Neuroimmune Regulation of Adult Hippocampal Neurogenesis by Complement Component 3 and Complement C3a Receptor

A thesis submitted for the degree of Doctor of Philosophy

Laura Jayne Westacott

School of Medicine

Cardiff University

September 2016

Declaration

This work has not been submitted in substance for any other degree or award at this or any other university or place of learning, nor is being submitted concurrently in candidature for any degree or other award.

Signed   (candidate)   Date

STATEMENT 1

This thesis is being submitted in partial fulfilment of the requirements for the degree of PhD

Signed   (candidate)   Date

STATEMENT 2

This thesis is the result of my own independent work/investigation, except where otherwise stated, and the thesis has not been edited by a third party beyond what is permitted by Cardiff University's Policy on the Use of Third Party Editors by Research Degree Students. Other sources are acknowledged by explicit references. The views expressed are my own.

Signed   (candidate)   Date

STATEMENT 3

I hereby give consent for my thesis, if accepted, to be available online in the University's Open Access repository and for inter-library loan, and for the title and summary to be made available to outside organisations.

Signed   (candidate)   Date

STATEMENT 4: PREVIOUSLY APPROVED BAR ON ACCESS

I hereby give consent for my thesis, if accepted, to be available online in the University's Open Access repository and for inter-library loans after expiry of a bar on access previously approved by the Academic Standards & Quality Committee.

Signed   (candidate)   Date

Thesis Summary

Neuroimmune Regulation of Adult Hippocampal Neurogenesis by Complement Component 3 and Complement C3a Receptor

New neurons are added to the dentate gyrus of the hippocampus throughout adult life, through the process known as adult hippocampal neurogenesis (AHN). This important form of structural plasticity supports learning and memory in mammalian species. AHN is tightly regulated by a myriad of factors, including the immune system. Previous evidence suggests that signalling via Complement Component 3 (C3) and Complement C3a Receptor (C3aR) may regulate AHN under physiological conditions, although the mechanism of this putative regulation is unclear. In addition, C3a/C3aR signalling may regulate neuronal morphology. Using $C3^{-/-}$ and $C3aR^{-/-}$ mice, I used a combined *in vitro* and *in vivo* approach to investigate the role of C3/C3aR signalling in AHN.

In **Chapter 2**, I demonstrate that C3a/C3aR signalling is able to directly influence hippocampal precursor cells in primary cultures. Furthermore, in the adult mouse brain, there is an increase in the number of immature neurons in the absence of C3 and C3aR, suggesting that C3a/C3aR signalling exerts an anti-neurogenic effect in the healthy brain.

In **Chapter 3** I report that the dendritic arborisation of newborn neurons is altered in the absence of C3aR, but not C3, suggesting involvement of an alternative ligand. Therefore, C3aR signalling via an as yet-unidentified ligand is important for maintaining the normal neuronal morphology of adult born neurons.

Both the net levels of AHN and immature neuronal morphology have important functional consequences for cognitive and affective processes involving the hippocampus, which I investigate in **Chapter 4**. I report superior performance of $C3^{-/-}$ and $C3aR^{-/-}$ mice in a hippocampus-dependent spatial discrimination task, consistent with their elevated levels of AHN. Furthermore, C3a/C3aR deficiency was associated with abnormal anxiety phenotypes.

In conclusion, these results demonstrate a novel mechanism for neuroimmune regulation of AHN, which is of functional consequence to learning, memory and affective behaviour.

Dedication

In loving memory of John Billot
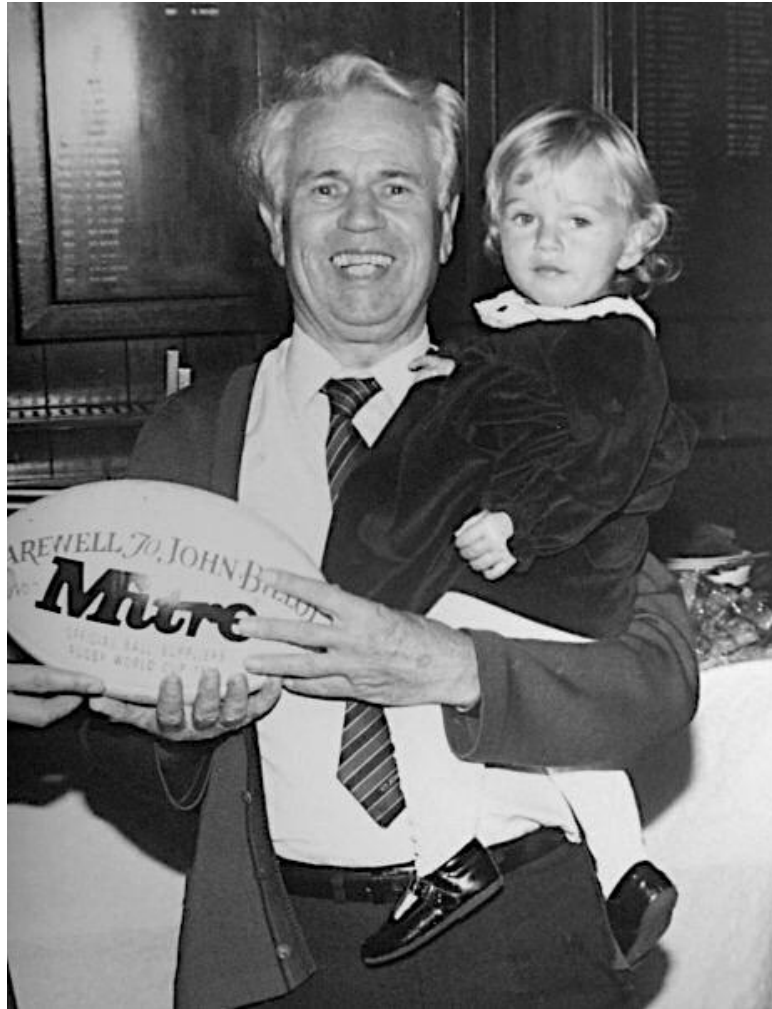
Acknowledgements

First and foremost, I would like to thank my supervisor Professor William Gray for his guidance, for believing in me when I didn't, and encouraging me to do my best; it has been of great benefit to me both academically and personally. I extend my gratitude to everyone in the Gray lab, whom have been a pleasure to work alongside. In particular I thank Malik Zaben, who was indispensible when I found myself at the foot of a steep learning curve, having chosen to transition from my prior field of Psychology to that of stem-cell biology. I am also grateful for the help, support and friendship of Dr Niels Haan. I also thank my close friends Damla Khan and Chen Liang, whose company always made long days in the lab a delight.

Thanks to Professor Paul Morgan and Dr Tim Hughes for their expertise and provision of the mouse strains used. I also thank Professor Lawrence Wilkinson for his and support and never-ending enthusiasm. Thanks also to Dr Trevor Humby, who was invaluable during the final months of my PhD. Dr Kate Binley has also been generous in sharing her knowledge, for which I am very grateful. I am indebted to the NMHRI and my funders, the Wellcome Trust, for giving me the opportunity to pursue my interests within the esteemed Neuroscience community at Cardiff University.

I am grateful to have shared this experience with many wonderful people who I now call friends; Hannah Furby, Stacy Littlechild, Zoe Noakes, Claris Diaz, Nick Clifton, Lucy Sykes, Emma Yhnell, Susanne Clinche, Yat Patel, Kat Christiansen, and many more. In particular, I thank my housemate Alison Costigan, for providing me with daily bouts of hysterical laughter over the past three years. Thanks also to my friends outside of work for their support and tolerance; Genevieve Clarke, Re-Becca Conely, Bina Higgins and Kim Hughes. I also thank Jay Williams and family, for all the good times, and providing refuge from the stresses of PhD life.

Thanks to my family for their endless support and patience throughout my many years of studying. I am especially grateful to my Dad for his keen interest in my work and proof reading of this thesis (in addition to his help in the prevention of catastrophic I.T. disasters). Mum, David, Emma, Andrew, Aunty Sue, Uncle Martin, Aunty Christine, Jen, Uncle Steve, Uncle Brian, Aunty Sue, Nan and Grandma-thank you all for always encouraging my endeavours and helping me to get where I am today. My final thanks go to my late grandfather, John Billot, to whom this work is dedicated. From an early age, he motivated me to learn, inspired me to do my best, and fostered an outlook on life that has guaranteed much fun and happiness whilst in pursuit of these values.

Table of Contents

Index of Figures

Index of Tables

List of Abbreviations

Abbreviation	Full name
-/-	Homozygous knockout
ABX	Antimycotic-antibiotic
AHN	Adult hippocampal neurogenesis
ANOVA	Analysis of variance
AUC	Area under the curve
BDNF	Brain-derived neurotrophic factor
BI	Branching Index
BLBP	Brain lipid binding protein
BrdU	5 Bromo-2'-deoxyUridine
BSA	Bovine serum albumin
C3	Complement component 3
C3aR	Complement C3a receptor 1
C3aRA	C3a receptor antagonist
C4	Complement component 4
C5aR	Complement C5a receptor 1
cDNA	Complementary DNA
CF	Close first
CFC	Contextual fear conditioning
CFH	Complement factor H
CFP	Properdin
CL	Close last
CLU	Clusterin
CNS	Central nervous system
Cr1	Complement receptor 1
CR2	Complement receptor 2
CR3	Complement receptor 3
CS	Conditioned stimulus
CS-US	Conditioned stimulus-unconditioned stimulus
DAF	Decay accelerating factor
DAMPs	Damage-associated molecular patterns
DAPI	4'6-Diamidino-2-phenylindole
DCX	Doublecortin
DG	Dentate gyrus
DIV	Days *in vitro*
dLGN	Dorsal lateral geniculate nucleus
DMEM	Dulbecco's Modified Eagle Medium
DMSO	Dimethyl sulfoxide
DNA	Deoxyribonucleic acid
EC	Entorhinal cortex
EdU	5-ethynyl-2´-deoxyuridine

EdU	5-ethynyl-2'-deoxyuridine
EE	Environmental enrichment
EGF	Epidermal growth factor
ELISA	Enzyme-linked immunosorbent assay
EPM	Elevated plus maze
ERK	Extracellular signal-regulated kinases
FBS	Fetal bovine serum
FF	Far first
FGF-2	Basic fibroblast growth factor
FL	Far last
GABA	γ-Aminobutyric acid
GC	Granule cell
GCL	Granule cell layer
GDNF	Glial derived growth factor
GFAP	Glial fibrillary acidic protein
GFP	Green fluorescent protein
GR	Glucocorticoid receptor
Hab	Habituation
HPA	Hypothalamic-pituitary axis
Iba-1	Ionized calcium binding adaptor molecule 1
IκBα	Nuclear factor of kappa light polypeptide gene enhancer in B-cells inhibitor, alpha
LD	Location discrimination task
LDH	Lactate dehydrogenase
LPS	Lipopolysaccharide
LS	Large squares
LTP	Long term potentiation
Map2ab	Microtubule-Associated Protein 2ab
MI	Must Initiate
mRNA	Messenger RNA
MT	Must touch
MTL	Medial temporal lobe
mTLE	Mesial temporal lobe epilepsy
MTT	3-(4,5-dimethylthiazol-2-yl)-2,5-diphenyltetrazolium
MWM	Morris water maze
NBA	Neurobasal A
NBA/B27/Abx/Glutamax	Standard culture medium
NeuN	Neuronal nuclei
NFκB	Nuclear factor kappa-light-chain-enhancer of activated B cells
NGF	Nerve growth factor
NMDA	N-Methyl-D-aspartic acid
NPCs	Neural precursor cells
NPY	Neuropeptide Y
NUMB	Numb-like protein
OF	Open field
PAMPs	Pathogen-associated molecular patterns

PBS	Phosphate buffered Saline
PBS-T	Phosphate buffered saline plus TritonX-100
PCR	Polymerase chain reaction
PFA	Paraformaldehyde
PI	Propodium Iodide
PI	Punish incorrect
PLL	Poly-L-Lysine
RA	Retinoic acid
Rcf	Relative centrifugal force
Rpm	Rotations per minute
SDF1	Stromal cell derived factor 1
SGZ	Subgranular zone
Sox-2	SRY (Sex Determining Region Y)-Box 2
SVZ	Subventricular zone
TUJ1	Neuron specific class III β-tubulin
US	Unconditioned stimulus
v/v	volume / volume
VEGF	Vascular endothelial growth factor
VGAT	Vesicular GABA transporter
VGF	Nerve-growth factor inducible protein
VGlut2	Vesicular glutamate transporter 1
VIP	Vasoactive intestinal peptide
w / v	weight / volume
WT	Wild type

1.   General Introduction

1.1 Overview - Adult hippocampal neurogenesis (AHN)

Neurogenesis, the creation of new neurons, was traditionally viewed as a phenomenon restricted to the developmental period in mammalian species. However, evidence to the contrary has accumulated since the first report of neurogenesis occurring in the adult rodent brain almost 50 years ago (Altman, 1963), and then in the human brain nearly 40 years on (Eriksson et al., 1998). In 2013, a seminal paper by Spalding et al. (2013) used nuclear-bomb testing generated ^{14}C dating to estimate that approximately 700 new neurons are added to the adult human hippocampus per day. It is now well accepted that neurogenesis is an ongoing process throughout adult life in mammalian species, and is acknowledged as a functionally relevant form of structural plasticity that supports learning and memory (Kempermann, Song, & Gage, 2015). It is therefore a unique process within the adult brain, and its relevance spans all levels of neuroscience; from molecular cell biology through to behaviour (Aimone et al., 2014).

Adult neurogenesis is an evolutionarily preserved trait that has been found in all vertebrate and mammalian species examined so far (Lindsey & Tropepe, 2006). In mammals, adult neurogenesis occurs in two principal regions; the subgranular zone (SGZ) of the hippocampal dentate gyrus (DG), which produces excitatory granule cell (GC) neurons, and the subventricular zone (SVZ), which gives rise to interneurons in the olfactory bulb. Within the canonical neurogenic zones reside highly specialized, tightly regulated microenvironments or niches that are permissive of neurogenesis in the otherwise anti-neurogenic brain (Kempermann et al., 2004). While prominent in rodents due to their reliance on olfaction, ongoing SVZ neurogenesis has not been detectable in humans (Arellano & Rakic, 2011). Consequentially, AHN has received considerably greater research interest

than its SVZ counterpart. The focus on AHN has also arisen due its important contribution to memory processes (Kempermann, 2012).

AHN itself is a complex and multi-faceted process, encompassing the progression from a primitive stem cell to the production of a mature, excitatory GC (Kempermann, Jessberger, Steiner, & Kronenberg, 2004; Riquelme, Drapeau, & Doetsch, 2008). AHN originates from stem cells with glial properties, which go through a series of sequential developmental steps. These cells are relatively quiescent, but give rise to an expansive population of transiently amplifying progenitor cells. After a period of highly selective survival, the few cells remaining become post-mitotic and begin to mature into GC neurons (Kempermann et al., 2004). This developmental stage sees large changes in the morphology and connectivity of adult born neurons (Zhao, Teng, Sumners, Ming & Gage, 2006), and ultimately their integration into pre-existing hippocampal circuitry.

AHN is a form of structural plasticity, and the process of generating new neurons is itself highly dynamic and amenable to influence. As such, there are many regulatory factors that act on the mechanisms controlling adult neurogenesis to influence its outcome. Critically, many stages of adult neurogenesis are regulated by local network activity (Ma, Kim, Ming, & Song, 2009). The continual turnover of new neurons in an activity-dependent manner therefore allows ongoing remodelling and fine-tuning of circuitry in line with environmental demands (Kempermann, 2012). Many other cell extrinsic factors, including the immune system, play important regulatory roles in AHN (Leiter, Kempermann, & Walker, 2016).

When neurogenesis fails, such as in the condition of mesial temporal lobe epilepsy (mTLE) cognitive deficits and mood disorders ensue, underlining the importance of this process for everyday life (Barkas et al., 2012; Coras et al., 2010; Helmstaedter, Kurthen, Lux, Reuber, & Elger, 2003; Illman, Moulin, & Kemp, 2015; Pauli, Hildebrandt, Romstöck, Stefan, & Blumcke, 2006). Deficits in AHN may be at the seat of many neuropsychiatric and neurological

disorders, but to date, the mechanisms contributing to neurogenic impairments are poorly understood (Kempermann, Krebs, & Fabel, 2008). It is therefore of great importance that we continue to expand our knowledge of AHN and the regulatory mechanisms that influence this integral process, both in the healthy and diseased brain.

1.2 Structure and connectivity of the dentate gyrus

Before presenting a detailed description of the process of adult neurogenesis, it is important to set the scene. The dentate is part of the hippocampal formation, a medial temporal lobe (MTL) structure critical for memory formation and storage (Eichenbaum, 2004). The dentate is comprised of three layers; the molecular layer, the GC layer (GCL), and the hilus (Figure 1.1A; Amaral, Scharfman, & Lavenex, 2007). The molecular layer consists of the dendritic trees of granule cells, which project from the GCL, as well as interneurons and projections from the nearby entorhinal cortex (EC). As seen in Figure 1.1A, the GCL is densely packed with GC neurons, and its blades form the characteristic 'V' shape that make the dentate such a distinctive structure. The transverse axis of the dentate is often divided into the suprapyramidal and infrapyramidal blades. As shown in Figure 1.1A, the former constitutes the more dorsal blade, which lies between the CA3 and CA1 hippocampal fields, whereas the latter lies opposite to this, below the CA3 region. The hilus is a cellular region enclosed by the GCL, which hosts the mossy fibres, the unmyelinated axons of GCs that project along the mossy fibre pathway to CA3 (Amaral & Pierre, 2009).

In order to understand the function of AHN, one must not only consider the structure of the DG, but perhaps more importantly, its connectivity. Neuroanatomically, the DG is a distinctive structure since most of its inputs and outputs are unidirectional and feed-forward in nature (Amaral et al., 2007). This connectivity has often been described as a 'tri-synaptic circuit' (Scharfman, 2007). As shown in Figure 1.1B, the major afferent projection to

3

the DG is via fibres known as the perforant path, which travel from the neighbouring EC (Cajal, 1893). The dentate is the termination point of these connections, which carry sensory information from the cortex. This suggests that the dentate serves as a initial step in the information processing that ultimately leads to memory formation (Amaral et al., 2007).
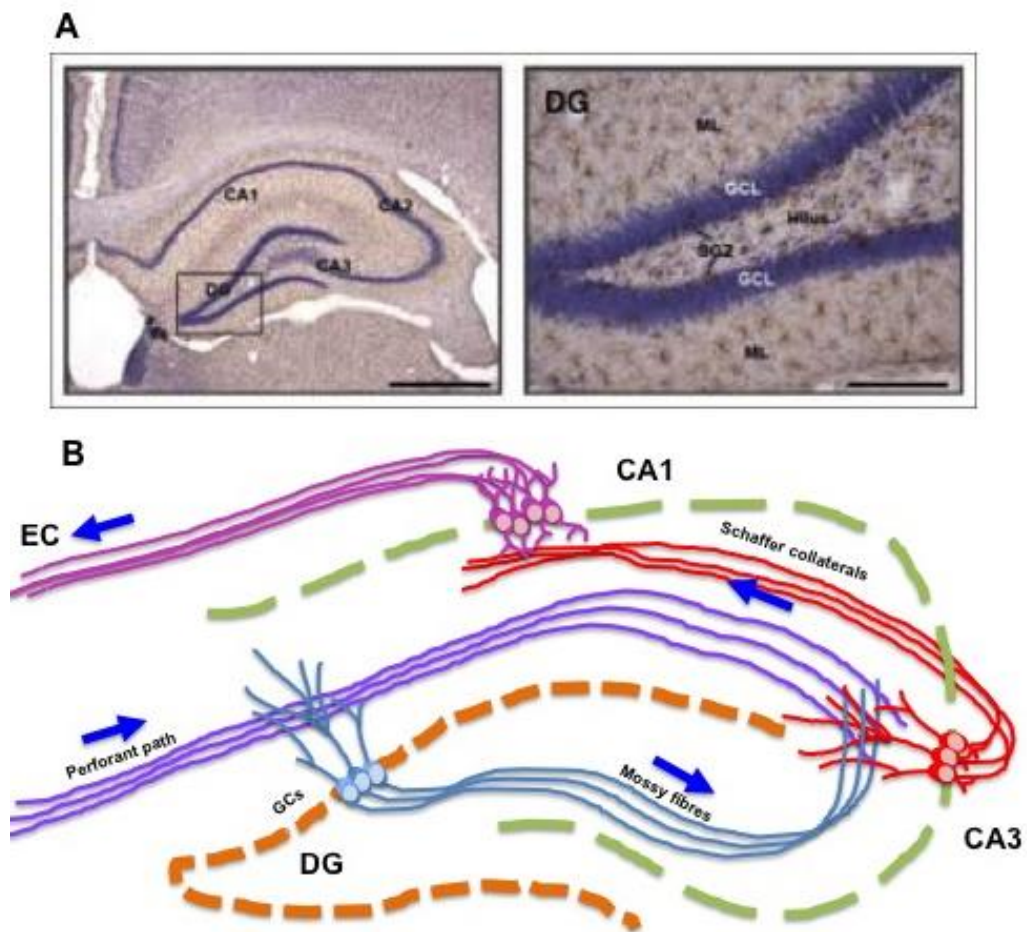
Figure 1.1. Example of dentate gyrus (DG) structure and connectivity in the murine hippocampus. A) Position of DG within the hippocampal formation (left panel, scale bar: 500 μm) and structure of the DG (right panel, scale bar: 100 μm). Image sourced from Liaury et al. (2012). **B)** Simplified illustration of the hippocampal tri-synaptic loop.

Importantly, these connections make contact with the dendritic spines of GCs situated in the GCL (Amaral & Pierre, 2009). The DG does not have reciprocal connections with the EC, rather, the mossy fibres of GCs project solely to the CA3 region (Amaral & Pierre, 2009). Here, the mossy fibres make contact

with the proximal dendrites of CA3 pyramidal cells. The axons of these cells, termed the Schaffer collaterals, project directly to pyramidal neurons in CA1 (Andersen, Bliss, & Skrede, 1971). Importantly, the axons of these cells form a recursive feedback loop as they circle back to the dendrites of cells within the same region (Andersen, Bliss, & Skrede, 1971). These connections complete the tri-synaptic circuit and relay back to the EC (Scharfman, 2007).

Each subfield (DG, CA3, CA1) receives direct cortical input from the perforant path (Yeckel & Berger, 1990), but also feed-forward excitation via sequential activation of the DG GCs, pyramidal cells in CA3, and pyramidal cells in CA1. This latter circuit is referred to as the 'intrinsic' circuit (Moser, 2011), and is thought to permit a step-by-step transformation of incoming sensory information into a 'network code' to enable memory storage and later retrieval (Colgin, Moser, & Moser, 2008).

1.2.1 Structural and functional heterogeneity of the longitudinal hippocampal axis

While the internal hippocampal circuitry is relatively homogeneous, heterogeneity exists in extrinsic connectivity along the longitudinal hippocampal axis (Bannerman, Sprengel, & Sanderson, 2014; Kheirbek et al., 2013; Strange, Witter, Lein, & Moser, 2014). The anterior hippocampus has connections with the entorhinal cortex (Dolorfo & Amaral, 1998), which is necessary for spatial learning (Steffenach, Witter, Moser, & Moser, 2005). The posterior hippocampus preferentially receives direct projections from limbic areas such the amygdala and hypothalamus, which are involved in fear and affective processes (Swanson & Cowan, 1979; Phillips & Ledoux, 1992). These observations have lead to the suggestion that the dorsal or anterior hippocampus is preferentially involved in learning and memory, whereas the posterior or ventral hippocampus participates in affective behaviours (Bannerman et al., 2014).

Levels of AHN also follow anatomical gradients. Greater numbers of adult born neurons are found within the anterior hippocampus (Snyder, Radik, Wojtowicz, & Cameron, 2009a; Ferland, Gross, & Applegate, 2002), and these cells show greater recruitment in hippocampus-dependent tasks than their posterior counterparts (Snyder et al. 2009a). However, in the posterior hippocampus, mature granule cells are more involved in spatial learning than those in the anterior hippocampus (Snyder et al. 2009a).

There are also differences in AHN and the functionality of newborn neurons between the two blades of the DG (Snyder et al. 2009a). Higher levels of AHN have been reported within the infrapyramidal blade (Snyder et al., 2009a; Schlessinger et al., 1975), although newborn neurons in the suprapyramidal blade are more active during spatial learning (Chawla et al., 2005; Snyder et al., 2009a). Therefore, clear anatomical gradients exist in hippocampal connectivity and AHN, with potential consequences upon functionality. Comparisons of newly born cells based on their anatomical location along the anterior-posterior and suprapyramidal-infrapyramidal axes will better help us understand the function of adult born neurons (Sahay & Hen, 2007).

1.3 Function of the DG and AHN within the long-term memory system

The function of AHN has been debated over many years. A consensus is now emerging however, and it is increasingly appreciated that newborn neurons serve a specific purpose with regards to cognition. Firstly, it is important to appreciate the basic structure of the long-term-memory systems involved. Declarative memory has been defined as conscious memory for facts and events (Squire, Stark, & Clark, 2004) and is thought to depend on the MTL system, including the hippocampus. Declarative memory is often contrasted with non-declarative, procedural memory such as that for habits, skills and procedures (Squire & Zola, 1996). Under the umbrella of declarative memory exists episodic memory; the conscious recollection of personal, autobiographical details occurring within a specific chronological and spatial

context (Aggleton & Brown, 2006a). For example, one may come across an individual, consciously recognise that you have met them before, and be able to recall exactly when and where you previously encountered them. This process, termed 'recollective recognition', has been contrasted with pure recognition or 'familiarity detection' (Aggleton & Brown, 2006b). This process may manifest as encountering an individual, knowing you are familiar with them, but not being able to recall any specific information about them or where you met them. Lively debate has surrounded this distinction within the scientific community (Aggleton & Brown, 2006b; Squire et al., 2004).

Evidence now demonstrates that these processes can be dissociated and attributed to separate, but interleaving memory systems (Aggleton & Brown, 2006b; Winters, 2004). Brown & Aggleton (2001) argued that the perirhinal cortex, a structure adjacent to the hippocampus, supports familiarity detection, whereas a system centred on the hippocampus is involved in recollective recognition. In agreement, it has been found that the hippocampus is preferentially engaged during recollection, but not during familiarity judgments (Yonelinas, Aly, Wang, & Koen, 2010). Furthermore, reports of clinical cases (Burgess, Maguire, & O'Keefe, 2002; Scoville & Milner, 1957) and animal lesion studies have suggested that recollective recognition is dependent on episodic memory, which itself is heavily dependent upon the hippocampal formation (Winters, 2004).

1.3.1 Pattern separation and pattern completion

Two key computational processes in the formation and recollection of episodic memories are known as 'pattern separation' and 'pattern completion'. Pattern separation involves the computational act of transforming similar sensory inputs into distinct, non-overlapping representations such that memories are separately stored, reducing interference and aiding retrieval (Figure 1.2A; Bakker, Kirwan, Miller, &

Stark, 2008). On the other hand, pattern completion refers is the process by which degraded or incomplete representations are 'filled in' based on representations previously stored; thus overlapping representations are made more similar (Figure 1.2B, Yassa & Stark, 2011). This process allows the retrieval of complete memories from partial cues (Lever & Burgess, 2012).

Recollective recognition places clear demand on pattern separation, and it has been argued that this process is the hallmark feature of episodic memory (O'Reilly & Norman, 2002). Recollection may not always require pattern separation however; if recalling two distinct episodes, which do not bear similarity to each other, then pattern separation would not be as necessary. However, if attempting to recall two highly similar events, such as where you parked your car yesterday, versus where you parked your car today within the same car park, then successful recall will depend on how well the memories have been separated based on their individual contextual, spatial and temporal details (Yassa & Stark, 2011). While it is not possible to test recollective, episodic memory in animals, pattern separation can nonetheless be tested in behavioural paradigms requiring rodents to discriminate between highly similar stimuli, spatial locations or contexts (McTighe, Mar, Romberg, Bussey, & Saksida, 2009; Shors et al., 2001).

1.3.2 The mechanical basis of pattern separation and completion

Traditionally, the DG has been regarded as the information gateway to the hippocampus and is thought to be pivotal in these processes (Aimone, Deng, & Gage, 2011; Lever & Burgess, 2012). This idea was first proposed based on the presumed role of the hippocampus in the formation of new memories, and the position of the DG within the hippocampal circuitry (Deng, Aimone, & Gage, 2010). Furthermore, the suggestion of David Marr that the hippocampus stores memories in associative networks led to the recognition

that highly separated inputs would be necessary to encode different representations or memories in the CA3 (Marr, 1971; Yassa & Stark, 2011).
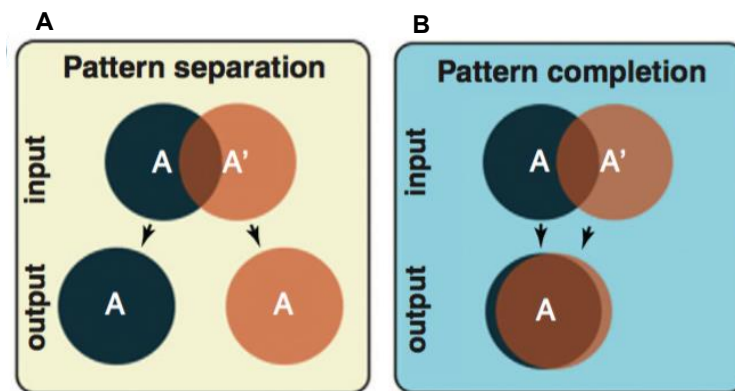
Figure1.2 Pattern separation and pattern completion. A) Pattern separation is the computational process of transforming similar or overlapping sensory inputs into distinct representations in order to aid learning and reduce interference. B) Pattern completion fills in partial or degraded representations to form an intact representation. Image sourced from Yassa & Stark, (2011).

Anatomically, the DG is well suited to perform pattern separation. The aforementioned tri-synaptic circuit supports this process, and adult born GCs in the GCL specifically carry out pattern separation. Importantly, the DG contains up to ten times more neurons than its primary input, the EC (Amaral et al., 2007), meaning that overlapping EC inputs can be encoded separately by the DG. Furthermore, the DG shows sparse coding, whereby events are encoded by a strongly activated but small set of GCs (Yassa & Stark, 2011). It is also is rarely active during behaviour and receives both feedforward and feedback inhibition from local interneurons (Deng, Aimone, & Gage, 2010). Therefore, it has been postulated that GCs are able to perform pattern separation on the distributed and overlapping representations which arrive from the EC, and project them on to CA3 pyramidal cells via the mossy fibre pathway (Yassa & Stark, 2011). Despite sparse activation of GCs, individual mossy fibres are able to strongly depolarize downstream CA3 pyramidal neurons, meaning that they can drive memory encoding. This supports learning and reduces interference. Furthermore, additional weaker projections which travel directly from layer II of the EC to CA3, bypassing the

DG (Witter, 1993) are thought to provide recall cues (Rolls & Kesner, 2006). Through connections within the associative hippocampal network, these memory cues are then able to activate the neurons which represent the stored memory or 'engram' itself, leading to successful recollection (Rolls & Kesner, 2006).

In support of this theory, lesion studies have reported a double dissociation between the DG and perforant path inputs into CA3 (Lee & Kesner, 2004). Lesions to the direct perforant path projections to CA3 impair retrieval but spare encoding, whereas lesioning the DG input into CA3 impairs encoding but not retrieval (Lee & Kesner, 2004). Furthermore, inactivation of the mossy fibres has been shown to impair learning of a spatial memory task in mice, but leaves memory consolidation and retrieval intact (Lassalle, Bataille, & Halley, 2000). Therefore, it has been proposed that the CA3 network associates input coming from the mossy fibres via GCs with direct perforant path input in order to enable later recall (Yassa & Stark, 2011).

1.3.3   Evidence implicating adult born neurons in pattern separation

Several experimental paradigms have been developed to either decrease or completely ablate neurogenesis (Zhao, Deng, & Gage, 2008). These techniques include but are not limited to the following; low dose irradiation of either the whole brain or specific brain regions (Winocur, Wojtowicz, Sekeres, Snyder, & Wang, 2006), the use of genetically engineered mice to eliminate neural progenitor cells (Saxe et al., 2006), and systemic treatment with antimitotic drugs including methylazoxymethanol (MAM) to inhibit the proliferation of precursor cells (Shors et al., 2001). Many initial studies using these techniques showed broad deficits in hippocampus-dependent behavioural tasks in animals with ablated neurogenesis (Saxe et al., 2006; Shors et al., 2001; Snyder, Hong, McDonald, & Wojtowicz, 2005; Winocur et al., 2006). While these studies suggested a potential role for AHN in cognition, results were somewhat inconsistent between studies (Zhao et al.

2008), likely reflecting the diversity of the behavioural paradigms used (Kempermann, 2013) and the variation in the efficiency and specificity of ablation techniques (Zhao et al. 2008). Furthermore, while many of these tasks may be hippocampus-dependent, they may not necessarily be hippocampal-neurogenesis dependent (Lledo, Alonso, & Grubb, 2006). Accordingly, studies that have specifically challenged the function of newly born neurons in performing pattern separation have provided greater clarity. Generally, rodents with ablated neurogenesis are impaired at discriminating stimuli which preferentially recruit pattern separation; for example, stimuli that are presented with little spatial separation as opposed to stimuli separated by a larger distance (Clelland et al., 2009) or highly similar contexts (Nakashiba et al., 2012; Tronel et al., 2015). In agreement, animals subjected to increases in AHN generally show improvements in pattern separation. Running has been demonstrated to increase AHN (van Praag et al., 2002) and is associated with enhanced spatial pattern separation (Creer, Romberg, Saksida, van Praag, & Bussey, 2010). Furthermore, inducible genetic expansion of adult born neurons (via increased survival) has also been used to augment AHN, and benefits discrimination of highly similar contexts (Sahay et al., 2011).

1.3.4 Age-dependent specialisation of GC function

Since the DG is one of the few areas in which adult neurogenesis occurs, this presents an unique situation whereby many neurons at distinct stages of maturation participate in the same neuronal network (Lopez-Rojas & Kreutz, 2016). As such, subtleties have emerged which suggest that GC neurons have distinct functions at varying stages of their maturation (Aimone et al., 2011). It has been shown that immature GCs differ from the older GC population as they initially possess greater excitability and plasticity (Esposito, 2005; Ge, Yang, Hsu, Ming, & Song, 2007), becoming increasingly silent within a few weeks of birth (Lopez-Rojas & Kreutz, 2016). Evidence also suggests an age-dependent specialization of function, whereby young GCs mediate pattern

separation, and old GCs are responsible for pattern completion (Nakashiba et al., 2012; Lever & Burgess, 2012).

1.3.5   Function of AHN in affective processes

Through its connections with the limbic system, a less appreciated and understood role of the hippocampus is in emotionality and affect (Kempermann et al., 2008). It has also been argued that AHN may mediate affective processes such as anxiety (Kheirbek & Hen, 2014; Bannerman et al., 2014). Anxiety is an emotional reaction to stimuli that are perceived as threatening, which may be innate or conditioned (Marques et al., 2016). While this reaction is adaptive and has evolved to promote avoidance of danger, anxiety can be pathological when prolonged or disproportionate to the threat (Cryan & Holmes, 2005). Kheirbek & Hen (2014) postulated that pattern separation might be integral to anxiety, as faulty pattern separation may impair the ability to discriminate between safe and threatening contexts. Deficits in AHN and thus pattern separation may therefore contribute to the tendency to over-generalise threat, as is often observed in anxiety and post-traumatic stress disorder (PTSD; Kheirbek et al., 2013). This may lead to inappropriate responses when an individual encounters similar, but harmless situations that had previously been associated with harm. This hypothesis has not yet received any experimental support in terms of its underlying mechanisms however.

AHN has also been implicated as an aetiological factor in major depression, and as a substrate for antidepressant action (Sahay & Hen, 2007). In contrast to our current understanding of the impact of AHN on anxiety, the mechanisms underlying this link have been well characterised. AHN is highly sensitive to stress (Mirescu & Gould, 2006) and it has long been known that the proliferation of hippocampal precursor cells is suppressed by corticosteroids (Gould, Cameron, Daniels, Woolley, & McEwen, 1992). Moreover, anti-depressants such as fluoxetine robustly increase AHN via

increased precursor cell proliferation (Encinas, Vaahtokari, & Enikolopov, 2006). Furthermore, antidepressants seem to preferentially increase AHN in the ventral portion of the hippocampus both in patients and rodents (Kheirbek et al., 2012). Importantly, AHN may also be required for the behavioural effects of antidepressant therapies via neurotrophic factor brain-derived neurotrophic factor (BDNF; Santarelli, 2003). On a mechanistic level, it has been found that BDNF and serotonin induce neuropeptide VGF (not an acronym), which has been found to increase AHN (Thakker-Varia et al., 2007).

Experimental evidence for a causal role of AHN in the pathogenesis of anxiety and depressive disorders remains limited however (Snyder, Soumier, Brewer, Pickel, & Cameron, 2011a; Gage, 2008a). Studies that have manipulated levels of AHN and measured subsequent affective behaviours have produced inconsistent results. There have been reports of increased anxiety (Revest et al., 2009) and depressive behaviours (Snyder et al., 2011a) in mice with ablated AHN, while others have reported no changes (Sahay et al., 2011). However it has also been reported that large increases in AHN induced by running are associated with heightened anxiety, which is ameliorated by irradiation treatment (Fuss et al. 2010a; Fuss et al. 2010b). The variation in these reports is likely due to the use of different ablation or augmentation techniques, as well as variation in behavioural paradigms used. Nonetheless, AHN can clearly contribute to some affective processes. In support, anxiety and depression are frequent comorbidities of mTLE, which is characterised by chronically impaired AHN (Groeticke, Hoffmann, & Loescher, 2008; Piazzini, Canevini, Maggiori, & Canger, 2001). Therefore, improving our understanding of the link between AHN and affect is of clinical importance.

1.4   The process of AHN

The ability of adult born neurons to perform the aforementioned cognitive and affective roles depends on their successful progression through a series of sequential developmental events, from neural precursor cells (NPCs) through to mature GC neurons (Kempermann et al., 2015). The process can be broken down into four distinct stages; a precursor cell stage, an early survival phase, a maturation phase in which cells become post-mitotic, and a late survival stage (Kempermann et al., 2015, Figure 1.3). Spanning these stages are six distinct 'milestones' of neurogenesis that can be distinguished based on protein expression and cell morphology (Kempermann et al., 2015). Briefly, radial glia-like stem cells give rise to intermediate, rapidly proliferating progenitors, which then generate NPCs (Bonaguidi, Song, Ming, & Song, 2012; Kempermann et al., 2004). These then become post-mitotic immature neurons, and finally mature GC neurons. The post-mitotic stage sees considerable change in terms of morphology, which is critical for functionality. The duration of AHN, from precursor cell to mature GC neuron has been estimated to take approximately 7 weeks in the rodent brain (Kempermann et al., 2015). Each stage and the corresponding cell phenotypes will now be considered in turn.

1.4.1 The precursor cell stage

This stage is associated with expansion of the precursor cell pool, a fraction of which eventually differentiate into neurons (Kempermann et al., 2015).

Type 1 cells

The most primitive stem cells in the adult hippocampus have been named type 1 cells, and have radial glia-like properties (Seri, Garcia-Verdugo, McEwen, & Alvarez-Buylla, 2001). Usually, radial glia are found only during development, where they generate progenitor cells and chaperon neurons to their correct destination before differentiating into astrocytes (Rakic, 1981).

14

However, they remain an integral feature of the adult DG throughout life. These cells can be identified by their characteristic morphology and position within the neurogenic niche. As shown in Figure 1.4, their triangular soma sits within innermost region of the GCL, the SGZ, and a single apical process extends through the GCL and ramifies in the molecular layer (Seri et al., 2001; Zhao et al., 2008). Type 1 cells can also be delineated by their expression of the astrocytic marker glial fibrillary acidic protein (GFAP) and radial glial marker brain lipid binding protein (BLBP), in combination with precursor cell associated proteins nestin and Sox2 (Fukuda, Kato, Tozuka, Yamaguchi, Miyamoto, & Hisatsune, 2003; Wei et al., 2002; see Figure 1.3).

Type 1 cells account for approximately two-thirds of the nestin expressing population in the adult mouse DG (Kempermann et al., 2004). Despite their prevalence, these cells account for only a small proportion of cell divisions. After pulse labelling with 5'-bromo-2-deoxyuridine (BrdU), a thymidine analogue that is incorporated into DNA during the S-phase of the cell cycle, (Wojtowicz & Kee, 2006), only 1% of type 1 cells show BrdU incorporation *in vivo* (Encinas et al., 2011). While the majority of type 1 cells are quiescent, they are capable of both symmetric self-renewal and multi-lineage differentiation via asymmetric division (Bonaguidi et al., 2011). Encinas et al. (2011) demonstrated that type 1 cells typically undergo three asymmetric divisions in rapid succession, before converting into astrocytes, although this cycle may be altered by pathology (Sierra et al., 2015).

A recent report has identified heterogeneity within the type 1 cell population, and suggested the existence of two distinct morphotypes of radial-glia like cells within the adult DG (Gebara et al., 2016). These cells, delineated as type α cells and type β cells, differ in terms of their morphology and proliferative activity. Lineage tracing showed that type α cells are proliferative and can generate neurons, type β cells, and astrocytes, whereas type β cells were non-mitotic. Therefore, it is possible that type β cells represent an intermediate stage between type α cells and their transformation into astrocytes (Gebara et al., 2016).
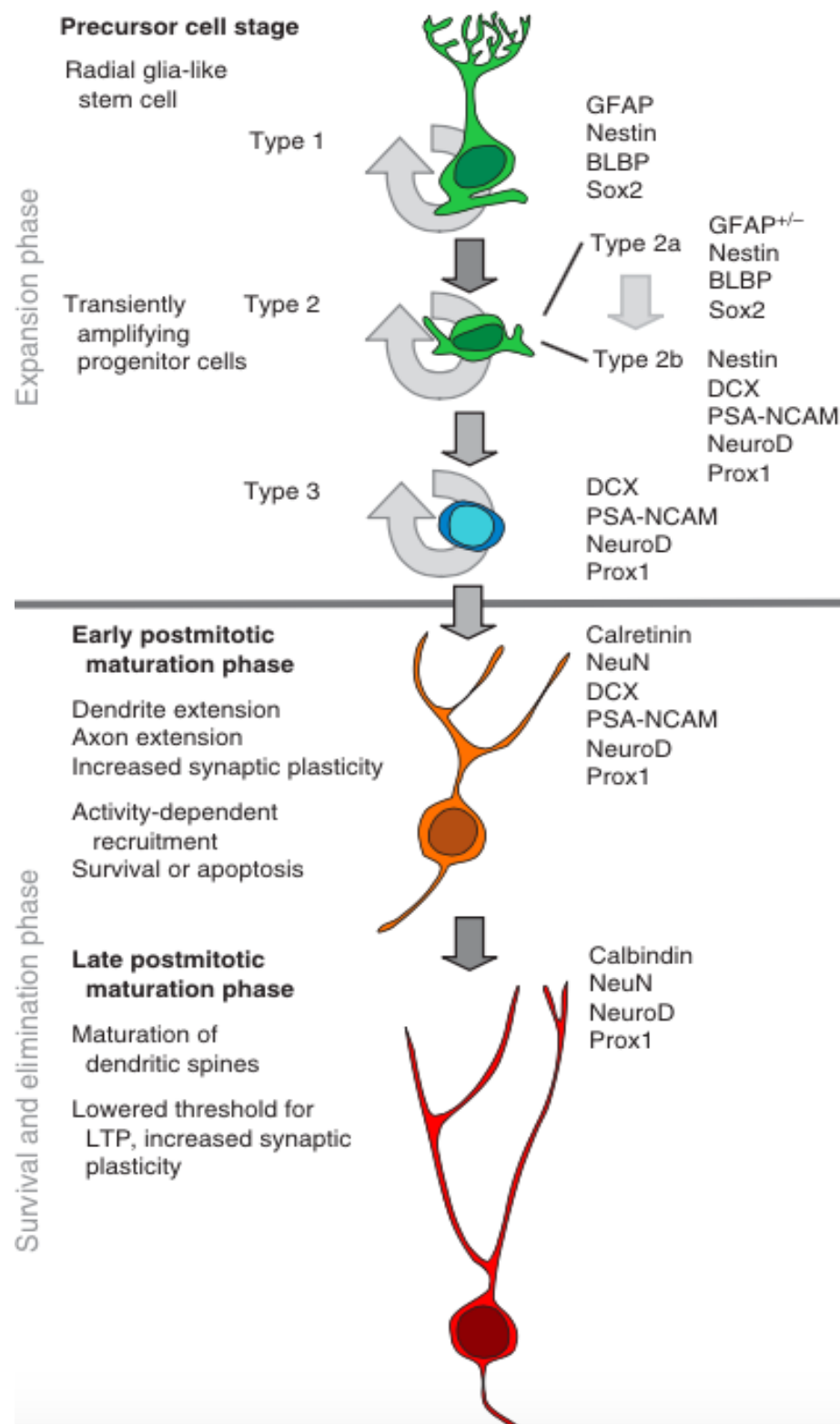
Figure 1.3 The milestones of adult hippocampal neurogenesis Schematic sourced from Kempermann et al. (2015).

Type 2a cells

The progeny of type 1 cells are known as the transit amplifying population or type 2 cells (Kempermann et al., 2004). These cells often have an oval morphology, with short bipolar processes if any, and are orientated tangentially to the GCL at the very base of the SGZ (Encinas et al., 2011; see Figure 1.4, left example of type 2 cell). Type 2a cells are characterised by their expression of the intermediate filament protein nestin, in combination with Sox2 and BLBP (see Figure 1.3; Steiner et al., 2006). A subset of these cells also retain expression of GFAP (Kempermann et al., 2015).

Mitotic activity is greatly increased at this stage of development; ten to twenty per cent of these cells show BrdU incorporation (Encinas et al., 2011). Overproduction due to this heightened proliferative activity is prevented by apoptosis and microglial phagocytosis (Sierra et al., 2010). It is thought that the fate choice of hippocampal neural precursor cells (NPCs) is made at the type 2a stage, since all later stages express neuronal lineage markers (Kempermann et al., 2015).

Type 2b cells

Neuronal lineage commitment and functional neuronal differentiation first become apparent in type 2b cells (Kempermann et al., 2004). While these cells retain expression of nestin, their expression of GFAP recedes and is replaced by immature neuronal markers including doublecortin (DCX). DCX is a microtubule associated protein that is often used as a marker for AHN, and is expressed for approximately two to three weeks from initial expression at the type 2b stage (Plümpe et al., 2006; Rao & Shetty, 2004). It has also been shown that DCX positive cells begin to migrate into the GCL (see Figure 1.4, type 2 cell), and are guided by the cell bodies of type 1 cells (Shapiro, Korn, Shan, & Ribak, 2005). These cells remain proliferative, and account for around ten per cent of all nestin positive cell divisions (Kronenberg et al., 2003). The subsequent phenotype to arise from type 2b cells, type 3 cells, spans both the precursor cell stage and the early survival stage.
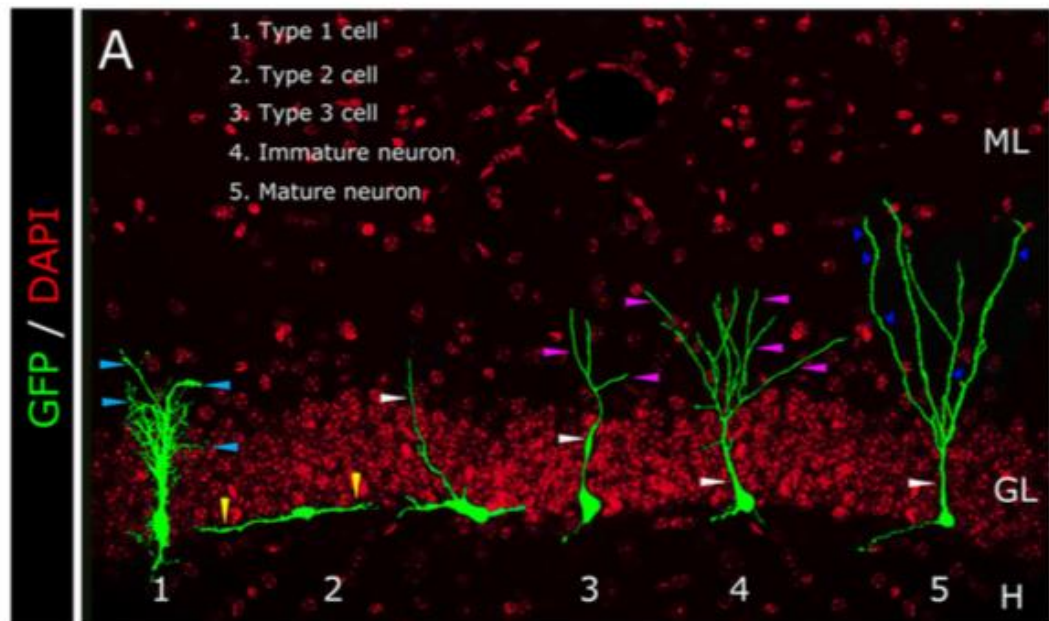
Figure 1.4 Morphological development in the adult dentate gyrus. GFP= green fluorescent protein, ML = molecular layer, GL= granule cell layer. Image sourced from Llorens-Martín, Rábano, & Ávila (2016).

1.4.2   The early survival stage

At this stage, many cells become post-mitotic, and their survival is highly selective. Most newborn cells are eliminated within a few days of their birth (Kuhn et al., 2005).   Surviving cells then enter a period of great morphological change (Llorens-Martín et al., 2016).

Type 3 cells
Type 3 represent a further advancement in the expression of neuronal features, and demonstrate the beginnings of GC morphology (Kempermann et al., 2004). Nestin expression ceases at this stage, whereas DCX persists. In addition, transcription factors NeuroD1 and Prox1 are upregulated (see Figure 1.3; Steiner et al., 2006). A subset of these cells retain limited proliferative activity (Kronenberg et al., 2003). Of the entire DCX positive population, approximately seventy per cent are post-mitotic (Plümpe et al.,

2006). These cells can express mature neuronal markers such as NeuN within a few days post-cell cycle exit (Kempermann et al., 2004). However, before they have the chance to mature and make functional connections, the majority of these cells are rapidly eliminated via apoptosis (Kuhn et al., 2005). For this reason, the overall quantity of proliferating cells in the adult DG is poorly predictive of net neurogenesis (Fabel, et al., 2009). It has been suggested that any cells surviving the first two weeks post-cell cycle exit are the 'chosen few' that will mature and become permanently integrated into the hippocampal circuitry (Kempermann, Gast, Kronenberg, Yamaguchi, & Gage, 2003). Therefore, the decision for long-term survival takes place at this stage (Kempermann et al., 2004).

The time-point at which dendrite development begins is highly variable within this population (Kempermann et al., 2015). By the end of this stage however, surviving cells have a triangular nucleus and a clear apical dendrite that is orientated vertically within the GCL (Llorens-Martín et al., 2016; see Figure 1.4). Furthermore, within a few days of cell cycle exit, an axon is extended to CA3, forming part of the mossy fibre tract (Zhao et al., 2006). However, spines do not yet form on these axons (Kempermann et al., 2015).

1.4.3 The post-mitotic maturation stage

This stage is characterised by the beginnings of functional integration (Zhao et al., 2006). Expression of markers remains similar to the preceding stage, however transient upregulation of Ca^{2+} binding protein calretinin is seen (Brandt, Jessberger, Steiner, & Kronenberg, 2003; See Figure 1.3). Complexity of the dendritic tree also begins to increase at this stage (Llorens-Martín et al., 2016), and spines begin to appear on the axonal contacts projecting to CA3 (Zhao et al., 2006).

1.4.4 The late survival stage

This period consists of the 'fine-tuning' of connectivity and function (Kempermann et al., 2015). Having survived the initial two to three weeks of post-mitotic life and integrated into the surrounding network, cells switch their expression of calretinin to calbindin (Brandt et al., 2003; Kempermann et al., 2015). Cells develop the morphology characteristic of mature GCs at this stage, which is of importance for their eventual function since connectivity relies upon dendritic-axonal arborisation and synaptic contacts (Zhao et al., 2006). The rate at which cells mature is highly dependent on the surrounding environment and network activity however (Zhao et al., 2006), which will be addressed in the following section. A critical period exists up to a month and a half after birth, where newborn neurons have enhanced synaptic plasticity, a lower threshold for induction of long-term potentiation (LTP) and are uninhibited by local interneurons, unlike mature GC neurons (Saxe et al., 2006; Schmidt-Hieber, Jonas, & Bischofberger, 2004). It is these particular properties of newly generated neurons which are thought to be responsible for the aforementioned role of AHN in pattern separation (Yassa & Stark, 2011). The plasticity permitted by the process of ANH therefore lies at the core of the functionality of the DG (Kempermann, Song, & Gage, 2015).

1.4.5 Adult versus postnatal neurogenesis

Adult neurogenesis has been said to recapitulate developmental neurogenesis (Kempermann et al., 2004). Whether this is the case has an important implication for experimental studies of AHN, since use of *ex vivo* postnatal tissue is a powerful approach to studying AHN *in vitro* (Namba, et al., 2007). In rodents, much GCL development occurs postnatally (Altman & Bayer, 1990), and studies have suggested that a peak of proliferation occurs between postnatal day 5 and 8 in the SGZ, after which these cells migrate to the GCL and become GC neurons (Namba at al., 2005). The GCL is indistinguishable from its adult form by postnatal day 19 (Namba et al.,

2007) This suggests that precursor cells present at this time are similar in nature to adult progenitors in terms of their differentiation potential and marker expression. Therefore, neurogenesis occurring at the postnatal stage is relevant and therefore suitable for modelling AHN (Namba et al, 2007). With regard to the morphological development of GC neurons, Esposito (2005) reported that the developmental rules for neuronal integration during embryonic development are maintained in the adult hippocampus. However, the entire process of morphological development occurs at a slower pace than is seen in the postnatal brain (Aimone et al., 2014; Zhao et al., 2006).

1.5   Regulation of AHN

The process of neuronal development within the adult DG is carefully controlled by cell intrinsic mechanisms. Many transcription factors vital for embryonic and postnatal hippocampal development also play a role in AHN (Li, Kataoka, Coughlin, & Pleasure, 2008). However, AHN is an extremely dynamic process, and these control mechanisms are subject to regulation by cell extrinsic factors, at both micro and macroscopic levels (Kempermann et al., 2004; Zhao et al., 2008). These regulatory factors can positively or negatively impact upon the levels of neurogenesis. Importantly, cells at distinct stages of the neurogenic lineage respond differently to modulating stimuli (Kronenberg et al., 2003) and can specifically alter their proliferation, survival or differentiation. Interestingly, different modulators of AHN can also affect the ultimate function of immature neurons upon their maturation (Clemenson et al., 2014). With regard to maturation and morphology, our knowledge of the regulatory genes necessary for neurite outgrowth and morphological maturation remains limited (Llorens-Martín et al., 2016), although dendritic maturation appears to be controlled by regulatory processes distinct to those that influence proliferation (Plümpe et al., 2006). In the following text, intracellular signalling pathways will be discussed

briefly, however the focus of this thesis lends itself more to the in-depth understanding of cell-extrinsic factors including the constituents of the neurogenic niche, local network activity and the immune system.

1.5.1 Intrinsic control of AHN

Maintenance and self-renewal

B-cell translocation 1 (Btg1) has been shown to play an important role in cell-cycle control and self-renewal of stem cells in the adult DG. Ablation of Btg1 causes a sharp decrease in the number of proliferating stem and progenitor cells, in combination with a high frequency of cell cycle exit and subsequent apoptosis (Farioli-Vecchioli, 2012; Tirone, Farioli-Vecchioli, Micheli, Ceccarelli, & Leonardi, 2013). Furthermore, Wnt proteins are important regulators of AHN in both embryonic and adult neurogenesis (Lie et al., 2005). In mice lacking Wnt7a, reduced self-renewal of stem cells and increased cell cycle exit was observed (Qu et al., 2013). Furthermore, cyclin-dependent kinase inhibitor 1C (p57) is vital for maintaining the quiescent state of type 1 cells; deletion of p57 in mice resulted in increased proliferation of type 1 cells, causing depletion of the adult stem cell pool (Furutachi, Matsumoto, Nakayama, & Gotoh, 2013).

Differentiation and fate choice

NeuroD1 is a basic helix-loop-helix (bHLH) transcription factor involved in regulating the expression of several genes involved in terminal differentiation of neurons (Schwab et al., 2000). Its expression has been shown in early differentiating progenitor cells in the DG (Seki, 2002). Strikingly, NeuroD1 deficient mice lack the granule cell layer of the DG (Liu et al., 2000) and display a number of abnormalities in AHN. Notably, the differentiation of granule cells is profoundly impaired. *In vitro,* Hsieh (2004) found that forced overexpression of NeuroD1 caused rat hippocampal neural progenitor cells to differentiate into more than seventy five per cent Tuj1$^+$

and MAP2ab^{+} neurons, and restricted their ability to adopt astrocytic and oligodendrocyte phenotypes.

Further to the role of Wnt7a in regulating self-renewal and proliferation of DG precursor cells, Wnt7a also plays a role in fate choice. Wnt7a regulates differentiation through downstream β-catenin activation of Neurogenin 2 (Ngn2), a bHLH transcription factor which has previously been implicated in neuronal differentiation (Thoma et al., 2012). Qu et al. (2013) reported that TUJ1^{+} cells decreased in number significantly when cells were transduced with Wnt7a siRNA.

Maturation

In addition to regulating differentiation, Wnt7a also plays a role in the morphological maturation of dentate granule neurons. Dendritic growth of newborn GCs was significantly decreased Wnt7a deficient mice, resulting in overall reduced dendritic complexity (Qu et al., 2013). These defects were also observed in cells cultured and transfected with Wnt7a siRNA.

Cyclin-dependent kinase 5 (cdk5) is pivotal to neurobiological processes such as neuronal migration, dendritic path finding, neurite extension, and learning and memory. Jessberger et al. (2008) used a retrovirus induced knock down of cdk5 targeted at newly generated DG granule cells. They found aberrant growth of dendritic processes and an altered migration pattern in newborn neuronal cells. Moreover, a large proportion of these cd5k-null cells failed to project their dendritic processes to the correct target zone of the ML, instead making aberrant synaptic connections in the hilus and GCL. This suggests that cdk5 is critical in the migration and morphological maturation of newborn granule cells within the DG.

Wnt, Sox2 and NeuroD1 crosstalk form a master regulatory pathway

The Wnt family of proteins are central in regulating multiple stages of neurogenesis. While some downstream targets have been identified (e.g., CyclinD1/Ngn2), little is known of the underlying molecular mechanisms (Lie et al., 2005). Kuwabara et al. (2009) described a novel mechanism

23

implicating Wnt mediated coordination of NeuroD1 and Sox2, in which Wnt signalling forms a dual regulatory switch controlling precursor cell self-renewal and neuronal differentiation in the hippocampus.

Using an adult rat hippocampal NPC line, Kuwabara et al. (2009) demonstrated that NeuroD1 promoter activity was upregulated in a dose-dependent manner after treatment with Wnt3a. This was dependent on the T cell factor/lymphoid enhancer factor (TCF/LEF) binding site, the primary downstream target of the noncanonical Wnt/ β-catenin pathway. Furthermore, they also identified binding sites in the NeuroD1 promoter region for Sox transcription factors, and some of these overlapped with the TCF/LEF sequences (referred to as Sox/LEF binding sites).   In undifferentiated cells, Sox2 was associated with the SOX/LEF site in the NeuroD1 promoter region. However, upon introduction of Wnt3a, β-catenin instead associated with the SOX/LEF binding site, consequently activating NeuroD1 expression and neuronal differentiation (Kuwabara et al., 2009). These findings suggest that the SOX/LEF sites act as bi-directional regulators of the balance between self-renewal of precursor cells and neuronal differentiation.

1.5.2 Cell extrinsic factors

The cell intrinsic factors described are the basic mechanisms that control the process of neuronal development. In addition, these control mechanisms are regulated by extrinsic factors that can be molecular through to behavioural in nature (Kempermann et al., 2015). This regulation lies at the heart of AHN, as exquisite sensitivity to the environment allows the experience-dependent structural plasticity for which it has evolved (Kempermann et al., 2015).

Much regulation occurs that the stage of neuronal development as opposed to the expansion phase (Kempermann, 2006). As such, NPC proliferation is amenable to a broad range of extrinsic factors in a non-specific manner, whereas survival is more finely tuned to respond to local network activity and hippocampal learning (Kempermann et al., 2015). Furthermore, AHN takes place within a highly specialized neurogenic niche, the constituents of which are vital for regulation of the neurogenic process (Riquelme et al., 2008). Firstly, how behavioural-level regulators, such as environmental enrichment, exercise or hippocampal learning are translated into changes in AHN will be considered, before moving on to describe the regulatory impact of cellular and molecular factors within the neurogenic niche itself.

1.5.3 Behavioural factors

Enriched environment and exercise

Environmental enrichment (EE) and exercise are potent stimulators of AHN, which affect differential phases of the neurogenic process (Olson, Eadie, Ernst, & Christie, 2006). EE is defined as an environment which provides social, motor and sensory stimulation (Aimone et al., 2014). For rodents, this may consist of home cage running wheels, tunnels or huts that increase the complexity of the environment (Aimone et al., 2014). EE has been shown to promote NPC survival (Kempermann, Kuhn, & Gage, 1997) by preventing spontaneous apoptosis of early post-mitotic type 3 cells (Young, Lawlor,

Leone, Dragunow, & During, 1999). In rats, the benefit of EE upon AHN is thought to depend on vascular endothelial growth factor (VEGF) upregulation (Cao et al., 2004), whereas the effect is dependent upon brain-derived neurotrophic factor (BDNF) in mice (Rossi et al., 2006).

In early studies, it was unknown which particular components of EE manipulations contributed to the observed effects on AHN. A study designed to tease apart the underlying constructs of EE showed that voluntary running is a highly salient feature, which has a dissociable effect to that of environmental complexity alone (Van Praag, Kempermann, & Gage, 1999). A dramatic increase in NPC proliferation was observed in mice that engaged in voluntary running (Van Praag et al., 1999). Furthermore, voluntary exercise also increased the dendritic tree length and morphological complexity of newborn neurons (Redila & Christie, 2006). These running mediated effects on AHN have been associated with improved hippocampus dependent cognition and pattern separation (van Praag, Kempermann, & Gage, 1999; Creer et al., 2010), and are thought to depend on VEGF signalling (Fabel et al., 2003). However, insulin-like growth factor 1 (IGF-1) and fibroblast-growth-factor 2 (FGF-2) have also been implicated in exercise-induced increases in AHN (Kempermann, 2015). Moreover, while the extent to which EE and running can individually enhance AHN vary in magnitude, these factors have a synergistic effect when combined (Fabel et al., 2009). Running and EE combined lead to a thirty per cent greater increase in new neurons compared to either stimuli alone (Fabel et al., 2009). Therefore, EE and running have potent pro-neurogenic effects on the adult DG.

Hippocampal learning

The relationship between hippocampal learning and AHN is mutual; not only does increased AHN benefit hippocampal learning, but the act of hippocampal learning also boosts AHN. This bi-directional relationship has proved complex however, and studies have been hindered by the diversity of learning paradigms available (Aimone et al., 2014). It has been reported that the survival of newborn neurons is increased by learning on hippocampus-

dependent, but not hippocampus-independent tasks (Zhao et al., 2008). Furthermore, it is not merely the act of training, but successful acquisition and performance that confers a survival benefit upon immature neurons (Gould, Beylin, Tanapat, Reeves, & Shors, 1999; Sisti, Glass, & Shors, 2007). Interestingly, Dupret et al. (2007) showed that hippocampus-dependent learning increases apoptosis of three-day old immature neurons, and blocking apoptosis during training lead to impaired performance. This suggests that intact hippocampal function requires both the selective survival and elimination of newborn neurons (Dupret et al., 2007; Zhao et al., 2008). In addition, hippocampus-dependent learning also modulates the morphology of the cells that survive. Tronel et al., (2010) reported that newborn neurons showed an accelerated rate of maturation and integration into the hippocampal network after learning, which was dependent on the level of cognitive demand.

Stress

An inherent weakness of a form of plasticity so sensitive to the environment is a vulnerability to negative environmental perturbations. AHN is extremely sensitive to many forms of stress (Aimone et al., 2014) and has been associated with reductions in NPC proliferation in mice (Ferragud et al., 2010) Furthermore, chronic stressors persistently reduce GC number in the DG (Gould & Tanapat, 1999). Decrements in survival and neuronal differentiation have also been reported in response to unpredictable chronic mild stress, a common paradigm for modelling depression (Mineur, Belzung, & Crusio, 2007). These effects are mediated by circulating glucocorticoids in the bloodstream, which have been shown to negatively regulate AHN both *in vivo* (Cameron & Gould, 1994; Gould et al., 1992) and *in vitro* (Fitzsimons et al., 2013). Despite this body of literature, more recent evidence suggests that a baseline level of stress may be important for maintaining normal AHN. Glucocorticoid receptors (GR) are expressed on nearly all cells within the neurogenic niche, and activation may positively regulate AHN at low levels. GR knockdown impaired the migration and differentiation of newborn

neurons, as well as their morphology and functional integration (Fitzsimons et al., 2013).

1.5.4 Activity dependent regulation

Local network activity and GABA

Local network activity signals changes in the external environment, such as those discussed, to NPCs within the neurogenic niche. Factors such as neurotransmitters and neuropeptides mediate this link. The major inhibitory neurotransmitter in the adult brain, amino acid γ-Aminobutyric acid (GABA), plays a pivotal role in activity-dependent regulation of AHN (Ge, Pradhan, Ming, & Song, 2007a). GABA receptors are found at the earliest stage of the neurogenic lineage, on type 1 radial glia-like cells (Song, Olsen, Sun, Ming, & Song, 2016). These cells are also responsive to tonic GABA signals, diffused from local parvalbumin interneurons. Song et al (2016) demonstrated that interneuron activity and levels of tonic GABA dictated whether type 1 cells adopted a quiescent or self-renewal (i.e., symmetric division) mode.

With increasing differentiation, NPCs begin to receive more direct GABAergic inputs, and activation proceeds from tonic to phasic at the type 2b/3 stage (Tozuka, Fukuda, Namba, Seki, & Hisatsune, 2005; Wadiche, Bromberg, Bensen, & Westbrook, 2005). As in the developing brain, GABA is depolarizing for NPCs and immature neurons, and promotes calcium influx. This excitation of NPCs favours neuron production via upregulation of pro-neuronal genes including NeuroD1, and suppression of glial fate genes (Deisseroth et al., 2004). Post-neuronal lineage commitment, depolarizing GABA is essential for normal maturation. In the absence of depolarizing GABA, immature neurons show delayed synapse formation and defective dendritic development (Ge et al., 2005; Chancey et al., 2013). GABA remains excitatory until immature neurons begin to develop their own glutamatergic phenotype, and make substantial contact with the surrounding circuitry

(Kempermann, 2015). Therefore, GABA is a key mediator in the activity dependent regulation of AHN.

Seizures

AHN is also regulated by aberrant circuit activity such as seizures. mTLE is characterised by recurrent seizures originating within the hippocampus, and this condition has a devastating effect on AHN. Experimental models have consistently shown that acute seizures cause an initial, transitory surge in neurogenesis (Bengzon et al., 1997; Gray & Sundstrom, 1998; Jessberger, Römer, Babu, & Kempermann, 2005; Parent et al., 1997). Otherwise quiescent type 1 radial-glia like cells are activated by seizures (Huttmann et al., 2003; Lugert et al., 2010; Walker et al., 2008), consistent with the demonstration of activity-dependent type 1 cell activation by Song et al. (2012). Recent work has shown that neuronal hyper-activation leading to sustained seizures caused type 1 cells to divide symmetrically, with both mother and daughter cells converting into reactive astrocytes (Sierra et al., 2015). This increased activation and symmetric division lead to exhaustion of the hippocampal stem cell pool and declined levels of AHN (Sierra et al., 2015). This is in line with the severe decline in AHN that is observed in chronic mTLE (Hattiangady, Rao, & Shetty, 2004). In addition, seizures cause abnormal migration of DCX[+] progenitors (Jessberger et al., 2007) and accelerated dendritic development and synaptic integration (Overstreet-Wadiche, Bromberg, Bensen, & Westbrook, 2006), which may be due to seizure induced increases in GABA (Ge, Pradhan, Ming, & Song, 2007b). This mechanism may contribute to the hallmark pathology seen in mTLE; dispersion of the GCL and mossy fibre sprouting (Jerome Engel, 2001). Chronic seizures thus have a deleterious regulatory effect upon many aspects of AHN.

1.5.5 Regulation by the neurogenic niche

The environment in which NPCs are situated largely defines the process of AHN. The neurogenic niche hosts a diverse population of cells, including NPCs, interneurons, mature astrocytes, endothelial cells and microglia (Riquelme et al., 2008; see Figure 1.5). Within the niche, both cell-cell contact, secreted factors and the surrounding cytoarchitechture play important regulatory roles (Aimone et al., 2014).

Local interneurons

Many classes of interneurons reside within the niche, and are in a prime position to regulate AHN (Masiulis et al., 2011). Not only do they sit in close proximity to the SGZ, but they also have highly complex dendritic and axonal projections which may be able to regulate neurogenesis based on activity in downstream regions such as CA1 or CA3 (Masiulis et al., 2011). Most DG interneurons are GABAergic, and the critical role of these cells is clear from the previous discussion of GABAergic mediated activity-dependent regulation by hilar interneurons (Tozuka et al., 2005).

It has also been shown that the neurotrophic factor BDNF promotes neuronal differentiation and maturation of NPCs via GABAergic signalling. BDNF mRNA is present in the dendrites of mature GCs, and GABAergic interneurons host the BDNF receptor, TrkB (Waterhouse et al., 2012). Knockdown of either BDNF expression in GCs or TrkB on interneurons lead to impaired GABA release, increased NPC proliferation and reduced neuronal differentiation, suggesting that BDNF enhances GABA release from interneurons to control neuronal lineage commitment (Waterhouse et al., 2012).

While GABAergic signalling has received most attention, these populations of interneurons also release other factors that modulate neurogenesis, such as stromal cell-derived factor 1 (SDF-1). The expression of this chemokine colocalises with GABA-containing synapses in basket cell terminals (Bhattacharyya et al., 2008). Early stage NPCs also express the receptor for

SDF-1, CXCR4 (Tran, Banisadr, Ren, Chenn, & Miller, 2007), meaning that SDF-1/CXCR4 signalling provides a direct route via which interneurons may regulate AHN (Masiulis et al., 2011). Indeed, it has been shown that GABAergic inputs on type 2 cells are enhanced by concomitant GABA/SDF-1 release from DG interneurons (Bhattacharyya et al., 2008), suggesting that this pathway may sensitize NPCs to activity-dependent regulation. Interneurons can also co-release peptide neurotransmitters (referred to as neuropeptides) that regulate AHN under certain firing conditions; vasoactive intestinal peptide (VIP) has been shown to promote the survival of proliferating type 2 NPCs (Zaben et al., 2009) whereas neuropeptide Y (NPY) promotes NPC proliferation (Howell et al., 2005; 2003) and also augments the action of FGF-2 (Rodrigo et al., 2010). Interestingly, these interneuron populations are lost in the chronically epileptic hippocampus, which may contribute to aberrant neurogenesis (Cunningham et al., 2014).

Astrocytes

Traditionally viewed as mere support cells within the CNS, astrocytes have now emerged as key mediators of many processes within the brain, including AHN (Riquelme et al., 2008). The relationship between NPCs and niche astrocytes is heavily dependent on their phenotype, which shows heterogeneity in terms of morphology and molecular expression profile (Fukuda et al., 2003). In addition to the type 1 radial glia which constitute the stem cells of the adult DG, nestin⁻ S100β⁺ 'horizontal' astrocytes are present, which send basal processes beneath the GCL (Kronenberg et al., 2003; see Figure 1.5). There is a close spatial relationship between NPCs and mature astrocytes, and astrocytes have been shown to make direct contact with NPCs, often surrounding the precursors in a 'cradle' or basket with their processes (Plümpe et al., 2006; Shapiro et al., 2005).

In culture, soluble factors derived from astrocytes strongly induced neuronal differentiation in hippocampal NPCs (Song, Stevens, & Gage, 2002). Key molecules that may mediate astrocytic effects upon NPC lineage determination include cytokines IL-6 and IL-1β, in combination with other
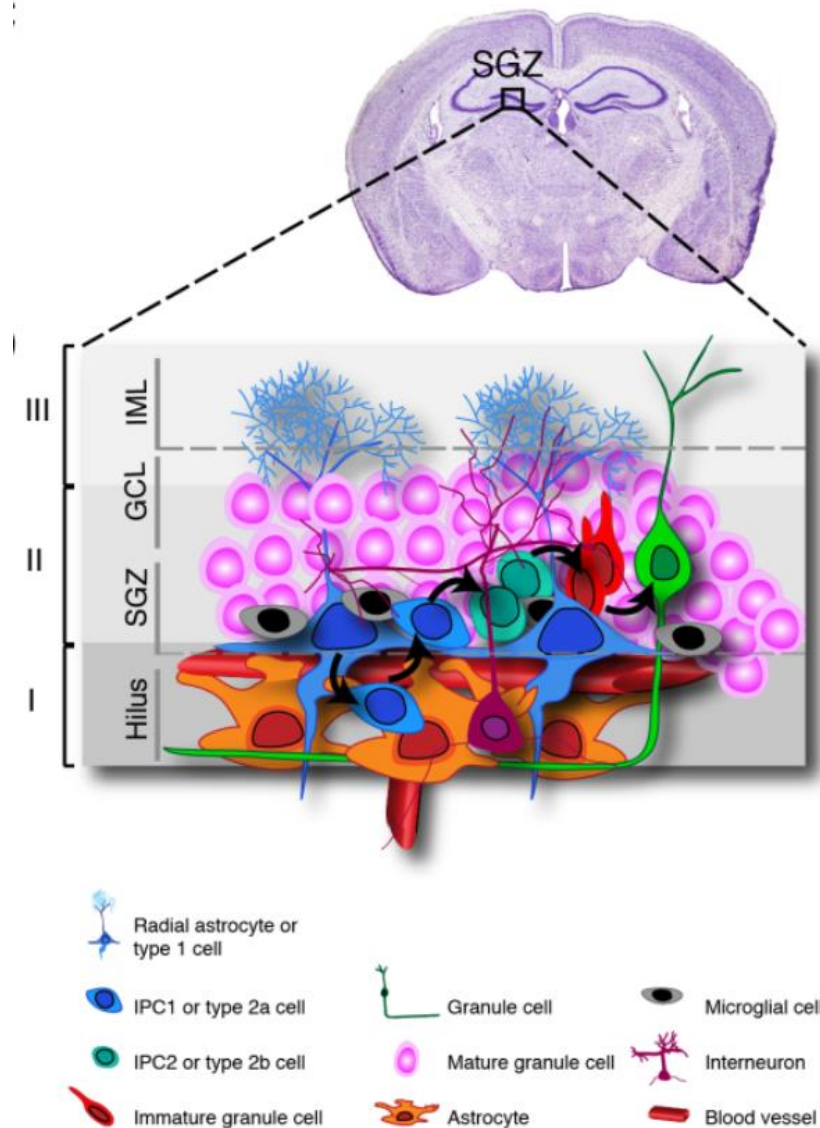
Figure 1.5 Constituents of the neurogenic niche. SGZ= subgranular zone. GCL= Granule cell layer. IMI= inner molecular layer. Image sourced from Bonafanti (2013).

astrocyte-secreted factors (Barkho et al., 2006) such as Wnt3a (Lie et al., 2005) and FGF-2 (Song et al., 2002). The latter is a highly potent modulator of stem cells, and *fgfr1* knockout animals show decreased NPC proliferation and neuronal differentiation (Zhao et al., 2007). Astrocytes are also a potential source of immune factors which may regulate AHN (Leiter et al., 2016). Moreover, astrocytes also influence the maturation of newly born neurons. Sultan et al. (2015) showed that direct contact between dendritic segments of newborn neurons and astrocytes was required for normal

dendritic maturation and spine formation. These effects were dependent on astrocytic D-serine release (Sultan et al., 2015). Astrocytes therefore play a pivotal role in regulating and guiding the many developmental stages of AHN.

Vasculature

Local vasculature presents an abundant supply of extrinsic factors for the regulation of AHN (Palmer, Willhoite, & Gage, 2000). There is a close physical connection between AHN and vasculature, as type 1 cells have been observed to wrap their end feed around blood vessels within the SGZ (see Figure 1.5; Filippov et al., 2003). Indeed, the SGZ is in close proximity to blood vessels, near which clusters consisting of proliferating endothelial precursor cells and NPCs have been reported (Palmer et al., 2000). This has led to the view that the DG niche supports not only neurogenesis, but also angiogenesis, and the two processes are highly interdependent (Riquelme et al., 2008). Both neurogenesis and angiogenesis may be jointly regulated by VEGF (Jin et al., 2002), in addition to other factors arriving in the niche via blood vessels including hormones, paracrine factors and cytokines from remote sources (Riquelme et al., 2008). Furthermore endothelial cells may themselves secrete factors that modulate neurogenesis, including BDNF (Leventhal, Rafii, Rafii, Shahar, & Goldman, 1999).

Microglia

Microglia are CNS resident macrophages, and the main immune effector cell in the brain (Gonzalez-Perez et al., 2012). Although they are of myeloid origin and share features with peripheral macrophages, they instead derive from the yolk-sac and migrate to the neural tube (Ginhoux, Lim, Hoeffel, Low, & Huber, 2013). They colonize the CNS during embryonic development, and it is now known that they dictate vital homeostatic and developmental roles from there on (Bilimoria & Stevens, 2015; Hughes, 2012; Ferrini & De Koninck, 2013). Microglia are also key mediators of AHN (Ekdahl, 2012) and are found within the hilus and distributed along the border of the GCL (see Figure 1.5; Wirenfeldt, Dalmau, & Finsen, 2003). Microglia are ideally suited to regulate neurogenesis due to their constant surveillance of the

surrounding parenchyma (Nimmerjahn et al., 2005) and their ability to sculpt and modulate local circuitry in interaction with the immune system, growth factors and neuronal activity (Schafer et al., 2012; Waterhouse et al., 2012; Zhang et al., 2014a).

The role of microglia in regulating AHN is complex, as both pro and anti-neurogenic effects have been described. These varying effects likely depend partly on their activation state, which too varies based on the surrounding context (Ransohoff, 2016). Under physiological conditions, or when in a resting state, microglia have a delicate morphology with branched processes (see Figure 1.6A). Alternatively, in the face of infection or damage-associated molecular patterns (DAMPs) microglia show enlarged cell bodies, short stubby processes and can appear phagocytic (see Figure 1.6B; Ransohoff & Perry, 2009). This former morphology has been deemed 'activated', although there is considerable debate in the literature as to whether resting and activated can be equated with anti-inflammatory and pro-inflammatory functions (Ransohoff, 2016). Instead, microglial activation seems to be a dynamic and complex process, the precise function of which depends on unique properties of the activating agent and the context within which it is encountered (Ransohoff & Perry, 2009).
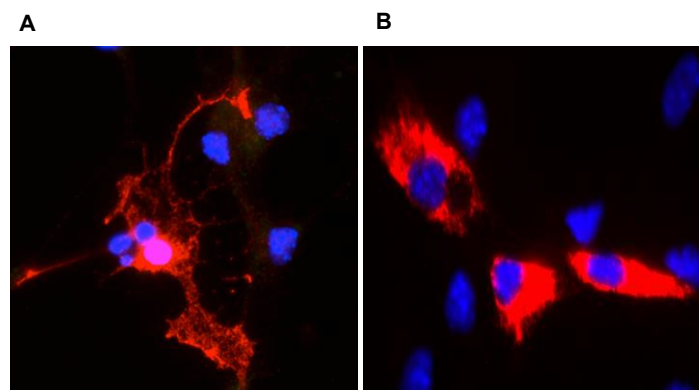
Figure 1.6 Microglial phenotypes. Image shows microglia isolated from postnatal murine hippocampus stained with ionized calcium-binding adapter molecule 1 (Iba-1; red). **A)** Typical 'resting' microglia showing ramified morphology. **B)** Activated microglia showing amoeboid morphology characteristic of activation.

Studies have indicated that in their resting state, microglia are beneficial to AHN. Disruption of the microglial fractalkine receptor CX_3CR1, which is essential for resting-state maintenance (Cardona et al., 2006), is associated with impaired proliferation and survival of NPCs *in vivo* (Bachstetter et al., 2011)*.* Furthermore, the phagocytosis of apoptotic newborn neurons by resting microglia in the SGZ is a critical regulatory mechanism preventing overexpansion of the NPC pool (Sierra et al., 2010). Microglia also release soluble factors that promote AHN. *In vitro,* microglia have been shown to promote NSC survival and proliferation via release the cytokine transforming growth factor beta (TGFβ; Battista et al., 2006). Furthermore, neuropeptide VIP stimulates microglial release of IL-4 via the VPAC1 receptor, which directly promotes proliferation and survival of NPCs (Nunan et al., 2014). Moreover, microglia can also exert pro-neurogenic effects in an activated state. *In vitro,* microglia activated by T-helper cell associated cytokines IL-4 or IFN-γ potently induced neurogenesis (Butovsky et al., 2006).

Conversely, certain forms of activation seem to be anti-neurogenic. Microglia activated by lipopolysaccharide (LPS), a component of bacterial cell walls, have been shown to dramatically impair the survival of newly born neurons in the adult DG, which is rescued by inflammatory blockade (Ekdahl, Claasen, Bonde, Kokaia, & Lindvall, 2003; Monje, Toda, & Palmer, 2003). Similarly, both Butovsky et al. (2006) and Cacci, et al. (2008) reported that microglia with a pro-inflammatory activation phenotype were detrimental to neurogenesis *in vitro*. Therefore, the relationship between microglial activation and AHN is complex, and likely dependent on the balance of pro and anti-inflammatory molecules secreted by these cells (Battista et al., 2006). Nonetheless, microglia are a central player in the neuroimmune regulation of AHN, which will now be considered in more depth.

1.5.6 Neuroimmune regulation of AHN

The aforementioned role of resting microglia in regulating AHN demonstrates how our understanding of immune function within the brain has changed within the last decade. Firstly, the notion of the CNS being 'immune-privileged' is rapidly fading, and it is now acknowledged that the brain has its own unique form of immunity, and that crosstalk with peripheral immunity also occurs (Leiter et al., 2016). Furthermore, it is becoming appreciated that inflammation is not always harmful in the brain, but inflammatory mediators can also protect and oversee homeostasis. However, far less is known about these 'non-immune' properties in physiological conditions than is known about inflammatory activities in pathological contexts (Leiter et al., 2016).

Some forms of inflammation are thought to be suppressive of AHN (Ekdahl et al., 2003; Monje et al. 2003). LPS-induced inflammation also induces morphological changes in adult born GCs, characterised by formation of multiple apical dendrites and reduced distal branching (see Figure 1.7; Llorens-Martín et al., 2014), and influences their functional integration (Jakubs et al., 2008). With the exception of microglia, relatively little is known of the cell types that mediate the immune effects upon AHN however. It has been noted that immune-deficient severe combined immunodeficiency (SCID) mice, which lack functional T cells and B cells (Bosma & Carroll, 1991) have decreased levels of AHN (Ziv et al., 2006). This phenotype was rescued by injection of T cells (Ziv et al., 2006), suggesting a pro-neurogenic effect of this cell type. This effect was found to be facilitated by CD4^{+} T cells mediated microglial activation, which promoted neurogenesis via microglial release of soluble cytokines and growth factors, which in turn augmented BDNF levels within the brain (Ziv et al., 2006). In our laboratory, we have additionally demonstrated that the neuropeptide VIP acts upon T cells to stimulate IL-4 production, which exerts both direct and indirect effects on NPCs via microglial BDNF release (Khan, 2014; PhD thesis). These mechanisms specifically increase NPC proliferation *in vitro.* Furthermore, mast cells are

Control   Neuroinflammation
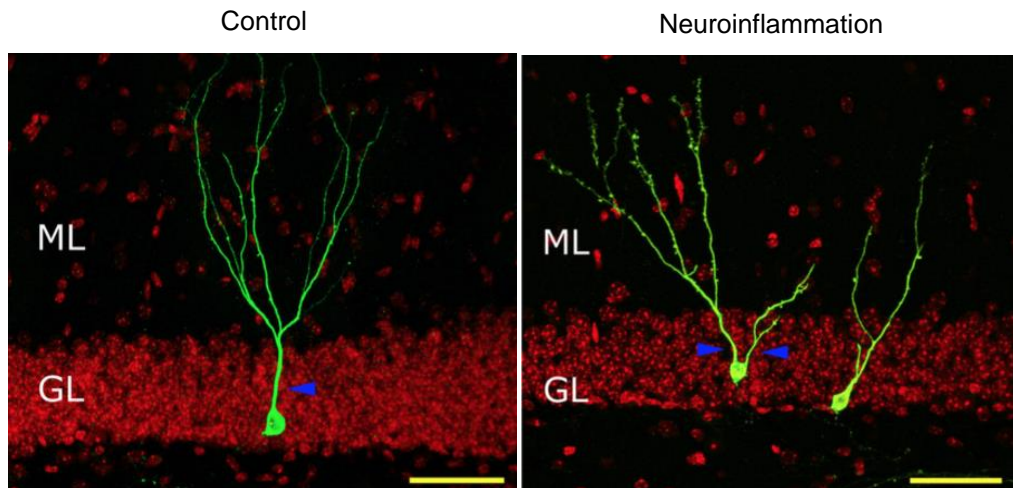
Figure 1.7 Neuroinflammation alters the morphology of adult born granule cells. Scale bars = 50 μm. ML= Molecular layer. GL= Granule cell layer. Image adapted from Llorens-Martín et al. (2016).

present within the brain and are a significant source of serotonin (Nautiyal et al., 2012). Mice deficient in these cells showed impaired AHN and hippocampal learning deficits, which were restored by the selective serotonin reuptake inhibitor fluoxetine (Nautiyal et al., 2012). Currently it is unknown whether other immune cells, including B cells, natural killer cells and dendritic cells, participate in regulation of AHN (Leiter et al., 2016).

More is known of immune molecules secreted by the aforementioned cells, in addition to microglia and astrocytes. Cytokines are the chemical messengers of the immune system and are produced by microglia as part of the innate immune response (Hanisch, 2002). Traditionally, pro-inflammatory cytokine secretion was thought to be restricted to pathological contexts, but evidence now indicates production under basal conditions (Leiter et al., 2016). Tumor necrosis factor (TNF-α) signalling via its TNFR1 is anti-neurogenic, whereas signalling via TNFR2 is pro-neurogenic (Widera, Mikenberg, Elvers, Kaltschmidt, & Kaltschmidt, 2006). Interleukin 1 beta (IL-1β) is also able to suppress NPC proliferation via the nuclear factor-κB pathway (NFκB; Koo & Duman, 2008). Furthermore, the previously discussed chemokine SDF-1 can also promote or inhibit NPC migration *in vitro*, in a concentration dependent

manner (Shinjyo, Ståhlberg, Dragunow, Pekny, & Pekna, 2009). This effect was found to dependent on the complement anaphylatoxin, C3a (Shinjyo et al., 2009).

Complement is a critical branch of the immune system which bridges the gap between innate and adaptive immunity (Morgan & Gasque, 1996). As shown in Figure 1.8, complement communicates with multiple immune cells that regulate AHN, including T cells, mast cells, macrophages, and is able to orchestrate their activity to shape immune reactions (Ricklin & Lambris, 2007). Complement has been implicated as an important regulator of both *in vitro* NPCs (Shinjyo et al., 2009) and *in vivo* AHN (Moriyama et al., 2011; Rahpeymai et al., 2006) and is the focus of this thesis. Furthermore, due to the involvement of complement activation in mTLE (Aronica et al., 2007; Vezzani, 2008), improving our understanding of the role of this system in regulating AHN in the healthy brain is integral. Therefore, the structure and function of the complement system will next be discussed.

1.6   Overview of the complement system

While diverse in function, the fundamental role of complement is immune 'surveillance and defence', and the rapid elimination of invading pathogens (see Figure 1.8; Klos et al., 2009; Ricklin, Hajishengallis, Yang, & Lambris, 2010). Estimated to be approximately 600-700 million years old, complement is an ancient defence mechanism, the evolution of which preceded that of adaptive immunity (Sunyer, Zarkadis, & Lambris, 1998). Indeed, there is a high degree of phylogenetic conservation among mammals and invertebrates (Beek, Elward, & Gasque, 2003; Ricklin et al., 2010). First described in 1891 by German bacteriologist Hans Buchner, it was identified as a heat-sensitive factor that 'complemented' the effects of antibody mediated immunity in the lysis of bacteria in serum (Carroll, 2004). It is now known that complement serves to detect and tag invading pathogens for rapid destruction via phagocytosis and cytolysis, whilst protecting host cells

(Beek et al., 2003). Complement activation has also been thought to exacerbate inflammation in areas of injury through the activity of the analphylatoxins (Beek et al., 2003)
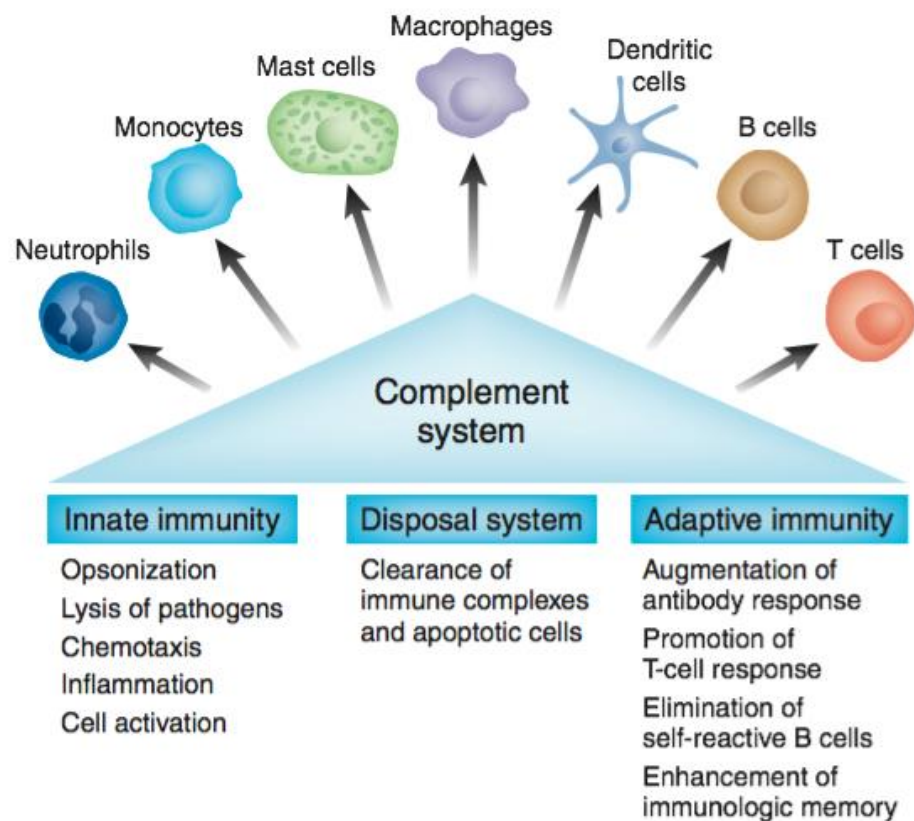
Figure 1.8 Complement system interactions and broad functions. Complement activates cells involved in both innate and adaptive immunity, and triggers a variety of immune activities. Complement also contributes to maintenance of homeostasis via disposal of cellular debris. Image sourced from Ricklin & Lambris, (2007)

For many years, the scientific community recognised little more than the aforementioned pathogen-clearance and inflammatory functions of complement. However, a paradigm shift has occurred within the last two decades (Mastellos, 2014) and an unexpected role for the complement system in non-immune, homeostatic functions has emerged within the CNS. This shift originated with reports of a complement protein expression, receptors and regulators within the CNS. Since the liver synthesizes ninety

per cent of complement components in plasma (Barnum, 1995), and the blood brain barrier prohibits their entry into the CNS, apparent extrahepatic production of complement proteins stimulated great research interest. Initially, questions were raised as to whether to blood brain barrier infiltration was responsible (Pasinetti, Johnson & Rozovsky, 1992), although in situ hybridization studies confirmed the phenomenon of CNS synthesized complement factors (Shen, Li, McGeer, & McGeer, 1997; Beek et al., 2003; Veerhuis, Nielsen, & Tenner et al., 1999). It is now known that the entire complement system is produced and operates within the brain (Davoust, Jones, Stahel, Ames, & Barnum, 1999; Nataf, Stahel, Davoust, & Barnum, 1999).

1.6.1 Structure and function of the complement cascade

The complement system consists of approximately thirty fluid-phase and membrane-associated proteins (Beek et al., 2003), including receptors, initiator molecules, inhibitors and regulators, which altogether account for approximately 4% of total blood proteins (Orsini, De Blasio, Zangari, Zanier, & De Simoni, 2014). Fluid-phase complement proteins are technically zymogens, since they circulate in an inactive state and are activated upon a proteolytic reaction whereby the zymogen is cleaved into smaller, active peptide fragments. These peptides then cleave downstream complement zymogens, thereby propagating the cascade of activation in a sequential manner (Orsini et al., 2014). Activation is also greatly amplified with each sequential reaction, generating many thousands of molecules (Beek et al., 2003).

As shown in Figure 1.9, the system consists of four 'recognition systems'; the classical pathway, the alternative pathway, the lectin pathway and the more recently identified extrinsic pathway (Huber-Lang et al., 2006). Each pathway is initiated by different stimuli, which can be either exogenous or endogenous danger signals, referred to as DAMPS or pathogen-associated

molecular patterns (PAMPS; Orsini et al., 2014). Despite these diverging initiators, all pathways converge on a single molecule, complement component 3 (C3), after which activation proceeds via a single terminal pathway.

C3 is a 185kDa plasma protein, possessing 13 domains; 8 of which are macroglobulin domains (Nilsson and Eldahl, 2012). Two polypeptide chains, the α-chain and β-chain, compose the C3 molecule, and these chains are linked by a disulphide bond and by non-covalent forces (Pekna, Hietala, Rosklint, Betsholtz, & Pekny, 1998). With the exception of the extrinsic pathway, activation of each complement pathway leads to the formation of the C3 convertase complex. This complex is able to cleave the central molecule of the complement system, C3. It is through C3 convertase mediated C3 cleavage that the main effectors of the complement system are generated, including the inflammatory anaphylatoxin C3a and the opsonin C3b. C3a can also be further cleaved, leading to formation of the C3a des Arg molecule (Janeway, Travers, Walport & Schlomchik, 2001). Similarly, many molecules of C3b are subject to further breakdown; stepwise-degradation occurs leading to formation of smaller fragments, including iC3b, C3c, C3dg and C3d (Janeway et al., 2001). When deposited on surfaces of pathogens or damaged host cells, intact C3b serves to attract phagocytic macrophages, a process known as opsonisation (Mastellos, 2014). Unbound C3b molecules can also associate with other complement molecules to form a C5 convertase complex. C5 is then cleaved in a similar manner to C3, thereby generating cleavage fragments C5a and C5b. This cascade of activation ultimately leads to assembly of the terminal complement effector; the membrane attack complex (MAC; see Figure 1.9; Cole & Morgan, 2003). Aggregation of MAC molecules on a target cell or pathogen creates pores in the cell membrane, leading to death by osmotic cell lysis (Cole and Morgan, 2003).
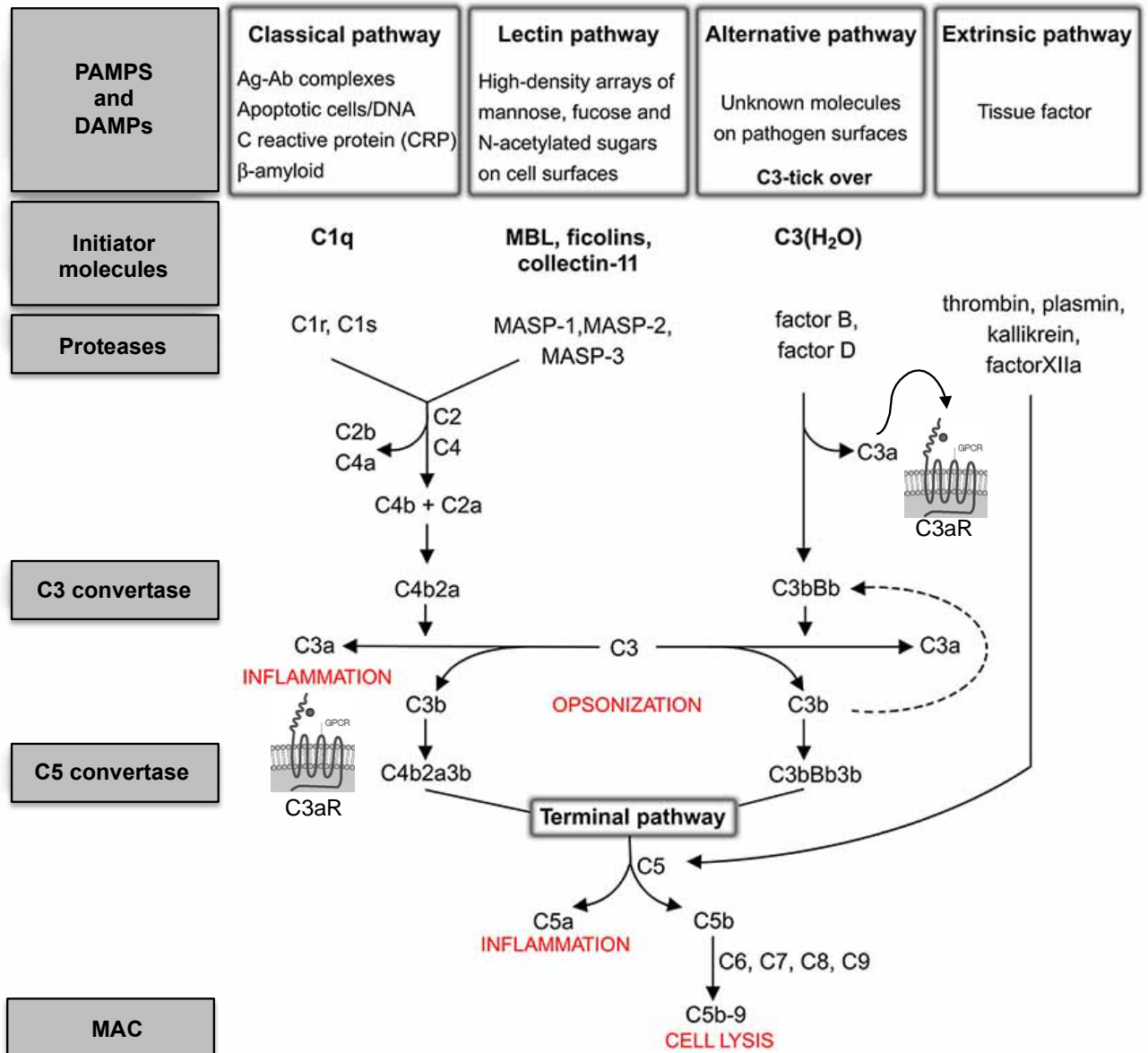
Figure 1.9 Structure of the complement system. The complement system is composed of four recognition pathways that are triggered by various stimuli associated with pathogens or host-damage. Classical, lectin and alternative pathway activation converge on the central C3 molecule, which is cleaved into fragments C3b and C3a. C3a is anaphylatoxin capable of both pro and anti-inflammatory activities, and signals via C3aR. C3b triggers opsonisation of bacterial or pathogens by macrophage phagocytosis. C3b also forms part of the C5 convertase molecule, which cleaves C5. This leads to terminal pathway activation (via C6, C7, C8 and C9) leading to assembly of the membrane attack complex (MAC; also know as C5b-9), which eliminates pathogens by cell lysis. Image adapted from Orsini et al., (2014).

1.6.2 Complement activation pathways and regulation

The complement pathways differ in their modes of activation, and consequently complement is well suited to recognize and respond to a diverse array of pathogenic and self-damage signals (Ricklin et al., 2010). There is also some evidence for spontaneous activation of the complement system.

Initiation of both the classical and lectin pathways is dependent upon recognition of specific PAMPS (see Figure 1.9). Activation of the classical pathway (consisting of C1q, C1r, C1s, C4, C2 and C3) is triggered by detection of antibody-antigen complexes by the initiator molecule of the classical pathway, C1q (Beek et al., 2003). C1q is then able to activate C1r and C1s, which cleave C4 and C2 to form the C3 convertase, C4b2a. The classical pathway is also activated by non-immune molecules, including nucleic acids, or by apoptotic or necrotic host cells (Ricklin and Lambris 2007, Gasque, 2004). C3 convertase then cleaves C3 into two fragments; C3b and C3a. The lectin pathway is initiated by the recognition of carbohydrates such as mannose upon pathogen surfaces by mannin-binding lectin (MBL), a molecule homologous to C1q of the classical pathway (Beek et al., 2003). Upon successful pattern recognition, MBL activates two serine proteases, MASP-1 and MASP-2, which then act to cleave classical pathway components C4 and C2 (Figure 1.9). Activation then proceeds in the same manner as the classical pathway, eventually leading to generation of C4b2a convertase and C3 cleavage (Beek et al., 2003).

The alternative pathway is the phylogenetically oldest pathway, and it differs from the classical and lectin pathways in that it does not require pathogen recognition to initiate activation (Beek et al., 2003). Rather, a continuous state of low level alternative pathway activation occurs, termed C3 tickover. This activation mode may account for the presence of C3a and C3b in the absence of inflammation, and thus is likely to underlie complement regulation of homeostatic processes. In this process, the internal thioester

bond of circulating C3 molecules is hydrolysed due to nucleophillic attack by H_2O. This process occurs at a slow yet constant rate, leading to the formation of $C3(H_2O)$ (Zipfel 2001). After a series of interactions with C3b and regulatory molecules (Factor B and Factor D), the alternative pathway C3 convertase is formed, $C3b(H_2O)Bb$ (Zipfel, 2001). This C3 convertase molecule can then cleave C3 molecules into C3b and C3a, as per the classical and lectin pathways (Nilsson and Ekdahl, 2012). This mechanism also serves as an 'amplification loop' whereby activation is greatly augmented (Ricklin et al., 2010). A similar 'C1-tickover' mechanism analogous to C3 tickover has also been described, suggesting there is also continual low-level activation of the classical pathway (Manderson, Pickering, Botto, Walport, & Parish, 2001).

While these mechanisms constitute the traditional activation pathways, our understanding of complement is far from complete. New activation mechanisms have been discovered within the last decade, and it is feasible that more will be unearthed (Ricklin & Lambris, 2007). For example, lectin pathway serine protease MASP-2 is capable of directly cleaving C3 molecules in a manner than bypasses the requirement for C3 convertase (termed 'C2 bypass pathway'; Daha, Kooten and Roos, 2006). Moreover, the serine protease thrombin is a key player in what is now recognized as the 'extrinsic' complement pathway, which possesses the capacity for direct cleavage of C3 and C5 (Huber-Lang et al., 2006).

Since complement is activation is rapidly propagated, should activity occur on host cells in an uncontrolled manner, there is potential for extensive self-damage (Gasque, 2004). Due to this capacity for self-harm, complement activation, both pathogen-induced and spontaneous, is tightly controlled by a sophisticated system of regulatory molecules that work to fine-tune the effects of complement activation (Alexander, Anderson, Barnum, Stevens, & Tenner, 2008). Regulation occurs primarily at the level of the convertase enzymes and the MAC, but mechanisms also exist for halting complement activation at multiple stages throughout the activation cascade. Several fluid-

phase and membrane bound regulatory proteins are responsible for these functions (Cole & Morgan, 2003).

1.6.3 Complement anaphylatoxins

Cleavage of C3 and C5 results in the production of the complement anaphylatoxins, C3a and C5a. The small polypeptides (77 and 74 amino acids, respectively) possess the most potent inflammatory effects of the complement cascade (Klos et al., 2009), although recent evidence suggests that they may induce anti-inflammatory, neuroprotective effects under some circumstances (Coulthard & Woodruff, 2015; Gavrilyuk, Kalinin, & Hilbush, 2005). The anaphylatoxins target a wide range of cells, both immune and non-immune (Klos et al., 2009). In the periphery, C5a and C3a exert highly pleiotropic effects including increasing vascular permeability, anaphylaxis, recruitment of macrophages, and chemotaxis, amongst others (Ricklin et al., 2010). Anaphylatoxin function within the brain is a relatively new concept, but it is known that they participate in cerebellar development and provide protection from neurotoxicity (Benard et al., 2008).

The effects of anaphylatoxins are exerted within the picomolar to nanomolar range (Beek et al., 2003), in close proximity to cells bearing the relevant receptors. The canonical receptor for C3a is complement C3a receptor 1 (C3aR), whereas C5a binds to both complement C5a receptor 1 (C5aR) and C5L2 (Mastellos, 2014). These high affinity receptors are members of the rhodopsin family of several transmembrane G-protein coupled receptors, with the exception of C5L2, which is structurally homologous to C5aR, but is not G-protein coupled (Hawksworth, Coulthard, Taylor, Wolvetang, & Woodruff, 2014). C5L2 was long thought to be a decoy receptor, although evidence now suggests functionality (Kalant et al., 2005; Scola, Johswich, Morgan, Klos, & Monk, 2009). The intracellular signals transduced by C3a/C3aR binding include PI3k/Akt and the mitogen activated protein kinase (MAPK) pathway, and C3a binding is known to elevate intracellular Ca^{2+}

concentration (Sayah et al., 2003; Bohanakashtan, 2004; Jacob, Bao, Brorson, Quigg, & Alexander, 2010).   Due to the aforementioned role of C3 in regulating AHN, this thesis will focus on C3aR signalling as opposed to C5aR/C5L2, the former of which is not thought to participate in AHN (Rahpeymai et al., 2006; note that C5L2 has not been investigated with regard to AHN).

Until recently, C3a was thought to signal solely through its canonical receptor C3aR, and C3a was thought to be the lone ligand for C3aR.   However, additional factors that intersect the C3a/C3aR axis are emerging (Coulthard & Woodruff, 2015). Strong and specific binding occurs between C3a and the receptor for advanced glycosylation end-products (RAGE), although the functional consequences of this are unknown (Ruan et al., 2010). C3a can also synergize with CpG oligonucleotide complexes to enhance IFN-α release from other immune cells (Ruan et al., 2010). There have also been controversial reports of C3a binding to C5L2 (Chen et al., 2007). With regard to C3aR, it has recently been shown that a breakdown product of the VGF neuropeptide is able to bind to C3aR upon conformational change of the receptor (Hannedouche et al., 2013).

1.6.4 C3 and C3aR knockout mouse models

Originally developed by Michael C. Carroll of the Immune Disease Institute at Harvard Medical School, and first reported by Wessels et al. in 1995, homozygous C3 deficient mice are a valuable tool for studying complement function.   These mice lack a functional C3 molecule, but possess intact complement components situated both upstream and downstream of C3 that are encoded by other regions of the genome (e.g., C1q, C2, C4, C5, C6, C7, C8 C9). Thus, while these animals can activate the classical and lectin pathways up to the stage of C3 convertase formation, activation is unable to proceed beyond this point due to the lack of C3. Therefore, C3 cleavage products C3a and C3b are absent in C3$^{-/-}$ mice. Furthermore, since C3b is required for the

assembly of the C5 convertase, C5 cannot be cleaved and thus C5b and C5a are also absent. This also means that the terminal pathway, leading to MAC assemblage, cannot occur. Moreover, due to the lack of a functional C3 molecule and its subsequent breakdown products, C3$^{-/-}$ mice also lack the alternative pathway, since this relies on the continuous low-level activation of C3. The phenotype of these mice is characterised by increased susceptibility to a range of pathogens and altered immune responses (Wessels et al. 1995). The C3$^{-/-}$ mouse therefore provides a model in which the main inflammatory, opsonisation and lytic properties of complement are absent. Further details of the genetic mutation are provided in Chapter 2, Section 2.2.3.

In addition, homozygous mice deficient in the C3aR receptor have been developed by Professor Craig Gerard of Boston Children's Hospital, USA, and were initially reported by Humbles et al. in 2000. These animals have fully functional complement activity with the exception of C3a/C3aR mediated functions. The phenotype of these animals in terms of vulnerability to infection is not as severe as C3$^{-/-}$ mice, although C3aR$^{-/-}$ strains do show altered secretion of some cytokines and protection from allergies (Humbles et al. 2000). Further details of the genetic mutation are provided in Chapter 2, Section 2.2.4. Combined with the C3$^{-/-}$ model, these strains can provide valuable insights into the functions attributable to C3/C3aR signalling.

1.7   Complement in the brain

There exists a baseline level of most complement components within cerebrospinal fluid (Morgan & Gasque, 1996), albeit at low levels compared to those seen in pathological conditions. As such, it has been proposed that physiological levels of complement contribute to non-immune processes, whereas pathogen invasion or injury is associated with rapidly elevated complement synthesis by neural cells (Beek et al., 2003; Woodruff, Ager, Tenner, Noakes, & Taylor, 2010). The specific cellular sources of complement

in the CNS has been elucidated over the past twenty years, though our knowledge remains far from complete (Stevens, 2008). Furthermore, complement receptor expression is abundant in the brain (Rutkowski et al., 2010). Ames et al. (1996) reported mRNA expression for the anaphylatoxin receptors C3aR and C5aR throughout the CNS, including the hippocampus. Evidence of constitutive expression by neural cells again substantiates the capability for complement to participate in homeostatic functions in the CNS (Mastellos, 2014).

1.7.1 Complement expression by glia

Complement proteins

Early reports implicated astrocytes as the primary immuno-competent cell phenotype capable of expressing complement proteins, with Lévi-Strauss & Mallat (1987) demonstrating release of C3 by rodent astrocytes *in vitro*. Later reports suggested that astrocytes are capable of producing a complete and functional complement system (Gasque, Fontaine, & Morgan, 1995b). C3 reactive-glia have also been reported within the healthy rat hippocampus (Morita et al., 2006). Data has now extended these observations to oligodendrocytes and microglia (Beek et al., 2003; Veerhuis et al., 2011). A recently published transcriptome database generated by RNA sequencing of purified cell populations from the postnatal mouse brain indicates that microglia are the principal cell type to express complement proteins, regulators and receptors (Zhang et al., 2014b). The purpose of complement synthesis in microglia appears to be largely related to phagocytosis (Stephan, Barres, & Stevens, 2012a). Furthermore, C3a can induce microglial 'priming', which encourages microglial activation and pro-inflammatory molecule expression (Ramaglia et al., 2012)

Complement receptors

Microglia express a variety of complement receptors, including C3aR and CR2 (Veerhuis et al., 2011; Zabel & Kirsch, 2013; Davoust et al., 1999).

Importantly, microglia are the only neural cell type to express complement receptor 3 (CR3, also known as CD11b; Stephan, Barres, & Stevens, 2012b). A variety of responses ensue upon microglial CR3 binding, from induction of phagocytosis and pro-inflammatory cytokine release (Zabel & Kirsch, 2013) to synapse remodelling (Stevens et al., 2007). Astrocytes similarly possess many complement receptors, including C3aR (Davoust et al., 1999; Gasque, Chan, Fontaine, Ischenko, et al., 1995a; Gavrilyuk et al., 2005; Gasque et al., 1996).

Complement regulators

Glia possess an array of complement regulators, in particular, MAC inhibiting CD59, and are therefore resistant to complement self-harm (Morgan & Gasque, 1996). This observation lead to the hypothesis that activation of locally generated complement may contribute to homeostatic CNS processes (Gasque, Fontaine, & Morgan, 1995b), with membrane expression of inhibitors by complement-competent cells preventing self-harm, and secreted fluid phase inhibitors limiting the radius in which locally produced complement can act (Gasque, 2004).

1.7.2 Neuronal complement expression

Complement proteins

Complement synthesis by neurons has been documented in response to neuropathology (Veerhuis et al., 2011), and there is some evidence of neuronal complement production under physiological conditions (Stephan, Barres, & Stevens, 2012b). In-situ hybridization of post mortem human brain tissue showed detectable mRNA expression of classical pathway components C1q to C3, and terminal components, C5 to C9, in the hippocampus and temporal cortex (Shen et al., 1997). Similar results were reported at the protein level by Terai, Walker, McGeer, & McGeer, (1997), and suggested that hippocampal pyramidal neurons are a particularly potent source of complement proteins. The precise function of complement expression in

neurons remains unclear however (Stephan, Barres, & Stevens, 2012a; Thomas, Gasque, Vaudry, Gonzalez, & Fontaine, 2000).

Complement receptors

Whereas glial cells take centre stage in complement synthesis, neurons seem to have a disproportionately larger share of complement receptors. Davoust et al. (1999) reported that neurons are the major cell type expressing C3aR in the unchallenged CNS, with hippocampal and cortical neurons expressing highest levels. Interestingly, expression of C3aR, C5aR (Rahpeymai et al., 2006) and complement receptor 2 (CR2; Moriyama et al., 2011) has been reported in hippocampal derived rat NPCs *in vitro* and in the DG. Moreover, using a ligand binding assay, Shinjyo et al. (2009) showed that binding of C3a to hippocampal adult NPCs via C3aR is direct and reversible. The same report suggested that C5a does not bind to NPCs, despite the presence of this receptor on this cell population. To date, the intracellular signalling pathways activated by C3a/C3aR binding on neurons have not been documented.

Complement regulators

In contrast to astrocytes, neurons can spontaneously activate locally produced complement *in vitro* and are vulnerable to self-harm due to their limited artillery of complement regulatory factors (Morgan & Gasque, 1996). Spontaneous activation of locally synthesized complement by neurons may be attributable to processes such as alternative pathway C3 tickover, or C1 tickover in the classical pathway. However, the key determinants of whether complement activation is detrimental or beneficial to host cells remain unknown.

1.7.3 Emerging role of complement in CNS homeostasis

Whilst complement CNS synthesis has been appreciated for the last two decades (Barnum, 1995), our understanding of its purpose beyond immune defence has lagged far behind. For years research focused on the ability of

complement to exacerbate damage in the context of neuropathology (Cowell, Plane, & Silverstein, 2003; Pasinetti et al., 1992). However, it is now appreciated that complement is also central to brain homeostasis and regeneration (Veerhuis et al., 2011). For this reason, complement is often referred to as a 'double edged sword' (Mastellos, 2014). Yet, compared to the peripheral and immune functions of complement, relatively little is known about the non-immunological functions of complement proteins within the normal CNS (Stephan, Barres, & Stevens, 2012b). Of relevance to this thesis are the purported roles of complement in adult neurogenesis, synaptic pruning and neuronal morphology.

As shown in Figure 1.10, C3 has been implicated in regulating AHN through two separate breakdown products and their receptors; the C3a/C3aR signalling pathway and C3d/CR2 signalling pathway. Adult C3$^{-/-}$ mice, and WT mice treated with a C3aR antagonist, showed reduced basal neurogenesis in both the SGZ and SVZ (Rahpeymai et al., 2006). Furthermore, Moriyama et al. (2011) reported that the C3 breakdown product, C3d, inhibits proliferation of NPCs *in vitro* via the CR2 receptor, and accordingly, CR2$^{-/-}$ mice show elevated basal neurogenesis. Therefore, two opposing regulatory roles have been assigned to breakdown products of C3, which suggest both pro and anti-neurogenic properties of C3. However, there are several methodological limitations of these studies that restrict the conclusions that can be drawn, and it is unclear whether C3 is able to act directly on NPCs and the neurogenic niche. These studies will be discussed in depth in Chapter 2.

Evidence has also suggested that C3a/C3aR signalling may modulate neuronal morphology. Impaired neuronal morphology has been documented in neurons exposed to high levels of C3, consisting of reductions in dendritic arborisation, length and complexity (Lian, Yang, Cole, Sun, Chiang, Fowler et al., 2015; Peterson, Nguyen, Mendez, & Anderson, 2015). However, the same reports have also suggested that basal C3aR signalling may also be important for maintaining normal neurite outgrowth and arborisation (Lian et al., 2015) and that C3a promotes neurite outgrowth (Shinjyo et al., 2009). These
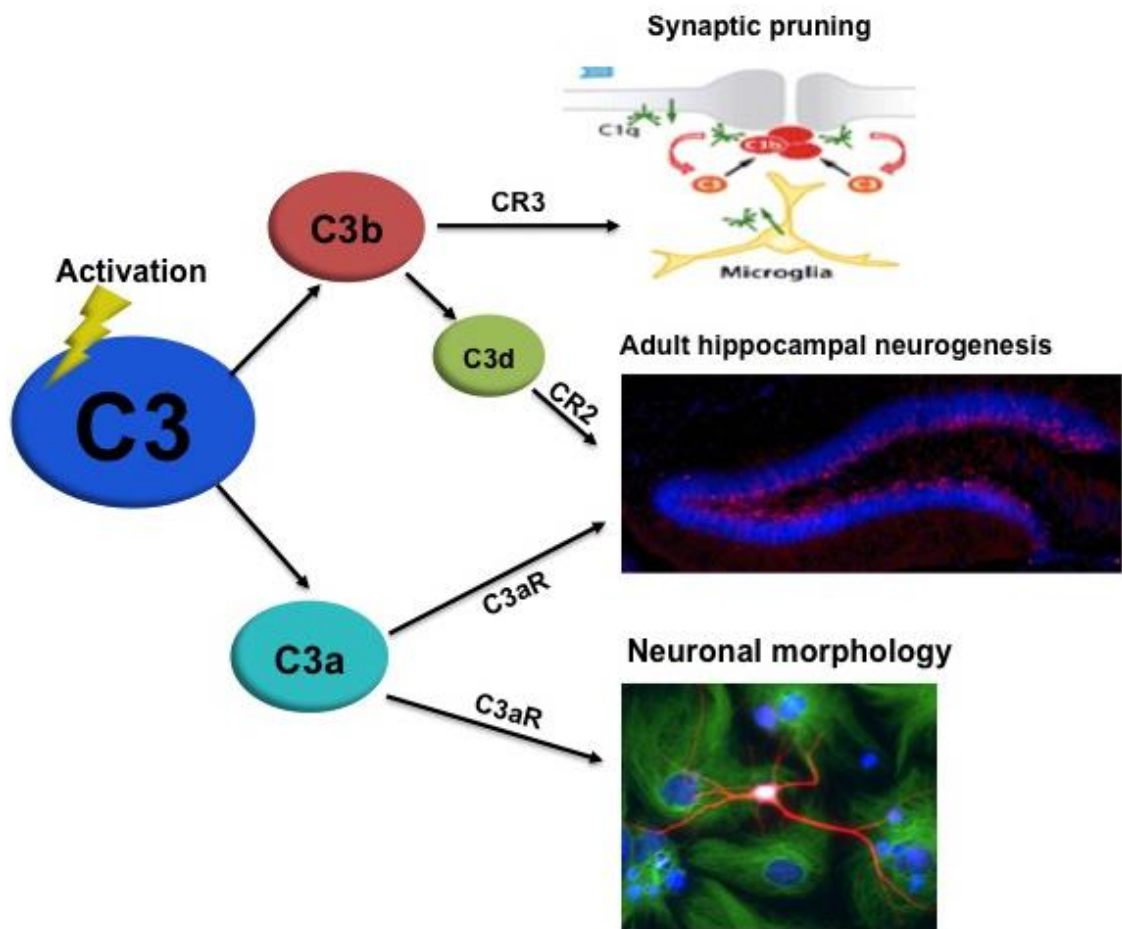
Figure 1.10. The role of C3 in adult hippocampal neurogenesis, neuronal morphology and developmental synapse elimination. C3 is activated by C3 convertase and proteolytically cleaved into breakdown products C3b and C3a. C3b has been implicated in developmental synaptic pruning in interaction with microglial CR3 (Schafer et al., 2012; Stevens et al., 2007). C3 may regulate adult hippocampal neurogenesis through both C3/C3aR and C3d/CR2 signalling pathways (Moriyama et al., 2011; Rahpeymai et al., 2006). C3d is a further breakdown product of C3b. C3a/C3aR signalling also modulates neuronal morphology (Lian et al., 2015). Top right image taken from Stevens et al., (2007).

reports will be discussed further in Chapter 3. Finally, via interaction with microglia, C3b/CR3 signalling contributes to the sculpting of neuronal circuitry in the developing brain (Shinjyo et al., 2009; Stevens et al., 2007). This constitutes a critical from of developmental synaptic plasticity. This literature will be considered further in Chapter 3. It is currently unknown whether these mechanisms pertaining to morphology and synaptic elimination also partake in the ongoing form of plasticity that is AHN.

An altered cognitive and affective phenotype has also been reported in C3$^{-/-}$ mice, which suggests improved spatial working memory (Perez-Alcazar et al., 2013; Shi et al., 2015). This finding is not in line with the decreased basal AHN reported by Rahpeymai et al. (2006), although the cognitive tasks used have not challenged pattern separation specifically. The relation of these phenotypes to AHN is therefore unclear, and this issue is considered in Chapter 4. Furthermore, the behavioural phenotype of C3aR deficient mice has not previously been investigated.

1.8   Project aims

In an attempt to better our understanding of the ability of complement regulation of AHN, this project aims to characterise the precise impact of C3 signalling upon various aspects of AHN, including the developmental milestones of neurogenesis, the maturation and morphology of newborn neurons, and the functional consequences of these processes upon hippocampal-dependent behaviour. Complementary *in vitro* and *in vivo* approaches will be taken in order to gain both an understanding of the direct effect of C3 on NPCs and cells isolated from the neurogenic niche *ex vivo*, in addition to a portrayal of function within the whole organism.

Chapter 2 will investigate the potential for the distinct pathways, C3a/C3aR and C3d/CR2 to regulate AHN, both *in vitro* and *in vivo*. In order to do this, primary cultures will be generated from the hippocampi of postnatal wild type, C3$^{-/-}$ and C3aR$^{-/-}$ mice. Within this controlled culture environment, I will separately examine the survival, proliferation and differentiation potential of hippocampal NPCs in the absence of C3 and C3aR. The use of this paradigm affords insight into whether complement is able to exert direct effects upon hippocampal precursor cells within a controlled and defined environment, without the confounding factors inherent in whole-organism studies. I also aim to determine whether the same mechanisms observed in culture also apply in the intact adult brain.

Chapter 3 will investigate a potentially novel role of C3/C3aR in the neuronal morphology of adult born neurons, both *in vitro* and *in vivo,* using techniques to carefully dissect various aspects of neuronal morphology. I will also examine whether the role of C3 in developmental synaptic pruning is relevant to the ongoing development and plastic network remodelling that is seen in AHN, by analysis of synapse density on newborn neurons *in vitro*.

In Chapter 4, a battery of behavioural tasks will be used to determine whether C3/C3aR mediated changes in AHN and newborn neuron morphology are of functional consequence for cognitive and affective processes associated with AHN, such as pattern separation and anxiety.

2.   The role of C3a/C3aR signalling in adult hippocampal neurogenesis

2.1   Introduction

Emerging evidence suggests that the complement system may regulate AHN (Moriyama et al., 2011; Rahpeymai et al., 2006; Shinjyo et al., 2009), with various factors implicated as pro or anti-neurogenic. Neurogenesis is a multifaceted process however, and precise answers regarding the specific effects of complement upon the proliferation, survival and differentiation of NPCs are lacking. This chapter therefore aims to provide a clearer understanding of these questions. Firstly, in a controlled culture system using precursor cells derived from the postnatal mouse hippocampus, I sought to determine whether complement C3/C3aR signalling exerts a direct effect upon hippocampal NPCs. Secondly, I investigated whether complement-mediated regulatory mechanisms were also applicable *in vivo.*

2.1.2 Effect of C3 on NPC proliferation

In vitro studies

CR2 and one of its several ligands, C3 fragment C3d, appear to exert an anti-proliferative effect on NPCs. Moriyama et al. (2011) generated neurospheres from primary hippocampal NPC's isolated from P0-P3 CR2$^{-/-}$ or WT mouse pups. While no differences were apparent in the number or size of spheres between genotypes, when exogenous human C3d was administered, neurosphere number decreased by one third. This effect was absent in CR2$^{-/-}$ spheres, suggesting dependency on CR2 signalling. Furthermore, co-administration of C3d and a CR2 blocking antibody saw reversal of the effect in WT cultures. These results imply that C3d functionally binds to CR2 on hippocampal precursor cells and exerts an inhibitory effect upon their

proliferation, resulting in the formation of fewer neurospheres. Parallel results were also obtained by Moriyama et al. (2011) using a rat NPC cell line, in which a reduction in total cell counts were observed after 48 hours of C3d treatment. Interestingly, no effects were seen with the addition of native C3, suggesting that C3 activation did not occur endogenously. Nonetheless, these results suggest that C3d/CR2 signalling exerts direct functional effects upon NPC proliferation.

The C3 breakdown product C3a has also been investigated with regard to proliferation. Using NPCs derived from the whole adult mouse brain, Shinjyo et al. (2009) investigated the effect of 100 nM purified human C3a treatment for 24 hours. No differences were found between C3a treated and control cells in the 3-(4,5-dimethylthiazol-2-yl)-2,5-diphenyltetrazolium (MTT) assay, which broadly reflects the metabolic activity of cells. In this assay, the MTT compound is converted to formazan by mitochondrial dehydrogenases in viable cells, resulting in a colorimetric change that can be detected spectrophotometrically (Edmondson, Armstrong, & Martinez, 1988). Shinjyo et al. (2009) therefore concluded that C3a does not affect NPC proliferation.

There are several limitations of the data reported by Shinjyo et al. (2009) and Moriyama et al. (2011). Foremost, the measures of proliferation used have been indirect. With regard to the techniques adopted by Moriyama et al. (2011), while variables such as neurosphere size, number and total cell counts are undoubtedly related to the proliferative capacity of cells, they do not directly assess proliferation. Similarly, the MTT assay used by Shinjyo et al. (2009) is indicative of the number of viable cells in culture and their metabolic activity, but is not a direct measure of proliferation. In both the neurosphere and MTT assay, it is therefore difficult to disentangle the combined influences of survival and proliferation. More direct measures would therefore provide clearer insight into the impact of complement factors upon proliferation. Techniques for direct assessment of proliferation include the thymidine analogues BrdU and 5-ethynyl-2'-deoxyuridine (EdU), in addition to endogenous cell-cycle marker Ki67 (Kee, Sivalingam, Boonstra,

& Wojtowicz, 2002). These two markers revolutionised the field of adult neurogenesis, as they readily permit assessment of newly born cells in the adult brain (Kee et al., 2002). BrdU is a maker of DNA synthesis, since dividing cells incorporate thymidine during the S-phase of the cell cycle. BrdU can be injected systemically or added exogenously to culture, and incorporation can later be detected immunohistochemically. BrdU is a powerful approach to studying AHN as it allows quantification of acute proliferation and the ability to lineage-trace NPCs using the pulse-chase paradigm (Taupin, 2006). Ki67 is a nuclear protein strictly associated with proliferation. It is expressed in the nucleus of dividing cells in all active phases of the cell cycle, and is absent from resting cells (Scholzen & Gerdes, 2000). Therefore, these markers are a valuable means to directly measure proliferation.

In addition, the cell types used in the aforementioned reports were not optimal for the study of AHN. For example, Moriyama et al, (2011) used precursor cells isolated from the mouse P0-3 hippocampus. While it is known that NPCs present in the rodent hippocampus from P5 are similar in nature to adult NPCs of the DG (Namba et al., 2005), the relevance of NPCs isolated prior to this stage is questionable. Moreover, although the NPCs used by Shinjyo et al. (2009) were of adult origin, their isolation from the whole mouse brain means heterogeneous cells from the SGZ and SVZ were likely present. It cannot be assumed that the effects are relevant to the hippocampal stem cell niche, as progenitor cells from differing regions have unique characteristics and respond to regionally specific cues (Riquelme, Drapeau, & Doetsch, 2008). Therefore, the use of a more relevant cell type is warranted in order to ensure conclusions are applicable to AHN. For example, a principal technique in our laboratory is the isolation of NPCs from the rodent hippocampus (Howell et al., 2005; 2003; Zaben et al., 2009). These cultures are generated from postnatal day 7 onwards, and therefore bear greater relevance to adult precursor cells than do embryonic or early postnatal cultures (Namba et al., 2005). Importantly, since our cultures are generated from the whole hippocampus, they also contain cell types found

57

within the neurogenic niche that are important for regulating AHN, including microglia and astrocytes.

In vivo studies

Moriyama et al. (2011) also examined the impact of C3d/CR2 signalling *in vivo.* Adult CR2$^{-/-}$ mice received daily injections of BrdU for 6 days, before being sacrificed 24 hours after final injection. No differences in the number of BrdU labelled cells were found in CR2$^{-/-}$ animals compared to WT controls, suggesting that CR2 deficiency did not affect the number of proliferating cells (or their survival; to be discussed). In light of the effect of exogenous C3d on neurosphere proliferation reported in the same paper, it is therefore possible that C3d/CR2 signalling does not influence NPC proliferation *in vivo* under physiological conditions.

Rahpeymai et al. (2006) also investigated the role of complement C3/C3aR in NPC proliferation *in vivo*. Adult WT mice were injected with either vehicle or C3aR antagonist SB290157 (Ames et al., 2001) for 10 days. C3$^{-/-}$ mice also received vehicle for this duration. Daily injections of BrdU were given to animals for the first 7 days, before sacrifice at day 10. Results showed no differences in the overall number of BrdU$^+$ cells in the DG, or in the number of proliferating type 1 cells (BrdU$^+$ cells co-expressing GFAP). Therefore, the authors concluded that C3 does not affect NPC proliferation.

However, the conclusions of these two reports are restricted due to methodological limitations. In both of these studies, animals received cumulative injections of BrdU over several days. This timeframe does not allow measurement of the number of cells in the S-phase of the cell cycle at one point in time however. The number of BrdU$^+$ cells remaining at sacrifice could reflect differences in survival, in combination with proliferation. For example, it is known that a large percentage of immature neurons born in the adult DG undergo apoptosis within a short time frame (Dayer, Ford, Cleaver, Yassaee, & Cameron, 2003; Kuhn et al., 2005). Therefore, it is important to

utilise experimental paradigms that can decipher the influence of proliferation independent of survival.

2.1.3 Effect of C3 on NPC survival

In vitro studies

NPC survival is as critical variable in adult neurogenesis (Sierra et al., 2010) and is more predictive of levels of net neurogenesis than NPC proliferation (Dayer et al. 2003). In order to investigate the effect of C3d/CR2 signalling on NPC survival, Moriyama et al. (2011) treated NPCs derived from a rat NPC cell line with either purified human C3 or C3d, before measuring the enzyme lactate dehydrogenase (LDH) in culture supernatant. LDH, a soluble cytoplasmic enzyme present in many cells, is commonly used as a measure of necrotic cell death (Cummings & Schnellmann, 2001). In necrotic cells, the plasma membrane is damaged, causing leakage of LDH into the cell culture medium, which can be detected colorimetrically by spectroscopy (Chan et al., 2013). Addition of C3 or C3d did not alter LDH release, suggesting that these molecules did not affect necrotic cell death. Furthermore, Shinjyo et al. (2009) reported no differences between whole adult mouse brain NPCs treated with human C3a or vehicle in the MTT assay, which also reflects overall cell viability.

As before, these studies are difficult to interpret due to the use of indirect measures. Alternative methods available for use *in vitro* include probes such as propodium iodide (PI), which labels dead or dying cells, and MitoTracker®, which labels viable cells. PI is a polar fluorescent DNA-binding dye, which penetrates dying cells due to their compromised cell membrane. PI cannot penetrate viable cells and is therefore a reliable measure of cell death (Cummings & Schnellmann, 2001). MitoTracker® is a fluorescent probe that diffuses across the plasma membrane of respiring cells and accumulates in active mitochondria, therefore labelling viable cells

(Poot et al., 1996). Combined, these two techniques allow specific insights into cell death and viability.

In vivo studies

While there have been many investigations into complement and survival in a variety of cell types (Veerhuis et al., 2011), little is known regarding complement and NPC survival *in vivo* specifically. Moriyama et al. (2011) reported no differences in the prevalence of activated caspase, a key protein mediator of apoptosis (McIlwain, Berger, & Mak, 2013), in the brains of $CR2^{-/-}$ mice. However, it is unclear from their report as to whether this marker was measured specifically in immature neurons of the DG, or throughout the whole brain.

2.1.4 Effect of C3 upon NPC differentiation

In vitro studies

The phenotype adopted by NPCs upon differentiation is another key variable in the study of adult neurogenesis. Shinjyo et al. (2009) investigated the effect of adding 100 nM purified human C3a to whole adult mouse brain NPCs. Differentiation was stimulated by the removal of growth factors for 24 hours prior to fixation. They observed a small but statistically significant 15% increase in the proportion of cells adopting a Microtubule-Associated Protein 2ab (Map2ab) positive phenotype, indicative of mature neurons, in cells treated with C3a. They conclude that C3a has a small effect upon the differentiation and maturation of neural precursor cells. It is debatable whether a change of this magnitude would have any biological relevance however.

Again, methodological limitations restrict the interpretation of these results. In addition to the previously discussed issue regarding use of whole adult mouse brain NPCs, these cells were also grown as neurospheres prior to the assays reported. Specifically, cells underwent nine consecutive passages

before being plated as monolayers for the differentiation assay reported by Shinjyo et al (2009). Although favoured as the most straightforward method of generating primary adult NPC cultures, the neurosphere paradigm is known to specifically propagate the population of stem and progenitor cells, since spheres are formed via proliferation of mitogen-responsive cells (Reynolds & Rietze, 2005). Such culture conditions are not supportive of the long-term survival of other cell types such as microglia, which provide important regulatory signals to NPCs in the hippocampal niche (Ekdahl, 2012). A culture paradigm that includes these cell types would therefore be a favourable approach. Additionally, it is known that cell properties such as gene expression, growth factor dependence, proliferation kinetics and adherence are amenable to change over the duration of long term sphere cultures (Seaberg & van der Kooy, 2002), such that the resulting cell population likely do not reflect the characteristics of those *in vivo* or those used in short term culture paradigms.

In vivo studies

In the healthy brain, it has been suggested that CR2 exerts an anti-neurogenic effect by decreasing the number of immature neuronal cells. Moriyama et al. (2011) quantified DCX, a marker of newly generated progenitor cells committed to the neuronal lineage (Rao & Shetty, 2004), in $CR2^{-/-}$ mice. In the absence of CR2, they observed a two-fold increase in immature DCX^+ neurons at two and five months of age, and a three-fold increase at thirteen months of age.

Furthermore, using a BrdU-pulse chase paradigm, Moriyama et al. (2011) demonstrated that CR2 deficiency is associated with a fate shift towards the neuronal lineage. Adult $CR2^{-/-}$ mice received daily injections of BrdU for six days and were sacrificed one day later. There was a significant increase in $BrdU^+ DCX^+$ immature neurons, and a concomitant decrease in $BrdU^+ GFAP^+$ type 1 radial glia cells. Moreover, when animals survived for 28 days post-injection, $CR2^{-/-}$ mice showed significantly more $BrdU^+ NeuN^+$ cells than WT,

suggesting that the absence of CR2 signalling promotes the differentiation and maturation of cells in the neuronal lineage.

CR2 is known to bind several ligands, including C3 derivatives iC3b, C3dg, and C3d (Molina et al., 1995) in addition to cytokine IFN-α, which has been shown to reduce proliferation in the adult rat DG (Kaneko et al., 2006). Therefore, in order to determine whether the observed effects were C3 mediated, Moriyama et al. (2011) infused human C3d protein into either the left or right dentate gyrus of WT and CR2$^{-/-}$ mice. A 35% decrease in BrdU$^+$ DCX$^+$ was shown in WT mice, whereas no effects were present in CR2$^{-/-}$ animals. These results conclusively demonstrate that C3d signalling via CR2 exerts an anti-neurogenic effect in the healthy brain, by reducing the differentiation of precursor cells into the neuronal lineage.

In contrast, a report by Rahpeymai et al. (2006) suggested a pro-neurogenic effect of C3a/C3aR signalling *in vivo.* BrdU was administered to WT, C3$^{-/-}$, C3aR$^{-/-}$ and C3aR antagonist treated WT animals (WT C3aRA) for 7 consecutive days, before sacrifice at either day 10 or day 21. A 33% decrease in BrdU$^+$ DCX$^+$ cells in C3$^{-/-}$ and WT C3aRA animals was seen at day 10, and a 22% decrease in BrdU $^+$ NeuN$^+$ cells was observed in C3$^{-/-}$ and C3aR$^{-/-}$ animals at day 21 (WT C3aRA animals were not included in this analysis, for unknown reasons). These results therefore implicate C3a/C3aR signalling as a stimulator of differentiation and/or maturation in the adult DG, and are in agreement with the *in vitro* report by Shinjyo et al. (2009) suggesting that C3a promotes neuronal fate choice.

Together, the reports of Moriyama et al. (2011) and Rahpeymai et al. (2006) suggest opposing pro and anti-neurogenic roles of C3a, C3d and their receptors. Considering that C3$^{-/-}$ mice also lack C3d, it is surprising that such differing conclusions have been reached. This suggests several possibilities. Firstly, C3d/CR2 signalling may not exert its proposed anti-neurogenic effect under physiological conditions. Alternatively, C3a/C3aR signalling may take precedence over C3d/CR2 signalling. It is also possible that other ligands

aside from C3d are partly responsible for the effects observed in CR2$^{-/-}$ animals, or are able to substitute for its absence.

While these papers provide convincing evidence that C3 fragments C3a and C3d influence AHN *in vivo*, the exact mechanisms through which complement affects hippocampal neurogenesis remain to be seen. For example, the observed increases or decreases in immature neurons may suggest specific effects upon neuronal fate determination, but could also be due to variations in the survival or proliferation of this cell type. Furthermore, it is difficult to determine whether the effects observed are a consequence of complement acting directly upon NPCs and the neurogenic niche, as many intervening signalling pathways exist in the whole organism. It is therefore imperative to use *in vitro* hippocampal neurogenesis models to gain a better understanding of the complement-mediated regulation of AHN.

2.1.5 Source of complement within the neurogenic niche

An important issue, which has not been addressed in much of the literature, is the source of the complement proteins thought to regulate AHN. Although Shinjyo et al. (2009) demonstrated specific and reversible C3a/C3aR binding on whole adult mouse brain derived NPCs upon addition of human C3a, little is known about the source of complement in the neurogenic niche. As outlined in Section 1.7, it is known that neurons (Thomas et al. 2007), astrocytes (Lévi-Strauss & Mallat, 1987), oligodendrocytes (Hosokawa, Klegeris, Maguire, & McGeer, 2003) and microglia (Gasque, Fontaine, & Morgan, 1995) are able to synthesize a complete set of complement proteins, receptors and regulators. Whether NPCs specifically synthesize complement factors or regulators is unknown.

While there have been no direct investigations in this area, it is interesting to note the findings of Moriyama et al. (2011) whereby effects of C3d/CR2 signalling in neurospheres were observed only when C3d was added to

culture media. This could suggest that if C3 is produced by NPCs, it is not activated to form C3d, or that NPCs do not endogenously produce C3. As discussed, neurosphere cultures do not favour the survival of immunocompetent cells such as astrocytes or microglia, which are a potent source of complement proteins (Zhang et al., 2014b). Therefore, while NPCs may not produce complement proteins, they may nevertheless be equipped with receptors and regulators, allowing them to respond to, and control local complement activation.

2.1.6 Aims and hypotheses

Based on the body of literature discussed (summarised in Table 1), I formulated several aims and hypotheses regarding the proliferation, survival and differentiation of NPCs, both *in vitro* and *in vivo*.

	Signaling pathway			
	C3d/CR2		C3a/C3aR	
	In vitro	*In vivo*	*In vitro*	*In vivo*
Publication	Moriyama et al. (2011)		Shinjyo et al. (2009)	Rahpeymai et al. (2006)
Proliferation	**Anti-proliferative**: C3d reduces neurosphere number	No differences in BrdU⁺ cells	No differences in MTT assay	No differences in BrdU⁺ cells
Survival	No differences in LDH release from neurospheres	No differences in activated-caspase staining	No differences in MTT assay	Not investigated
Differentiation	Not investigated	**Anti-neurogenic**: C3d causes decreases in BrdU⁺ DCX⁺	**Pro-neurogenic:** promotes neuronal phenotype	**Pro-neurogenic:** decrease in BrdU⁺ DCX⁺/ BrdU⁺ NeuN⁺ in absence of signaling

Table 2.1 Summary of prior literature regarding complement signalling pathways C3d/CR2 and C3a/C3aR and their effects upon proliferation, survival and differentiation of NPC's both *in vitro* and *in vivo.*

Proliferation

To overcome the aforementioned methodological shortcomings of previous studies, I aimed to utilise EdU incorporation as a direct measure of acute proliferation in primary hippocampal cultures isolated from postnatal WT, $C3^{-/-}$ and $C3aR^{-/-}$ mice. *In vivo,* I used the endogenous proliferation marker Ki67 to compare the number of proliferating cells in the adult DG between genotypes. I also aimed to investigate the impact of C3/C3aR on the proliferation of specific cell phenotypes, such as type 1, 2a, 2b and 3 cells, both *in vitro* and *in vivo,* using co-localisation of phenotype specific markers with proliferative markers.

Based on the report of Moriyama et al. (2011) I hypothesised that if C3d/CR2 signalling affects NPC proliferation, I would observe an increase in EdU incorporation in $C3^{-/-}$ cultures, but not $C3aR^{-/-}$ or WT cultures. An increase in $Ki67^+$ cells would also be observed in the hippocampi of $C3^{-/-}$, but not WT or C3aR-/- animals, *in vivo.*

Survival

Again, in order to gain a clearer understanding of the impact of complement upon NPC survival, I aimed to use PI and MitoTracker® staining as specific measures of cell death and viability in primary hippocampal cultures. Despite the limitations of prior techniques used to investigate cell death, based on the report of Moriyama et al. (2011) I hypothesised there would be no alterations in cell death or viability in the absence of C3. I did not form any prior hypotheses with regard to the impact of C3aR specifically, since this has not been previously investigated (see Table 1).

Differentiation

While the prior evidence regarding complement and differentiation is compelling, I aimed to further investigate the proposed effects of complement *in vitro* and *in vivo* using a range of markers to distinguish immature and mature neurons. Two opposing hypotheses are possible based on the reports of Moriyama et al. (2011) and Rahpeymai et al. (2006), since

C3$^{-/-}$ mice lack both C3a and C3d, and these ligands have seemingly opposite effects. Therefore, if the absence of C3d is of functional relevance under physiological conditions, one would expect to observe greater numbers of immature neuronal and mature neuronal cells in C3$^{-/-}$ mice, but not in C3aR$^{-/-}$ or WT, since C3d/CR2 signalling is present. However, if the C3a signalling exerts a greater effect on basal neurogenesis than does C3d, then I hypothesised that there would be a reduction in the number of immature and mature neuronal cells both *in vitro* and *in vivo,* as per Rahpeymai et al. (2006).

Source of complement

I also aimed to explore the expression of complement pathway proteins, receptors and regulators in postnatal hippocampal cultures. Since these cultures provide a relatively pure population of precursor cells (~70% nestin$^+$) in addition to other cell types important in the neurogenic niche, this experimental paradigm is well suited to examine the expression of complement by specific cell types. Since this investigation was exploratory in nature, no prior hypotheses were made.

2.2   Methods

2.2.1 Animals

All animals were kindly provided by Professor Paul Morgan at the Institute of Infection and Immunity, Cardiff University. C57Bl6 Thy1.1 and C3$^{-/-}$ strains were originally sourced from The Jackson Laboratory (strain B6.PL-Thy1a/CyJ and B6;129S4-C3tm1Crr/J respectively), whereas the C3aR$^{-/-}$ strain was provided by Professor Craig Gerard of Boston Children's Hospital, USA, as a collaboration via Professor Morgan. All strains were on a C57Bl6-J background.

2.2.2 Wild type

C57Bl/6 Thy1.1 was used as WT controls in all experiments. While not of relevance to this thesis, it should be noted that these animals carry a homozygous allelic variant on chromosome 9 known as Thy1 (thymus cell antigen 1). This locus determines a surface antigen present on cells of the brain, lymph nodes, thymus and spleen cells (Snell and Cherry, 1972). Many researchers use this model since it allows easy discrimination of donor T cells from recipient T cells via flow cytometry. This strain was used in our experiments as it was the standard wild type C57Bl6 colony present in the unit.

2.2.3   C3$^{-/-}$

Developed by Michael C. Carroll of the Immune Disease Institute at Harvard Medical School, this model was derived via homologous recombination in embryonic stem cells (Wessels et al., 1995). A PGK-neomycin resistance cassette was inserted into an exon of the C3 gene on chromosome 17, resulting in the deletion of approximately 600 nucleotides. The deleted segment included 364 nucleotides of coding sequence for the C-terminal

67

region of the β chain, and the N-terminal region of the α chain. This sequence also includes the site for processing of the pro-C3 molecule into its mature form found in serum. Therefore, as described in Section 1.6.4, complement activation cannot proceed past C3 in this model. Consequentially, these mice lack the main inflammatory functions of complement, in addition to the C3 and C1 tickover mechanisms. These animals are viable and are capable of breeding on a homozygous background, although reduced fetal weight is common (Chow et al., 2009).

2.2.4 C3aR$^{-/-}$

The C3aR deficient model was originally generated on a BALB/cJ background by Professor Craig Gerard of Boston Children's Hospital, USA. Using homologous recombination, a 736 base pair sequence containing the translation start site and coding sequences for the N-terminal region of the C3aR protein was targeted for deletion by vector, and replaced with a neomycin-resistant gene driven by a PGK promoter (Humbles et al. 2000). These animals were later backcrossed onto a C57Bl/6-J background. The strain are homozygous viable, but produce less frequent and smaller litters than WT C57Bl/6-J animals.

2.2.5 Animal housing

All animals were housed in conventional cages on a 12:12 light/dark cycle. For *in vitro* experiments, breeding triplets consisting of one male and two females housed together in conventional caging. Litters remained within the breeding cage until use at P7 or P8. For *in vivo* experiments, adult males were group housed with up to 5 littermates per cage until the time of sacrifice.

2.2.6 *In vitro* methods

Generation of primary hippocampal cultures

The following protocol was adapted from a previously used protocol in our laboratory for generating hippocampal cultures from rat pups (Ahmed et al., 2012; Howell et al., 2003, 2005; Zaben et al., 2009a). Cultures were generated from P7 or P8 WT, $C3^{-/-}$ and $C3aR^{-/-}$ pups (of mixed sex) in separate isolations, using approximately 6 to 8 animals per culture, and maintained in serum-free conditions for up to 14 days. An overview of the process is shown in Figure 2.1.

Preparation of tissue culture coating

Prior to commencing isolation, tissue culture plasticware was prepared fresh on the same day. 13mm glass coverslips (previously autoclaved to ensure sterility) were placed into 24 well plates and coated with 250 µl of 50 µg/ml poly-L-lysine (PLL, Sigma) per well for 30 minutes at room temperature. After three washes with sterile PBS, 250 µl of pre-warmed 10 µg/ml mouse laminin (Sigma) diluted in sterile phosphate-buffered saline (PBS) was added to each well to permit better adherence. Wells were then incubated in laminin solution at 37°C for 30 minutes. Wells were then washed a further three times with PBS, and as per manufacturers instructions, were allowed to dry fully prior to cell plating.

Isolation protocol

The following protocol was adapted for use with mouse tissue from previous protocols for the generation of primary hippocampal rat cultures (Howell et al., 2003; 2005; Zaben et al., 2009b). Litters of 6-8 mixed sex pups were swiftly culled by cervical dislocation. Carcasses were sprayed with 70% ethanol and decapitated inside a fume hood. The skin was carefully cut before the skull was parted and folded back, allowing the brain to be removed. The hippocampi were then dissected and placed into petri dishes containing 200 µl of Gey's balanced salt solution (Sigma Aldrich)

supplemented with 4.5 mg/ml glucose (Sigma), chilled to 4°C until all brains were dissected and ready to proceed to the following step.
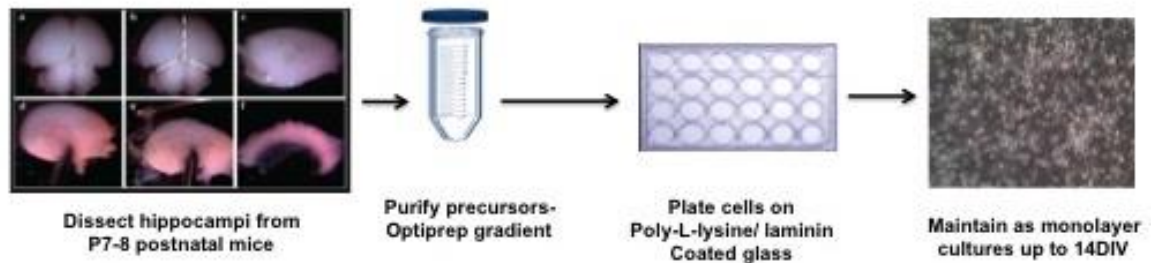
Figure 2.1. Overview of protocol for generation of primary hippocampal cultures from postnatal mouse pups. Hippocampi are dissected from postnatal day 7 pups, after cervical dislocation and decapitation. After enzymatic digestion, cells are purified from debris using an Optiprep gradient of a 10% solution atop 20% solution, upon which the cells are placed. After spinning, cells are collected and plated at the required density of 100,000 cells per ml on to pre-coated glass coverslips in tissue culture plates. Cells can then be maintained as monolayer cultures for up to 14DIV.

Cell release and dissociation

Hippocampi were pooled and placed on the stage of a MciIwain Tissue Chopper and sliced into 400 µm sections, cut perpendicular to the long axis of the hippocampus. This step was included to aid tissue digestion and cell viability. Subsequently, tissue was immediately transferred to a pre-prepared enzymatic solution to aid digestion. Papain (Sigma, 2 mg/ml) was pre-filtered and sterilised using a 0.2 µm syringe filter (Millex-GV, Millipore). Papain was prepared in 5 mls of standard culture medium, consisting of Neurobasal A (NBA; Life Technologies), 2% B27® (Life Technologies), 1% antibiotic-antimycotic (ABX; Life Technologies) and 0.25% Gibco™Glutamax™ (Life Technologies; from here on standard culture medium will be referred to as NBA/B27/Abx/Glutamax) and pre-warmed to 37°C in a water bath for at least 30 minutes before introducing to tissue. Tissue sections were incubated in papain solution for 30 minutes at 37°C in a petri dish.

After 30 minutes, the solution was transferred to a 15 ml centrifuge tube and centrifuged at 1100 rpm for 3 minutes to sediment the tissue. The

supernatant was carefully aspirated in order to ensure that the majority of papain was removed, and replaced with 1 ml of pre-warmed NBA/B27/Abx/Glutamax. The pellet was then mechanically triturated 5-10 times to initiate cell release, until the cell pellet was fully dissociated, resulting in a single cell suspension.

This suspension was then diluted in an additional 1 ml of NBA/B27/Abx/Glutamax to allow reliable trituration. In order to partially purify cells from debris an Optiprep (Sigma) gradient was used. Optiprep is a sterile ready-made solution of iodixanol in water that is non-toxic to cells and therefore does not require extensive washing. The Optiprep gradient consisted of 2 mls of NBA/B27/Abx/Glutamax, with the 1st ml consisting of 20% Optiprep and the 2nd ml consisting of 10% Optiprep. The 10% solution was carefully pipetted on top of the 20% to create an interface, inside a 15 ml centrifuge tube. The cell suspension was then carefully pipetted on to the top of the Optiprep gradient. The gradient was then centrifuged for 15 minutes at 1900 rpm.

After centrifugation, the cell-containing fraction (found at the 2 ml mark) was collected and diluted in 1 ml of fresh NBA/B27/Abx/Glutamax. The solution was then centrifuged at 1100 rpm for 5 minutes at room temperature, after which the supernatant was carefully aspirated to remove any remaining debris or Optiprep solution. The pellet was then resuspended in 1 ml of fresh NBA/B27/Abx/Glutamax, and then diluted in the appropriate volume of NBA/B27/Abx/Glutamax media in preparation for plating (1 ml per animal used). The density of cells per ml was then calculated using a haemocytometer, and cell suspension was further diluted to a concentration of 1×10^5 cells per ml in NBA/B27/Abx/Glutamax.

Cell plating and maintenance
Cells were then plated in a volume of 500 μl per well in 24 well plates prepared as previously discussed in Section 2.2.6. For experiments requiring collection of RNA, cells were instead plated at 5×10^5 cells per ml in 1 ml of

NBA/B27/Abx/Glutamax, in a pre-prepared 6 well plate, in order to ensure adequate yield of RNA.

Two hours post-plating, all medium was aspirated in order to remove non-attached cells and debris. Wells were replenished with fresh NBA/B27/Abx/Glutamax supplemented with 20 ng/ml Epidermal growth factor (EGF; Sigma) and 20 ng/ml Basic fibroblast growth factor (FGF-2; Sigma), as these growth factors are necessary for the expansion and survival of mouse hippocampal cultures (Babu et al. 2007; Babu et al., 2011). Partial medium changes were performed every 3 days to provide fresh growth factors and remove build-up of dead cells. Cells were maintained in a tissue culture incubator at 37°C, in 5% CO_2 and 9% O_2.

2.2.7 Generation of pure microglial cultures

At the time of hippocampal cell harvest, cortical tissue was also collected. The same protocols were followed as per hippocampal cultures for mechanical and enzymatic cell dissociation, but the purification step was omitted in order to generate mixed glial cultures. Cells were washed of papain before being plated at high density in 6 well plates pre-coated with poly-L-lysine. Cells were maintained in Dulbecco's Modified Eagle Medium (DMEM; Life Technologies) supplemented with 0.25% Glutamax, 10% fetal bovine serum (FBS) and 1% ABX, for up to two weeks until confluent. While these cortical cultures do initially contain neurons, the addition of FBS favours the proliferation and survival of glia over neurons.

In such cultures, it is known that microglia sit atop the confluent layer of astrocytes and can be detached by mechanical shaking (Tamashiro, Dalgard, & Byrnes, 2012). I used a procedure previously developed in our laboratory by Nunan et al. (2014). Culture plates were attached to a shaker heated to 37°C for 30 minutes and shaken at 1200 rpm. After shaking, microglia were dislodged by several hard taps to the bottom of the plate, and supernatant

was collected. Cell density was estimated using a haemocytometer and cells were plated in fresh PLL coated plates. Purified microglia were maintained the same culture medium as described for mixed glial cultures, and were kept for up to one week. In order to activate microglia, LPS (from Escherichia coli, L5293; Sigma) was added at a concentration of 10 μg / ml for 24 hours before supernatant was collected and stored at -80°C until further use.

2.2.8 *In vitro* assays

Detection of acute proliferation

All media was aspirated and replaced with growth factor free NBA/B27/Abx/Glutamax medium containing 20 μM EdU (Invitrogen), from a stock solution in Dimethyl sulfoxide (DMSO), for the terminal 6 hours prior to fixation. Cells were then fixed in 4% paraformaldehyde solution for 30 minutes at 4°C, before being washed three times with PBS. Detection of EdU was performed using the Click-It EdU kit (Invitrogen) according to manufacturer's instructions. Briefly, cells were washed three times for 5 minutes each in PBS containing 3% w/v bovine serum albumin (BSA, Sigma Aldrich), incubated in PBS containing 0.5% Triton-X (Sigma Aldrich) to allow permeabilization, before detection of EdU for 30 minutes at room temperature, protected from light. The detection reaction is catalysed by copper at room temperature and results in formation of a covalent bond between an alkyne group present in EdU and the Azide present in fluorescent dye (Cieślar Pobuda & Los, 2013). Cells were washed once more in PBS containing 3% BSA, before proceeding to standard immunocytochemistry (described in Section 2.2.9).

Quantification of live/dead cells in culture

To detect dead cells in culture, cells were incubated with 1 μg/ml PI (Life Technologies) for 40 minutes at 37°C. Wells were then washed once with warm   NBA/B27/Abx/Glutamax,   and   incubated   with   fresh

NBA/B27/Abx/Glutamax containing 100 nM/ml MitoTracker® Green (Invitrogen) for a further 40 minutes at 37°C. To mark all nuclei in culture, 5 μg/ml 4',6-diamidino-2-phenylindole (DAPI) was added for the final 15 minutes. All medium was then aspirated and replenished with fresh NBA/B27/Abx/Glutamax, and cells were live-imaged using an inverted fluorescence Leica microscope (DMi6000B) inside a chamber supplied with 5% CO_2 and air and heated to 37°C. Six fields were sampled per well, with four in the periphery and two in the centre of each well.

Differentiation conditions

To stimulate differentiation, at 5DIV all media was aspirated, cells were washed gently with pre-warmed NBA/B27/Abx/Glutamax and replenished with growth-factor free NBA/B27/Abx/Glutamax media. Cells were then fixed 24 hours later (6 DIV) or 9 days later (14 DIV) as per experimental requirements.

2.2.9 Immunocytochemistry

Cells were fixed in 4% paraformaldehyde solution for 30 minutes at 4°C, prior to washing three times with PBS, before being blocked for 30 minutes at room temperature in 250 μl/well PBS containing 0.1% Triton-X (Sigma Aldrich) and 5% normal donkey serum (Life Technologies). Primary antibodies (see Appendix A) were applied in 250 μl/well 0.1% PBS-T overnight at 4°C. After three PBS washes, cells were incubated in the appropriate AlexaFluor secondary antibodies (see Appendix A) in 250 μl per well 0.1% PBS-T for two hours at room temperature, protected from light. Secondary antibodies were then removed, plates washed three times in PBS and counterstained with 1 μg/ml DAPI in distilled H_2O for 6 minutes, protected from light. After a final wash, coverslips were carefully removed from wells and mounted face-down onto microscope slides in Mowiol (Sigma) mounting solution in preparation for imaging.

2.2.10 Imaging and cell counting

Mounted coverslips were imaged on an upright Leica DM6000B fluorescence microscope. Micrographs from 6 fields per well were systematically random sampled, with four on the periphery and two in the centre, were obtained for analysis. Cell counts were performed using ImageJ Cell Counter plugin (http://imagej.nih.gov/ij/). Cells per mm^2 were calculated, as well as the proportions of different phenotypes of cells relative to the total (DAPI) cell count.

2.2.11 Polymerase chain reaction (PCR)

RNA was harvested from cultures plated at 5×10^5 cells / ml at 5DIV in 500 μl of Trizol (Life Technologies). RNA was extracted and genomic DNA removed using Precision DNAse kit (Primer Design), before performing reverse transcription using NanoScript 2 Reverse Transcription kit (Primer Design, Southampton, UK). Complementary DNA (cDNA) quality was then measured and diluted to 1 μg / 10 μl.

Primers were designed using UCSC Genome Browser (https://genome.ucsc.edu/, see Appendix B for primer sequences, gene names and approved nomenclature) Positive control cDNA was obtained from combined liver and brain samples taken from P7 mouse pups at the same time as hippocampal cell harvest. All primers were tested on positive control samples as well as hippocampal cell culture RNA. 25 ng of cDNA was used per PCR reaction, with 10 μm primer mix, 10 μl 2xPrecisionFAST Mastermix (Primer Design, Southampton, UK) and nuclease free water. The PCR cycle was as follows: 5 minutes at 95°C, followed by 40 cycles of 15s at 95°C, 15s at 60°C, 30s at 72°C. DNA product was then run on a 2% agarose gel and visualised to determine absence or presence of transcripts.

2.2.12 Sandwich Enzyme-linked immunosorbent assay (ELISA)

Supernatant from WT, C3$^{-/-}$ and C3aR-$^{/-}$ primary hippocampal cultures was collected and pooled prior to cell fixation at 5DIV. Supernatant was also collected from purified microglial cultures treated with LPS as described in Section 2.27 to serve as a positive control. Supernatant was then centrifuged for 20 minutes at 4°C at 1000 × rcf to separate cell debris, and then stored at -80°C until further use. Sandwich ELISA was carried out according to manufacturer instructions (Cloud-Clone Corp, Houston, TX). The minimum detectable dose of the kit used was cited as 6.1 pg/ml.

2.2.13 *In vivo* methods

Animals

Groups consisted of 6 adult males per genotype, between 8 and 12 weeks of age at time of sacrifice. All animals were reared in the same breeding room and were group-housed with littermates.

2.2.14 Perfusion fixation

Animals were sacrificed through administration of a lethal dose of Euthetal. Once the heartbeat had ceased, the animal was placed in a dorsal position and the thorax opened, and the ribcage cut away to expose the heart. The perfusion needle was inserted into the right ventricle and the left atrium snipped. In order to remove blood from the circulatory system, approximately 200 ml PBS was first infused, followed by 200ml of 4% paraformaldehyde. The brain was then removed and post-fixed in 4% paraformaldehyde for a further 24 hours. Brains were then transferred into a 30% w/v sucrose solution in PBS until brains had sunk to the bottom of the tube.

2.2.15 Tissue processing

Each brain was embedded in OCT (Thermo Scientific) and stored at -80°C until further processing. Brains were then sectioned in the coronal plane at 40 μm using a Cryostat, and collected as free floating sections in 24 well plates in 500 μl of PBS.

2.2.16 Immunohistochemistry

Appropriate sections were selected using a stereological sampling rate of 1/10, starting from the most anterior hippocampal section identified. As shown in Figure 2.11B, 6 sections were collected per animal, spanning the longitudinal axis of the hippocampus beginning approximately -0.94 mm from Bregma and ending at approximately -3.40 mm from Bregma (Franklin & Paxinos, 2008).

Sections were first blocked in 250 μl/well 0.1% PBS-T containing 3% normal donkey serum for 2 hours at room temperature. Subsequently, primary antibodies (see Appendix A) were diluted in 250 μl/well 0.1% PBS-T containing 0.2% normal donkey serum and incubated overnight at 4°C. The next day, sections were washed three times with PBS for periods of 10 minutes. Secondary antibodies at appropriate dilutions were then applied in 250 μl/well 0.1% PBS-T for 2 hours at room temperature, protected from light. Subsequently, another three 10 minute PBS washes were performed, interspersed by a 6-minute incubation with DAPI at a concentration of 0.5 μg/ml in distilled H_2O. Tissue sections were then mounted onto microscope slides, with 20 μl of Mowiol added per section and then sealed with glass coverslips.

2.2.17 Imaging of tissue sections

Tissue sections were imaged on an upright Leica DM6000B fluorescence microscope using tile scanning at 40x magnification to capture the entire left and right dentate gyri in each section. Before cell counting, tile scan files were genotype blinded to the experimenter using KeyGen software (designed and provided by Nicholas Clifton).

2.2.18 Cell counting and analyses

The number of DCX$^+$, Ki67$^+$, and Ki67$^+$ GFAP$^+$ / Ki67$^+$ DCX$^+$ double positive cells were counted in the left and right dentate gyri of each section, in 6 sections per animal, from 6 animals per genotype. In order to estimate the total number of cells in the whole dentate gyri of each animal, the number of cells counted in the left and right dentate gyri were summed and multiplied by the intersection interval (10) to obtain the total number of cells for the region spanning the current section until the next section. This was repeated for each of 6 sections, and the estimates obtained were summed in order to give a measure of the total number of cells present in the entire DG per animal. Similarly, the total number of cells in either sections 1, 2 and 3, or 4, 5 and 6, were summed to estimate the total number of cells in the anterior and posterior hippocampal regions respectively (see Figure 2.11B). Missing data is as follows; 1 full section from 1 animal in WT due to tissue folding, 1 and ½ full sections from 1 C3$^{-/-}$ animal due to tissue folding, and 1 full section from 1 C3aR$^{-/-}$ animal due to high background/occlusion of tissue by debris. In these instances, the mean cell count from the same section in all other animals in their experimental group was substituted.

2.2.19 Statistics

Data screening

Prior to statistical analyses, whether data met the assumptions of ANOVA was assessed. The shape of the distribution was first visually inspected in a histogram of frequency distributions using a bin width of 20 units. The D'Agostino-Pearson omnibus K2 test was also used to assess whether data was sampled from a population with a Gaussian distribution (Rani Das, 2016). Homogeneity of variance was assessed using the Brown-Forsythe test (M. B. Brown & Forsythe, 1974). Outlier screening was performed using the ROUT method (Motulsky & Brown, 2006).

Statistical tests

Where appropriate, unpaired two-tailed *t*-tests were performed, or in the instance of multiple genotype experiments analysis of variance (ANOVA) was used. An α level of 0.05 was used for all statistical tests. All statistics were conducted using GraphPad Prism software (La Jolla, CA). In the instance of a significant omnibus ANOVA, Tukey's HSD test was used for post-hoc comparisons, since all possible pairs of means were compared.

2.3   Results

2.3.1 mRNA expression of complement proteins, receptors and regulators in hippocampal cultures

In order to investigate endogenous complement expression within WT hippocampal cultures, a PCR screen for expression of complement proteins, receptors and regulators was conducted. As shown in Figure 2.2A, product was visible for C1qs, C1s, C1r, and C4a. A faint band was observable for C3. There was strong expression of receptors C3aR and CR1l, and weaker expression of C5aR, CR1 and C1qR (Figure 2.2B, see Appendix B for gene names and approved nomenclature). A variety of complement regulators, including DAF, CFP, Cd59t1, CLU, CD59, CFB and CFH were also present in WT cultures (Figure 2.2C). These results suggest that a range of complement proteins, receptors and regulators are endogenous to the WT culture system.

2.3.2 C3 positive cells are present in primary hippocampal cultures

As C3 is the central protein of interest in this thesis, it was important to determine whether C3 mRNA is translated into protein. Hippocampal cultures were fixed at 5DIV and processed using immunocytochemistry with the antibody 11H9 (Hycult Biotechnology, Uden, NL). This antibody recognises both intact C3 and its cleavage products C3b, iC3b, C3d and C3dg. Negative controls were obtained both by staining 5DIV cells from C3$^{-/-}$ hippocampal cultures, and also by staining WT cells in absence of primary antibody to assess auto-fluorescence and non-specific secondary antibody binding. As seen in Figure 2.3A, C3/iC3b/C3d/C3dg positive cells were present in WT cultures, with 23.88 ± 3.77 cells per mm^2 in WT cultures, accounting for 4 ± 0.9 % of the total cell populations measured by DAPI (Figure 2.3F). Negative controls shows minimal signal (Figure 2.3B & C), suggesting that positive signal observed in WT cells represents
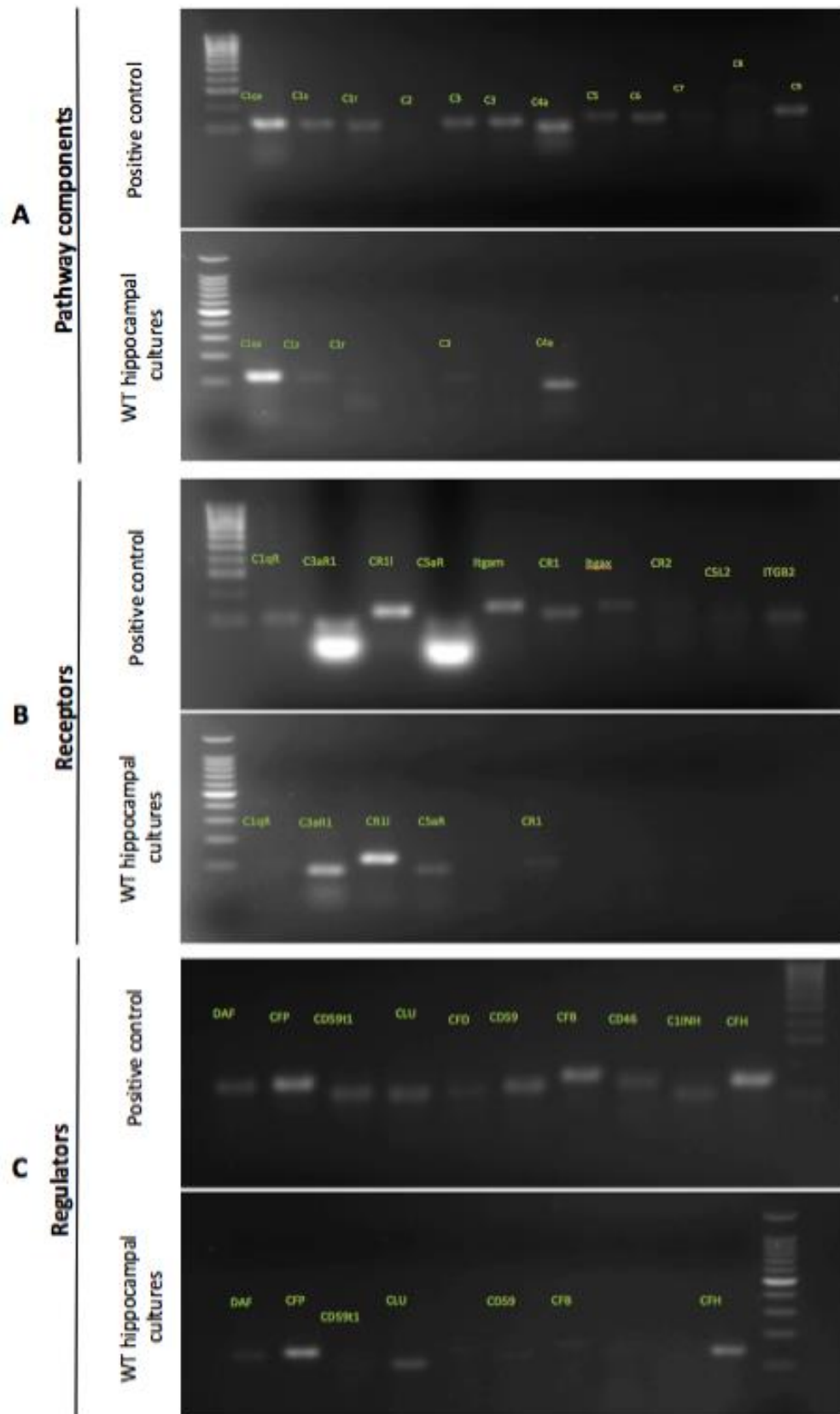
Figure 2.2 PCR screen for complement mRNA in wild type hippocampal cultures. All primers were tested on positive control samples of combined liver/brain RNA from WT mice**. A)** Complement proteins **B)** Complement receptors **C)** Complement regulators. N= pooled mRNA samples from 4 wells, from 1 experiment. See Appendix B for gene names and approved nomenclature

true expression. Whether any alteration to C3 levels occurred in C3aR$^{-/-}$ cultures was also investigated. Despite a significant difference in DAPI counts between WT 595.8 ± 76.63 per mm^2 and C3aR$^{-/-}$ cultures 289.4 ± 38.21 per mm^2 in these experiments (unpaired t test, $t_{(18)}$= 3.07, p < 0.01, Figure 2.3D), there were no differences in the number of C3$^+$ cells 13.05 ± 2.98 per mm^2 ($t_{(18)}$= 2.06, p = 0.053, Figure 2.3E) or the proportion of C3$^+$ cells in C3aR$^{-/-}$ cultures compared to WT (4 ± 1 %, $t_{(18)}$= 0.07, p=0.93). These data suggest that the genetic deletion of C3aR does not affect *in vitro* C3 expression levels in cultures deficient in this receptor.

2.3.3 Phenotype of C3 expressing cells

Having established C3 expression in culture, the phenotype of C3$^+$ cells was investigated. Since microglia are known to produce complement, WT and C3aR$^{-/-}$ primary hippocampal cultures were co stained with 11H9 to detect C3/iC3b/C3d/C3dg, and microglial marker Iba1 (Wako Chemicals USA, Richmond, VA, see Figure 2.4A). Results demonstrated that in WT cultures, approximately 24 ± 5 % of C3$^+$ cells were Iba1$^+$ (Figure 2.4B). In C3aR$^{-/-}$ cultures, 43 ± 14 % of C3$^+$ cells were Iba1$^+$, although this was not significantly different to WT ($t_{(18)}$= 1.42 , p=0.17, Figure 2.4B). Of the total population of Iba1$^+$ microglia, approximately 50 ± 9 % were C3$^+$ in WT cultures, whereas 72 ± 13 % of microglia were C3$^+$ in C3aR $^{-/-}$ cultures (Figure 2.4C). This difference did not reach statistical significance in an unpaired t-test ($t_{(18)}$= 1.39 , p=0.18).

Between genotypes, there was a comparable number of C3$^+$ Iba1$^+$ cells per mm^2 (WT 5.55 ± 1.32, C3aR$^{-/-}$ 4.72 ± 1.53; $t_{(18)}$= 0.40 , p=0.68, Figure 2.4E). Of the total cell population, C3 expressing microglia accounted for an extremely small proportion of cells in both WT (1 ± 0.3 %) and C3aR$^{-/-}$ (2 ± 0.7 %) cultures ($t_{(18)}$= 1.04 , p=0.30, Figure 2.4D). There were also no differences in the number of microglia present in WT, C3$^{-/-}$ or C3aR$^{-/-}$ cultures (see Appendix C). This data demonstrates that a significant proportion of C3
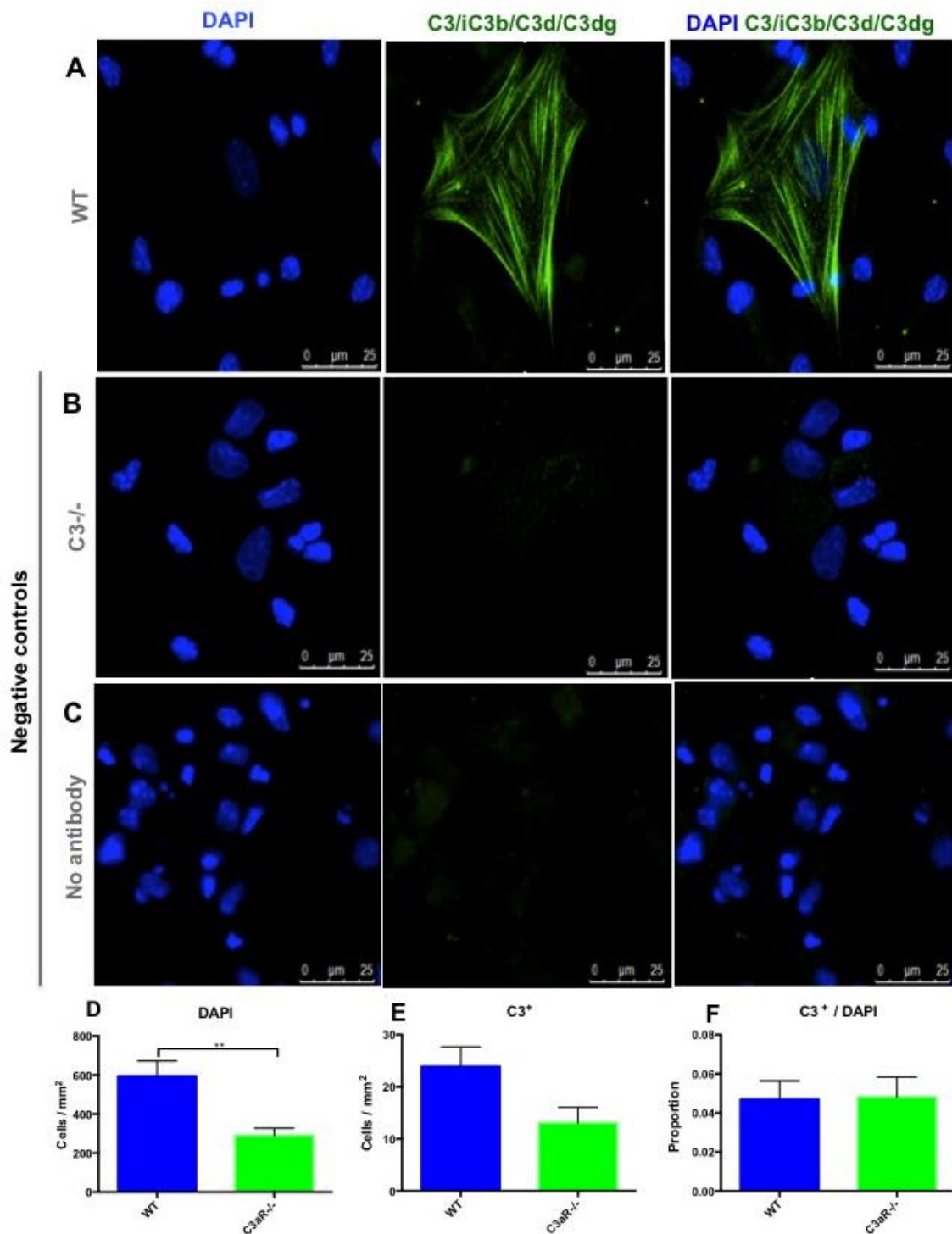
Figure 2.3. C3 expression in WT primary hippocampal cultures at 5DIV. A). Example of C3/iC3b/C3d/C3dg positive cells in WT hippocampal cultures. **B)** Negative control was conducted using C3$^{-/-}$ cells, showing minimal signal **C)** A negative control omitting the primary antibody showed minimal background staining. Figure comprises representative images taken from WT cultures and C3$^{/-}$ cultures. **D)** DAPI cells per mm^2 corresponding to data shown in **E** and **F. E)** Number of C3$^+$ cells per mm^2 **F)** C3$^+$ cells as a proportion of total cell count. WT N= 12 wells from 3 independent cultures, C3aR$^{-/-}$ N= 8 wells from 2 independent cultures. Scale bar = 25 μm Data points represent mean ± SEM. * = p < 0.05, ** = p < 0.01, *** = p < 0.001, **** = p<0.0001

83

expressing cells are microglia, and there are comparable numbers of these cells in WT and C3aR cultures.
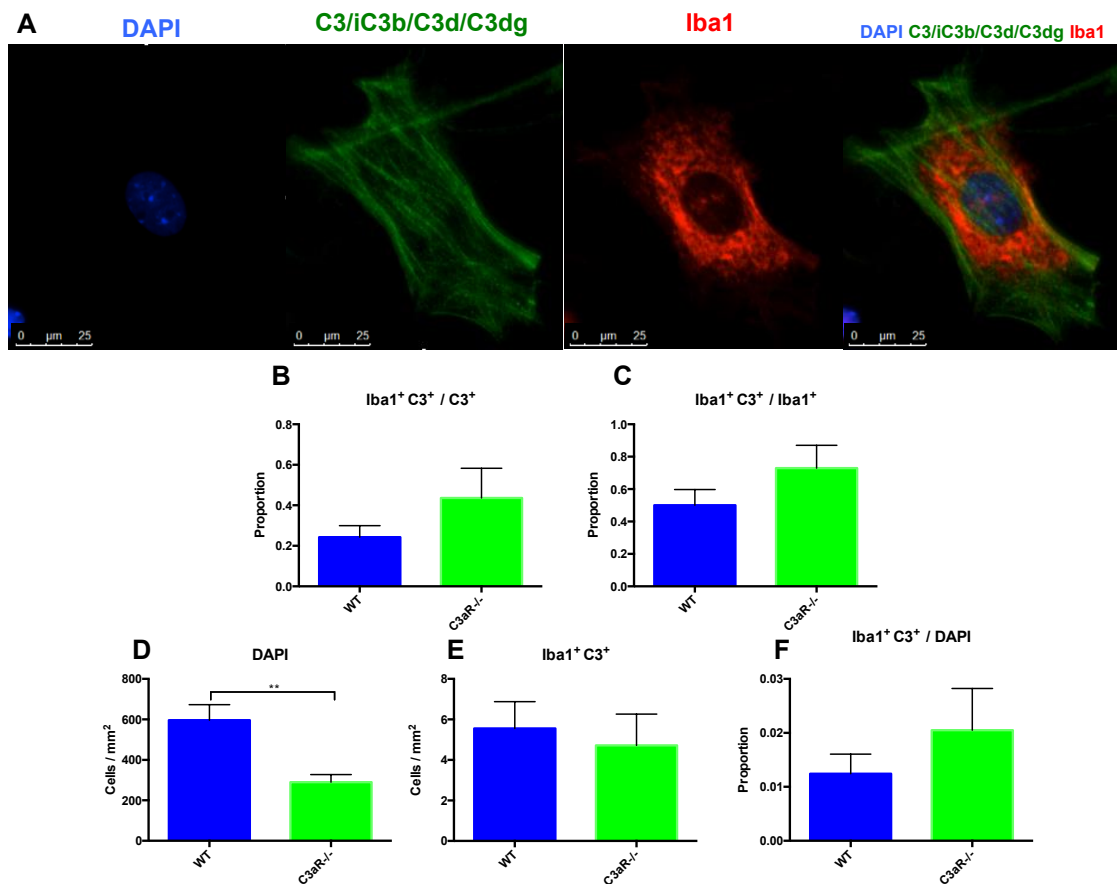
Figure 2.4. Phenotype of C3 expressing cells in primary hippocampal cultures. A) Example of C3 and Iba1 co-localisation. **B)** Proportion of C3$^+$ cells identified as microglia by Iba1 co-localisation **C)** Proportion of microglia expressing C3 **D)** Total cell counts measured by DAPI (cells per mm^2) for data shown in E and F. **E)** Number of Iba$^+$ C3$^+$ cells per mm^2 **F)** Iba$^+$ C3$^+$ cells as a proportion of total cell counts. WT N= 12 wells from 3 independent cultures, C3aR$^{-/-}$ N= 8 wells from 2 independent cultures. Data points represent mean ± SEM. Scale bar = 25 μm *=p<0.05,**=p<0.01,***=p<0.001,****=p<0.0001.

2.3.4 C3 activation in culture

The previous data demonstrates that several complement factors are expressed at the mRNA level, and C3 protein is present in primary hippocampal cultures. However, since the 11H9 antibody detects both intact

C3 and its breakdown products, it cannot be concluded that C3 is activated in culture based on immunocytochemistry alone. Therefore, sandwich ELISA was used to determine whether C3 is activated to produce the breakdown product C3a. In WT, C3aR and C3$^{-/-}$ cultures, the values obtained were below the given detection limit of the kit. As shown in Figure 2.5, 2.86 ± 1.7 pg / ml of C3a was detected in WT hippocampal cultures, compared to 1.65 ± 2.8 pg / ml in C3$^{-/-}$ and 2.47 ± 1.26 pg / ml in C3aR$^{-/-}$ cultures. WT microglia treated with LPS showed higher levels of C3a however, with 8.29 ± 3.65 pg / ml. These results suggest extremely low levels of C3 activation in culture, which was below the detectable range of the ELISA kit used.
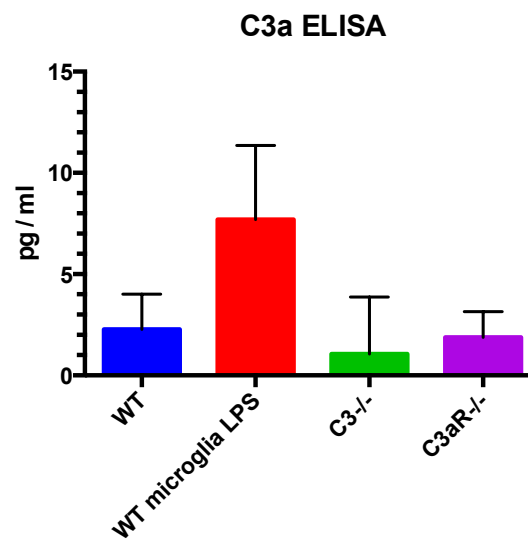
Figure 2.5. Activation of C3 in culture using C3a sandwich ELISA. WT N = 3 supernatant samples analysed in duplicate from three independent cultures, WT microglia N= 2 supernatant samples analysed in duplicate from two independent cultures, C3-/- N= 3 supernatant samples analysed in duplicate from 3 independent cultures, and C3aR-/- N= 2 supernatant samples analysed in duplicate from 2 independent cultures. Data points represent mean ± SEM.

2.3.5 Effect of C3/C3aR deficiency on total cell number

I next investigated whether the absence of C3 or C3aR had any effects upon hippocampal cells *in vitro*. Cultures were maintained for either 3, 5 or 14 days *in vitro* (DIV)*,* before being fixed and stained. A 3 (genotype; WT, C3$^{-/-}$, C3aR$^{-/-}$) $\times$ 3 (time-point; 3DIV, 5DIV, 14DIV) between-subjects ANOVA was carried out to analyse the effects of genotype on the total number of cells per mm^2, measured by DAPI counterstaining, at each time-point. Results showed a significant main effect of time-point ($F_{(2,200)}$= 26.43, p < 0.0001, Figure 2.6), but no main effect of genotype ($F_{(2,200)}$= 2.81, p = 0.06). The interaction of these two factors was not significant ($F_{(4,200)}$= 1.68, p =0.15).

Tukey post-hoc comparisons were made across genotypes between the three levels of the time-point factor. Results showed a significant increase in cell number between 3DIV (234.43 ± 14.49 cells per mm^2) and 5DIV (546.91 ± 22.66 cells per mm^2, p < 0.0001) across genotypes, and between 3DIV and 14DIV (503.12 ± 19.07 cells per mm^2, p < 0.0001) across genotypes. There were no significant differences between total cell counts at 5DIV and 14DIV however (p = 0.42). These results suggest that cell expansion peaked between 3 and 5DIV, and was stable from thereon. This pattern was not affected by the absence of C3/C3aR signalling. However, it was noted that considerable variability occurred in total cell counts between separate isolations. Therefore, while this was not influenced by genotype, analyses of DAPI cells per mm^2 are included each in the following experiments in order to aid interpretation of changes in cell types per mm^2.
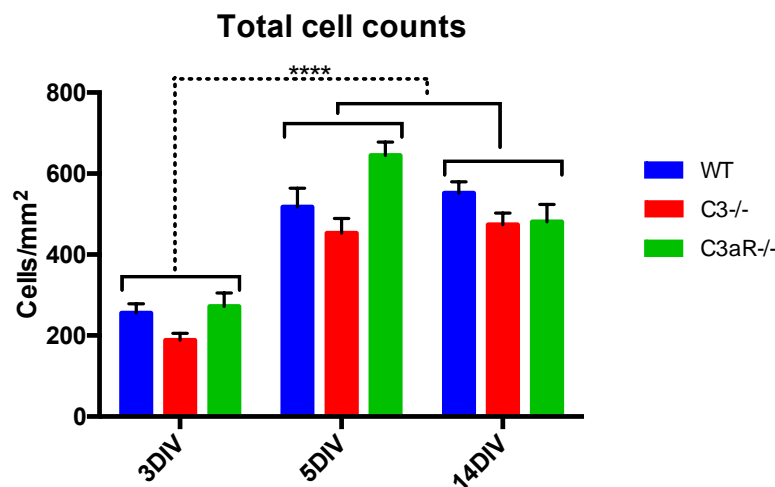
Total cell counts

Figure 2.6 Total cell counts over 3, 5 and 14 days *in vitro*. 3DIV WT N= 12 from 2 separate experiments, C3$^{-/-}$ N= 12 from 2 separate experiments, C3aR$^{-/-}$ N= 8 from 2 separate experiments. 5DIV WT N= 33 from 8 independent cultures, C3$^{-/-}$ N= 44 from 9 independent cultures, C3aR$^{-/-}$ N= 52 from 13 independent cultures. 14DIV WT N=17 from 3 independent cultures, C3$^{-/-}$ N= 18 from 3 independent cultures, C3aR$^{-/-}$ N= 13 from 3 independent cultures. Data points represent mean ± SEM. * = p < 0.05, ** = p < 0.01, *** = p < 0.001, **** = p < 0.0001.

2.3.6 Cell survival and viability

In order to examine the effect of C3/C3aR deficiency on cell viability, 5DIV cells were incubated with PI to mark dead or dying cells and MitoTracker® Green to mark viable cells. Cells were also counterstained with DAPI to label all nuclei.

There was variability in the total cell counts (measured by DAPI cells per mm^2) between genotypes in these experiments, which was borderline significant ($F_{(2,38)}$= 3.150, p = 0.054, Figure 2.7A). There was a significant difference in the number of PI$^+$ cells between genotypes ($F_{(2,38)}$= 3.355, p < 0.05, Figure 2.7B), and post-hoc analyses showed a significant increase in C3aR$^{-/-}$ PI$^+$ cells (139.60 ± 12.75 per mm^2) compared to C3$^{-/-}$ cultures (96.59 ± 11.88 per mm^2, p < 0.05), consistent with an increase in overall DAPI cells in C3aR$^{-/-}$ cultures. C3aR$^{-/-}$ did not significantly differ to WT (112.6 ± 10.36

per mm^2, p = 0.28). There was no significant difference in PI$^+$ as a proportion of the total cell count however ($F_{(2,38)}$=0.46, p= 0.63, Figure 2.7C).

As seen in Figure 2.7D, there was a trend towards a decrease in MitoTracker$^+$ cells in both C3 and C3aR deficient cultures compared to WT ($F_{(2,18)}$=3.84, p < 0.05). This decrease was significant only in C3aR$^{-/-}$ cultures (454.30 ± 53.64 per mm^2) compared to WT (701.10 ± 78.01 mm^2, p < 0.05). The number of MitoTracker$^+$ cells per mm^2 found in C3$^{-/-}$ cultures (463.20 ± 52.11 mm^2) was not significantly different to WT (p= 0.12). There were no proportional differences in MitoTracker$^+$ cells between WT (80 ± 1 %), C3$^{-/-}$ (71 ± 2 %) or C3aR$^{-/-}$ (73 ± 2 %) cultures at 5DIV however ($F_{(2,18)}$=1.86, p=0.18, Figure 2.7E). These results suggest that C3/C3aR does not affect the viability or survival of cells in culture.
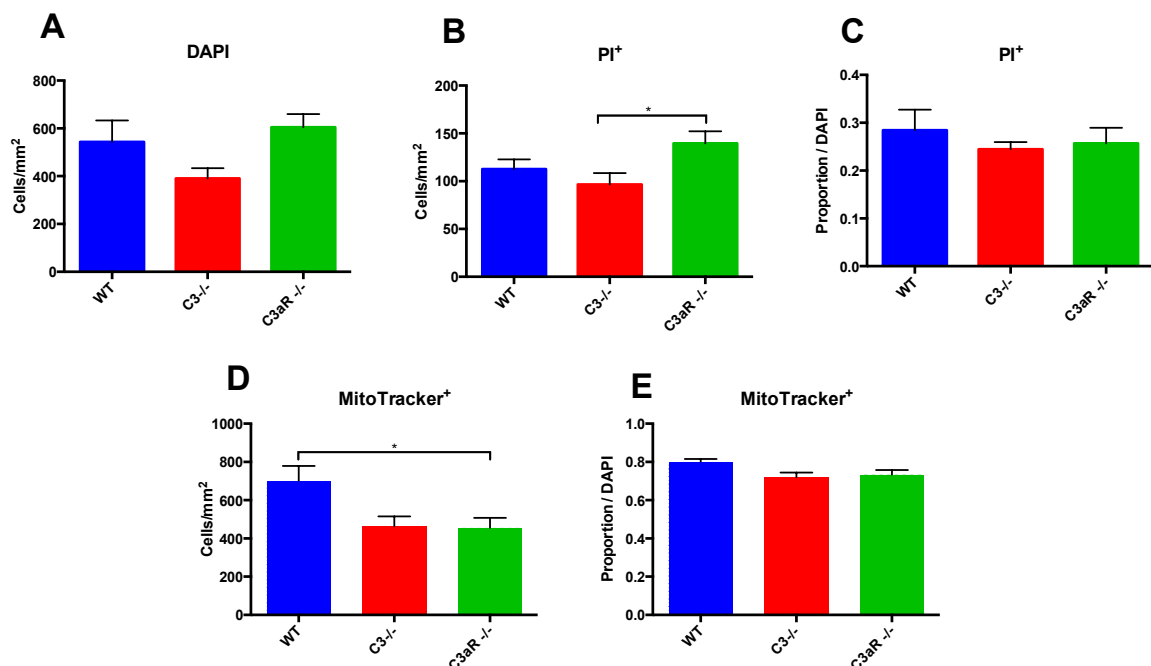
Figure 2.7. Survival and viability are unchanged in C3$^{-/-}$ and C3aR$^{-/-}$ cultures at 5DIV. A) DAPI total cell counts. **B)** Mean number of PI cells per mm^2 **C)** Proportion of total cell count accounted for by PI positive cells **D)** Mean number of MitoTracker cells per mm^2 **E)** Proportion of total cell count accounted for by MitoTracker positive cells. WT N= 13 from 3 independent cultures, C3$^{-/-}$ N= 16 from 3 independent cultures and C3aR$^{-/-}$ N= 12 from 3 independent cultures. Data points represent mean ± SEM. * = p < 0.05, ** = p < 0.01, *** = p < 0.001, **** = p < 0.0001.

2.3.7 The effect of C3/C3aR deficiency on cell phenotypes

C3/C3aR deficiency causes a phenotypic shift in early progenitor cell phenotypes

Having observed no alterations in cell number, survival or viability, I moved on to examine whether C3/C3aR deficiency affected cell fate. Primary hippocampal cultures were grown for 5DIV before being fixed and co-stained for Nestin and GFAP. Co-localisation of Nestin and GFAP (Nestin$^+$ GFAP$^+$) indicates a radial glial stem cell phenotype, classified as type 1 or type 2a cells (Kempermann et al., 2004). Cells expressing nestin in absence of GFAP were classified as type 2a or 2b cells, as type 2a can have either presence or absence of GFAP expression (see Section 1.4).

In this set of experiments, there was a significant difference in the total cell counts indicated by DAPI, between genotypes ($F_{(2,31)}$=11.63, $p > 0.001$, Figure 2.8B). Post hoc analyses showed a significant increase in C3aR$^{-/-}$ DAPI cells per mm^2 (700.4 ± 49.73), compared to both WT (402.0 ± 59.91 mm^2; $p < 0.0001$) and C3$^{-/-}$ cultures (460.5 ± 18.17 mm^2; $p < 0.01$). Total cell counts in C3$^{-/-}$ cultures did not significantly differ to WT ($p = 0.73$).

The number of type 1/2a cells, characterised by co-expression of Nestin and GFAP, was significantly different between genotypes ($F_{(2,31)}$=15.68, $p < 0.0001$, Figure 2.8C). A greater number of type 1/2a cells were present in both C3$^{-/-}$ (293.6 ± 17.11 per mm^2) and C3aR$^{-/-}$ cultures (370.2 ± 25.36 per mm^2) compared to WT (166.3 ± 26.41 mm^2; $p < 0.01$ and $p < 0.0001$, respectively). Furthermore, type 1/2a cells as a proportion of the total DAPI count were also significantly altered between genotypes ($F_{(2,31)}$=17.55, $p < 0.0001$, Figure 2.8D), again due to a higher proportion of type 1/2a cells in C3$^{-/-}$ (63 ± 2 %) and C3aR$^{-/-}$ (57 ± 2 %) cultures compared to WT (41 ± 1 %; $p < 0.0001$ and $p < 0.001$, respectively).

There were also significant changes in the number of type 2a/2b cells between genotypes ($F_{(2,31)}$=5.53, $p < 0.01$, Figure 2.8E), which arose due to

greater numbers of this cell type in C3aR^{-/-} cultures (161.7 ± 21.59 per mm^2) compared to C3^{-/-} (70.31 ± 11.94 per mm^2, $p < 0.01$), but this was not significantly different to WT (134.4 ± 19.04 per mm^2, $p = 0.63$). This difference likely reflected the increase in overall DAPI cells seen in C3aR^{-/-} cultures. WT and C3^{-/-} cultures had comparable numbers of this cell type ($p = 0.13$). There were also significant differences in the proportion of type 2a/2b cells between genotypes ($F_{(2,31)}=11.58$, $p < 0.001$, Figure 2.8F). Type 2a/2b cells accounted for a smaller proportion of the total cell count in C3^{-/-} (15 ± 2 %) and C3aR^{-/-} (21 ± 2 %) cultures than in WT cultures (34 ± 2 %; $p < 0.0001$ and $p < 0.01$, respectively). This data suggests that C3/C3aR signalling favours the differentiation of type 1/2a cells into type 2a/2b cells.

2.3.8 C3/C3aR deficiency increases the proliferation of progenitor cells

Type 1, 2a and 2b cells are mitotic (Kempermann et al., 2004) and I therefore investigated whether a change in their proliferation could account for the phenotypic shifts observed. Cultures were maintained for 5DIV before EdU was added for the terminal 6 hours prior to fixation. Immunocytochemistry was then performed to label cells expressing Nestin, GFAP and EdU (example shown in Figure 2.8A). This allowed the identification of proliferating type 1 and 2a cells (Nestin[+] GFAP[+] EdU[+]) and proliferating type 2a and 2b cells (Nestin[+] GFAP[-] EdU[+]).

In this set of experiments, there were significant differences in total cell counts between genotypes ($F_{(2,17)}=7.79$, $p < 0.01$, Figure 2.8G). C3aR^{-/-} cultures had a greater number of DAPI nuclei per mm^2 (722.1 ± 73.16) compared to WT (402.0 ± 59.01 per mm^2, $p < 0.01$) and C3^{-/-} cultures (442.2 ± 13.56 per mm^2, $p < 0.05$). The number of DAPI cells per mm^2 in C3^{-/-} cultures was not significantly different to WT ($p = 0.92$).

There was a significant difference in the number of proliferating type 1/2a cells between genotypes ($F_{(2,17)}=17.54$, $p < 0.0001$, Figure 8h). Both C3^{-/-} (145.1 ± 18.29 per mm^2) and C3aR^{-/-} (211.6 ± 26.18 per mm^2) cultures had a

greater number of EdU$^+$ type 1 and type 2a cells than was observed in WT cultures at 5DIV (Figure 2.8H, 59.02 ± 7.20 per mm^2; p < 0.05 and p < 0.0001, respectively). There were also changes in the proportion of proliferating type 1/2a cells between genotypes ($F_{(2,17)}$=15.45, p < 0.001, Figure 2.8I). Of the total type 1/2a cell population, approximately double the proportion was proliferating in C3$^{-/-}$ (32 ± 3 %) and C3aR$^{-/-}$ (29 ± 1 %) cultures compared to WT (15 ± 2 %, both comparisons p < 0.001). The proportion of proliferating type 1/2a cells was comparable between C3$^{-/-}$ and C3aR$^{-/-}$ cultures (p= 0.60).

There were also changes in the number of proliferating type 2a/2b cells at 5DIV ($F_{(2,17)}$=6.11, p < 0.01, Figure 2.8J). There were more proliferating type 2a/2b cells per mm^2 in C3aR$^{-/-}$ cultures (123.0 ± 21.36 per mm^2) compared to WT (48.49 ± 7.79 per mm^2, p < 0.01). There were no significant differences between C3$^{-/-}$ (65.95 ± 17.49 per mm^2) and WT (p = 0.79) or C3$^{-/-}$ and C3aR$^{-/-}$ (p= 0.11) however. The proportion of the total type 2a/2b population accounted for by proliferating type 2a/2b cells was significantly different between genotypes ($F_{(2,17)}$=6.51, p < 0.01, Figure 2.8K), with a near doubling of this cell type in C3$^{-/-}$ (71 ± 17 %) and C3aR$^{-/-}$ (69 ± 5 %) cultures compared to WT (38 ± 4 %; p < 0.05 and p < 0.01, respectively). These results demonstrate that C3/C3aR signalling may suppress the proliferation of type 1 and type 2a/2b cells.
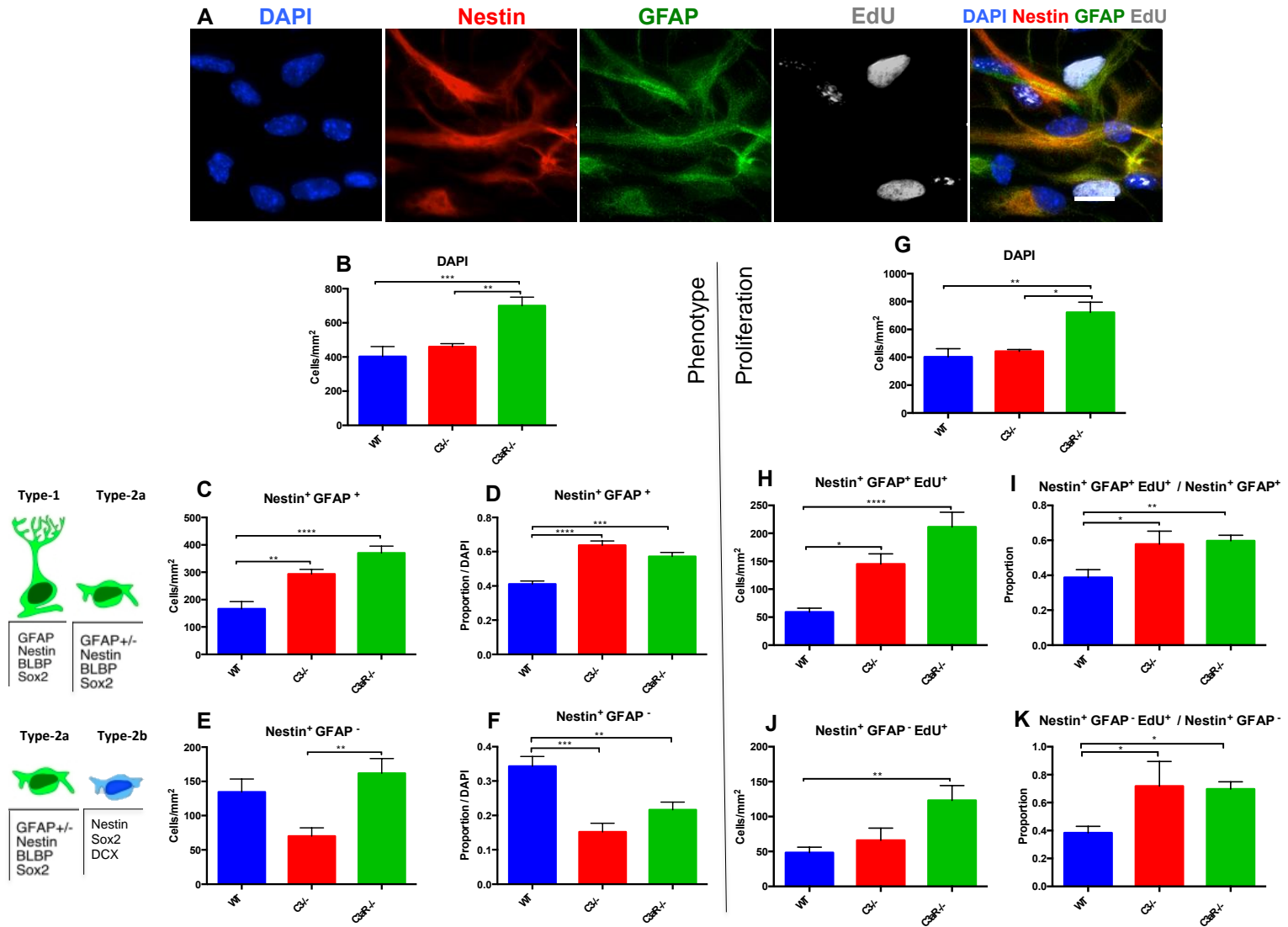
Figure 2.8. At 5DIV, C3/C3aR deficiency causes a phenotypic shift and alters proliferation. A) Example of Nestin/ GFAP / EdU immunostaining **B)** Total cell counts for Nestin/GFAP experiments measured by DAPI. **C)** Nestin⁺ GFAP⁺ cells per mm² **D)** Nestin⁺ GFAP⁺ as a proportion of DAPI. **E)** Nestin⁺ GFAP⁻ cells per mm² **F)** Nestin⁺ GFAP⁻ as a proportion of DAPI **G)** Total cell counts for Nestin/GFAP/EdU experiments. **H)** Nestin⁺ GFAP⁺ EdU⁺ cells per mm². **I)** Nestin⁺ GFAP⁺EdU⁺ as a proportion of Nestin⁺ GFAP⁺. **J)** Nestin⁺ GFAP⁻ EdU⁺ cells per mm² **K)** Nestin⁺ GFAP⁻ EdU⁺ as a proportion of Nestin⁺ GFAP⁻. WT N= 9 from 2 independent cultures, C3⁻/⁻ N= 10 from 2 independent cultures and C3aR⁻/⁻ N= 16 from 4 independent cultures. Data points represent mean ± SEM. Scale bar = 5 μm. * = p < 0.05, ** = p < 0.01, *** = p < 0.001, **** = p < 0.0001.

2.3.9 C3/C3aR deficiency decreases DCX⁺ neuronal progenitors

To assess whether the early phenotypic shift observed had a knock-on effect on later cell types of the neurogenic lineage, I used the marker DCX to label immature neuronal cells. This marker is expressed by type 2b cells, type 3 cells and early post-mitotic neurons (Kempermann et al., 2004, see Section 1.4). Primary hippocampal cultures were maintained for 5DIV before being fixed and processed using immunocytochemistry and stained for DCX and TUJ1 (see Figure 2.9A). Since TUJ1 is expressed later than DCX in our culture system, and does not overlap with Nestin expression, co-staining of DCX and TUJ1 allows discrimination of type 2b (DCX⁺ TUJ1⁻) versus type 3 (DCX⁺ TUJ1⁺) cells.

There was a statistically significant increase in total cell counts ($F_{(2,25)}$=4.1, p<0.05, Figure 2.9B) in this set of experiments, which was attributable to greater cells per mm² in C3aR⁻/⁻ (581.67 ± 76.40) cultures compared to C3⁻/⁻ (295.1 ± 55.08 per mm², p < 0.05), although this increase was not significantly different to WT (456.1 ± 65.98 per mm², p = 0.42).

There was a trend towards a decrease in the number of DCX⁺ TUJ1⁻ type 2b cells per mm² in both C3⁻/⁻ and C3aR⁻/⁻ cultures compared to WT (Overall ANOVA $F_{(2,25)}$=5.44, p < 0.001, Figure 2.9C) however only C3⁻/⁻ (18.01 ± 6.72 per mm²) reached statistical significance when compared to WT levels (82.56 ± 21.76 per mm², p < 0.01). C3⁻/⁻ and C3aR⁻/⁻ (43.53 ± 8.69 per mm²) cultures showed comparable levels of DCX⁺ TUJ1⁻ cells per mm² (p = 0.34). As seen in Figure 2.9D, there was a significant proportional decrease in DCX⁺ TUJ1⁻ cells in both C3 ⁻/⁻ (6 ± 2 %) and C3aR⁻/⁻ cultures (8 ± 1 %) compared to WT (16 ± 2 %; both comparisons p < 0.05, overall ANOVA $F_{(2,25)}$=5.60, p < 0.001).
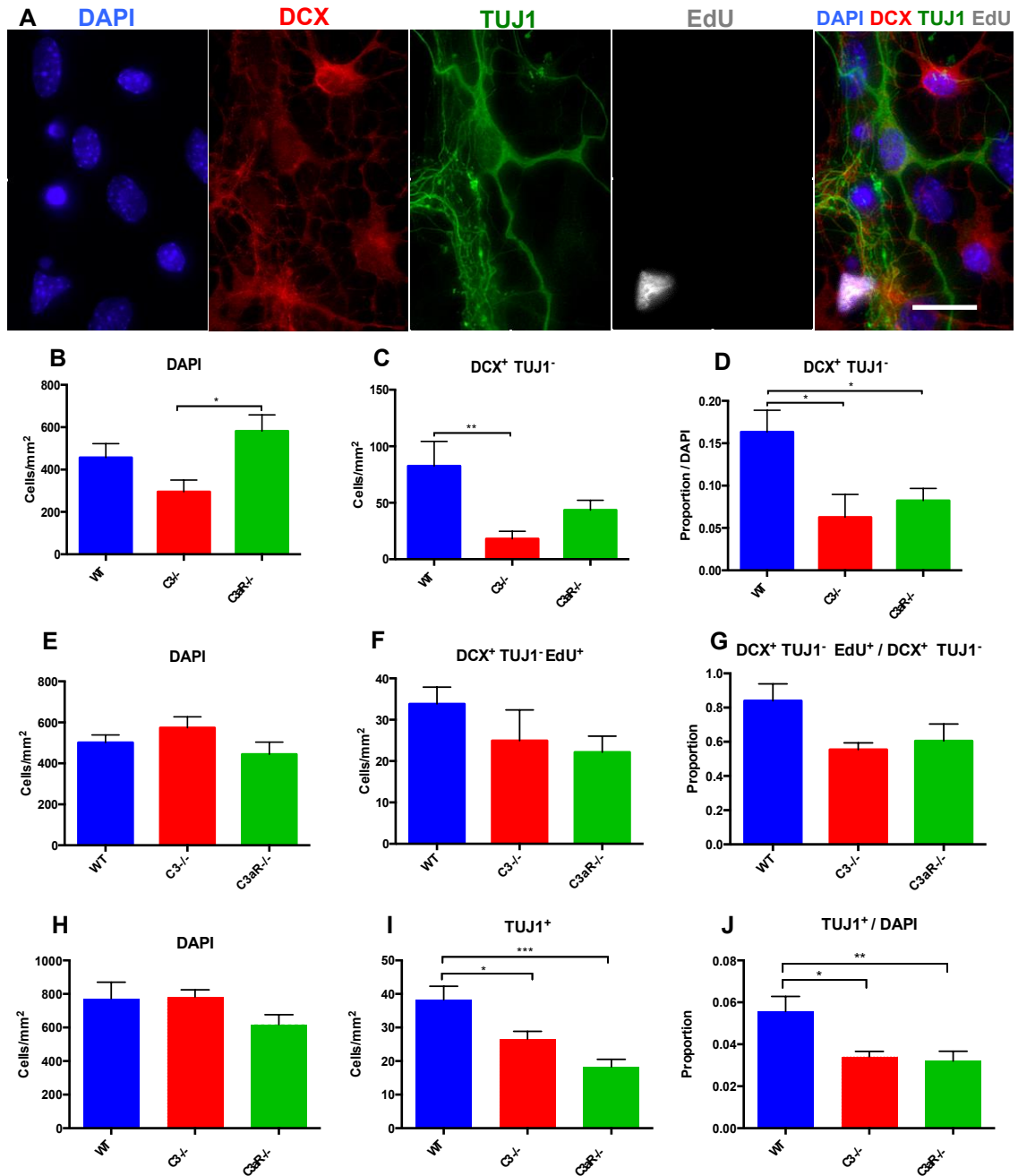
Figure 2.9. C3/C3aR deficiency causes a decrease in early neuronal progenitors and immature neuronal phenotypes. A) Example of DCX TUJ1 EdU immunostaining **B)** DAPI cells per mm^2 for DCX TUJ1 co-staining experiment. **C)** DCX+TUJ1- cells per mm^2 **D)** DCX+TUJ1- as a proportion of total cell count **E)** DAPI counts for DCX/TUJ1/EdU experiment. **F)** DCX+TUJ1- EdU+ cells per mm^2 **G)** DCX+TUJ1- EdU+ as a proportion of DCX+TUJ1- . N WT = 8 from 2 independent experiments, C3-/- N= 8 from 2 independent experiments, C3aR-/- N= 12 from 3 independent experiments. **H)** DAPI cells per mm^2 for 6DIV TUJ1 data. TUJ1+ density per mm^2 is shown in **I** and proportion over DAPI in **J.** Data represents WT N = 13, C3-/- N= 13, C3aR -/- N= 12, from three separate cultures per genotype. Data points represent mean ± SEM. Scale bar = 5 μm * = p < 0.05, ** = p < 0.01, *** = p < 0.001, **** = p < 0.0001

In the present culture system, cells expressing DCX[+] in the absence of TUJ1 appear to be type 2b cells due to their co-expression of nestin, and ability to divide. Therefore I also investigated the proliferation of these cells using EdU. Between genotypes, there were no differences in the number of DCX[+] TUJ1^{-} cells incorporating EdU per mm^2 ($F_{(2,25)}$=1.53, p = 0.23, Figure 2.9F). When EdU[+] DCX[+] TUJ1^{-} cells were considered as a proportion of the entire DCX[+] TUJ1^{-} population however, there was a trend towards a decrease in both C3^{-/-} (55 ± 4 %) and C3aR^{-/-} (60 ± 9 %) compared to WT (83 ± 9 %). This difference failed to meet conventional levels of statistical significance however ($F_{(2,25)}$=3.06, p = 0.06, Figure 2.9G). Therefore, C3/C3aR deficiency decreases the number and proportion of type 2b cells in culture, and may affect their proliferation.

2.3.10 C3/C3aR deficiency decreases TUJ1^{+} immature neuronal cells at 6DIV

In order to assess mature neuronal phenotypes, primary hippocampal cultures were maintained for 5DIV under standard conditions, before growth factors were withdrawn for the terminal 24 hours to slow proliferation and allow differentiation. Cells were then fixed and stained for TUJ1. In this particular culture system, TUJ1 cells are exclusively post-mitotic. These cells can therefore be thought of as a more mature neuronal phenotype than the aforementioned DCX[+] TUJ1^{-} phenotype.

There were no differences in the total cell counts between genotypes in this set of experiments ($F_{(2.35)}$=1.68, p = 0.19, Figure 2.9H). There was a decrease in the number of TUJ1 cells per mm^2 however ($F_{(2.35)}$=11.33, p < 0.001, Figure 2.9I) in both C3^{-/-} (26.58 ± 2.26 per mm^2) and C3aR^{-/-} (18.29 ± 2.02 per mm^2) compared to WT (38.28 ± 3.9 per mm^2; p < 0.05 and p < 0.001, respectively). TUJ1^{+} cells per mm^2 were comparable between C3^{-/-} and C3aR^{-/-} cultures (p = 0.13). The proportion of the total cell count accounted for by TUJ1^{+} cells varied between genotypes ($F_{(2.35)}$=6.53, p < 0.01, Figure 2.9J), with a smaller

proportion of TUJ1 cells in both C3$^{-/-}$ (3 ± 0.2 %) and C3aR$^{-/-}$ (3 ± 0.4 %) cultures compared to WT (5 ± 0.07 %; p < 0.05 and p < 0.01 respectively). The TUJ1$^+$ proportion in C3$^{-/-}$ and C3aR$^{-/-}$ cultures did not significantly differ (p = 0.95). These results show that C3/C3aR deficiency also compromised neuronal maturation.

2.3.11 Neurogenesis in C3/C3aR deficient cultures normalises by 14DIV

In order to assess whether the observed decrease in neuronal progenitors at 5DIV and immature neurons at 6DIV resulted in a deficit in subsequent neuronal maturation, primary hippocampal cultures were maintained for a further 9DIV after growth factor withdrawal at 5DIV. Cells were fixed and stained for TUJ1 alongside mature neuronal marker NeuN in order to determine the neuronal maturation (see Figure 2.10A). Co-expression of these markers enabled identification of mature neurons. Cultures were also co-stained with GFAP, to assess the number of cells adopting a glial as opposed to a neuronal phenotype.

As seen in Figure 2.10B, DAPI cells per mm^2 were similar between genotypes ($F_{(2,45)}$=1.83, p = 0.17). Despite the aforementioned decrease in TUJ1 cells at 6DIV, the number of these cells was comparable between genotypes at 14DIV ($F_{(2,45)}$=2.32, p = 0.10, Figure 2.10C). TUJ1$^+$ cells as a proportion of the total cell count was also unaffected by genotype ($F_{(2,45)}$=1.52, p = 0.22, Figure 2.10D). Furthermore, the number of NeuN$^+$ cells was unchanged between genotypes in both density ($F_{(2,45)}$=2.07, p = 0.13, Figure 2.10G) and as a proportion of the total cell population ($F_{(2,45)}$=0.91, p=0.40, Figure 2.10H). There were no differences in the number of mature neurons (TUJ1$^+$ NeuN$^+$) per mm^2 ($F_{(2,45)}$=2.07, p = 0.13, Figure 2.10I). Of the total TUJ1$^+$ population, C3/C3aR deficiency did not affect the proportion of TUJ1$^+$ cells that co-expressed NeuN ($F_{(2,45)}$=0.07, p = 0.93, Figure 2.10J).

In all genotypes, many more cells adopted a glial rather than neuronal phenotype by 14DIV. Across all genotypes, approximately 76 ± 1 % of the total cell population expressed GFAP, whereas only 6 ± 0.5 % of the total cell population expressed TUJ1 (data not shown, N= 42 from 12 independent cultures, pooled across genotype). The density of GFAP$^+$ cells was equal between genotypes ($F_{(2,45)}$=1.19, p = 0.31, Figure 2.10E) as was the proportion of GFAP cells relative to total DAPI counts ($F_{(2,45)}$=0.93, p = 0.40, Figure 2.10F). These results suggest that the previously observed differences in immature neuronal cells were abolished after 14DIV.

2.3.12 Summary of *in vitro* results

These results show that C3 is expressed in NPC cultures, and is able to directly influence cells isolated from the postnatal mouse hippocampus. Data indicated an increase in the number of type 1/2a cells in the absence of C3/C3aR signalling, and a subsequent decrease in type 2a/2b cells. There were also fewer type 3 cells and post-mitotic immature neurons in the absence of C3/C3aR. Furthermore, C3a/C3aR deficiency altered proliferation in culture. Type 1/2a cells showed increased mitotic activity, whereas there was a trend towards reduced proliferation in type 2b cells. These effects were noted in the absence of a general survival effect upon cells in cultures. These results suggest that C3/C3aR signalling jointly causes a fate shift and a change in the proliferative properties of early progenitor cells. Having observed these results, I next questioned whether C3/C3aR signalling exerted similar effects upon AHN *in vivo.*

Figure 2.10. Neuronal maturation normalises after 14 days in culture. A) Example of TUJ1 / NeuN/ GFAP immunostaining. **B)** DAPI cells per mm². TUJ1+ density **(C)** and proportion **(D). E)** GFAP cells per mm² **F)** GFAP cells as a proportion of DAPI **G)** NeuN+ cells per mm² **H)** NeuN+ as a proportion of DAPI **I)** TUJ1+ NeuN+ cells per mm² **J)** Proportion of TUJ1+ cells expressing NeuN. Data represents WT N= 17 from 3 independent experiments, C3-/- N= 18 from 3 independent experiments, C3aR -/- N= 13 from 4 separate experiments. Data points represent mean ± S.E.M Scale bar = 5 µm.

2.3.13 *In vivo* neurogenesis

In order to assess both the phenotype and proliferation of cells in the DG, sections were co-stained with Ki67 to identify proliferating cells, GFAP to label type 1 radial glia, and DCX to demarcate immature neuronal progenitors. An example of staining is shown in Figure 2.11. As highlighted in Section 1.2.1, topographical differences in neurogenesis and the functions of adult born neurons exist along the longitudinal (i.e., anterior / posterior) hippocampal axis (Jinno, 2011; Snyder et al., 2009). The distribution of newly born neurons also varies along the transverse dentate axis, which is separated into the suprapyramidal and infrapyramidal blades (Snyder et al., 2009). Therefore, the distribution of the major cell types was investigated according to these anatomical distinctions.

2.3.14 Dentate size is unaltered in the absence of C3/C3aR

Firstly, to check for differences in DG size between genotypes, the inner border of the GCL (corresponding to the SGZ) was measured in each section of a stereological sample from 6 animals per genotype. There were no differences in the average length of the GCL in WT (2,045 ± 82.51 μm), C3$^{-/-}$ (1,980 ± 98.86 μm) or C3aR$^{-/-}$ (2,010 ± 104.70 μm) sections throughout the entire hippocampus ($F_{(2,211)}$=0.11, p = 0.88, Figure 2.12A). There were also no differences in the length of the suprapyramidal blade of the DG between genotypes (WT 1,208 ± 43.83 μm; C3$^{-/-}$ 1,208 ± 53.59 μm; C3aR$^{-/-}$ 1,258 ± 65.20 μm; $F_{(2,177)}$=0.27, p = 0.76, Figure 2.12B), nor the infrapyramidal blade (WT 1,005 ± 26.45 μm; C3$^{-/-}$ 973.0 ± 33.91 μm; C3aR$^{-/-}$ 968.2 ± 34.73 μm; $F_{(2,211)}$=0.39, p = 0.67, Figure 2.12B). Therefore, all cell counts were analysed as raw data per animal, as opposed to the cell number normalised per μm.
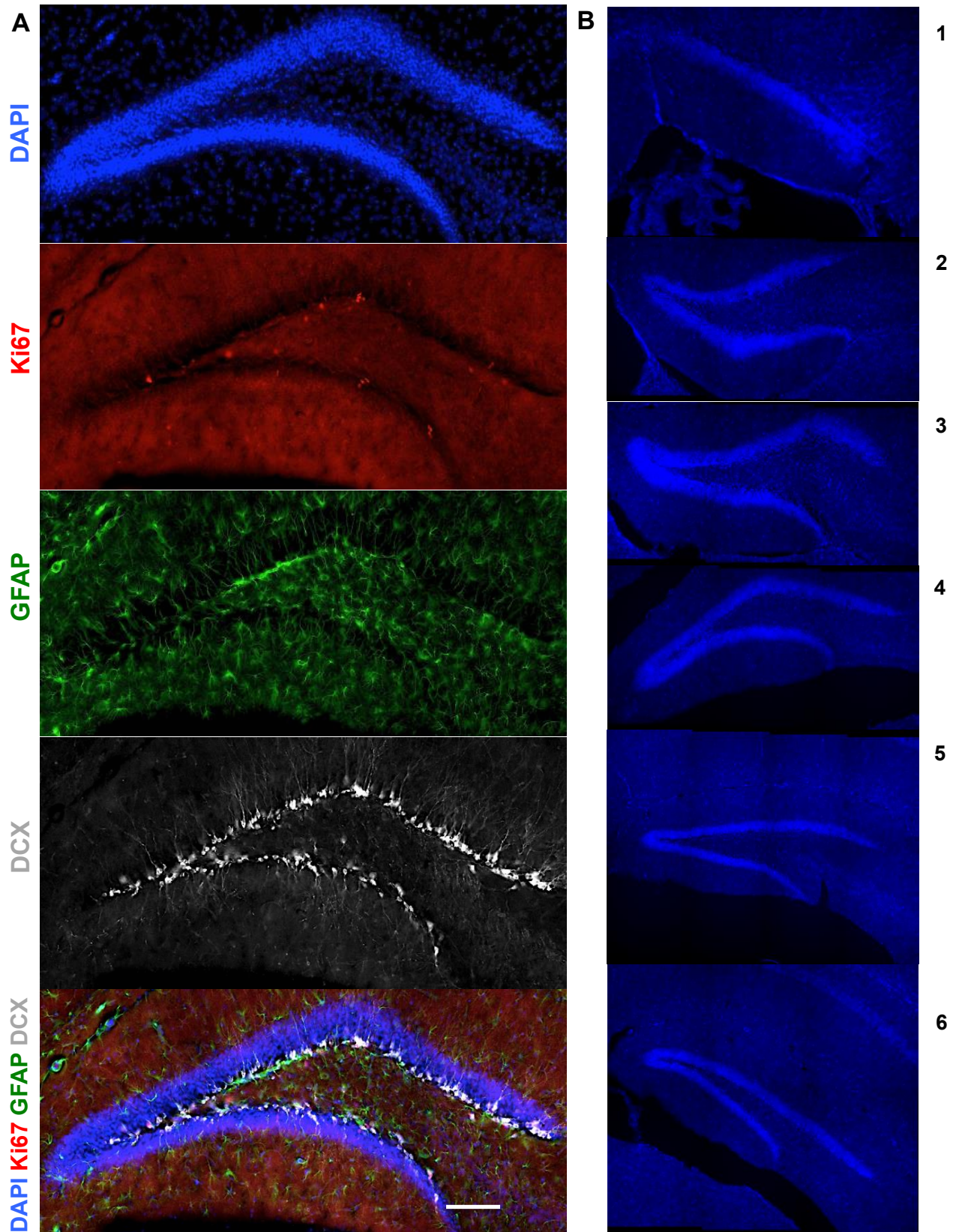
Figure 2.11. A) Representative example of Ki67 (red) GFAP (green) and DCX (grey) immunostaining in the adult mouse DG. Scale bar = 150 μm. **B)** Representative example of sections 1 to 6. In regional analyses, sections 1 to 3 were grouped and considered anterior hippocampus, whereas sections 3 to 6 were regarded as posterior hippocampus.

100
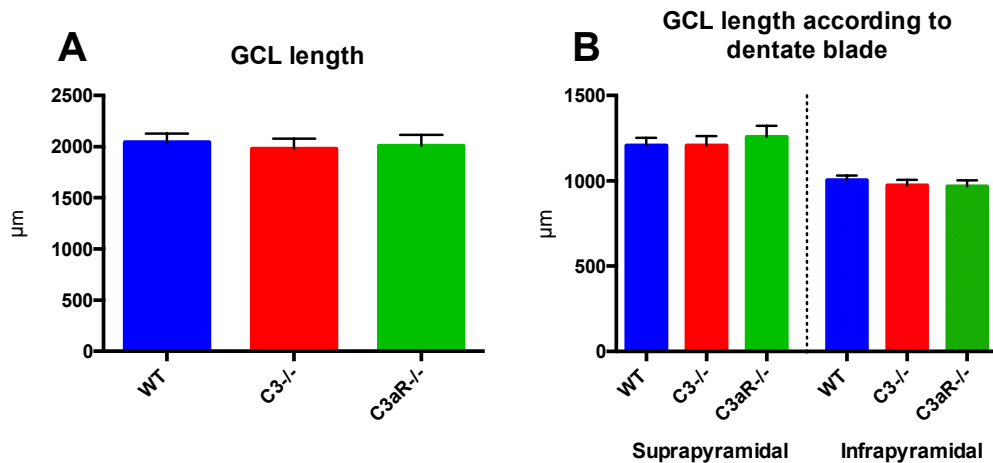
Figure 2.12. The length of the subgranular zone (SGZ) is unchanged between WT, C3^{-/-} and C3aR^{-/-} animals. **A)** Average length of the GCL per animal throughout entire hippocampus **B)** Average length GCL length per animal according to suprapyramidal blade or infrapyramidal blade. N= 12 dentate gyri from 6 sections per animal, from 6 animals per genotype. Data points represent mean ± SEM.

2.3.15 Granule cell layer volume is increased in C3^{-/-} and C3aR^{-/-} animals

I also measured the volume of the GCL as an index of the number of granule cells present in the adult dentate gyrus per animal. In each section, the outer perimeter of each GCL was traced using ImageJ. The measured area was then multiplied by the intersection interval (10). The data was then transformed to millimetre scale, before being multiplied by the section size (40 μm) to obtain an estimated measure of GLC volume (mm³) per animal.

Despite equivalent DG length in all genotypes (Figure 2.12), there were significant differences in GCL volume measured across the whole dentate (One-way ANOVA, $F_{(2,15)}$=12.00, p < 0.001, Figure 2.13A). This difference was attributable to increases in estimated whole GCL volume in C3^{-/-} (0.59 ± 0.03 mm³) and C3aR^{-/-} (0.60 ± 0.01 mm³) compared to WT (0.46 ± 0.006 mm³; Tukey post-hoc comparisons, both < 0.01).

Due to the aforementioned topographical differences in neurogenesis along the anterior-posterior hippocampal axis, I questioned whether GCL volume

increases were region-specific. A mixed 3×2 ANOVA consisting of two between-subjects factors of genotype (WT, C3$^{-/-}$, C3aR$^{-/-}$) and region (anterior, posterior) was used to analyse whether regional differences in GCL volume existed between genotypes. Results showed a significant main effect of region ($F_{(1,30)}$= 73.82, $p < 0.0001$), reflecting a greater estimated GCL volume in the posterior dentate than in the anterior dentate (Figure 2.13B). There was also a significant main effect of genotype ($F_{(2,30)}$= 16.92, $p < 0.0001$, post-hoc analyses were not conducted as this analysis duplicates that shown in Figure 2.13A). The interaction of these two factors was not significant ($F_{(2,30)}$= 0.92, p =0.40). This data suggests that in the absence of C3/C3aR, the volume of the GCL is increased throughout the anterior-posterior axis of the hippocampus. This may be indicative of greater levels of adult neurogenesis.
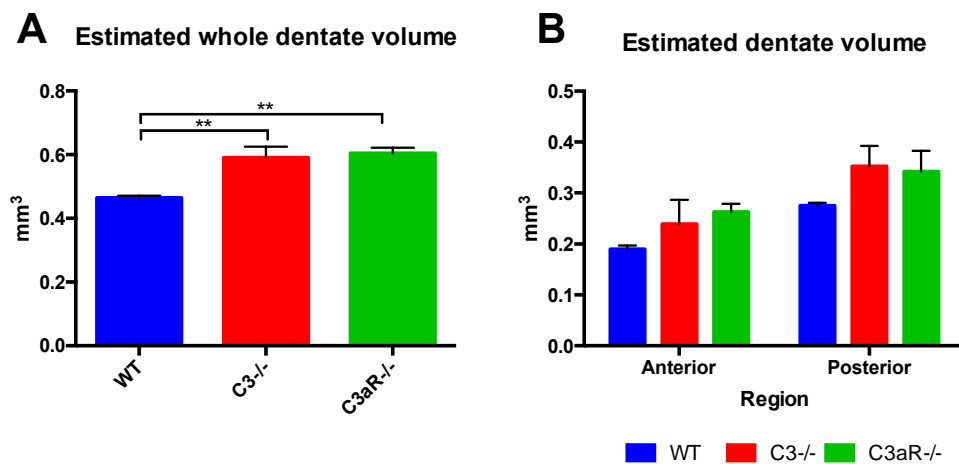
Figure 2.13. C3/C3aR deficiency increases granule cell layer (GCL) volume. A) Estimated volume of the GCL across all hippocampal regions per animal. **B)** Estimated GCL volume in anterior and posterior hippocampal regions per animal. N= 12 dentate gyri from 6 sections per animal, from 6 animals per genotype. Data points represent mean ± SEM. * = p < 0.05, ** = p < 0.01, *** = p < 0.001, **** = p < 0.0001

2.3.16 Absence of C3/C3aR does not affect proliferation *in vivo*

In light of the differences observed in NPC proliferation *in vitro,* Ki67 staining was used to assess the total number of proliferating cells *in vivo*. The average estimated number of Ki67$^+$ cells throughout the entire hippocampus was 1,612 ± 173.0 cells per WT animal, compared to 1,996 ± 178.7 cells per C3$^{-/-}$ animal and 1,737 ± 194.8 cells per C3aR$^{-/-}$ animal. These differences did not reach statistical significance (one-way ANOVA, $F_{(2,15)}$= 1.15, p = 0.34, Figure 2.14A).

I also investigated whether the distribution of Ki67$^+$ cells varied along the anterior-posterior and transverse (suprapyramidal *vs.* infrapyramidal) hippocampal axes between genotypes. A 3 (genotype; WT, C3$^{-/-}$, C3aR$^{-/-}$) × 2 (region; anterior, posterior) between subjects ANOVA indicated a significant main effect of region ($F_{(1,30)}$= 6.16, p < 0.05), due to a greater number of Ki67$^+$ cells in the posterior hippocampus in all genotypes (Figure 2.14B). The main effect of genotype was non-significant ($F_{(2,30)}$=1.44, p = 0.25) and there was no significant interaction between region and genotype ($F_{(2,30)}$= 0.28, p = 0.75).   Furthermore, a 3 (genotype; WT, C3$^{-/-}$, C3aR$^{-/-}$) × 2 (blade; suprapyramidal, infrapyramidal) between-subjects ANOVA showed no main effect of genotype ($F_{(2,30)}$= 1.52, p = 0.23) but a significant main effect of blade ($F_{(1,30)}$= 10.19, p < 0.01), reflecting a greater number of Ki67$^+$ cells in the suprapyramidal blade (Figure 2.14C). There was no significant interaction between genotype and blade ($F_{(2,30)}$= 0.83, p = 0.44). Together, these results demonstrate that more proliferating cells reside in the suprapyramidal blade of the DG, and in the posterior region of the hippocampus. The absence of C3/C3aR did not affect the number of proliferating cells, or their distribution within the DG however.
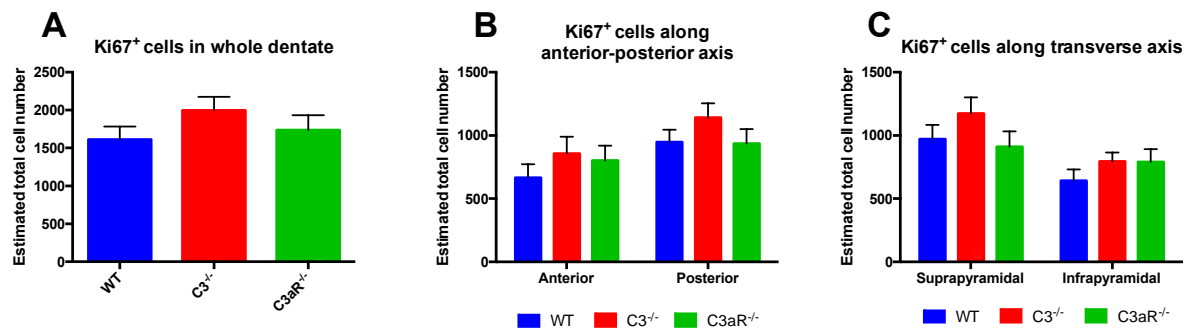
Figure 2.14. C3/C3aR deficiency does not affect the number or distribution of proliferating cells in the adult DG. **A)** Estimated total number of Ki67+ cells per animal throughout the entire hippocampus. **B)** Number of Ki67+ cells per animal in either the anterior or posterior regions of the dentate **C)** Number of Ki67+ cells per animal in either the suprapyramidal or infrapyramidal blade of the DG. N= 12 dentate gyri from 6 sections per animal, from 6 animals per genotype (total N= 18). Data points represent mean ± SEM. * = p < 0.05, ** = p < 0.01, *** = p < 0.001, **** = p < 0.0001

2.3.17 C3/C3aR does not impact upon proliferation of type 1/2a cells *in vivo*

Based on the differences observed in the proliferation of type 1/2a cells in C3$^{-/-}$ and C3aR$^{-/-}$ *in vitro,* I estimated the total number of proliferating type 1/2a cells in the DG, per animal. Proliferating type 1/2a cells were identified through immunostaining and morphology. While GFAP marks all astrocytes in the brain, co-localisation of Ki67 with GFAP in the GCL, and presence of the characteristic triangular morphology with an apical process extending into the GCL, is indicative of type 1 radial glia (Kempermann et al., 2004; see Figure 2.15A for example). However, since type 2a cells are also proliferative and can also express GFAP, It cannot be excluded that these cells were not also sampled. I therefore refer to type 1/2a cells in the following sections.

Results showed no differences in the total number of this cell type between genotypes (WT 283.5 ± 48.80; C3$^{-/-}$ 357.9 ± 63.91; C3aR$^{-/-}$ 292.8 ± 60.30; F$_{(2,15)}$=1.06, p=0.37, Figure 2.15B). Furthermore, there were no significant differences in the proportion of Ki67+ cells expressing GFAP between

genotypes (WT; 14 ± 2 %; C3$^{-/-}$ 17 ± 2 %; C3aR$^{-/-}$ 16 ± 1 %, F$_{(2,15)}$= 0.50, p = 0.72, Figure 2.15C). To test for any differences in the regional distribution of Ki67^{+}GFAP^{+} cells along the anterior-posterior hippocampal axis, a 3 (genotype; WT, C3$^{-/-}$, C3aR$^{-/-}$) × 2 (region; anterior, posterior) between-subjects ANOVA was conducted. There was no significant main effect of region (F$_{(1,30)}$= 0.90, p = 0.34) or genotype (F$_{(2,30)}$= 1.34, p = 0.27), and no significant interaction of these factors   (F$_{(2,30)}$= 1.12, p = 0.33, Figure 2.15D). These results suggest that the proliferation of type 1/2a cells was not affected by the absence of C3/C3aR.
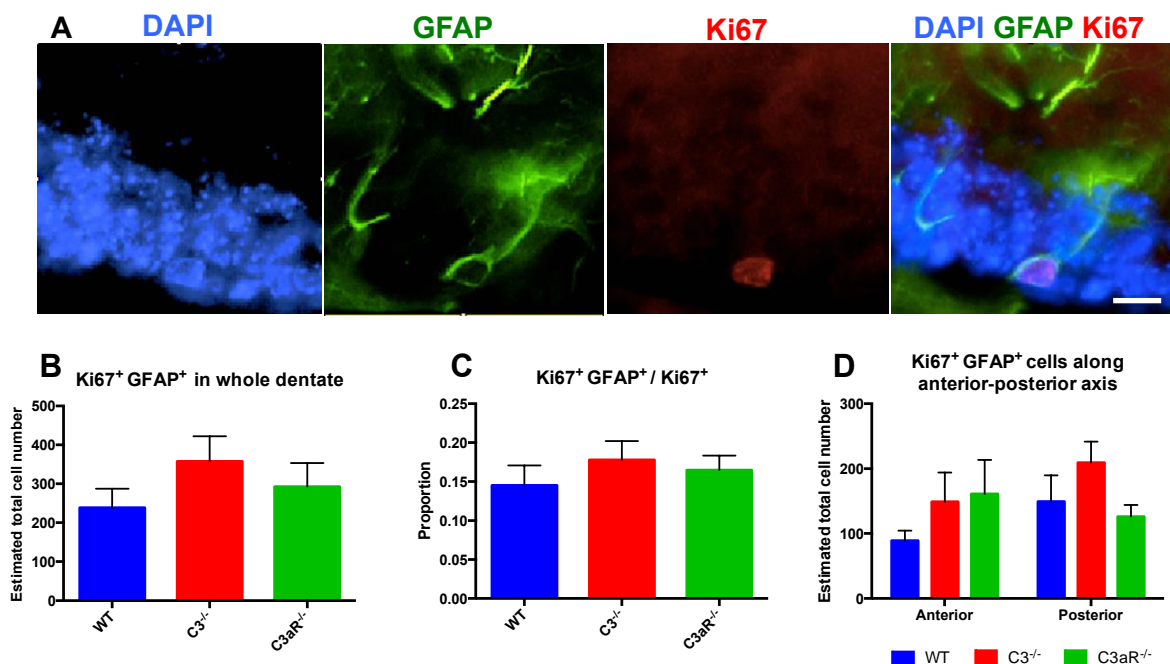
Figure 2.15. C3/C3aR does not affect the proliferation of type 1/2a radial glial cells in the adult DG A) Representative example of type 1 cell based on Ki67 GFAP co-localisation. Note characteristic morphology with apical process extending into granule cell layer **B)** Estimated total number of type Ki67^{+} GFAP^{+} cells per animal in the whole dentate **C)** The proportion of Ki67^{+} population accounted for by type 1 cells throughout entire DG **D)** Estimated total number of Ki67^{+} GFAP^{+} cells per animal in anterior and posterior hippocampal regions. N= 12 dentate gyri from 6 sections per animal, from 6 animals per genotype (total N= 18). Data points represent mean ± SEM. Scale bar = 5 μm. * = p < 0.05, ** = p < 0.01, *** = p < 0.001, **** = p < 0.0001.

2.3.18 Immature neurons are increased in the absence of C3/C3aR

Subsequently, I examined newly generated immature neurons *in vivo* using DCX immunostaining. There was a significant difference between genotypes in the estimated number of DCX$^+$ cells per animal in the whole hippocampus ($F_{(2,15)}$=5.98, $p < 0.05$, Figure 2.16A & B). Post-hoc comparisons using Tukey's HSD test revealed a significantly greater estimated total cell count in C3$^{-/-}$ animals (21,107 ± 2,027 cells per animal) compared to WT (13,670 ± 424.7 cells per animal, $p < 0.05$). There were also a greater number of DCX$^+$ cells in C3aR$^{-/-}$ animals (19,302 ± 1,805 cells per animal) compared to WT. Uncorrected (i.e,, Fisher's LSD test) contrasts yielded a p value of 0.02 for this comparison, yet when subjected to Tukey's HSD test the reported p value equalled 0.058. However, considering an increase of this size and its comparable magnitude to that seen in C3$^{-/-}$ brains, this result is likely to be biologically meaningful despite not reaching conventional levels of statistical significance.

To determine whether regional differences in DCX cell numbers were present, I examined the distribution of DCX cells along the anterior-posterior axis of the hippocampus, depending on section number (1= most anterior; 6 =most posterior). As seen in Figure 2.17A, there was an elevated number of DCX cells throughout the anterior-posterior axis in C3$^{-/-}$ and C3aR$^{-/-}$ animals compared to WT. To analyse this data, the area under the curve (AUC) was calculated for each animal. One-way ANOVA showed significant differences in the average AUC (arbitrary unit) between genotypes ($F_{(2,15)}$=6.40, $p < 0.01$, Figure 2.17B) . Post hoc tests showed a significant difference in the AUC between WT (1,305583.33 ± 156.45) and C3$^{-/-}$ (1,907700 ± 274.61, $p < 0.05$) and between WT and C3aR$^{-/-}$ (1,793300 ± 261.48, $p < 0.05$), again suggesting elevated numbers of DCX cells in the absence of C3/C3aR.

In order to confirm the differential distribution of DCX cells in anterior and posterior hippocampal regions between genotypes, DCX counts for sections 1

106
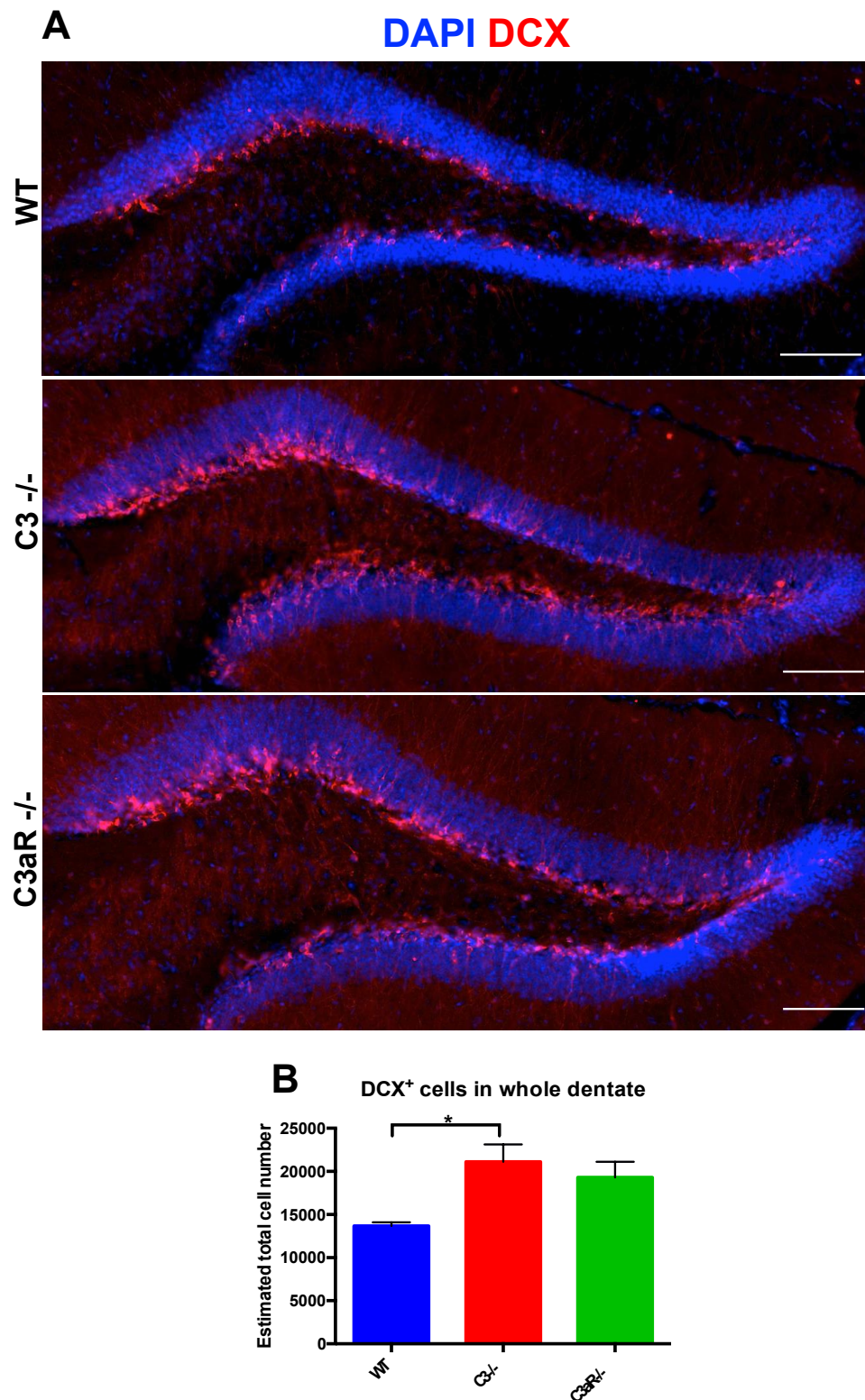
Figure 2.16. There are greater numbers of DCX+ immature neurons in the adult DG in the absence of C3 and C3aR. A) Representative examples of DCX staining from WT, C3-/- and C3aR-/- animals. **B)** Estimated total number of DCX cells per dentate, per animal. N= 12 sections per animal from 6 animals per genotype. Data points represent mean ± SEM. Scale bar = 150 µm * = $p < 0.05$, ** = $p < 0.01$, *** = $p < 0.001$, **** = $p < 0.0001$.

to 3 were pooled and counted as anterior, whereas sections 4 to 6 were counted as posterior. A 3 (genotype; WT, C3$^{-/-}$, C3aR$^{-/-}$) $\times$ 2 (region; anterior, posterior) between-subjects ANOVA indicated a significant main effect of region (F$_{(1,30)}$=9.47, p < 0.01, Figure 2.17C), reflecting a greater number of DCX cells in the posterior hippocampus, and a significant main effect of genotype (F$_{(2,30)}$= 8.84, p < 0.001; post-hoc tests were not conducted as this analysis duplicates that depicted in figure 2.16). The interaction of genotype and region was non-significant (F$_{(2,30)}$=0.54, p = 0.58).

I also estimated the total cell number in the suprapyramidal and infrapyramidal blades of the DG per animal (Figure 2.17D). A 3 (genotype; WT, C3 $^{-/-}$, C3aR$^{-/-}$) $\times$ 2 (blade; suprapyramidal, infrapyramidal) between-subjects ANOVA showed a significant main effect of genotype (F$_{(2,15)}$=5.98, p < 0.05), a borderline significant main effect of blade (F$_{(1,30)}$=3.83, p = 0.059) and no significant interaction of blade and genotype (F$_{(2,30)}$=0.89, p = 0.41). The main effect of genotype was not followed up as this analysis duplicates that shown in Figure 2.16B (i.e., total DCX cell count regardless of location within the hippocampus). These results suggest that C3 and C3aR deficient animals showed increases in immature neurons throughout both the longitudinal (anterior-posterior) and transverse (suprapyramidal-infrapyramidal) hippocampal axes.

2.3.19 C3/C3aR does not affect the proliferation of immature neurons

I also questioned whether there were any changes in the proliferation of immature neurons via DCX co-localisation with Ki67 (see Figure 2.18A for example). There were no significant genotype differences in the mean number of proliferating DCX cells in the DG per animal (WT 560.4 ± 58.43 cells; C3$^{-/-}$ 719.0 ± 67.24 cells; C3aR$^{-/-}$ 642.6 ± 80.33 cells; F$_{(2,15)}$=1.31, p = 0.29, Figure 2.18B). The proportion of Ki67^{+} cells expressing DCX was also unchanged between genotypes (F$_{(2,15)}$= 0.97, p = 0.40, Figure 2.18C).
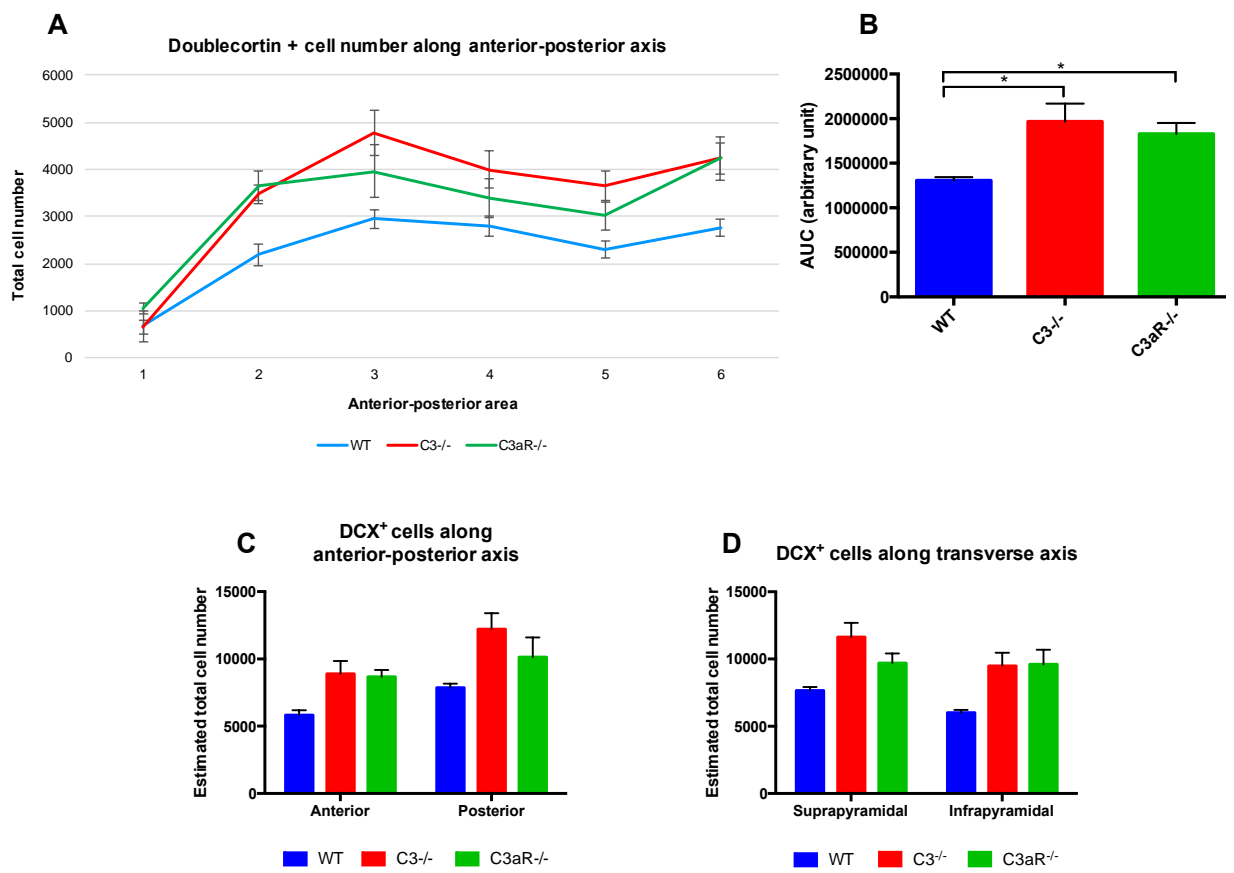
Figure 2.17. C3 and C3aR deficient animals have increased numbers of immature neurons throughout the hippocampus. **A)** Estimated DCX cell number in sections 1 (most anterior) through to 6 (most posterior) in WT, C3$^{-/-}$ and C3aR$^{-/-}$ brains. **B)** Area under the curve (AUC) analysis of the profile shown in B. **C)** Estimated DCX cell number in anterior (sections 1-3, pooled) and posterior (sections 4-6, pooled) hippocampal regions, in WT, C3$^{-/-}$ and C3aR$^{-/-}$ animals**. D)** DCX cells in the suprapyramidal vs. infrapyramidal blades, in WT, C3$^{-/-}$ and C3aR$^{-/-}$ animals. N= 12 sections per animal from 6 animals per genotype. Data points represent mean ± SEM. * = p < 0.05, ** = p < 0.01, *** = p < 0.001, **** = p < 0.0001.

Furthermore, a 3 (genotype; WT, C3$^{-/-}$, C3aR$^{-/-}$) × 2 (region; anterior, posterior) between-subjects ANOVA showed no significant main effect of genotype ($F_{(2,30)}$= 1.72, p = 0.29) or region ($F_{(1,30)}$= 2.69, p = 0.11), and no significant interaction of genotype and region ($F_{(2,30)}$= 0.16, p = 0.84, Figure 2.18D). Therefore, these results suggest that the absence of C3/C3aR increased the number of immature neurons without affecting their proliferation.
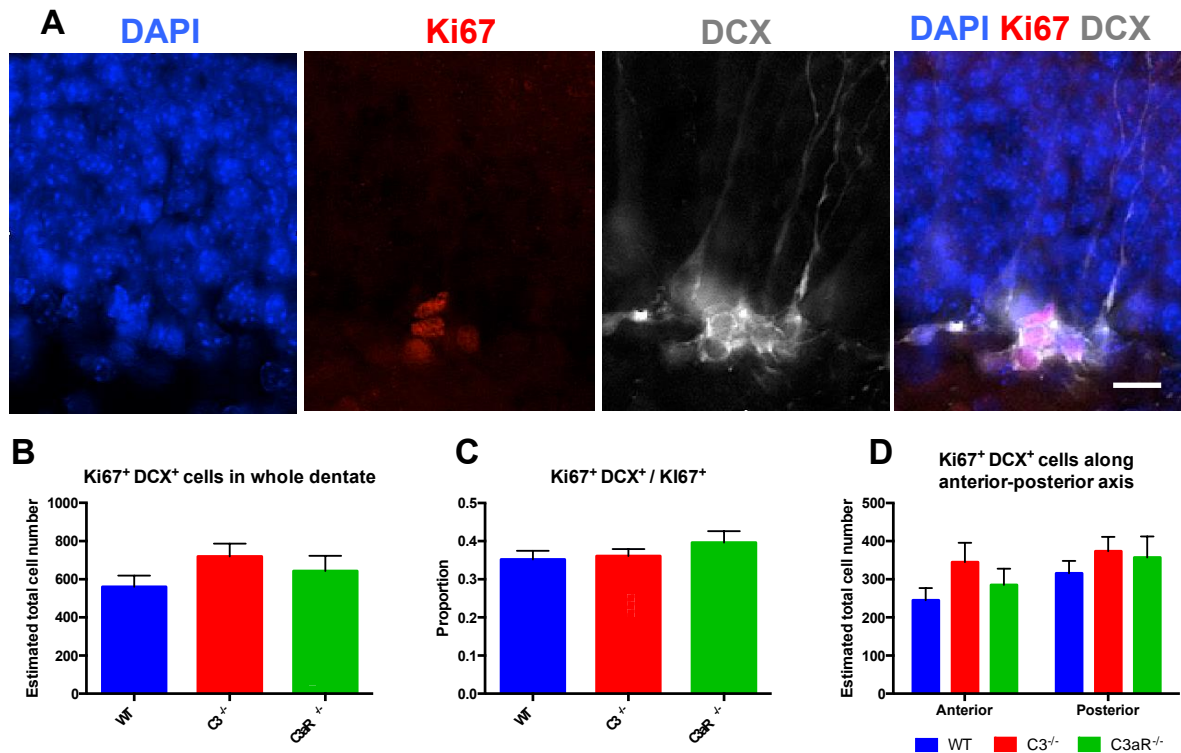
Figure 2.18. C3/C3aR does not affect the proliferation of newly born neurons in the adult DG. **A)** Example of Ki67+ DCX cells **B)** Estimated total number of DCX+ Ki67+ cells throughout the entire DG **C)** Ki67+ DCX+ as a proportion of Ki67+ in the whole DG **D)** Regional breakdown of Ki67+ DCX+ total cell number in anterior and posterior sections. N= 12 dentate gyri from 6 sections per animal, from 6 animals per genotype (total N= 18). Data points represent mean ± SEM. Scale bar = 7 μm * = p < 0.05, ** = p < 0.01, *** = p < 0.001, **** = p < 0.0001.

2.3.20   Summary of *in vivo* results

The data presented here suggest no effect of C3/C3aR signalling upon overall proliferation (Ki67+ cell number) within the adult mouse DG. The proliferation of type 1/2a cells (GFAP+Ki67+) and type 2b/3 cells (DCX+Ki67+) cells was also unchanged in C3 and C3aR deficient animals. There was however, a significant increase in the total number of DCX cells per animal in C3 deficient animals, and a trend of comparable magnitude in the absence of C3aR, which fell marginally short of statistical significance. This increase in immature neurons was present throughout both the longitudinal and transverse hippocampal axes. Together with the finding of increased GCL volume, and in absence of an effect of C3/C3aR deficiency on

proliferation of DCX⁺ cells, this data suggests that C3/C3aR signalling is anti-neurogenic under physiological conditions.

2.4 Discussion

2.4.1 Overview of results

The central complement component C3 and its breakdown products, C3a and C3d, have previously been implicated in regulating AHN (Moriyama et al., 2011; Rahpeymai et al., 2006). However, from the existing body of knowledge, it has been unclear whether complement is able to directly modulate NPCs. This chapter therefore aimed to investigate the potential for C3/C3aR signalling to regulate AHN. To do this, I adopted an *in vitro* approach, generating primary hippocampal precursor cell cultures from C3 and C3aR deficient mouse lines, combined with an *in vivo* approach in the adult brain. Results demonstrated that C3/C3aR signalling is able to directly modulate NPCs, although the local environment is an important modulatory factor in the relationship between C3/C3aR signalling and adult neurogenesis. Furthermore, this data conclusively demonstrates a role for C3a/C3aR signalling in regulation AHN, in opposition to that of C3d/CR2. In my *in vivo* experiments, I documented a substantial increase in the number of immature DCX+ neurons throughout the entire dentate in C3 and C3aR$^{-/-}$ animals. Furthermore, the increased volume of the GCL observed in these strains suggests that the elevated number of DCX cells also survive and mature into mature granule cells. Therefore, C3/C3aR signalling exerts an anti-neurogenic *in vivo*.

2.4.2 *In vitro* results I: Complement is expressed in primary NPC culture

While it is well established that complement is produced locally within the CNS, primarily by astrocytes and neurons (Nataf et al., 1999), less is known about complement expression within the neurogenic niches, or indeed by NPCs. Therefore, I first sought to determine whether the receptor and ligand of interest, C3 and C3aR, were present in WT hippocampal cultures, before

proceeding to experiments featuring the genetic deletion of C3 and C3aR. I also questioned whether other complement receptors, proteins and regulators were expressed. The results of an exploratory PCR screen in WT hippocampal cultures showed expression of classical pathway components of the C1 complex, C3 and C4. A variety of receptors were also expressed in culture, including C3aR, C5aR and complement receptor 1 (CR1). Hippocampal cultures also produced complement regulatory factors including factor P (CFP, also known as Properdin) and factor H (CFH). Interestingly, Properdin is one of the only positive regulators of complement activity, serving to promote C3b and factor B association, thus leading to assembly of alternative pathway C3 convertase C3bBb. This may therefore be a means for C3 activation to occur in culture via the C3 tick over mechanism (as outlined in Section 1.6.2). In contrast, Factor H is a fluid phase alternative pathway regulator which accelerates the decay of the alternative pathway C3 convertase, C3bBb (Zipfel & Skerka, 2009). The presence of these two factors suggests that hippocampal precursor cells have the capacity to regulate alternative pathway tick over.

Despite weak mRNA expression of C3, positive and specific C3 immunocytochemistry was demonstrated, suggesting that C3 mRNA is translated to protein in hippocampal cultures. A quarter of C3+ cells were microglia, determined by co-localisation with Iba1. Further experiments will be conducted to determine the identity of the remaining 75% of C3+ cells. As shown in Figure 2.19, a pilot experiment (data yet to be quantified) has indicated that many of these cells co-express nestin, suggesting a precursor cell identity. Whether this indicates production of C3 by NPCs, or deposition of C3 on their cell surfaces, is unclear however. It will also be of interest to further examine the activation status of the 50% of microglia that were C3+. This could be probed jointly through the use of ED-1 immunocytochemistry, a protein expressed by phagocytic microglia (Damoiseaux et al., 1994) and microglial Sholl analysis (Norris, Derecki & Kipnis, 2014), since activation states are associated with distinct morphologies.
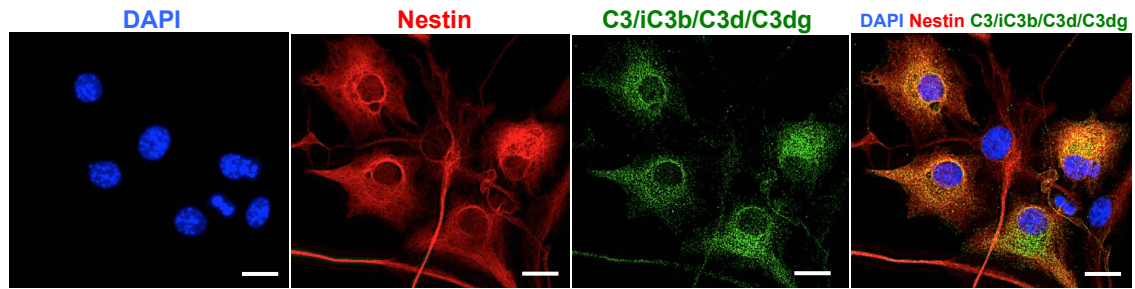
Figure 2.19. Pilot data showing expression of C3 and/or and breakdown products (green) on nestin+ precursor cells. Scale bar = 5 μm.

I also investigated whether C3 is activated in culture. Sandwich ELISA did not detect C3a in the culture supernatant from WT hippocampal cells. However, it is known that C3a exerts effects at picomolar to nanomolar concentrations (Beek, Elward & Gasque, 2003) and thus may be below detection limits of many commercial ELISA kits. Moreover, C3a produced by LPS treated microglia only marginally surpassed the detection limit, suggesting that the levels produced in hippocampal cultures under physiological conditions may indeed be extremely low. Nevertheless, given the range of effects seen in $C3^{-/-}$ and $C3aR^{-/-}$ cultures, it is possible that C3 activation occurring at extremely low levels is still of functional relevance.

2.4.3 *In vitro* results II: C3/C3aR deficiency does not affect total cell numbers or survival

I next moved on to consider the effects of C3/C3aR genetic deletion on hippocampal precursor cells isolated from $C3^{-/-}$ and $C3aR^{-/-}$ mouse pups. Firstly, whether C3/C3aR deficiency altered the total number of cells in culture was examined. Analyses of DAPI cells in culture at 3, 5 and 14 days *in vitro* showed a similar pattern between genotypes, characterised by expansion between days 3-5 followed by a plateau in numbers between days 5-14. This pattern closely mirrored that seen previously in our lab using primary hippocampal rat cultures (Howell et al., 2005; Nunan, et al., 2014;

Zaben et al., 2009) Therefore, C3/C3aR deficiency did not affect the total number of cells in culture.

I then asked whether C3/C3aR affected cell survival or viability in cultures at 5DIV. Due to a large amount of variability in total cell counts in these experiments, which is characteristic of primary hippocampal mouse cultures, the proportion of dead/dying (PI[+]) or alive (MitoTracker[+]) is more reliable than raw data in this instance. This data showed no differences in the proportion of dead or alive cells in C3^{-/-} or C3aR^{-/-} cultures compared to WT. While C3a has previously been shown to affect the survival of a variety of cell types, including astrocytes (Shinjyo, de Pablo, Pekny, & Pekna, 2015), neurons (Pavlovski et al., 2012) and other immune cells (Strainic et al., 2008), this data suggests that it does not impact upon NPC survival specifically.

2.4.4 *In vitro* results III: C3/C3aR deficiency causes a phenotypic shift towards type 1/2a radial glia cells and decreases subsequent phenotypes in the neurogenic lineage

In absence of any effect upon total cell number or survival, I investigated the phenotype of cells in culture using antigens specific to each stage of neurogenesis. As summarised in Table 1, the results demonstrate that C3/C3aR deficiency alters the phenotype of hippocampal precursor cells by causing a shift towards a primitive radial glial type 1/2a phenotype (GFAP[+] Nestin[+]), as there were significantly greater numbers of these cells present in C3 and C3aR^{-/-} cultures compared to WT at 5DIV. This phenotypic shift was associated with a decline in subsequent cell types; fewer type 2a/2b cells (Nestin[+] GFAP[-] DCX[+]), type 2b (DCX[+] TUJ1^{-}) and 3 cells (DCX[+] TUJ1^{+}) were found in C3^{-/-} and C3aR^{-/-} cultures between 5DIV and 6DIV. I did not find any differences in the number of mature neurons present after 14 days however, suggesting that the deficit in neurogenesis caused a temporary delay in

neurogenesis as opposed to a permanent decrease. The reasons behind this pattern of results are likely to be a methodological artefact however, and will be discussed in Section 2.4.11.

Since type 1/2a cells accounted for a large percentage of the total cell population, in which survival was unchanged, I questioned whether the proliferation of these cells was altered. Using an acute EdU pulse-chase paradigm, I found that more type 1/2a cells were proliferating in C3$^{-/-}$ and C3aR$^{-/-}$ cultures. Interestingly, other phenotypes also showed altered proliferation (see Table 1); Nestin$^+$ GFAP$^-$ type 2a/2b cells also showed a greater degree of proliferation, whereas there was a trend suggestive of lowered proliferation of Nestin$^+$ DCX$^+$ type 3 cells in the absence of C3/C3aR (p=0.06). Therefore, C3/C3aR signalling appears to affect the proliferation of cells at distinct stages of the neurogenic lineage.

Cell type	Markers	Number	Proliferation
Type 1/2a	GFAP$^+$ Nestin$^+$	↑	↑
Type 2a/2b	GFAP$^-$ Nestin$^+$	↓	↑
Type 2b	DCX$^+$ TUJ1$^-$	↓	↓
Type 3	DCX$^+$ TUJ1$^+$	↓	n/a
Mature neurons	TUJ1$^+$ NeuN$^+$	Unchanged	n/a

Table 2.2. Summary of *in vitro* results.

2.4.5 Potential mechanisms underlying C3/C3aR induced phenotype shift

Increased proliferation of type 1/2a cells may be expected to lead to greater levels of neurogenesis acutely, as has been reported in some *in vivo* disease models such as temporal lobe epilepsy (Sierra et al., 2015). However, this is not fitting with the decrease in neurogenesis observed here. An explanation

that may account for this pattern of results is that C3/C3aR altered not just the number of type 1 cells proliferating, but also their division symmetry. These cells are known to divide infrequently and asymmetrically to produce a nestin positive type 2 daughter cell (Kempermann, Jessberger, Steiner, & Kronenberg, 2004). If the absence of C3a should cause type 1 cells to alter their mode of division to favour symmetric divisions, the pool of type 1 cells would expand, as was observed in my experiments. This would also explain the decrease in subsequent phenotypes observed, due to a lower amount of type 1/2a cells differentiating into the type 2a/2b transient amplifying population required for the generation of new neurons (Kempermann et al., 2004). The increased proliferation of type 2a/2b nestin$^+$ GFAP$^-$ cells may be a compensatory mechanism to account for the lack of neurogenic output from the stem cell pool. Therefore, under basal conditions, C3/C3aR may stimulate neurogenesis by increasing the rate at which type 1 cells generate type 2a and 2b cells. This would result in more radial glial stem cells exiting their normally quiescent state and therefore speeding up the rate of neurogenesis.

However, it should be noted that the proliferation of cells in culture is highly driven by the addition of EGF and FGF-2. Therefore, this effect may be dependent on growth factors and thus normalised upon growth factor withdrawal at 5DIV, leading to normal levels of neurogenesis by 14 days (see Section 2.4.11 for further discussion of this point). Nonetheless, follow up work will utilise NUMB immunocytochemistry to address whether complement alters division symmetry in culture. This approach has previously been used by our lab with primary rat hippocampal cultures (Zaben et al., 2009). Since unequal distribution of NUMB protein during mitosis leads to asymmetric division (Shen et al., 2016), co-staining cells with NUMB, nestin and GFAP will allow quantification of the proportion of type 1 cells dividing symmetrically versus asymmetrically. Therefore, if C3/C3aR absence causes increased symmetric division, a greater number of NUMB$^+$ Nestin$^+$ GFAP$^+$ cells can be expected in culture. It is also possible that postnatal C3 and C3aR deficient animals had a greater number of type 1 cells in the hippocampus prior to isolation, thus explaining the current pattern of

results. This possibility has not been elucidated in the *in vivo* data presented here, and will be investigated in future work by assessing numbers of BLBP+ type 1 cells present in the DG of C3 and C3aR deficient mice.

2.4.6   Relation to previous *in vitro* literature

With regard to my hypotheses, the increase in proliferation I have observed is not consistent with the findings of Moriyama et al. (2011), who demonstrated an anti-proliferative effect of C3d/CR2 signalling in primary hippocampal rat neurospheres. While the absence of C3d in C3$^{-/-}$ cultures could account for the increases I have observed in proliferation of type 1/2a and 2a/2b cells, this is negated by the fact that these same findings were mirrored in C3aR$^{-/-}$ cultures, where C3d/CR2 is present. Therefore, C3d/CR2 does not appear to contribute to proliferation of NPCs under basal conditions. However, my results do suppose those of Shinjyo et al. (2009), who documented a pro-neurogenic effect of exogenous C3a on whole-mouse-brain derived NPCs, suggesting that hippocampal precursor cells are also sensitive to regulation by endogenous C3a/C3aR signalling.

The current work constitutes the most thorough and relevant investigation of C3/C3aR signalling in adult neurogenesis to date. While informative, the aforementioned studies by Shinjyo et al. (2009) and Moriyama et al. (2011) are limited by their use of either cell lines or neurosphere cultures, and through use of indirect measures of proliferation (i.e., neurosphere size) and survival (i.e., MTT assay). They were also unable to conduct phenotypic analyses, which I have been able to carry out through use of primary monolayer cultures. Therefore, the current paradigm affords greater methodological validity than has previously been seen in the *in vitro* literature regarding complement and adult neurogenesis. These results also suggest that complement can exert direct effects upon NPCs, although it may

also modulate the other cell types isolated from the DG that are present within cultures, including microglia.

2.4.7   *In vivo* results: C3/C3aR signalling is anti-neurogenic under physiological conditions

Despite the many differences between *in vitro* and *in vivo* approaches, I was interested to determine whether the results obtained in culture were applicable to the whole brain. Firstly, based on my *in vitro* data suggesting a phenotypic shift towards type 1 radial glia *in vitro,* I assessed both the total number of Ki67$^+$ cells and the proportion of these cells which co-expressed GFAP, as a marker of radial glia. Results demonstrated that C3/C3aR deficiency did not affect the overall number of proliferating cells in the DG, nor did it affect the number of proliferating radial glia.

I next examined whether there were any changes to later stages of the neurogenic process by staining for DCX, a marker of newly born neurons. There was a considerable increase in DCX$^+$ cells in C3$^{-/-}$ animals, and a borderline significant increase in C3aR$^{-/-}$ animals (p=0.06). These increases were observed throughout the entire DG, in both the suprapyramidal and infrapyramidal blades, and along the anterior-posterior hippocampal axis. This suggests that C3/C3aR signalling exerts an anti-neurogenic effect in the healthy brain by reducing the number of immature neurons formed. To follow up this result, I conducted joint Ki67/DCX immunohistochemistry to determine whether the increases in DCX cells were due to greater proliferation of this cell type. The number of Ki67$^+$ DCX$^+$ cells was unchanged however, suggesting that an alternative mechanism, namely either enhanced survival or greater neuronal differentiation, was responsible for the increased levels of immature neurons observed.

2.4.8 Potential mechanisms underlying increases in *in vivo* neurogenesis

As previously mentioned, C3a has been implicated in cell survival, although whether it exacerbates death or facilitates survival is highly dependent upon cell type and context (Coulthard & Woodruff, 2015). The most well described, albeit indirect, mechanism through which C3 contributes to cell death is through C3b/CR3 signalling (Zabel & Kirsch, 2013). DAMPs trigger complement activation, leading to cleavage of C3 and generation of breakdown product C3b, which remains bound to the membrane of the dead or dying cell. As outlined in Section 1.6.1, C3b is an opsonin, which attracts macrophages or phagocytic microglia hosting the CR3 receptor, leading to engulfment of dead/dying cells and associated debris (Stephan, Barres, & Stevens, 2012). This mechanism is not always directed towards dead or dying cells however; it has been found to underlie complement mediated elimination of weak synapses during post-natal development (Stephan et al., 2012; Stevens et al., 2007). While C3a/C3aR signalling has not previously been directly implicated in this process, C3a has chemo-attractant properties which enable it to recruit and activate macrophages in the periphery (Stephan et al., 2012). Moreover, microglia are also known to constitutively express C3aR in the CNS (Gasque, Singhrao, Neal, & Sedgwick, 1998). It has therefore been suggested that C3a may attract microglia to synaptically dense regions in the developing brain (Klos et al., 2009), and it is possible that C3a may direct microglia to apoptotic progenitor cells in the SGZ.

Critically, the maintenance of normal AHN is dependent upon phagocytosis of immature neurons undergoing apoptosis by unchallenged microglia resident in the hippocampal niche (Sierra et al., 2010). The current results suggest that complement may be involved in this process. While numbers of microglia are unaltered in the dentate gyrus of C3$^{-/-}$ mice (Perez-Alcazar et al., 2013), it is possible that the absence of C3a/C3aR leads to reduced clearance of apoptotic immature neurons. This may also lead to increased GCL volume, as a greater proportion of dead cells may crowd the GCL. This

question will be addressed in future work by assessing characteristic nuclear signs of apoptosis, including nuclear fragmentation (karyorrhexis) and DNA condensation (pyknosis) in combination with immunostaining for caspase-3 activation (McIlwain, Berger, & Mak, 2013), which reliably marks apoptotic cells in the SGZ (Sierra et al., 2010). Double immunohistochemistry for DCX and microglial marker Iba-1 would also allow investigation of the interaction between microglia and immature neurons in the absence of C3/C3aR. Furthermore, should this mechanism indeed be complement/microglia mediated, this may explain the failure to observe similar effects upon DCX cells *in vitro*, as microglia were present at a much lower ratio to NPCs than would be found *in vivo*. Therefore, microglia are likely to be a key factor in the divergence of the *in vitro* and *in vivo* results presented in this chapter.

It is also possible that C3a/C3aR directly mediates survival by influencing apoptosis pathways. In murine astrocyte cultures subjected to chemical ischemia, Shinjyo et al., (2015) demonstrated that C3a treatment protected WT but not C3aR$^{-/-}$ astrocytes from death. C3a was shown to inhibit astrocytic caspase-3 activation via reduced ERK-phosphorylation (Shinjyo et al., 2015). C3a also protected neurons from *N*-Methyl-D-aspartic acid (NMDA) induced death (Van Beek et al., 2001). However, whether complement is neuroprotective or exacerbates cell death has been long debated, with many scenarios described in which the anaphylatoxins contribute to cell death or pathology (Cowell, Plane, & Silverstein, 2003; Brennan, Anderson, Taylor, Woodruff, & Ruitenberg, 2012; Veerhuis et al., 2011). For example, in primary cultured mouse cortical neurons, C5a triggered apoptotic but not necrotic cell death (Pavlovski et al., 2012). One potential explanation for the disparity in survival effects observed is via C3a/NGF signalling; C3a induces NGF expression in astrocytes (Heese, Hock, & Otten, 1998), which can exert either trophic or pro-apoptotic effects depending on the balance of neuronal receptors TrkA or p75[NTR] (Shinjyo et al., 2015). Moreover, the action of the anaphylatoxins is highly pleiotropic with regards to different cell types and developmental stages (Mastellos, 2014; Reiman et al., 2005). It is possible that C3a/C3a signalling directly

influences the susceptibility of adult born hippocampal neurons to apoptotic cell death. In its absence, this possibility would lead to a greater number of viable immature neurons surviving and maturing into GCs within the GCL, which is again consistent with my observation of increased GCL volume. The potential for this outcome will be elucidated in the aforementioned experimental design examining apoptotic markers, but also through the use of a long term BrdU-pulse chase paradigm to assess whether more immature neurons successfully mature in the absence of C3/C3aR using joint BrdU/NeuN staining.

For methodological reasons, effects on differentiation or fate choice cannot be ruled out however. Due to time constraints, total numbers of other relevant phenotypes in the neurogenic cascade (i.e., type 1 and 2a cells) are yet to be examined. Future work will use BLBP to selectively label all type 1 radial glial cells in the DG (Feng, Hatten, & Heintz, 1994), in combination with nestin / sox-2 to demarcate type 2a (Nestin/Sox-2$^+$ GFAP$^{+/-}$) cells. In combination with DCX staining, this experimental design will allow determination of whether the absence of C3/C3a favours greater neuronal differentiation, or whether the effect is specifically upon survival post-neuronal lineage commitment. At present, these possibilities cannot be distinguished as an increase in GCL volume could reflect both a failure to clear apoptotic nuclei or an increase in healthy, adult born granule cells. Also, it would be of use to conduct experiments utilising both short-term and long-term BrdU pulses. In particular, it will be important to examine BrdU$^+$ NeuN$^+$ cells using a long-term BrdU pulse paradigm in C3$^{-/-}$ and C3aR$^{-/-}$ animals, to determine whether GCL volume increases are a consequence of greater survival of adult born neurons, or an accumulation of apoptotic nuclei.

2.4.9 Relation to previous *in vivo* literature

Finally, with regard to my hypotheses concerning differentiation, distinct outcomes were predicted depending on signalling via C3d/CR2 or C3a/C3aR pathways. Results demonstrated increased DCX cells in the absence of C3, which is in line with the observations of Moriyama et al. (2011) in CR2$^{-/-}$ mice. However, since a trend of similar magnitude was seen in C3aR$^{-/-}$ mice, and these animals possess C3d/CR2, it is more likely that these effects are attributable to C3/C3aR than C3d/CR2 signalling. However, it remains possible that both ligands and receptors jointly contribute to maintaining the balance of neurogenesis *in vivo.* My results are discordant with that of Rahpeymai et al. (2006) however, who reported a decline in AHN in C3$^{-/-}$ and C3aRA treated mice.

There are several methodological differences that may account for the opposing conclusions reached. Firstly, Rahpeymai et al. did not assess the total number of DCX cells, only the number of BrdU$^+$ DCX cells. Since I found no differences in the proliferation of DCX cells via Ki67$^+$ immunolabelling, it is possible that their analyses missed any increases in total DCX cell number. Furthermore, although Rapheymai et al*.* reported a reduction of NeuN$^+$BrdU$^+$ cells *in vivo,* their post-injection survival time was only two weeks. It is possible that many precursors incorporating BrdU did not have sufficient time to mature and express NeuN, meaning that their analyses may have missed the increase in mature GCs suggested by the present data regarding GCL volume. It should also be noted that Rahpeymai et al. utilised a different C3$^{-/-}$ model (generated by Pekna et al., 1998). While the effects of the particular genetic manipulation serve to render C3 non-cleavable, and should therefore have comparable effects to our model, this is another potential source of variation.

2.4.10 Consideration of differences between *in vitro* versus *in vivo* paradigms: Developmental differences in complement expression

The differing *in vitro* and *in vivo* results presented in this chapter demonstrate that the manner in which complement regulates AHN is heavily dependent on the local environment. Two key elements that are likely to have contributed to these results are developmental variations in complement between the postnatal and adult brain, and cell-extrinsic factors, which are absent from the culture dish.

Firstly, the expression of complement factors is developmentally regulated. Here, cultures were generated from the postnatal mouse brain, as precursor cells present at this time are relevant to the study of adult neurogenesis (Namba et al., 2005) and are comparatively easier to culture than adult tissue. However, there are considerable differences in complement expression in the postnatal versus adult brain. For example, in the murine brain, C1q protein levels have been found to dramatically increase between the early postnatal-stage and adulthood. In contrast, C3 levels peak during the first postnatal week (from which our cultures are derived), after which they decrease (Stephan et al., 2013). C4 is also abundant until the sixth postnatal week (Johnson, Pasinetti, & Finch, 1994). It is also likely that the roles of complement are developmentally variable also (Benard et al., 2008). Therefore, complement is likely to have differing roles and expression levels in the postnatal brain, from which my cultures were generated, to those it may have in the adult brain, from which my *in vivo* data was derived. Further experiments examining postnatal hippocampal neurogenesis *in vivo,* or alternatively primary cultures generated from the adult as opposed to postnatal hippocampus, may provide insight into the influence of these factors in the pattern of results reported here.

2.4.11 Consideration of differences between *In vitro* versus *in vivo* paradigms: Environmental factors

Consideration of the factors that are either present or absent *in vitro* versus *in vitro* may offer important insights into the interpretation of our results. Foremost, it must be emphasised that cell culture is an inherently artificial environment that inevitably changes many cellular properties due to the cell-extrinsic factors that are absent, such as the anatomical organisation of the neurogenic niche. It does however afford insight into mechanisms that are dependent on cell-cell contact and soluble factors released from other cells within the neurogenic niche.

The process of AHN is highly dependent on the composition of the niche in which NPCs are immersed (Battista et al., 2006). Firstly, although cell-cell contact occurs in monolayer cultures, the influence of 3D cycoarchitechture is lost in monolayer cultures. 3D culture systems, including neurosphere cultures, are advantageous in this regard. Nevertheless, the use of monolayer cultures in this chapter was valuable as a means to study cell phenotype, which would not be possible to the same extent in neurosphere cultures. In addition, the various cell types highlighted in Section 1.5.5 as important niche constituents may be missing, or present at lower proportions in culture than *in vivo.* For example, the influence of the vascular niche is not present in culture, and the mature interneurons important for activity-dependent regulation are entirely absent. Moreover, microglia constitute approximately 1% of the total population in WT cultures, yet these cells are a critical link in the neuroimmune modulation of adult neurogenesis *in vivo* (Ekdahl et al.; 2003; 2012; Butovsky et al., 2006; Sierra et al., 2010; Nunan et al., 2014). Furthermore, mature astrocytes account for less than 5% of the total cell population present in 5DIV hippocampal mouse cultures. Mature astrocytes are intimately associated with the neurogenic process and promote neuronal differentiation *in vitro* when co-cultured with postnatal hippocampal NPCs (Song, Stevens, & Gage, 2002). The altered prevalence of these cell types

125

relative to NPCs, and lack of paracrine factors secreted by these cells, is likely to play an important role in the pattern of results reported here.

Despite these inherent shortcomings of an *in vitro* approach, it is nonetheless a valuable technique to permit assessment of the direct effect of experimental variables on cell types present within the niche, independent of the myriad factors that complicate *in vivo* whole-brain studies. While culturing NPCs within a controlled environment in defined media is advantageous in this respect, it should be considered that successful culture of mouse NPCs (as opposed to rat NPCs) is highly dependent on the addition of several factors to the culture medium, the concentrations of which may not be physiologically relevant. For example, mitogens EGF and FGF-2 are conventionally used at high doses in adult mouse NPC culture (Gage, 2000), and in the case of mouse hippocampal NPCs these factors are vital for successful cultures (Babu, Cheung, Kettenmann, Palmer, & Kempermann, 2007; Babu et al., 2011; Ray & Gage, 2006). Consequently, the proliferation of precursor cells in culture is non-representative of the *in vivo* situation. In our WT cultures, type 1/2a (Nestin$^+$ GFAP$^+$) accounted for approximately 38 ± 4 % of all dividing cells in a short-term EdU pulse paradigm. Using a similar culture protocol, Babu et al., (2011) reported that the majority of cells in adult mouse hippocampal cultures express Ki67$^+$ in the presence of 20 ng / ml EGF and FGF-2, as was used in the present experiments. *In vivo,* type 1 radial glia account for only 5% of nestin$^+$ cell divisions (Kronenberg et al., 2003). Therefore, the artificial drive placed upon cell division greatly inflates the natural rate of proliferation, and is likely to change the course of neurogenesis in the culture dish. This may also contribute to the observation of altered proliferation *in vitro* compared to *in vivo.*

Another noteworthy feature of our culture system is the use of retinoic acid (RA). B27 supplemented with RA was used as it has been shown to promote survival of adult mouse hippocampal cultures, which is otherwise poor (Babu et al., 2011; Ray & Gage, 2006). However, the benefits of RA upon mouse NPC survival are counteracted by its impact upon neuronal differentiation. While

126

RA is beneficial to neuronal differentiation and maturation in rat hippocampal NPCs (Palmer, 1997), it produces low levels of neuronal differentiation in mouse NPCs. Instead, RA favours glial differentiation in mouse NPCs (Ray & Gage, 2006), as was evident in our culture system at 14DIV. These intra-culture factors are likely to participate in the differing impact of complement upon NPCs in culture compared to the brain. Moreover, there are many other factors that control adult neurogenesis *in vivo* that are absent *in vitro*, such as neurotrophic factors VEGF and BDNF (Doetsch, 2003), neuropeptides NPY and VIP (Howell et al., 2005; Zaben et al., 2009; Nunan et al., 2014) and neurotransmitters such as GABA (Tozuka et al., 2005; Ge, 2005).

Due to the features of the in vitro paradigm discussed, it is possible that my *in vitro* findings are partially an artefact of the culture system. Together, the use of EGF/FGF-2 and RA in these cultures may have contributed towards a greater proportion of type 1/2a cells, and lower than usual levels of neuronal differentiation. Potentially, this could explain why I did not see the same increase in DCX+ cells in the absence of C3/C3aR *in vitro* as was observed *in vivo.* Furthermore, this could account for the return of TUJ1+ neurons to WT levels in C3/C3aR deficient cultures by 14DIV, as growth factors were then absent, yet the continued presence of RA may have inhibited the increases in mature neurons observed *in vivo* via GCL volume*.*

Nevertheless, it is important to note that differences were observed between genotypes, despite being exposed to the same culture conditions, suggesting that C3/C3aR signalling alters the interaction between NPCs and local niche factors, such as their sensitivity or responsiveness to growth factors. Therefore, in absence of the important cell-extrinsic factors discussed, my *in vitro* data does nonetheless demonstrate genuine regulatory effects of complement upon neurogenesis. These effects may be mediated either by direct signalling to NPCs, cell-cell contacts, or soluble factors released from microglia or astrocytes within culture. These effects may be overridden by

other cell extrinsic factors *in vivo,* or the manner of interaction between complement, NPCs and the local environment may be altered.

2.4.12 Concluding remarks

The *in vitro* data described here demonstrates that C3/C3aR can modulate the phenotype and proliferation of NPCs. *In vivo,* adult C3$^{-/-}$ and C3aR$^{-/-}$ animals showed heightened levels of neurogenesis, suggesting that C3/C3aR signalling is anti-neurogenic in the healthy brain. Combined, this data suggests that the effects of C3/C3aR signalling on AHN are dependent on interactions with local environment factors, such as microglia within the neurogenic niche. Furthermore, this data suggests that the C3a/C3aR pathway plays a greater regulatory role in AHN than the aforementioned C3d/CR2 pathway. Future work will seek to determine whether the mechanisms responsible for this effect are via survival or neuronal differentiation. Either way, the alterations to the level of net neurogenesis observed might have important implications for both the development of new neurons and their function, which will be investigated in the following chapters.

3. The role of C3/C3aR signalling in regulating neuronal morphology

3.1 Introduction

AHN is an important form of structural plasticity in the adult brain. Within this process, important variables include not only the net addition of new neurons, but also their morphology and functional integration into the existing hippocampal circuitry (Lledo, Alonso, & Grubb, 2006). Alterations in dendritic morphology are of significance, since the dendritic branch is a functional synaptic unit needed for memory storage (Govindarajan, Israely, Huang, & Tonegawa, 2011) and changes in neuronal branching, morphological complexity and migration may have widespread effects on the synaptic integration and function of newly born neurons (Llorens-Martín et al., 2016).

The maturation of dentate granule cells (DCGs) is highly plastic and can be modulated by several intrinsic (Ge et al., 2006) and extrinsic factors (Redila & Christie, 2006), including immune system proteins (Boulanger, 2009). An emerging line of evidence suggests that complement may be an important regulatory factor in both synaptic and morphological plasticity. Complement has been shown to sculpt synaptic circuitry in both the developing (Schafer et al., 2012; Stephan, Barres, & Stevens, 2012; Stevens et al., 2007) and adult brain (Shi et al., 2015), in addition to influencing the neurite outgrowth and dendritic structure of neurons in culture (Shinjyo et al., 2009; Lian et al., 2015). Whether these processes also apply to the ongoing neuronal development occurring within the adult hippocampus remain to be seen however. In this chapter, I investigated the capacity for C3/C3aR signalling to influence neuronal morphology and synaptic density using primary hippocampal mouse cultures. I also investigated the dendritic morphology of newly generated neurons in the brains of C3 and C3aR deficient mice.

3.1.1   The effect of C3/C3a signalling upon neuronal morphology

Previous reports have produced mixed results regarding the role of complement in regulating neuronal morphology. Using progenitor cells derived from the whole adult mouse brain, Shinjyo et al. (2009) reported that the addition of 100 nM C3a for 24 hours in the absence of growth factors significantly increased process length of Map-2ab^{+} neurons from 25.3 to 36.9 μm, suggesting a benefit of C3a in neuronal maturation and growth. At pathological levels however, C3 has been shown to compromise neurite outgrowth. Peterson, Nguyen, Mendez, & Anderson (2015) isolated neurons from the early postnatal rat cortex and co-cultured them with myelin to recapitulate spinal cord injury. When treated with a high dose of C3 (250 μg / mL; approximately 1.35 μM), the outgrowth of TUJ1^{+} neurons was significantly reduced compared to control. In contrast, treatment with C1q encouraged neurite outgrowth in this context, and was found to directly reduce neuronal growth inhibitory signalling (Peterson et al., 2015).

Together, these studies suggest C3/C3a can modulate neurite outgrowth, but whether this effect is beneficial or detrimental may be context (i.e., healthy versus diseased brain) and dose-dependent. These papers also suggest that complement can affect the morphology of diverse neuronal subtypes, including postnatal cortical neurons and adult progenitor-derived neurons. However, these studies are limited in scope regarding morphology, as measuring neurite length alone neglects many aspects of overall neuronal morphology, including complexity and arborisation. More detailed measures of neuronal morphology such as Sholl analysis (Sholl, 1953), a technique that quantifies the overall complexity of dendritic arbours, would be considerably more informative in assessing the impact of C3/C3a on neuronal morphology.

Lian et al. (2015) recently published a report featuring this technique. In this report, an astroglial-specific knock down of IκBα, an important regulator of NFκB, was used to induce C3 overexpression. This manipulation was shown

to cause uncontrolled NFκB activation, and consequent upregulation of C3 mRNA, a direct downstream target of NFκB. In order to investigate the effects of C3 on hippocampal neuronal morphology, neurons were isolated from the P0 WT mouse hippocampus and co-cultured with either WT (physiological C3 expression levels) astrocytes or IκBα knock down astrocytes (elevated C3 expression). After 14 days in culture, hippocampal neurons cultured in the presence of high levels of C3 had reduced total dendritic length, and Sholl analysis indicated that their morphology was significantly less complex than that of neurons cultured with WT astrocytes. Crucially, a dose-dependent relationship between decreased morphological complexity and exogenously-added human C3 was observed in hippocampal neurons, with doses ranging from 5 nM /ml to 27 nM / ml. In opposition to the results of Shinjyo et al. (2009), this suggests that C3 can impair neuronal morphology.

Lian et al. (2015) also performed a series of controls, which provide convincing evidence that C3/C3aR is responsible for the observed effects. Firstly, the morphological phenotype of hippocampal neurons co-cultured with IκBα knock down astrocytes was rescued when C3 was depleted from the culture media. Hippocampal neurons isolated from C3aR$^{-/-}$ P0 mice also showed preserved morphology when cultured with IκBa deficient astrocytes compared to WT hippocampal neurons exposed to these conditions. Furthermore, addition of C3aR antagonist SB290157 (Ames et al., 2001) to hippocampal neurons co-cultured with IκBa deficient astrocytes (thus exposed to high levels of C3) also rescued their dendritic length and morphological complexity. However, when hippocampal neurons co-cultured with WT astrocytes (thus exposed to physiological C3 levels) were treated with C3aRA, their morphology was compromised compared to non-C3aRA treated neurons also co-cultured with WT astrocytes. This suggests that while high levels of C3a/C3aR activity may harm neuronal morphology, critically, C3a signalling may also play a role in maintaining normal neuronal morphology under physiological conditions.

Therefore, this paper provides robust evidence that C3a/C3aR signalling impacts upon both dendritic length and overall neuronal morphology. While it has been shown that the processes guiding neuronal maturation and differentiation are maintained between embryonic development and the adult hippocampal niche (Esposito, 2005; Zhao et al., 2006), whether the morphology of postnatal and adult hippocampal neurons is also regulated by C3a/C3aR in the same manner has not previously been investigated. Furthermore, the aforementioned studies have exclusively examined the addition or upregulation of C3 release in culture. This may be problematic in the instance of adding exogenous C3, as commercially available products are often of human origin and the stability of such proteins can be extremely sensitive. This may explain the apparently contradictory results seen between the reports of Shinjyo et al., (2009; who used 100 nM C3a and observed a benefit upon neurite outgrowth), Lian et al. (2015; who used a maximum of 5 nM and observed a decrement in neurite length), and Petersen et al. (2015; who used an extremely high dose and reported impairment of morphology). Additionally, while the report by Lian et al. (2015) provided thorough controls to demonstrate the dependence of effects upon C3/C3aR, their IκBa knock down model is likely to have diverse impact upon the functioning of many other inflammatory pathways, which may interact with C3/C3aR to influence results. Therefore, a specific knock out of C3/C3aR would also be informative in this regard, and would also permit *in vivo* investigations*.

3.1.2 C3 dependent modulation of synapse density and phenotype

Recently, it has been demonstrated that plasticity-related proteins involved in long-term potentiation (LTP) and synaptic tagging can be synthesized within dendritic branches (Redondo & Morris, 2011). Changes in synapses and consequently neuronal excitability are thought to be a neural substrate for long term memory storage (Bliss, 1973; Johnston & Narayanan, 2008;), and are therefore also important to consider. In addition to modulating

dendritic structure, complement has also been implicated in directing synaptic pruning in the developing brain. In these studies, the visual system has been used as a model system for synaptic plasticity, taking advantage of the activity-dependent synaptic refinement occurring in the thalamic relay neurons of the dorsal lateral geniculate nucleus (dLGN) during the postnatal period (Stevens et al., 2007). There is now a strong body of evidence demonstrating that mice deficient in classical pathway components C1q, C3 (Stevens et al., 2007) and C4 (Sekar et al., 2016), as well as C3b receptor CR3 (Schafer et al., 2012), show parallel defects in developmental synapse elimination that persist into adulthood. Compared to WT animals, neurons in the dLGN of these animals retain a greater number of functional axonal inputs from retinal ganglion cells, which are normally eliminated in favour of one or two stronger inputs (Stevens et al., 2007). Consequently, C3$^{-/-}$ animals were shown to have a 1.3 fold increase in the number of VGluT1-2 containing synapses in the LGN compared to WT controls (Schafer et al., 2012). Moreover, the mechanism underlying complement-dependent synaptic pruning has been attributed to phagocytic microglia engulfing pre-synaptic inputs (Schafer et al., 2012), and is dependent both upon neuronal activity and the C3b/CR3 microglial signalling pathway (Stephan et al., 2012).

Interestingly, it has also been shown that this failure to prune excessive synapses during development is associated with cortical epileptogenesis at P20 in C1q $^{-/-}$ mice, suggesting that these findings may apply to brain areas other than the visual system, thereby constituting a widespread CNS pruning mechanism (Chu et al., 2010). Indeed, using electrophysiology, Perez-Alcazar et al, (2013) reported that hippocampal neurons derived from C3$^{-/-}$ mice have an increased number of glutamatergic synapses, yet demonstrate decreased release probability. This evidence therefore implicates C3 as a regulator of both the quantity, and functionality, of glutamatergic synapses.

Synapse density has also been investigated *in vitro* by Lian et al. (2015) using the previously described culture system. After 14 days in culture, Map-2ab positive neurons were co-stained with the synaptic markers synaptophysin,

VGluT1 and VGAT. Synaptophysin is an integral membrane glycoprotein found in the presynaptic vesicles of all neurons (Wiedenmann & Franke, 1985) Due to its ubiquitous expression, it can be used as a pan-synaptic marker. VGluT1, a vesicular glutamate transporter, has been shown to be present in the axons of glutamatergic neurons (Kaneko, Fujiyama, & Hioki, 2002), whereas VGAT is a vesicular GABA transporter associated with excitatory neurons (Zander et al., 2010). Lian et al. (2015) sampled 10 μm sections from the dendritic arbours of MAP-2 positive cells, and quantified the density of each type of synaptic puncta. Results showed that hippocampal neurons co-cultured with IκBα knock down astrocytes, thus exposed to high levels of C3, had a reduced numbers of synaptophysin+ puncta. This reduction in overall synapses was attributable to a significant reduction in the density of VGluT1+ puncta specifically. No changes in the density of VGAT puncta were observed. Moreover, exogenously administered recombinant human C3 showed that the effect was dose-dependent, with increasing doses of C3 incurring greater reductions in synapse number. Therefore, these results suggest that C3 is a negative regulator of excitatory synapses density on hippocampal neurons *in vitro,* and is in line with the increase in glutamatergic synapses reported by Perez-Alcazar et al. (2013) in C3$^{-/-}$ mice.

3.1.3 Mechanisms underlying complement dependent changes in neuronal morphology and synapse density

Is it important to note that the effects of complement upon dendritic structure and synaptic pruning are postulated to depend on separate C3 breakdown products and signalling pathways. The effects of C3 on dendritic morphology were shown to be dependent upon C3aR signalling by Lian et al. (2015), whereas the role of complement in synaptic pruning has been shown to be mediated by C3b/CR3 signalling on microglia by Schafer et al. (2012). However, Lian et al. (2015) argue against a role for microglia in their synapse density results, since microglia accounted for only 1% of cells in their

astrocyte-neuron co-culture system. It is therefore possible that C3 influences synapse density via a distinct pathway to that previously posited in the literature.

3.1.4 Aims and hypotheses

In this chapter, I aimed to investigate whether the morphology and synaptic phenotype of newly generated neurons in the adult hippocampus are also subject to regulation by C3, as previously described for other cell types *in vitro* and *in vivo*. Therefore, I examined both neuronal morphology and synapse density in hippocampal neurons generated from the postnatal mouse hippocampus. To do this, I utilised the technique of Sholl analysis, alongside immunostaining for synaptic markers. I also aimed to investigate the effects of C3/C3aR deficiency on newly born neurons within the adult mouse hippocampus, to determine whether effects are modulated by the surrounding niche that is absent *in vitro*.

Hypotheses

Regarding neuronal morphology, based on the data of Lian et al. (2015) and Peterson et al. (2015) I hypothesised that if C3/C3aR plays a role in neuronal morphology under physiological conditions, the constitutive absence of C3/C3aR would result in greater process length and more complex dendritic morphologies of newly born hippocampal neurons, both *in vitro* and *in vivo*. Regarding synaptic number and phenotypes, I also hypothesised that C3/C3aR deficiency would increase the number of overall synapses and specifically the number of excitatory synaptic puncta on mature hippocampal neurons *in vitro* when compared to WT.

3.2   Methods

3.2.1 Analyses for *in vitro* and *in vivo* neuronal morphology

Sholl analyses and profile

The Sholl analysis is conducted by superimposing the tracing of a neuron upon a series of concentric circles. The number of intersections at each radii are then calculated until the terminal point of the dendrites are reached (Sholl, 1953; see Figure 3.1C for example). To obtain a Sholl profile, the number of intersections versus the radial distance from the cell soma is plotted (Gutierrez & Davies, 2007). For all experiments detailed, radii separated by a distance of 10 μm were used.

Some previous reports have compared the number of intersections obtained at each individual radii statistically, however this method is likely prone to false positives due to the large number of multiple comparisons involved in analysis of cells with long processes. Therefore, I opted to compare Sholl profiles using a single metric, the area under the curve (AUC). This measure was calculated using the trapezoidal rule for each profile (Binley, Ng, Tribble, Song, & Morgan, 2014) using Microsoft Excel macros, designed and provided by Kate Binley (School of Optometry, Cardiff University).

Branching index (BI)

The BI was developed as a new algorithm to address shortcomings in Sholl analysis, as differences in number of intersection crossings can reflect both neurite length and neurite branching (Garcia-Segura & Perez-Marquez, 2014). The BI produces a value that is proportioned to differences in the pattern of neurite ramification, and is relative to the amount of branches a neurite possesses. As shown in Figure 3.1B, the difference in the number of intersections made in pairs of circles relative to the distance from the neuronal soma is compared (Garcia-Segura & Perez-Marquez, 2014). For

A TUJ1 DAPI   Trace

B

$$BI = \sum (\text{Intersections circle}_n - \text{Intersections circle}_{n-1})r_n$$

C

BI = 0   BI = 32
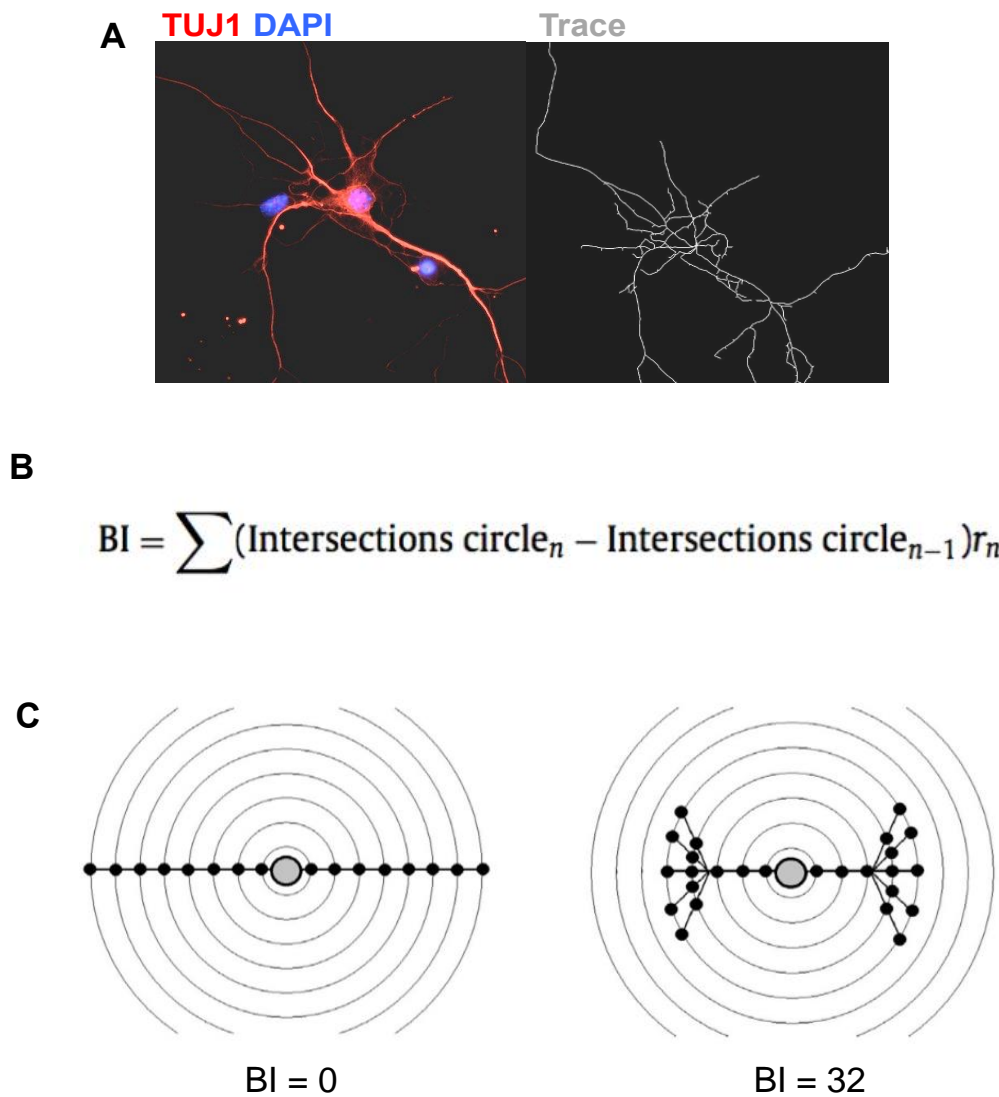
Figure 3.1 Example of Sholl tracing and calculation of the Branching Index (BI). A) TUJ1+ cell in culture (left) and tracing (right). **B)** BI equation (Garcia-Segura & Perez-Marquez, 2014). **C)** Example of BI application to a neuron with no ramification (left) versus ramification (right). Image adapted from Garcia-Segura & Perez-Marquez, (2014).

example, if the number of intersections in the outer circle is smaller than or equal to the number in the inner circle, the neurites have not ramified and the BI value will be 0 (see Figure 3.1C, left panel). Conversely, when the number of intersections in an outer circle is larger than the number in an inner circle, the BI will have a positive value (as shown in Figure 3.1C, right panel). Comparisons are made between consecutive circles, progressively in distance away from the cell soma. In these experiments, the BI was calculated using a Microsoft Excel macro, again designed and provided by Kate Binley.

Path length

In order to assess process length, all dendrites of an individual cell were classified as either primary paths or branches. Primary paths were defined as processes emanating directly from the soma, whereas branches were defined as any process originating from a primary process. The length of primary paths and branches, as well as the summation of primary paths and branches to calculate total path length, was analysed.

Branch and junction number

The number of branches, and their associated junctions (expected at approximately a 2:1 ratio) were also calculated as part of Sholl analyses.

3.2.2 *In vitro* methods

Animals

WT, $C3^{-/-}$ and $C3aR^{-/-}$ mice were used for all experiments, as detailed in Chapter 2 sections 2.2.1- 2.2.4.

3.2.3   Primary hippocampal cultures

Hippocampal cultures were generated from postnatal day 7 pups as described in Section 2.2.6. Cells were maintained NBA/B27/Glutamax/Abx with the addition of 20 ng/ml EGF and FGF-2 for the first 5 days in culture, with a partial medium change on day 3. After 5 days, media was aspirated and replaced with fresh NBA/B27/Glutamax/Abx devoid of growth factors in order to stimulate differentiation. After 24 hours, cells were fixed with 4% PFA and processed immunohistochemically (as detailed in Section 2.2.9) for immature neuronal marker TUJ1 and counterstained with DAPI to mark all nuclei. Cells were then mounted on microscope slides and imaged on a Leica DM6000B upright fluorescent microscope at 40 x magnification. For Sholl

analyses, TUJ1+ cells were sampled at random from 4 coverslips per condition.

3.2.4 Sholl analysis

Micrographs of TUJ1+ cells from WT, C3-/- and C3aR-/- cultures were first blinded using KeyGen software (kindly designed and provided by Nicholas Clifton). Cells were then traced individually (see Figure 3.1A for example) using Fiji image processing software (http://fiji.sc/Fiji) plugin Simple Neurite Tracer (http://fiji.sc/Simple_Neurite_Tracer). Any micrographs containing TUJ1+ cells that were off centre, so that their processes could not be traced in their entirety, were excluded. TUJ1+ cells in close proximity to each other or with inter-twined processes were also excluded from analyses. For each cell, processes were traced manually. Primary and secondary path lengths were extracted, before Sholl analysis was performed. Further analyses were then conducted using a series of Microsoft Excel macros to calculate the AUC and BI. A minimum of 15 TUJ1+ cells were analysed from 4 coverslips per experiment, from three independent experiments per genotype.

3.2.5 Synaptic analyses

I investigated the density and type of synapses present in primary hippocampal cultures after 14DIV. Cells were fixed and immunostained for TUJ1 and either synaptophysin, VGLUT1 or VGAT (an example of VGLUT1 staining is shown in Figure 3.7a). Micrographs of TUJ1+ processes were then acquired at 100 x magnification, with the experimenter blind to synaptic staining. Upon analysis, a section of neurite was chosen per image and the synaptic staining was un-blinded. Using ImageJ, the number of synapses was estimated by setting an image threshold using the particle count feature. The

number of synaptic puncta per 10 µm of dendrite was used as the dependent variable.

3.2.6 *In vivo* methods

Animals

Groups consisted of 6 adult males per genotype, between 8 and 12 months of age at time of sacrifice. All animals were reared in the same breeding room and were group-caged with littermates. Animals were transcardially perfused as detailed in Section 2.2.14, and brains processed as outlined in Section 2.2.15.

3.2.7 Sholl analysis of DCX+ cells

In order to analyse the morphology of newly born neurons in the adult hippocampus, 40 µm tissue sections were processed for doublecortin (DCX) immunohistochemistry as outlined in Section 2.2.16. Six stereotactic sections were collected per animal, and from each slice four doublecortin cells were selected for Sholl analysis. Within each hippocampi, two cells from the infrapyramidal and suprapyramidal dentate gyrus was selected. Each micrograph was transformed to grey scale and traced in the same manner as TUJ1+ cells *in vitro,* using Simple neurite tracer plug in on Fiji (see Figure 3.2 below for example, also described in Section 3.2.4).

3.2.8 Statistics

All statistics were conducted using GraphPad Prism software (La Jolla, CA). To determine whether assumptions for ANOVA were met, the shape of the

= Primary path
= Branches
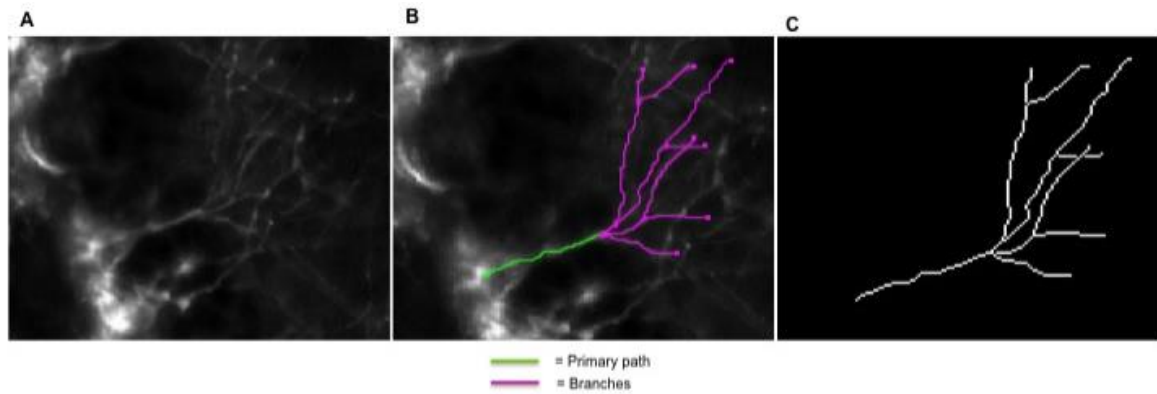
Figure 3.2. Example of *in vivo* Sholl tracing. **A)** DCX[+] immature neuron situated within the GCL. **B)** Tracing in progress, showing primary process in green and branches in magenta. **C)** The resulting trace, upon which Sholl analysis is based.

distribution was first visually inspected in a histogram of frequency distributions using a bin width of 20 units. D'Agostino-Pearson omnibus K2 test was used to assess normality. To assess departure from horizontal symmetry, skewness was examined, and the peak of the curve was assessed using kurtosis. Equal variance was assessed using the Brown-Forsythe test. In the case of heteroscedasticity, data was normalised between 0 and 100%, with 0 representing the lowest value in each dataset, and 100 representing the largest value in each data set. Data was then expressed as percentages.

Outliers were identified and removed using the ROUT method, which is based upon the False Discovery Rate (FDR). Q, or the maximum desired FDR, was set to 5%. Therefore, I aimed for no more than 5% of the identified outliers to be false, and at least 95% to be actual outliers.

One-way between subjects ANOVA was used to analyse differences between genotypes. Tukey post-hoc test was then used to correct for multiple comparisons when a significant overall ANOVA result was obtained. In the instance of non-normally distributed data, or data with unequal variances, Kruskal-Wallis non-parametric test was used as an alternative to ANOVA to compare three or more unmatched groups. Dunn's multiple comparison test was then used to conduct post hoc analyses.

141

3.3   Results

3.3.1 *In vitro* results

C3aR-/- neurons have altered morphological complexity in vitro

As seen in Figure 3.3A, the Sholl profiles suggested differential neuronal morphology between genotypes. The AUC was calculated for the Sholl profile of each genotype. One way ANOVA showed a significant difference between genotypes on this measure ($F_{(2,179)}$=10.61, p < 0.0001, Figure 3.3B). Post hoc analyses showed that the AUC was significantly greater in C3aR$^{-/-}$ cells (1323 ± 67.72) compared to both WT (922.5 ± 62.06, p < 0.0001) and C3$^{-/-}$ cells (1061 ± 58.90, p < 0.05). Since the Sholl curve reflects a range of variables, including process length and ramification, a range of other variables were next examined.

3.3.2   C3aR$^{-/-}$ increases neurite ramification

I next assessed the ramification of neurons between genotypes using the BI. There were significant differences in the BI between genotypes ($F_{(2,179)}$=8.07, p < 0.01, Figure3.4), reflecting a greater BI in C3aR$^{-/-}$ cells (624.4 ± 55.44) compared to WT (348.0 ± 42.75, p < 0.001) but not C3$^{-/-}$ (504.2 ± 48.27, p = 0.20).
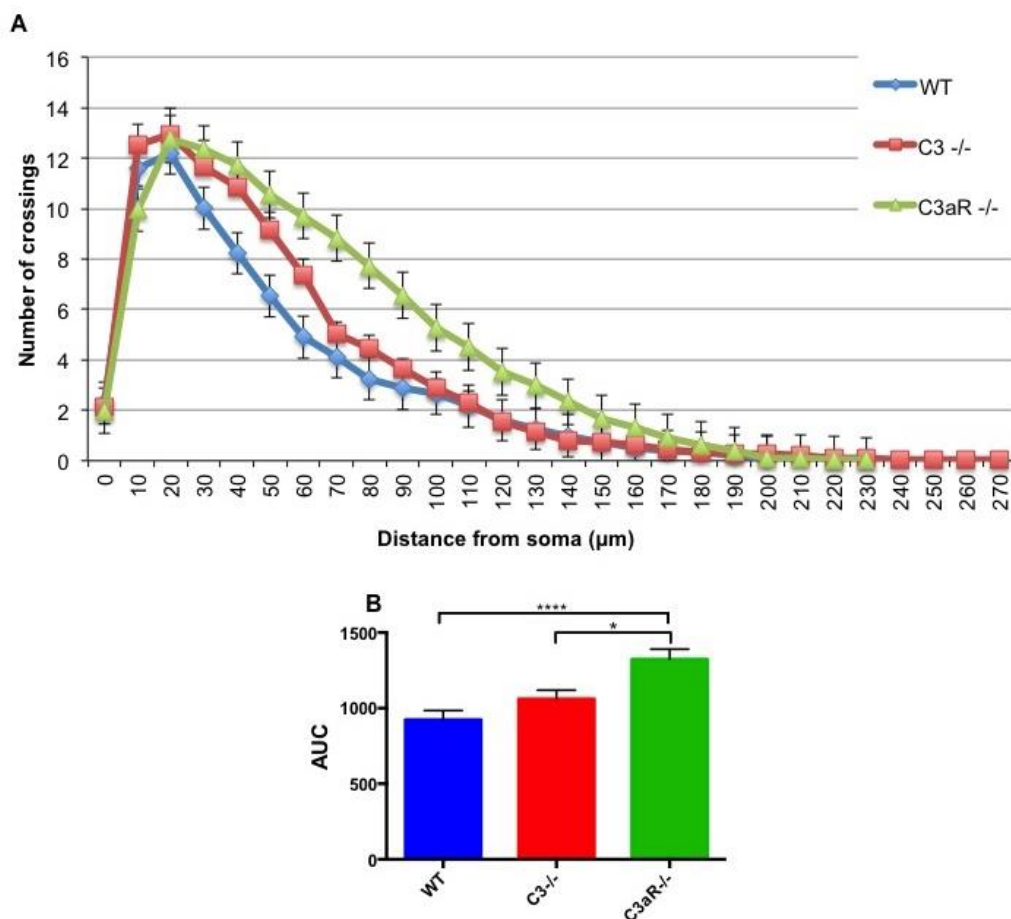
Figure 3.3. Sholl profiles of TUJ1+ cells from 6DIV WT, C3-/- and C3aR-/- cultures. A) Sholl profile **B)** Area under the curve. WT N= 61 neurons, C3-/- N = 57 neurons, C3aR-/- N=61 neurons. All cells were sampled from three separate cultures per genotype (minimum 15 per experiment). Data points represent mean ± SEM.. * = p < 0.05, ** = p < 0.02, *** = p < 0.001, **** = p < 0.0001
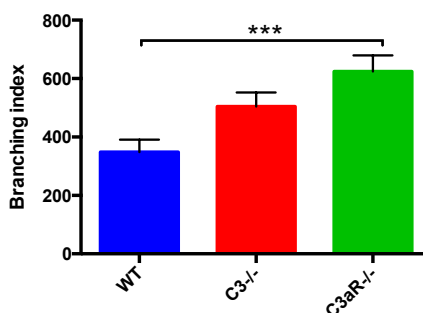
Figure 3.4. Branching index (BI) of WT, C3-/- and C3aR-/- TUJ1+ cells. WT N= 61 neurons, C3-/- N = 57 neurons, C3aR-/- N=61 neurons. All cells were sampled from three separate cultures per genotype (minimum 15 per experiment). Data points represent mean ± SEM.. * = p < 0.05, ** = p < 0.02, *** = p < 0.001, **** = p < 0.0001.

3.3.3 Absence of C3aR increases process length

As seen in Figure 3.5A, there was a significant difference in the average primary path length ($F_{(2,176)}$=11.27, $p < 0.0001$) and average branch length ($F_{(2,174)}$=17.99, $p < 0.0001$, Figure 3.5B) between genotypes. Post hoc analyses suggested that C3aR$^{-/-}$ (83.09 ± 3.01 μm) primary paths were, on average significantly longer than both WT (63.22 ± 3.74 μm, $p < 0.0001$) and C3$^{-/-}$ (65.82 ± 3.00 μm, $p < 0.001$). This pattern was also found in average branch lengths (C3aR$^{-/-}$ 34.94 ± 1.57 μm, WT 23.09 ± 1.35 μm, $p < 0.0001$ and C3$^{-/-}$ 27.44 ± 1.35 μm, $p < 0.001$). There were no significant differences between the average primary path lengths or branch lengths of C3$^{-/-}$ cells when compared to WT (p= 0.84 and p= 0.09, respectively).

For each cell, the primary process length and individual branch lengths were summed to create a total path length. Again, this measure showed variation between genotypes ($F_{(2,177)}$=11.04, $p < 0.0001$, Figure 3.5C). C3aR$^{-/-}$ cells had a significantly greater total path length (1588 ± 98.85 μm) than WT (1010 ± 79.87 μm, $p < 0.0001$) and C3$^{-/-}$ cells (1240 ± 86.16 μm , $p < 0.05$).
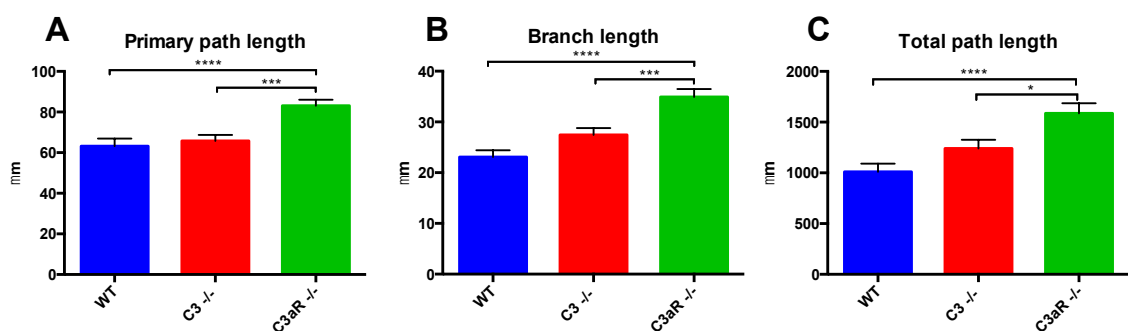
Figure 3.5 Process lengths in 6DIV TUJ1$^+$ cells from WT, C3$^{-/-}$ and C3aR$^{-/-}$ hippocampal cultures. A) Primary path length **B)** Branch length **C)** Primary paths and branches were summed per cell to obtain a total path length. WT N= 61 neurons, C3$^{-/-}$ N = 57 neurons, C3aR$^{-/-}$ N=61 neurons. All cells were sampled from three separate cultures per genotype (minimum 15 per experiment). Data points represent mean ± SEM.. * = $p < 0.05$, ** = $p < 0.02$, *** = $p < 0.001$, **** = $p < 0.0001$

3.3.4   C3/C3aR deficiency does not affect number of branches

The number of branches, and their associated junctions were measured across genotypes.   The number of branches was unchanged between genotypes ($F_{(2,181)}$= 1.57, p = 0.20, WT 121.5 ± 12.52, C3$^{-/-}$ 140.7 ± 13.66, C3aR$^{-/-}$ 152.4 ± 11.93, Figure 3.6A), as was the number of junctions ($F_{(2,174)}$=1.83, p = 0.16, WT 64.02 ± 6.99, C3$^{-/-}$ 71.91 ± 7.39, C3aR$^{-/-}$ 82.14 ± 6.33, Figure 3.6B).
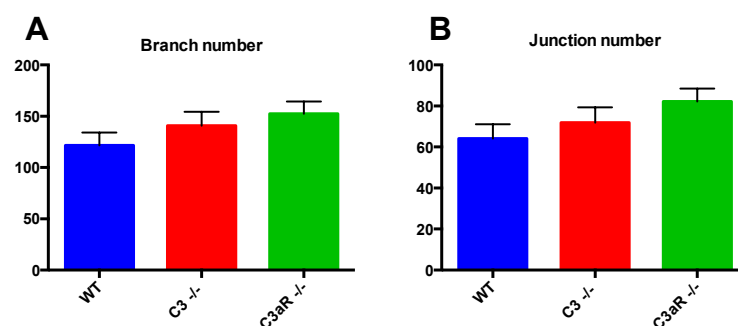
Figure 3.6. The number of branches and associated junctions of 6DIV TUJ1$^+$ cells from WT, C3$^{-/-}$ and C3aR$^{-/-}$ cultures. **A)** Branch number **B)** Junction number. WT N= 61 neurons, C3$^{-/-}$ N = 57 neurons, C3aR$^{-/-}$ N=61 neurons. All cells were sampled from three separate cultures per genotype (minimum 15 per experiment). Data points represent mean ± SEM.. * = p < 0.05, ** = p < 0.02, *** = p < 0.001, **** = p < 0.0001

3.3.5 Effect of C3/C3a deficiency on synapse density and phenotype

The density of synaptophysin puncta per 10 μm dendrite was comparable between genotypes ($F_{(2,171)}$=0.1005, p = 0.90, WT 3.65 ± 0.37 μm, C3$^{-/-}$ 3.91 ± 0.46 per 10 μm, C3aR$^{-/-}$ 3.70 ± 0.44 per 10 μm, Figure 3.7B). The density of VGLUT1$^+$ puncta also did not significantly differ between genotypes ($F_{(2,170)}$=1.75, p = 0.17, WT 2.46 ± 0.40 per 10 μm, C3$^{-/-}$ 3.44 ± 0.36 per 10 μm, C3aR$^{-/-}$ 3.07 ± 0.33 per 10 μm, Figure 3.7C). The density of VGAT$^+$ puncta was unchanged by C3/C3aR deficiency ($F_{(2,176)}$=1.30, p = 0.27, WT 1.37 ± 0.28 per 10 μm, C3$^{-/-}$ 0.88 ± 0.18 per 10 μm per 10, C3aR$^{-/-}$ 1.33 ± 0.20 per 10 μm, Figure 3.7D).
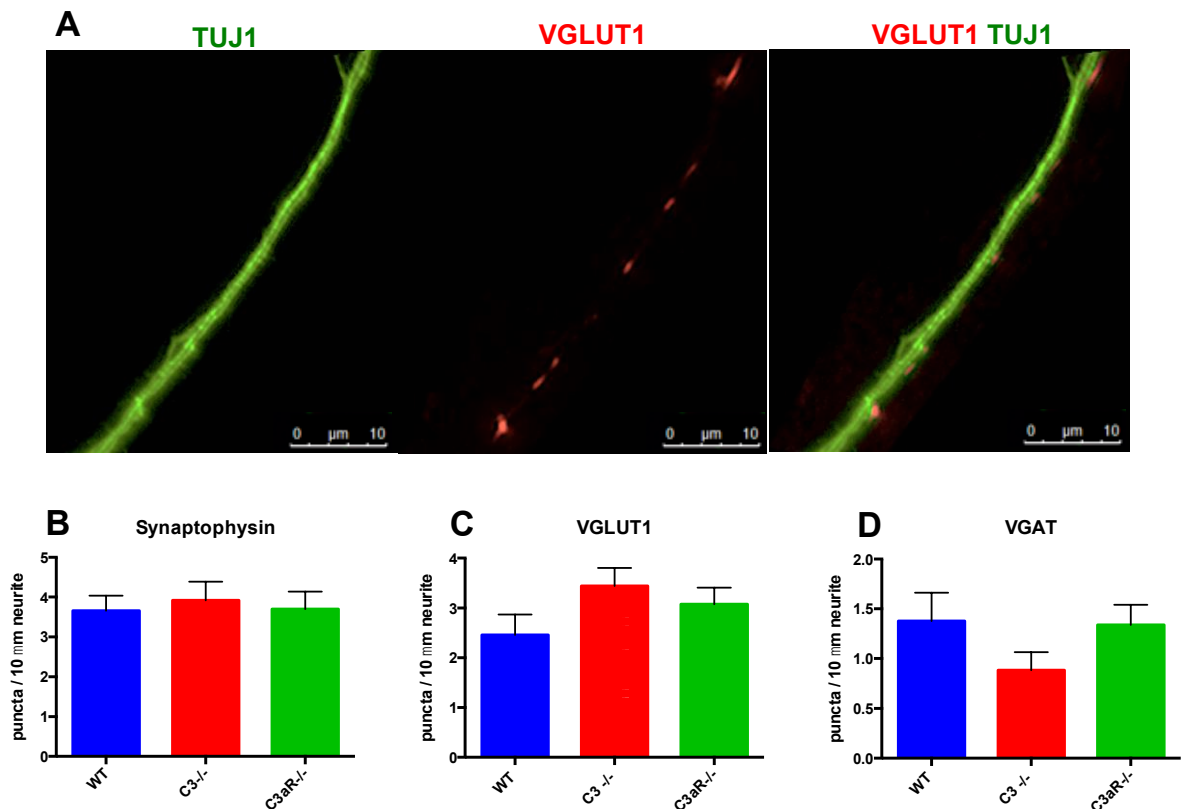
Figure 3.7 Synapse density and type in WT, C3^{-/-} and C3aR^{-/-} primary hippocampal cultures at 14DIV. A) Example of immunostaining. Sections of TUJ1^{+} neurites were sampled and the density of synaptic puncta (synaptophysin, VGluT1 [pictured] or VGAT) was counted. **B)** Density of synaptophysin puncta per 10 μm neurite sections. N= WT 53 neurons, C3^{-/-} 55 neurons, C3aR^{-/-} 66 neurons, from 3 independent cultures per genotype. **C)** Density of VGluT1^{+} puncta N= WT 64 neurons, C3^{-/-} 50 neurons, C3aR^{-/-} 59 neurons from 3 independent cultures per genotype. **D)** VGAT density. WT N= 63 neurons, C3^{-/-} N= 54 neurons, C3aR^{-/-} N= 62 neurons from 3 independent cultures per genotype. Data points represent mean ± SEM.

3.3.6 *In vivo* data

Newborn neurons have differing morphology in the suprapyramidal and infrapyramidal DG

I chose to examine the morphology of DCX^{+} cells with vertically orientated apical processes within the GCL, as these are typically Nestin[-] DCX[+] type 3 cells (Kempermann, Jessberger, Steiner, & Kronenberg, 2004; Kempermann et al., 2004), the stage at which the greatest morphological changes occur (Llorens-Martín et al., 2016). In addition, differences in the dendritic trees of newly born neurons have been reported between the suprapyramidal and

146

infrapyramidal blades of the DG (Claiborne, Amaral, & Cowan, 1990; Desmond & Levy, 1985). I therefore analysed the morphology of DCX cells based on this anatomical distinction. In WT animals, newly generated neurons in the suprapyramidal blade had greater overall complexity than those situated in the infrapyramidal blade (AUC 202.4 ± 11.74 suprapyramidal vs. 120.1 ± 6.42 infrapyramidal, $t_{(127)}$= 6.36 , p < 0.0001, Figure 3.8A and 3.8D). This pattern was observed in all genotypes (C3$^{-/-}$ suprapyramidal vs. infrapyramidal AUC $t_{(128)}$= 4.17 , p < 0.0001, Figure 3.8B and 3.8D, C3aR$^{-/-}$ suprapyramidal vs. infrapyramidal AUC $t_{(131)}$= 3.24 , p < 0.001, Figure 3.8C and 3.8D). Therefore, cells from each blade were distinguished in all further analyses.

3.3.7 C3aR$^{-/-}$ morphological complexity is altered in the suprapyramidal DG

Next, I compared the AUC obtained from Sholl analysis between genotypes. As shown in Figure 3.9 A and B, there were significant differences in the morphology of cells in the suprapyramidal blade between genotypes ($F_{(2,177)}$= 4.73, p < 0.01, Figure 3.9A and B). There was a trend towards a smaller AUC in C3$^{-/-}$ DCX$^+$ cells (169.4 ± 8.97) and C3aR$^{-/-}$ DCX$^+$ cells (160.9 ± 9.25) compared to WT (202.4 ± 11.74), although post-hoc tests showed significant differences between WT and C3aR$^{-/-}$ only (p < 0.01). The Sholl profile of cells sampled from the infrapyramidal blade were comparable between genotypes ($F_{(2,209)}$= 1.19, p = 0.70, Figure 3.9C and 3.9D).
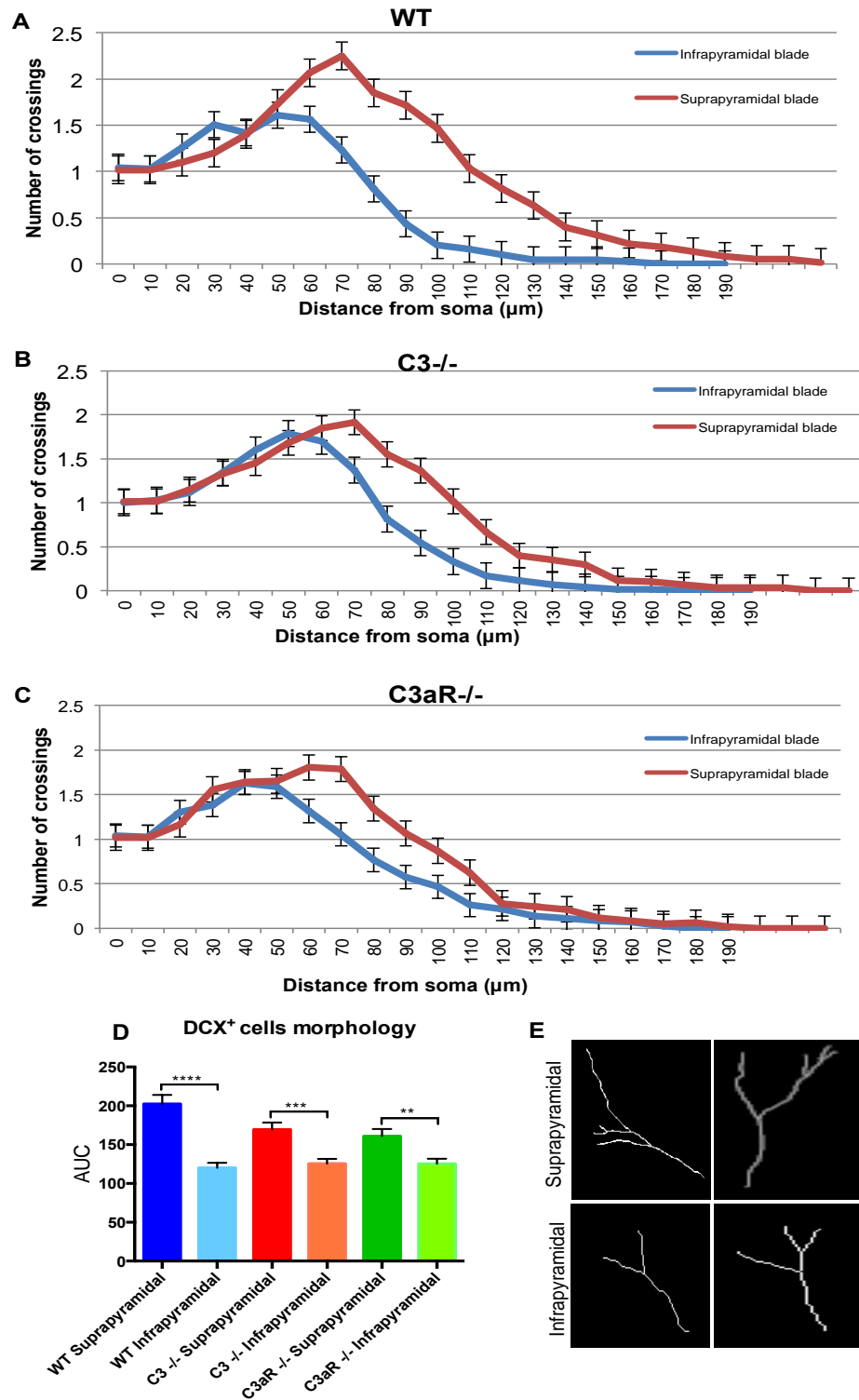
Figure 3.8. Sholl profile of DCX+ immature neurons situated in either the suprapyramidal or infrapyramidal blade of the dentate gyrus, across genotypes. A) Sholl profile for WT cells **B)** Sholl profile for C3^{-/-} cells. **C)** Sholl profile for C3aR^{-/-} cells. **D)** Area under the curve (AUC) analyses for all genotypes comparing the magnitude of differences between dentate blades. N= WT 60 cells suprapyramidal blade, 69 cells infrapyramidal blade; C3^{-/-} 60 cells suprapyramidal blade, 70 cells infrapyramidal blade; C3aR^{-/-} 60 cells suprapyramidal blade, 73 cells infrapyramidal blade, from 6 animals per genotype. **E)** Representative examples of tracings obtained from suprapyramidal and infrapyramidal blade cells. Data points represent mean ± SEM, * = $p < 0.05$, ** = $p < 0.02$, *** = $p < 0.001$, **** = $p < 0.0001$.
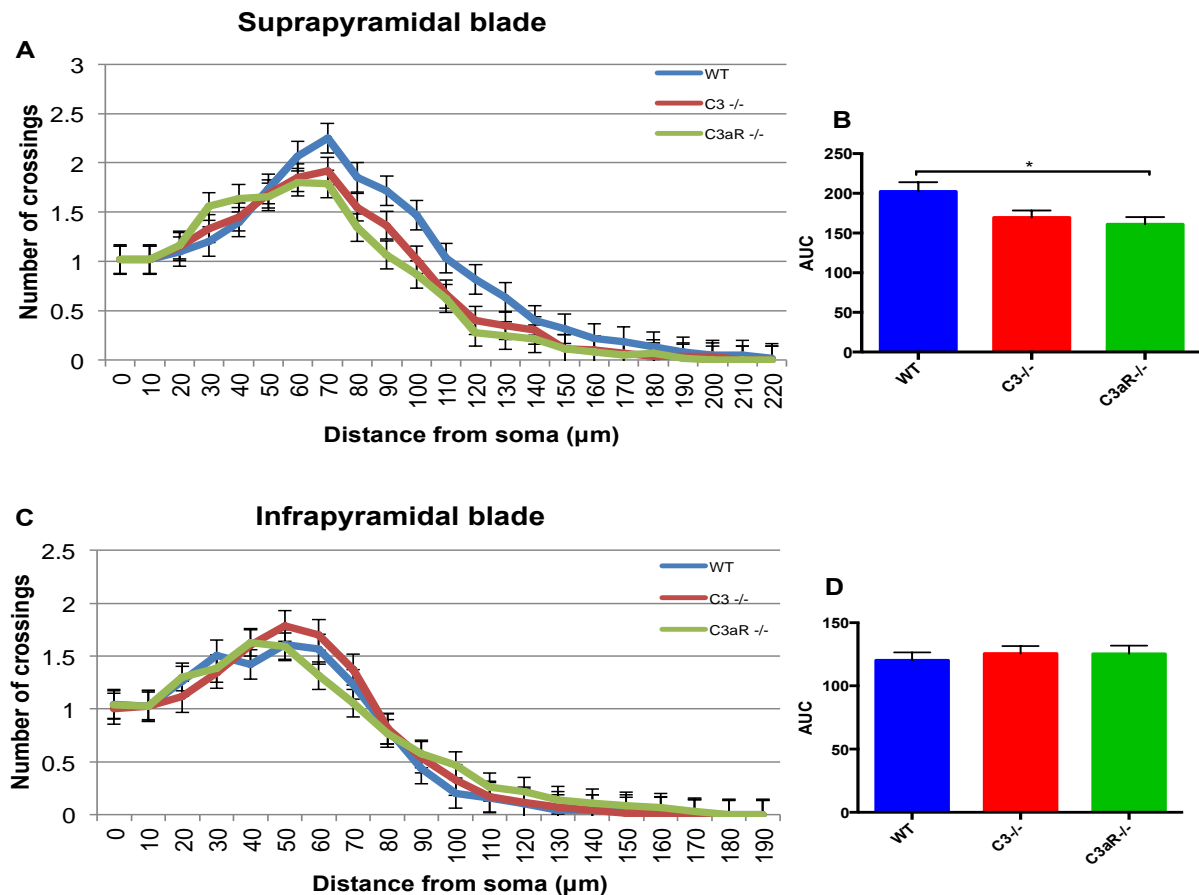
Figure 3.9. Sholl profile of DCX⁺ immature neurons between genotypes *in vivo*. A) Sholl profile for WT, C3$^{-/-}$ and C3aR$^{-/-}$ cells situated in the suprapyramidal blade of the DG **B)** AUC for suprapyramidal blade Sholl profiles shown in A. N= 60 cells per genotype, from 6 animals per genotype **C)** Sholl profile for WT, C3$^{-/-}$ and C3aR$^{-/-}$ cells situated in the infrapyramidal blade of the DG **D)** AUC analyses for all genotypes in the infrapyramidal DG. N= WT 69 cells, C3$^{-/-}$ 70 cells, C3aR$^{-/-}$ 73 cells, from 6 animals per genotype. Data points represent mean ± SEM, * = p < 0.05, ** = p < 0.02, *** = p < 0.001, **** = p < 0.0001.

3.3.8 C3aR$^{-/-}$ neuronal progenitors show decreased ramification in the suprapyramidal blade of the DG

I next examined the BI as a specific measure of neurite ramification. Within genotypes, DCX⁺ cells in the suprapyramidal blade had significantly greater BI values than those in the infrapyramidal blade (Figure 3.10A, unpaired *t*-tests). Between genotypes, I observed a significant difference in the BI of DCX cells in the suprapyramidal blade (F$_{(2,176)}$= 3.17, p < 0.05, Figure 3.10B). Post

hoc analyses showed a significant reduction of the BI in C3aR$^{-/-}$ cells (80.00 ± 10.11) compared to WT (117.9 ± 11.25, $p < 0.05$). Comparisons between C3$^{-/-}$ (107.7 ± 11.73) and WT or C3aR$^{-/-}$ were non significant. No differences were observed between genotypes in the BI of DCX cells situated in the infrapyramidal blade (Figure 3.10C).
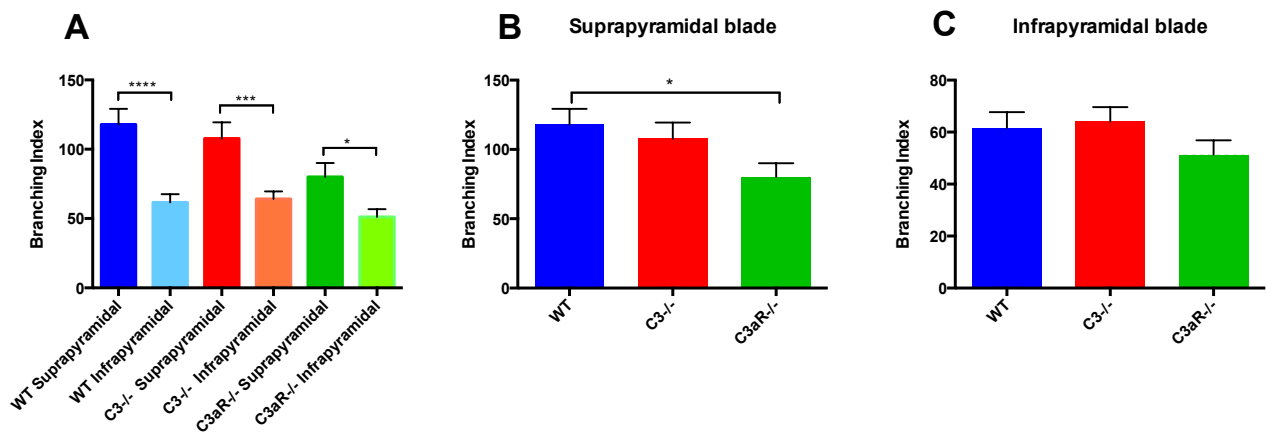
Figure 3.10. Branching index (BI) of DCX$^+$ cells *in vivo*. A) Comparison of the BI for DCX cells situated in either the suprapyramidal or infrapyramidal DG, across genotypes. **B)** BI of DCX cells in the suprapyramidal blade between genotypes N= WT 58 cells, C3$^{-/-}$ 60 cells, C3aR$^{-/-}$ 61 cells, from 6 animals per genotype. **C)** BI of DCX cells in the infrapyramidal blade between genotypes. N= WT 69 cells, C3$^{-/-}$ 70 cells, C3aR$^{-/-}$ 73 cells, from 6 animals per genotype. Data points represent mean ± SEM, * = $p < 0.05$, ** = $p < 0.02$, *** = $p < 0.001$, **** = $p < 0.0001$.

3.3.9 Path lengths are altered in C3aR$^{-/-}$ DCX cells

The average length of primary paths differed between the suprapyramidal and infrapyramidal blade ($F_{(5,383)}$= 5.26, $p < 0.0001$, Figure 3.11A). WT and C3$^{-/-}$ animals showed a significantly greater primary path length in the suprapyramidal blade (WT 91.45 ± 6.37 µm suprapyramidal vs. 63.99 ± 3.72 µm infrapyramidal, $p < 0.001$, C3$^{-/-}$ 79.57 ± 4.96 µm vs. 60.82 ± 3.59 µm $p < 0.05$). C3aR$^{-/-}$ cells did not significantly differ in this regard (71.52 ± 6.04 µm suprapyramidal vs. 65.65 ± 5.05 µm infrapyramidal, $p = 0.78$).

The average branch length of DCX$^+$ cells was also found to differ between the two dentate blades ($F_{(5,1093)}$= 11.58, p < 0.0001, Figure 3.11B). The average branch length of DCX$^+$ cells was significantly different in WT animals (suprapyramidal 42.53 ± 2.32 μm vs. infrapyramidal 27.31 ± 1.50 μm, p < 0.0001) and in C3aR$^{-/-}$ animals (suprapyramidal 45.45 ± 2.59 μm vs. infrapyramidal 34.00 ± 12.09 μm, p < 0.001), but this pattern was not present in C3$^{-/-}$ cells (suprapyramidal 34.72 ± 2.10 μm vs infrapyramidal 30.16 ± 1.42 μm, p = 0.27, Figure 3.11B).

In the suprapyramidal blade specifically, there were no differences in the average primary path length of DCX cells between genotypes (Figure 3.11D). There were differences in the average branch length in this region however ($F_{(2,557)}$= 5.52, p < 0.01, Figure 3.11E), attributable to a lower average branch length in C3$^{-/-}$ DCX cells (34.72 ± 2.10 μm) compared to both WT (42.53 ± 2.32 μm, p < 0.05) and C3aR$^{-/-}$ (45.45 ± 2.59 μm, p < 0.01). In the infrapyramidal blade, there were again no differences in average primary path lengths between genotypes (Figure 3.11G). However, there was a significant difference in average branch length between genotypes ($F_{(2,536)}$= 3.94, p < 0.05, Figure 3.11H) due to a greater average branch length in C3aR$^{-/-}$ DCX cells (34.00 ± 2.09 μm) compared to WT (27.31 ± 1.50 μm, p < 0.05) but not C3$^{-/-}$ (30.16 ± 1.42 μm, p = 0.24).

3.3.10 Total path lengths are decreased by C3aR$^{-/-}$

I next calculated the sum of all paths per cell to obtain the total path length. When comparing between suprapyramidal and infrapyramidal blades, there was a trend towards greater total path length in the suprapyramidal blade in WT   animals   (232.9   ±   13.19   μm   vs   138.8   ±   7.31   μm
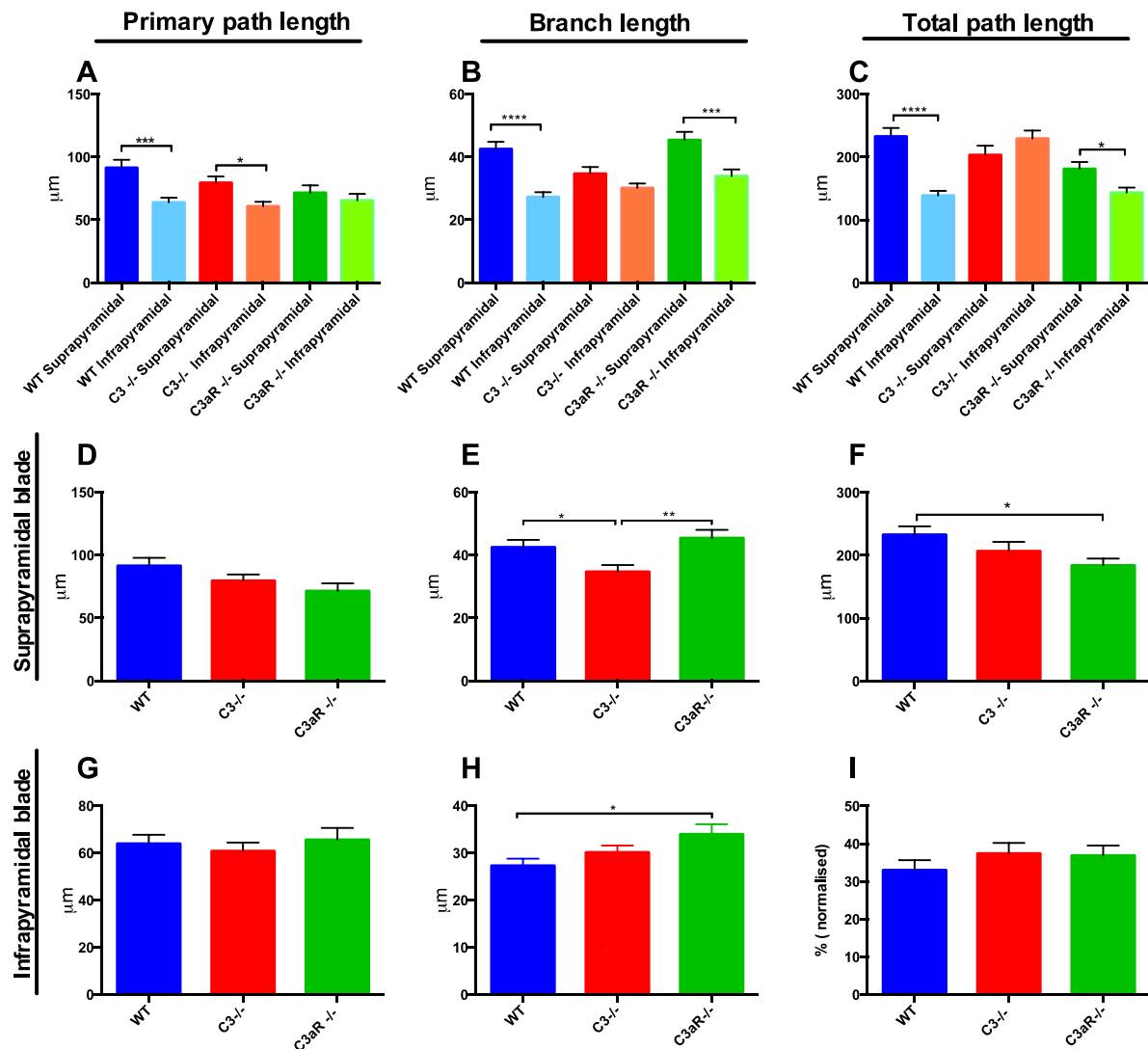
Figure 3.11 Average path lengths of DCX⁺ cells *in vivo* A) Comparison of the average primary path length for DCX cells situated in either the suprapyramidal or infrapyramidal DG, across genotypes. **B)** Comparison of the average branch length. **C)**. Comparison of the total path length. **D)** Average primary path length of DCX cells in the suprapyramidal blade N= WT 60 cells, C3$^{-/-}$ 59 cells, C3aR$^{-/-}$ 60 cells, from 6 animals per genotype. **E)** Average branch length of DCX cells in the suprapyramidal blade. N= WT 211 branches, C3$^{-/-}$ 199 branches, C3aR$^{-/-}$ 150 branches, from WT 60 cells, C3$^{-/-}$ 59 cells, C3aR$^{-/-}$ 60 cells, from 6 animals per genotype. **F)** Total path length of DCX cells in the suprapyramidal blade. N= WT 61 cells, C3$^{-/-}$ 59 cells, C3aR$^{-/-}$ 60 cells, from 6 animals per genotype. **G)** Average primary path length of DCX cells in the infrapyramidal blade N= WT 70 cells, C3$^{-/-}$ 68 cells, C3aR$^{-/-}$ 71 cells, from 6 animals per genotype. **H)** Average branch length of DCX cells in the infrapyramidal blade. N= WT 190 branches, C3$^{-/-}$ 189 branches, C3aR$^{-/-}$ 160 branches from WT 70 cells, C3$^{-/-}$ 68 cells, C3aR$^{-/-}$ 71 cells, from 6 animals per genotype. **I)** Total path length of DCX cells located in the infrapyramidal blade. N=WT 70 cells, C3$^{-/-}$ 68 cells, C3aR$^{-/-}$ 72 cells from 6 animals per genotype. Data points represent mean ± SEM, * = p < 0.05, ** = p < 0.02, *** = p < 0.001, **** = p < 0.0001.

infrapyramidal, p < 0.0001, Figure 3.11C) and C3aR$^{-/-}$, but post hoc tests did not meet conventional levels of statistical significance (181.11 ± 10.99 μm vs 143.5 ± 7.90 μm, p = 0.0506, Figure 3.11c). This trend was not present in C3$^{-/-}$ animals however (203.0 ± 14.67 μm vs 229.2 ± 12.56 μm respectively, p = 0.28). When total path lengths were analysed in DCX cells located in the suprapyramidal blade only, there was a significant difference between genotypes ($F_{(2,177)}$= 3.60, p < 0.05, Figure 3.11F) owing to a decreased total path length in C3aR$^{-/-}$ DCX cells (184.2 ± 10.74 μm) compared to WT (232.9 ± 13.19 μm, p < 0.05). With regard to total path length in the infrapyramidal blade, data was found to be positively skewed, not normally distributed and in violation of homogeneity of variance. The dataset was therefore normalized as detailed in Section 3.2.8. Based on the ROUT method, one outlier was identified and removed from the C3$^{-/-}$ data. One-way ANOVA did not show any significant differences between genotypes on this measure (Figure 3.11 I).

3.3.11 Newly born neurons have fewer branches in the absence of C3aR

There were significant differences in the number of branches on DCX cells between dentate blades ($F_{(5,382)}$= 7.54, p < 0.0001, Figure 3.12A). Post hoc analyses showed this was due to a greater number of branches on WT DCX cells located in the suprapyramidal blade compared to the infrapyramidal blade (7.45 ± 0.48 vs. 5.37 ± 0.31 infrapyramidal, p < 0.001). There were similar trends in C3$^{-/-}$ (7.33 ± 0.49 vs. 6.10 ± 0.40) and C3aR$^{-/-}$ cells (5.89 ± 0.46 vs. 4.60 ± 0.26), but these did not reach statistical significance (p= 0.09 and p= 0.07, respectively). Between genotypes, there were significant differences in the branch number in the suprapyramidal blade ($F_{(2,175)}$= 3.20, p < 0.04, Figure 3.12c). Compared to WT, there was a trend approaching significance in C3aR$^{-/-}$ cells (7.33 ± 0.49 WT vs. 5.89 ± 0.46 C3aR$^{-/-}$, p =0.06). A similar pattern was observed in the infrapyramidal blade ($F_{(2,207)}$= 5.13, p < 0.01, Figure 3.12E). This was a consequence of fewer branches on the DCX cells in C3aR$^{-/-}$ mice compared to WT (4.60 ± 0.26 vs. 6.10 ± 0.40, p < 0.01).

Closely associated with branch number is junction number. This variable again showed differences between dentate blades ($F_{(5,382)}$= 7.96, p < 0.0001, Figure 3.12B) due to a significantly greater difference in the number of junctions in C3$^{-/-}$ cells in the suprapyramidal compared to infrapyramidal blade (3.23 ± 0.24 vs. 2.17 ± 0.15, p < 0.001). There were significant differences in junction number in the suprapyramidal blade ($F_{(2,175)}$= 3.55, p < 0.05, Figure 3.12D) due to a decrease in C3aR$^{-/-}$ cells compared to C3$^{-/-}$ (suprapyramidal C3aR$^{-/-}$ 2.40 ± 0.22 vs. C3$^{-/-}$ 3.23 ± 0.24, p < 0.05) but not WT (3.18 ± 0.26, p = 0.06). Differences were also present in the infrapyramidal blade ($F_{(2,207)}$= 3.22, p < 0.01, Figure 3.12F), where there was a significant decrease in junction number of C3aR$^{-/-}$ DCX$^+$ cells 1.74 ± 0.13 vs. WT 2.53 ± 0.21 (p < 0.01).
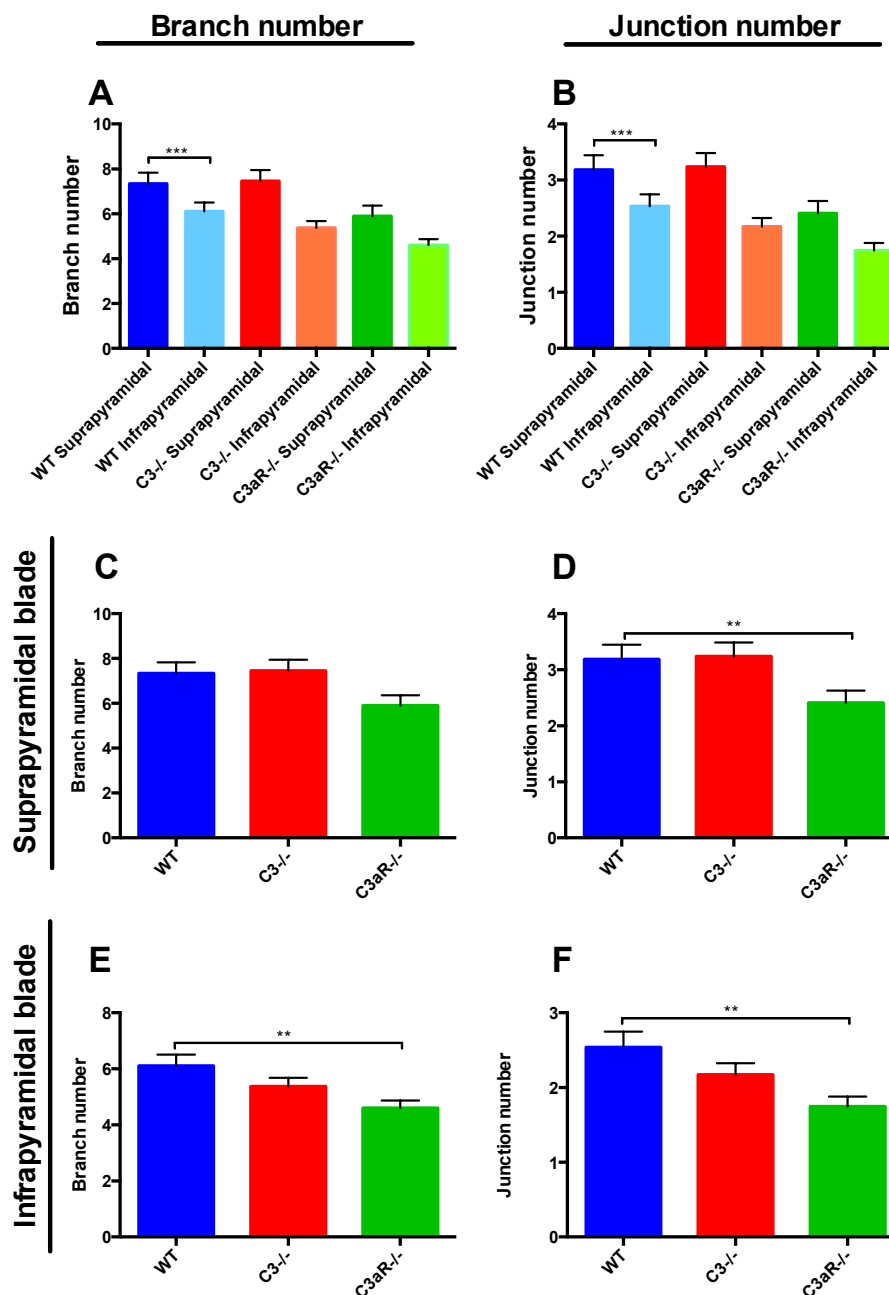
Figure 3.12. Number of branches and junctions on DCX⁺ cells *in vivo* A) Comparison of the branch number for DCX cells situated in either the suprapyramidal or infrapyramidal DG, across genotypes. **B)** Comparison of the junction number **C)** Number of branches on DCX cells in the suprapyramidal blade between genotypes. N= WT 60 cells, C3⁻/⁻ 59 cells, C3aR⁻/⁻ 59 cells from 6 animals per genotype. **D)** Number of junctions on DCX cells in the suprapyramidal blade between genotypes. **E)** Number of branches on DCX cells in the infrapyramidal DG, between genotypes N= WT 69 cells, C3⁻/⁻ 70 cells, C3aR⁻/⁻ 71 cells, from 6 animals per genotype **F)** Number of junctions on DCX cells in the infrapyramidal blade between genotypes. Data points represent mean ± SEM, * = $p < 0.05$, ** = $p < 0.02$, *** = $p < 0.001$, **** = $p < 0.0001$.

3.4   Discussion

The morphology of newly born neurons is an important aspect of AHN. This chapter investigated the capacity for C3/C3aR signalling to modulate neuronal morphology, both *in vitro* and *in vivo,* alongside a potential role in synaptic phenotype and density *in vitro.* Results showed that C3aR had effects upon morphology, both in culture and in the adult hippocampus. However, these effects differed depending on the environment, suggesting important modifiers of the C3aR-morphology relationship exist within the whole brain that are absent *in vitro*. Critically, I did not observe significant effects in the absence of C3, suggesting that other ligands may be accountable for the effects seen in the absence of C3aR.

3.4.1   C3a/C3aR signalling is not responsible for changes in neuronal morphology

As previously discussed, Lian et al. (2015) reported morphological changes in neurons exposed to C3 in a dose dependent manner. Peterson et al. (2015) also found that high levels of C3 reduce neurite length. Based on this literature, I hypothesised that an absence of C3 would therefore increase the morphological complexity of immature neurons. This hypothesis was not supported, neither in culture, nor in the whole brain. Regarding the *in vitro* results described here, in the previous chapter I demonstrated that C3a levels in our WT culture system are extremely low (below 6 pg/ml; see Section 2.3.4), and therefore may not be comparable to the concentrations of C3 used in the previous literature. Therefore, the previously reported effects may be concentration-dependent, and neuronal morphology may only be perturbed at levels that are irrelevant to the healthy brain. Therefore, these results suggest that C3 does not influence morphology under physiological conditions.

Instead, these results indicate morphological changes in C3aR$^{-/-}$ immature neurons, both *in vitro* and *in vivo,* suggesting that the effects are not mediated by C3a/C3aR signalling. As mentioned in the general introduction, it has been speculated that C3aR may possess multiple ligands (Gao et al., 2003). Indeed, the VGF derived peptide TLQP-21 has recently been shown to bind to murine C3aR (Hannedouche et al., 2013). There are several characteristics of VGF expression that make it a prime candidate for explaining the effects I have observed upon neuronal morphology.

Firstly, evidence implicates VGF in neuronal differentiation. Using in-situ hybridisation in the developing rat brain, Snyder, Pintar, & Salton (1998b) demonstrated that while VGF expression was widespread, expression was not found in areas of active proliferation, but rather appeared when developing neurons reached their target region and began to differentiate. Furthermore, they noted that the peak of VGF expression, during the first two weeks of postnatal development, coincides with periods of significant axonal outgrowth and synaptic remodelling. Furthermore, in this study, expression was observed in a developmentally regulated manner throughout the hippocampus, and expression of VGF was observed in granule cells of the dentate gyrus at P10 (Snyder, Pintar, & Salton, 1998b). This expression pattern persisted into adulthood, suggesting that VGF is of relevance to AHN and neuronal differentiation.

Moreover, VGF expression is known to be rapidly induced by neurotrophins including Nerve Growth Factor (NGF), BDNF and Glial Derived Growth Factor (GDNF; Ferri, Noli, Brancia, D'Amato, & Cocco, 2011). These factors have been reported to separately regulate the proliferation, differentiation and survival of adult born hippocampal neurons (Chen, AI, Slevin, Maley, & Gash, 2005; Frielingsdorf, Simpson, Thal, & Pizzo, 2007). In particular, BDNF is required for terminal differentiation, and newly born hippocampal neurons show reduced dendritic maturation in the absence of this factor (Chan, Cordeira, Calderon, Iyer, & Rios, 2008). Interestingly, C3a has been shown to induce NGF expression in astrocytes (Heese, Hock, & Otten, 1998), suggesting the

possibility for interaction between NGF-induced expression of VGF via C3a/C3aR. In addition, VGF expression is also inducible by neuronal activity. In rat PC12 cells, KCl induced depolarisation was shown to upregulate VGF mRNA (Salton, Fischberg, & Dong, 1991). Kainate-induced seizures also stimulated VGF mRNA expression in neurons of the DG and hippocampus, amongst other areas (Snyder et al., 1998a), whereas blocking retinal activity during the critical period of visual development strongly repressed VGF expression (Snyder et al., 1998a). Furthermore, a role for VGF has been elucidated in regulating AHN. VGF treatment was demonstrated to enhance neuronal lineage commitment and survival of hippocampal NPCs *in vitro,* although these were isolated from the embryonic brain (Thakker-Varia et al., 2007). *In vivo,* intra-hippocampal VGF infusion increased the number of BrdU labelled cells adopting a neuronal phenotype (Thakker-Varia et al., 2007).

TLQP-21, the VGF derived peptide found to bind to C3aR, is multi-functional in nature. Roles for this peptide have been described in regulating metabolism, nociception, the gastrointestinal system, the stress response, as well as mammotrophic cell differentiation (Cero et al., 2014; Hannedouche et al., 2013). In combination with the body of literature describing the expression and function of VGF, my results suggest that TLQP-21 signalling via C3aR may modulate the neuronal morphology of adult born neurons in the hippocampus. In order to investigate this possibility, follow up experiments will first screen for VGF expression in hippocampal cultures using qPCR, followed by ELISA to detect TLQP-21 in culture supernatant. TLQP-21 peptide could also be added to WT cultures to assess whether neuronal morphology is altered. Furthermore, if dependent on C3aR signalling, addition of the peptide to C3aR$^{-/-}$ cultures should fail to recapitulate effects seen in WT cultures.

3.4.2 C3aR deficiency increases morphological complexity of immature neurons *in vitro*

Using Sholl analysis of 6DIV neurons, C3aR deficient TUJ1⁺ cells were shown to have a more complex morphology (see Table 3.1 for summary of results). Examination of the separate variables that contribute to the overall Sholl profile revealed that absence of C3aR caused greater neurite ramification, and an increase in process length, affecting both branches and primary processes. There was not an increase in the number of branches however, suggesting that in the absence of C3aR, neurons had longer processes with a more complex ramification pattern, rather than more branches per se.

The finding that the absence of C3aR increases morphological complexity in culture does not agree with the finding reported by Lian et al. (2015), whereby hippocampal neurons showed decreased morphological complexity when treated with C3aRA. There are several potential factors that may contribute to this discrepancy. Firstly, the pharmacological action of C3aRA SB290157 is ill-defined, with some groups reporting full agonist activity in certain cell lines (Therien, 2005; Woodruff & Tenner, 2015). Differences may also be explained by the use of embryonic hippocampal precursors by Lian et al. (2015), versus postnatal day 7 cells in the current experiments, in addition to the astrocyte co-culture approach adopted by Lian et al. (2015).

3.4.3 C3/C3aR signalling does not affect synapse density or phenotype *in vitro*

Based on previous reports of the role of C3 in developmental synapse pruning *in vivo* (Stevens et al., 2007) and synapse density *in vitro* (Lian et al., 2015), I hypothesised that the absence of C3/C3aR *in vitro* would increase the density of VGluT1⁺ excitatory synapses specifically. Between genotypes, no differences were found in the density of overall synapses, or in the density

159

	In vitro		In vivo			
			Suprapyramidal	Infrapyramidal	Suprapyramidal	Infrapyramidal
	C3-/-	C3aR-/-	C3-/-		C3aR-/-	
AUC	n.s	↑	n.s	n.s	↓	n.s
BI	n.s	↑	n.s	n.s	↓	n.s
Average primary path length	n.s	↑	n.s	n.s	n.s	n.s
Average branch length	n.s	↑	↓	n.s	n.s	↑
Total path length	n.s	↑	n.s	n.s	↓	n.s
Branch number	n.s	n.s	n.s	n.s	n.s	↓
Junction number	n.s	n.s	n.s	n.s	↓	↓

Table 3.1 Summary of morphology results *in vitro* and *in vivo*. N.s indicates non-significant compared to WT.

of inhibitory or excitatory synapses however. Nonetheless, across genotypes, VGluT1 accounted for a greater proportion of all synapses than did VGAT. This is in accordance with the majority of neurons in culture expressing NeuN at this stage (see chapter 2, Figure 10J) and the excitatory phenotype of mature granule cell neurons *in vivo* (Gomez-Lira, 2005; Gutiérrez, 2003), suggesting that neuronal maturation occurs normally within our culture system. Since complement mediated synaptic-pruning is thought to depend on the interaction of weak synapses with microglia (Schafer et al., 2012), the low prevalence of this cell type in culture could also account for the absence of this effect *in vitro.*

It is possible that the methods used to estimate synapse number in the present data may not be sensitive enough to detect changes. While useful as an overall measure of density, the technique is sub-optimal where areas of high synapse density are concerned as proximal synapses may be grouped together and thus counts underestimated. Due to time constraints, even with the use of 100 X magnification it was not possible to count synapses by eye, although this would be a consideration for future studies. Furthermore, it is acknowledged that counting individual synaptic puncta does not give any indication of functionality. Perez-Alcazar et al., (2013) showed that despite

increased excitatory synapse numbers, compensatory mechanisms were present in C3$^{-/-}$ mice suggesting that the resultant electrophysiology is of central importance. Future work could therefore conduct more detailed analyses of synaptic density, alongside electrophysiological studies to investigate the impact of potential synaptic and morphological phenotypes upon network functionality.

3.4.4   C3aR deficiency decreases morphological complexity of newborn neurons *in vivo*

Sholl analysis of DCX$^+$ neurons in the adult mouse hippocampus also revealed effects of C3aR deficiency upon morphology. However, the direction of effect was in opposition to that observed in culture. Rather, C3aR deficient immature neurons in the suprapyramidal blade of the DG showed a less complex overall morphology (see Table 3.1). This was characterised by decreased neurite ramification and total process length, in combination with fewer branches. Interestingly, in the infrapyramidal blade, DCX cells also had fewer branches, but on average these branches were longer. In C3$^{-/-}$ brains, I observed effects only in the suprapyramidal blade, where immature neurons showed a decreased branch length. In contrast to my *in vitro* data, these results suggest C3aR encourages the neurite outgrowth and branching of newly born neurons under physiological conditions.

Again, the lack of results in the C3$^{-/-}$ strain suggests that C3/C3a does not partake in neurite outgrowth or dendritic branching under physiological conditions *in vivo*. My result regarding C3aR dependent morphological effects agrees in part with the finding of Lian et al. (2015), whereby hippocampal neurons co-cultured with WT astrocytes (therefore producing physiological levels of C3), showed impaired morphology when treated with C3aRA compared to untreated neurons in the same condition. This suggests that C3aR plays a role in maintaining normal neuronal morphology under basal conditions, as I have demonstrated *in vivo.*

On the majority of measures, there were significant differences between cells situated within the suprapyramidal versus the infrapyramidal blade, within genotype. This is in agreement with previous literature (Rahimi & Claiborne, 2007; Claiborne et al., 1990; Desmond & Levy, 1985) suggesting that newly generated neurons in the suprapyramidal blade have a more complex morphology and longer reaching branches than their infrapyramidal counterparts. It is also interesting to note that between genotypes, I found variations in branch length and number, but not primary path length, implying that the former is more amenable to modulation by complement *in vivo*.

In considering the functional impact of these morphological changes, it is interesting to note that most effects were found in the suprapyramidal blade of the DG. Functional divisions along the traverse hippocampal axis have been less thoroughly investigated than those of the longitudinal hippocampal axis (Jinno, 2011). However, some differences in connectivity have been reported between blades. Claiborne et al (1986) reported that dendrites arising from the infrapyramidal blade make contact with the proximal CA3 region via the hilus, whereas suprapyramidal cells contact the stratum lucidim via the stratum radiatum. Therefore, should the abnormal morphological phenotype of immature neurons observed persist in the fraction of cells surviving to maturity, it is possible that these connections may be disturbed in C3aR$^{-/-}$ animals. Blade-dependent differences in functionality have also been described (as outlined in Section 1.2.1). In particular, the suprapyramidal blade displays more c-Fos reactivity after water maze training and physical activity than the infrapyramidal blade (Snyder et al. 2009). Therefore, it is possible that the morphological alterations seen in immature neurons in these experiments may compromise hippocampal spatial learning and memory.

Important anatomical gradients of neurogenesis and functionality also exist along the longitudinal hippocampal axis (Strange, Witter, Lein, & Moser, 2014), which have not been investigated in this data due to insufficient

sample size. It is likely that the functional impact of any morphological alterations will depend on the location of cells within this axis, and therefore follow up experiments aim to sample more cells to gain greater power to conduct these analyses.

3.4.6 Potential mechanisms underlying C3aR dependent morphological changes

The potential mechanism underlying morphological changes may be via a direct effect of C3aR on neurite growth, or via an intermediate cell type such as microglia. With regard to the former possibility, little is known of the downstream consequences of C3a/C3aR binding, let alone of the more recently discovered TLQP-21/C3aR binding which may be responsible for the results obtained here. Cero et al. (2015) reported that TLQP-21/C3aR binding increased intracellular Ca^{2+} and activated the MAPK/ERK pathway, similar to the proposed downstream effects of C3/C3aR in astrocytes (Sayah et al., 2003; Shinjyo et al., 2015). Lian et al. (2015) also demonstrated that C3aR plays a role in regulating intra-neuronal calcium. Therefore, C3aR-mediated activation of these transduction pathways would likely have important functional effects, such as growth factor and cytokine production (Sayah et al., 2003), which may impact upon neuronal growth and thus morphology.

With regard to the possibility of microglial involvement, while these cells are known to prune synapses and dendritic spines, less is known about whether they are able to phagocytose dendritic arbours directly, or whether dendrite retraction is a certain consequence of synaptic pruning (Schafer et al., 2012). Previous papers have argued against a contribution of microglia in C3aR dependent dendritic morphological changes. In the co-culture system used by Lian et al. (2015), microglia comprised 1% of the total cell population. This is comparable to the proportion of microglia present in the current culture system (see Appendix C). Lian et al. (2015) argue that such a low

concentration of microglia rules out a potential contribution of this cell type in their results. Nevertheless, despite a low proportion of microglia, these cells are highly motile when activated, and release many factors which are of importance to both neurogenesis and neuronal network functioning (Ferrini & De Koninck, 2013; Wake, Moorhouse, Miyamoto, & Nabekura, 2013). Therefore, the potential contribution of microglia is an interesting avenue for future experiments.

The potential for microglial involvement via dendritic pruning could be examined in culture. Microglia have been shown to be important for AHN in primary hippocampal rat cultures (Nunan et al., 2014) and completely removing microglia is likely to perturb neurogenesis and morphology. Therefore, the differing actions of the compounds MAC-1-SAP (a saporin-conjugated anti-CD11b monoclonal antibody) and minocycline could be exploited to answer this question. Minocycline is an antibiotic known to inhibit motility of microglia, and thus in this context this would inhibit potential 'pruning' whilst preserving the benefit of microglial-secreted factors released into culture medium. Neurons grown under this condition could be compared to both those grown with MAC-1-SAP, which selectively depletes microglia, and neurons grown in control conditions. Investigation of the resulting neuronal morphology may elucidate whether microglia contribute to the observed effects upon neuronal morphology via dendritic pruning.

3.4.5 Methodological considerations of morphological analyses

Given the methods used, a degree of selection bias was unavoidable in the current set of experiments. Although cells were sampled at random *in vitro,* the sample may not be representative of the majority of neurons in culture. Immature neurons often congregated in monolayer cultures, and possessed extremely intertwined processes that would not permit accurate Sholl tracing. Therefore, isolated cells have been used for these analyses. I cannot

exclude the possibility that the morphology of these cells is altered due to their lack of neighbouring neurons and likely synaptic contacts. Similarly, *in vivo* analyses presented a similar problem due to the tightly packed nature of DCX cells along the hilar border of the GCL, meaning that deciphering which processes belong to which cell can often be ambiguous. This again limited the number of cells available for sampling to those with clearly defined processes. In order to circumvent such selection bias, future experiments will utilise sparse labelling as opposed to immunohistochemical labelling. This can be achieved in monolayer cultures, in hippocampal slice culture or in fixed tissue using multicolour DiOlistic labelling (Gan, Grutzendler, Wong, & Wong, 2000). This technique delivers lipophilic dye-coated particles via a gene gun, and simultaneously labels many different cells with subtly differing hues, rendering the processes of densely packed cells discernable. In fixed tissue, this technique could be combined with immunohistochemistry to identify immature neurons, or jointly with BrdU injections prior to sacrifice to assess the morphology of more mature neurons.

3.4.7 Differences between *in vitro* and *in vivo* paradigms

As discussed in the previous chapter (Section 2.4.10 and 2.4.11), many factors may contribute to the opposing direction of effects observed *in vitro* versus *in vivo.* Pertaining to neuronal maturation in particular, a critical factor may be the lack of surrounding cycoarchitecture in culture. *In vivo,* there exists an intimate relationship between radial glial cell bodies and newborn neurons. Shapiro, Korn, Shan, & Ribak, (2005) demonstrated that the non-radial processes of GFAP expressing cells wrap around DCX cells to 'cradle' them within the SGZ. Principally, radial glia also appear to provide a scaffolding for the neurite outgrowth of immature neurons; the apical processes and growth cones of DCX cells were found to extend along the radial glial processes that permeate the GCL (Shapiro et al., 2005). Furthermore, mature astrocytes are key constituents of the neurogenic niche,

yet account for a small proportion of the total cell population in primary hippocampal mouse cultures at 5DIV. It has been demonstrated that the dendritic development of adult born neurons relies on direct contact between their dendritic trees and mature astrocytes situated on the outer-GCL border, in addition to astrocytic D-serine release (Sultan et al., 2015). This mechanism has important implications for the survival, synaptic integration and ultimate function of adult born neurons. Therefore *in vitro,* where neurite growth is unconstrained in comparison, it perhaps should not be surprising to observe dramatic alterations in morphology. The differences I have observed between the culture dish and the whole brain therefore underscore the importance of the environmental factors in neuronal maturation and morphology.

Another potential variable that should be considered is the use of different markers *in vitro* and *in vivo.* In culture, I used TUJ1 as a marker of immature neurons, whereas *in vivo* I used DCX for this purpose, as this is conventional for identifying newly generated neurons (Rao & Shetty, 2004)*.* One could argue that in order to compare like with like, the morphology of DCX cells should also be examined *in vitro,* which will be followed up in future experiments. However, for several reasons, I believe that these cell types are comparable despite the use of a different marker. In primary hippocampal cultures, type 3 cells (Nestin⁻ DCX⁺) show extremely low proliferative activity (see Appendix D), and TUJ1 cells were found to be exclusively post-mitotic (i.e., EdU incorporation was never detected). The majority of TUJ1 cells also co-expressed DCX (see Appendix D). This co-expression was maintained up until 14DIV in some TUJ1 cells. *In vivo,* most of the DCX⁺ cells sampled showed a 'Y' shaped morphology, and were vertically positioned within the GCL. Based on visual comparison to report by Zhao et al. (2006; see Figure 1.4, p.18) which presents a time course of the maturation of granule cells, the present sample mainly consisted of post-mitotic immature neurons approximately 10 days post-differentiation. Therefore, the populations sampled *in vitro* and *in vivo* may overlap considerably, and the aforementioned differences in environment are likely to play a larger

causative role in the differences observed than the use of differing markers per se.

3.4.8 Concluding remarks

This chapter has demonstrated that C3aR signalling modulates the morphology of newly born neurons, both in primary hippocampal cultures and in the whole brain. Whether C3aR perturbs or promotes dendritic branching and neurite outgrowth appears to depend on the surrounding microenvironment however. Furthermore, this effect was not observed in C3 $^{-/-}$ cells, suggesting independence of C3a and its canonical receptor, C3aR. Rather, it is speculated that TLQP-21/C3aR signalling constitutes an alternative pathway that may underlie the observed effects. Since the dendritic arborisation and synaptic contacts of a cell are important determinants of its connectivity, these variables are therefore critical to the functionality of hippocampal circuitry. Whether the morphological alterations observed in this chapter have any functional consequences for hippocampal-dependent cognition will be investigated in the subsequent chapter.

4.   Influence of C3/C3aR on pattern separation and affective behaviour

4.1   Introduction

As outlined in Section 1.3, the hippocampal formation participates in episodic memory and the form of recollective recall that features contextual, temporal and spatial information (Aggleton & Brown, 2006b). Adult born GCs are thought to support this process by performing the computation referred to as 'pattern separation' on cortical input arriving from the EC. This allows highly similar inputs to be distinguished, thereby reducing interference and permitting efficient memory storage and retrieval (Yassa and Stark, 2011). Furthermore, through the connections of adult born neurons with structures such as the amygdala, AHN is thought to partake in affective processes such as fear and anxiety (Bannerman et al. 2014; discussed in Sections 1.2.1 and 1.3.5).

In the previous chapters, I observed increased levels of newly born neurons in the adult hippocampus in C3 and C3aR deficient mice, alongside morphological changes in this population of cells in the absence of C3aR. Such alterations in adult neurogenesis, and in the connectivity of newly born neurons, have been associated with measurable changes in hippocampus-dependent behavioural tasks (Clelland et al., 2009; Monje, Toda, & Palmer, 2003; Barkas et al., 2012; Sahay et al., 2011) and paradigms measuring anxiety (Hill, Sahay, & Hen, 2015b; Kheirbek & Hen, 2014; Revest et al., 2009). Therefore, in this chapter I sought to determine whether the neurogenic and morphological changes observed have functional correlations with hippocampal dependent cognition and anxiety.

This introduction gives an overview of behavioural paradigms relevant to the testing of hippocampal-dependent cognition and emotionality, before considering the impact of abnormal neurogenesis on each faculty and task

performance. The previous literature regarding complement deficient animals and their behavioural phenotype is then reviewed.

4.1.1 Behavioural paradigms for testing spatial memory and their relevance to AHN

Hippocampal function is commonly probed in behavioural tasks that manipulate spatial information. The Morris water maze (MWM) is one of the most commonly used tasks in behavioural neuroscience and has a wide range of applications (D'Hooge & De Deyn, 2001). As depicted in Figure 4.1, a rodent is immersed in a large circular pool, with opaque liquid. Over a series of acquisition and probe trials, an animal must learn and retain the location of a hidden submerged platform, based on extra-maze spatial cues (Morris, 1984). The MWM is particularly sensitive to hippocampal lesions in rodents (D'Hooge & De Deyn, 2001; Logue, Paylor, & Wehner, 1997; Morris, Garrud, Rawlins, & O'Keefe, 1982), and it has been established that adult born hippocampal neurons between five and eight weeks of age are preferentially recruited by water maze training (Kee, Teixeira, Wang, & Frankland, 2007). Animals with chronically decreased neurogenesis have shown deficits in the MWM (Barkas et al., 2012), although increases in neurogenesis do not always benefit MWM probe trial performance (Sahay et al., 2011).

Many spatial learning tasks also incorporate reversal learning, a commonly used measure of cognitive flexibility or executive functioning (Clark, Cools, & Robbins, 2004). This requires an animal to adapt their behaviour to meet changes in stimulus-reward contingencies. Reversal learning can be incorporated into tasks such as the MWM, by changing the location of the platform or changing the rewarded spatial location between trials. This facet of the task requires cognitive flexibility, since the animal must abandon their previous search strategy and acquire the novel platform location (Vorhees & Williams, 2006). Furthermore, inclusion of a reversal element in such tasks

can allow discernment of changes in executive function from changes in learning and memory. In rodents and nonhuman primates, lesions to the orbitofrontal frontal cortex and the ventral striatum cause a perseverative response tendency, characterised by an inability to adapt responses to such changes in stimulus-reward contingencies, suggesting these areas participate in reversal learning (Annett, McGregor, & Robbins, 1989; Clark et al., 2004; Jones & Mishkin, 1972).
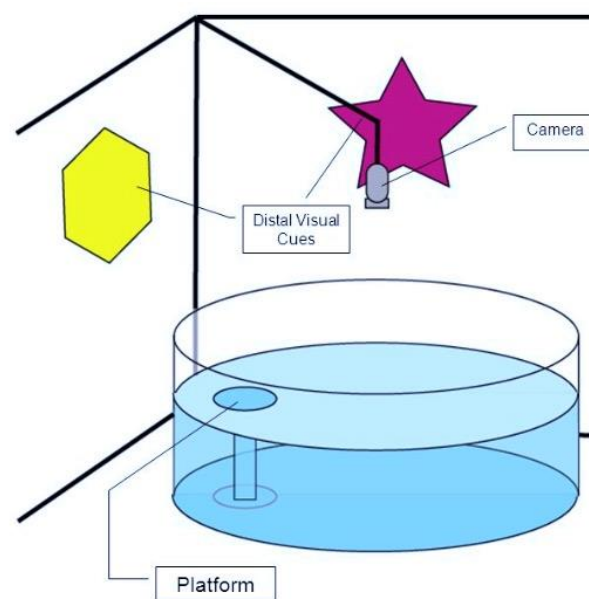
Figure 4.1. **Example of the Morris water maze apparatus**. Image sourced from http://www.radiantthinking.us/memory-theory/ii-behavioral-assessments-in-rodents.html

Whether AHN in involved in cognitive flexibility is unclear. Garthe, Roeder, & Kempermann (2015) proposed that AHN is essential for adding flexibility to hippocampus-dependent learning. However, disruptions of AHN have been found to spare spatial reversal learning (Hernández-Rabaza et al., 2009), suggesting that AHN is not needed for this aspect of cognitive flexibility. Furthermore, Saxe et al. (2007) reported that ablation of AHN actually improved performance in working memory tasks, but only in scenarios where non-relevant information from previous trials had to be ignored or forgotten, as is the case in reversal tasks.

4.1.2   Previous investigations of spatial reversal learning in complement deficient mice

There have been three previous reports of the performance of complement deficient mouse models in spatial reversal learning paradigms. Shi et al. (2015) reported no differences in 4-month-old $C3^{-/-}$ mice and age matched WT littermate controls in either the acquisition or reversal stage of the MWM. This research was conducted from the viewpoint of age-related cognitive decline and presented some interesting findings in aged C3 deficient mice. 16 month old $C3^{-/-}$ mice showed no differences compared to WT in their initial acquisition of the platform location (Shi et al., 2015). Upon switching of the platform location in the reversal trial however, $C3^{-/-}$ animals showed a significantly higher percentage of correct choices compared to aged WT controls. This finding suggests that C3 deficiency does not affect the rate of spatial learning or acquisition, but specifically benefits spatial reversal learning. Moreover, this report would suggest that the enhanced cognitive abilities of $C3^{-/-}$ mice are age-dependent.

Since C1q and C3 are two critical proteins of the classical cascade, and $C1q^{-/-}$ and $C3^{-/-}$ mice share a similar synaptic phenotype characterised by an excess of connections (Stevens et al., 2007), the behavioural phenotype of C1q deficient animals is also of relevance. Similar to Shi et al. (2015) Stephan et al. (2013b) also found no differences between $C1q^{-/-}$ and WT animals at either 3 months or 17 months of age on the acquisition stage of the MWM. Aged, but not young mice, exhibited superior performance on the reversal stage however. Indeed, the performance of 17-month old $C1q^{-/-}$ mice was equivalent to 3-month old WT mice on this measure. Therefore, absence of the classical complement cascade (including both C1q and C3) appears to improve spatial reversal learning and cognitive flexibility, and may counteract age-related cognitive decline.

171

Using a different approach to the MWM, Perez-Alcazar et al. (2013) investigated spatial reversal learning in young adult male C3$^{-/-}$ mice using the IntelliCage platform, which permits behavioural testing in the home cage environment. Group-housed animals were trained to nose poke in a corner of their home cage to attain reward (access to water bottles). After an introductory period, a place-learning phase was implemented in which reward was randomised to one corner of the cage, and all other corners were programmed as incorrect. This was individualised to each animal. If an animal performed a nose poke in the correct corner, a door would open allowing access to water bottles. After five consecutive days, reward was randomised to a new corner (from which the previous corner was excluded) to measure spatial reversal learning. Results showed that C3$^{-/-}$ animals made significantly fewer visits to incorrect corners, both during the initial corner phase and after a reversal to a different corner, compared to WT animals. This data again suggests that, in the absence of C3, the acquisition of spatial information and subsequent spatial reversal learning are enhanced. In contrast to the data obtained by Shi et al. and Stephan et al. in the MWM, this suggests that differences are observable in young adult C3$^{-/-}$ mice.

4.1.3 The contextual fear conditioning paradigm and its relevance to adult neurogenesis

Another frequently used paradigm, contextual fear conditioning (CFC), is a form of Pavlovian conditioning (Phillips & Ledoux, 1992). As shown in Figure 4.2, an animal is placed inside a conditioning chamber (which serves as the conditioned stimulus; CS) and receives an aversive unconditioned stimulus (US), such as a foot shock. When reintroduced to the chamber, the context in which the CS-US association was initially formed, rodents display a defensive response termed 'freezing' whereby they become immobile (Rudy, Huff, & Matus-Amat, 2004). In order to test the ability to distinguish between two highly similar contexts, and therefore test elements of pattern separation,

animals may be reintroduced to contexts with varying degrees of similarity to that first encountered (Sahay et al., 2011). In rats, lesions to the amygdala impaired learning of both the CS and the context, whereas hippocampal lesions impaired conditioning of the context but not the CS. This suggests that the hippocampus is important for fear conditioning when there is a spatial or contextual element involved.

AHN has also been shown to be involved in CFC, and it is thought that successful context-US recall requires pattern separation performed by the DG (McHugh et al., 2007; Sahay et al., 2011). Loss of AHN, either through focal x-irradiation or genetic depletion of GFAP$^+$ progenitor cells, impaired contextual fear responses (Hernández-Rabaza et al., 2009; Pan, Chan, Kuo, Storm, & Xia, 2012; Saxe et al., 2006), but spared cued fear responses (Saxe et al., 2006). Other studies, however, have reported no changes in contextual fear conditioning after ablation of adult neurogenesis (Shors, Townsend, Zhao, Kozorovitskiy, & Gould, 2002). Sahay et al. (2011) used a genetic gain-of-function approach to elevate levels of AHN, by overriding *Bax*-dependent programmed cell death of newly born neurons. These mice were superior in their ability to distinguish between highly similar contexts in the CFC paradigm, suggesting enhanced pattern separation.
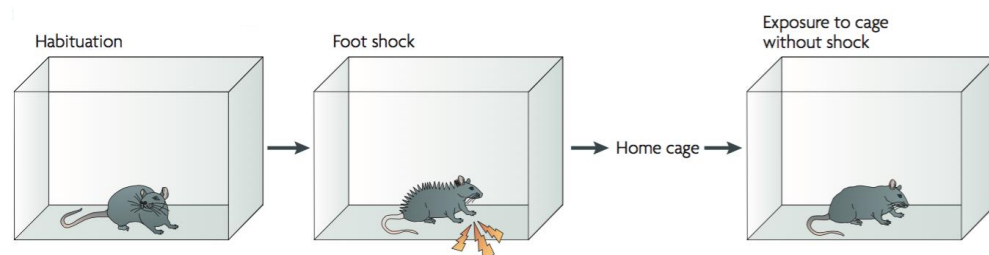
Figure 4.2 Example of contextual fear conditioning paradigm. An animal is first habituated to a testing chamber, before receiving a foot shock. The animal is returned to the home cage before being reintroduced to the testing chamber. Should the animal have formed a context-shock association, they will display freezing behaviour when placed back in the chamber despite the absence of further aversive stimuli. Image adapted from Dantzer, et al. (2008).

173

4.1.4   Previous investigations of CFC in C3$^{-/-}$ mice

Similar to the MWM, young C3$^{-/-}$ mice were comparable to WT mice in their retention of the shock-context association at 4 months of age (Shi et al., 2015). On the other hand, aged C3$^{-/-}$ mice showed superior retention of the shock-context association 24 hours after initial exposure, indexed by greater freezing responses compared to WT (Shi et al., 2015). This would suggest an enhancement in hippocampus-dependent contextual learning in the absence of C3. Evidence for the involvement of complement in cognition has also come from overexpression models. Lian et al. (2015) investigated CFC in an astrocytic IκBα knock down mouse model. Since IκBα is an inhibitor of NFκB, its knockdown causes aberrant NFκB signalling, a downstream signal of which is C3. As such, C3 mRNA was found to be upregulated in IκBα knockout animals. These animals showed an impaired CFC response, characterised by significantly lesser freezing behaviour when reintroduced to the context in which a foot shock was previously encountered. Critically, freezing deficits were restored when animals were treated with C3aR antagonist SB290157 (Ames et al., 2001) suggesting that the cognitive impairment observed was dependent on C3/C3aR signalling. This suggests that high levels of C3a/C3aR activation are detrimental to hippocampal-dependent cognition. This conclusion is in line with the aforementioned MWM and CFC literature demonstrating enhanced spatial and contextual learning in C3 deficient mice.

4.1.5   Testing anxiety in rodents

Anxiety is routinely tested in exploration based paradigms such as the elevated plus maze (EPM) or open field (OF), which rely on competition between rodents natural tendency to explore novel environments against their unconditioned fear of heights and open spaces (Walf & Frye, 2007). As shown in Figure 4.3A, the OF apparatus consists of a square, high-walled field with zone markings to demarcate central and outer zones. Each animal's

exploration is recorded over a brief trial, during which a greater duration spent in the central zone of the field is indicative of anti-anxiety behaviour, whereas remaining in the outer zone or close to walls, termed 'thigmotaxis', is increased with anxiety.

The EPM is a widely used paradigm for investigation of unconditioned anxiety in rodents (Pellow, Chopin, File, & Briley, 1985). The apparatus consists of a plus-shaped maze, featuring two open arms and two arms enclosed by high walls (see Figure 4.3B). An animal is placed into the central junction of the maze, and the number of entries into each arm and the duration spent in open compared to closed arms is recorded by the experimenter (Walf & Frye, 2007). Behaviour in the EPM reflects a conflict between a rodents innate motivation to explore novelty and their preference for protected, enclosed spaces (Walf & Frye, 2007). Therefore, a greater number of entries or duration spent in open arms is thought to be reflective of anti-anxiety or approach-orientated behaviour, whereas greater closed arm entries or duration spent in closed arms suggests anxiety. Other ethological parameters can be measured in the EPM, including dips of the head over the side of the open arms, and 'stretch attend postures' where an animal stretches out into an open arm from the safety of a closed arm. These behaviours are regarded as a form of 'risk assessment' (Walf & Frye, 2007; Wall & Messier, 2001).

A less commonly used paradigm for testing anxiety in rodents is the assessment of food neophobia. If presented with a novel food or drink in an unfamiliar context, at first mice will consume very limited quantities of the amounts available. Anxiolytic agents increase total consumption of a novel food or drink source in an unfamiliar context (Crawley, 1985) .
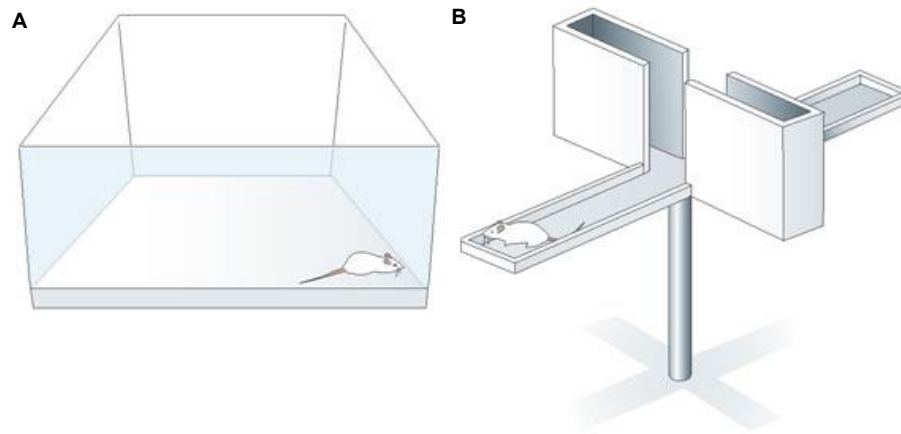
Figure 4.3 Behavioural tests of anxiety in rodents. A) Open field test. **B)** Elevated plus maze apparatus. Image adapted from Cryan & Holmes, (2005).

4.1.6 The role of hippocampal neurogenesis in emotionality and anxiety

AHN, and the process of pattern separation, have been suggested to regulate aspects of anxiety (see Section 1.3.5; Kheirbek & Hen, 2014; Kheirbek, Klemenhagen, Sahay, & Hen, 2012; Revest et al., 2009). However, studies in which anxiety has been assessed in animals with altered neurogenesis have provided inconsistent results. Revest et al. (2009) found that deficits in AHN via inducible transgenic ablation of newborn DG neurons increased anxiety-associated behaviour in the EPM. In contrast, Snyder et al. (2011) found no differences in the behaviour of animals in the EPM, despite observing a 99% decrease in BrdU$^+$DCX$^+$ progenitors in animals treated with a specific genetic ablation virus versus untreated controls. Findings are also unclear regarding increases in AHN. Sahay et al. (2011) reported that mice in which the pro-apoptotic gene *Bax* is deleted from adult NPCs, thus enhancing their survival, showed a decrease in anxiety-like behaviour in the OF. These animals were comparable to controls in the EPM however. Another study using the same inducible transgenic model reported that animals with augmented neurogenesis did not differ in their baseline anxiety in the OF or EPM (Hill, Sahay, & Hen, 2015b). However, Branchi et al. (2006) reported that

176

augmented AHN due to social enrichment was also associated with elevated anxious behaviour in both the EPM and OF. There have also been reports of increases in neurogenesis via voluntary wheel running increasing anxiety in C57Bl6 mice (Fuss et al., 2010a). Interestingly, a post-exercise irradiation treatment administered to reduce elevated levels of neurogenesis reversed the anxiety phenotype previously observed in this study (Fuss et al., 2010b). Although there are many inconsistencies within the literature, it is possible that that abnormal levels of hippocampal neurogenesis, whether increased or decreased, can lead to maladaptive anxiety (Fuss et al., 2010a).

4.1.7   Previous investigations of anxiety in C3$^{-/-}$ mice

Shi et al. (2015) reported no differences in the OF or EPM when testing young adult C3$^{-/-}$ mice. However, aged C3$^{-/-}$ animals spent an increased portion of their time in the centre of an OF, despite comparable levels of locomotion to WT, suggesting an anti-anxiety phenotype in the absence of C3. This was confirmed in the EPM, where aged C3$^{-/-}$ mice made significantly more open arm entries compared to WT. Aged C3$^{-/-}$ mice also showed more approach-orientated behaviour in an object-habituation task, indicating greater motivation to explore novelty, possibly due to decreased anxiety levels (Shi et al., 2015). This study suggests that C3 may contribute to anxiety and avoidance behaviour under physiological conditions, although there is age-specificity in the manifestation of this behavioural phenotype.

4.1.8 Summary of previous literature regarding neurogenesis, complement, cognition and anxiety

Our current knowledge regarding the impact of either increases or decreases in AHN and performance of tasks such as the MWM or CFC is lacking clarity. The many conflicting results likely reflect the diversity in techniques for both

manipulating neurogenesis, and the behavioural testing of cognitive outcomes. A clearer picture has emerged from the few studies examining complement and cognition however. In summary, absence of the classical complement cascade seems to boost performance on hippocampus-dependent tasks, since both C3 and C1q deficient animals demonstrate enhanced performance relative to WT animals (Shi et al., 2015; Stephan et al., 2013b) although not necessarily at the same age, suggesting age-related variability. In particular, the absence of the classical complement cascade seems to improve cognitive flexibility, as measured in the reversal element of spatial learning paradigms by Perez-Alcazar et al. (2013), Shi et al. (2015), and Stephan et al. (2013a). In contrast, it seems that where there are high levels of C3 and C3aR signalling, hippocampal learning and memory functions are compromised as shown by Lian et al. (2015). In terms of emotionality, the absence of C3 has been associated with an anti-anxiety phenotype in the OF and EPM in older, but not young adult C3$^{-/-}$ mice (Shi et al., 2015).

4.1.9   Limitations of previous investigations

While these reports show that complement does impact upon cognition, there have been no prior investigations of these animals from the perspective of AHN. Therefore, it is unclear whether the behavioural phenotypes described are relevant to AHN due to the hippocampal tasks used, many of which are not necessarily hippocampal neurogenesis-dependent (Shors et al, 2002; Lledo, Alsonso & Grubb, 2006). For example, the MWM has provided inconsistent and sometimes paradoxical results with regard to manipulations of AHN (Ehninger & Kempermann, 2006). Neither significant increases or decreases in rodent AHN have demonstrated consistent, specific behavioural phenotypes in this paradigm (Kempermann, 2013). In a 2013 review, Kempermann concluded that this fact may suggest that adult neurogenesis contributes to "highly specific functional aspects of spatial learning that

become apparent only when certain task demands are faced" (p.1), rather than benefitting hippocampal function as a whole (Kempermann, 2013).

Furthermore, there are also methodological limitations of some tasks that restrict their utility for studying AHN. It has been reported that training in the MWM leads to a robust decrease in BrdU$^+$ cell counts in the DG of trained animals compared to non-trained controls (Ehninger & Kempermann, 2006), an effect that is likely due to the stress induced by forced swimming. Due to the sensitivity of AHN to stress, behavioural paradigms that are aversive in nature may therefore confound results of studies examining subtle changes in AHN. The use of a non-aversive behavioural task that is sensitive to the function of newly born neurons in performing pattern separation would therefore be a valuable addition to the existing literature.

4.1.10 The location discrimination task (LD) as a measure of fine pattern separation

Tasks such as the automated touchscreen location discrimination (LD) task developed by the laboratory of Tim Bussey (Horner et al., 2013; Hvoslef-Eide et al., 2013; McTighe et al., 2009) provide a relatively specific measure of pattern separation, and have proved sensitive to systematic alterations in AHN. As shown in Figure 4.4, the basic task involves training mice to respond to one of two stimuli locations presented on a touch screen, the proximity of which is manipulated. The supposition is that close stimuli separation discriminations will tax fine pattern separation to a greater extent than far stimuli discriminations (Yassa & Stark, 2011). Typically, the task also incorporates a reversal learning manipulation; animals are trained to reach a criterion defined by correct responses to either a left or right situated stimulus, before stimulus-reward contingencies are switched. Methodologically, this paradigm is advantageous over other tasks such as the MWM or CFC due to its appetitive as opposed to aversive nature, ease of

manipulation of stimuli due to the programmable touchscreen platform, and its high degree of automation (Horner et al., 2013). It also incorporates a spatial reversal component, which can allow dissociations to be made between changes in pattern separation and executive function (Hvoslef-Eide et al., 2013).

Furthermore, the neurobiological substrates underlying this task are highly relevant to my current experimental aims. McTighe et al. (2009) showed that lesions of the dorsal hippocampus impaired rats performance on the LD task when the locations discriminated were in close proximity, but not when they were situated far apart. Furthermore, mice receiving low-dose x-irradiation to focally ablate AHN showed impairments on the LD task when the stimuli presented were close together, but performed normally on discriminations where stimuli were spatially distinct from each other (Clelland et al., 2009). Also using the touchscreen LD task, Creer et al. (2010) found that a running intervention selectively enhanced performance when discriminating closely separated stimuli, but did not affect discriminations of far-apart stimuli. Importantly, a positive correlation was found between task performance in the close stimuli separation condition and the number of newly born neurons in the adult DG. Therefore, this task provides a behavioural readout that is of direct relevance to AHN. The use of this task would provide valuable insight into whether the observed alterations in AHN in the absence of C3/C3aR have specific consequences upon the functioning of newly born neurons.

4.1.11 Aims and hypotheses

Previous experimental chapters have demonstrated that C3 and C3aR deficient animals have an increased number of immature neuronal cells in the adult DG, alongside alterations in the morphology of these newly born cells in the absence of C3aR. To assess whether this is of behavioural significance, I aimed to investigate the cognition of $C3^{-/-}$ and $C3aR^{-/-}$ animals
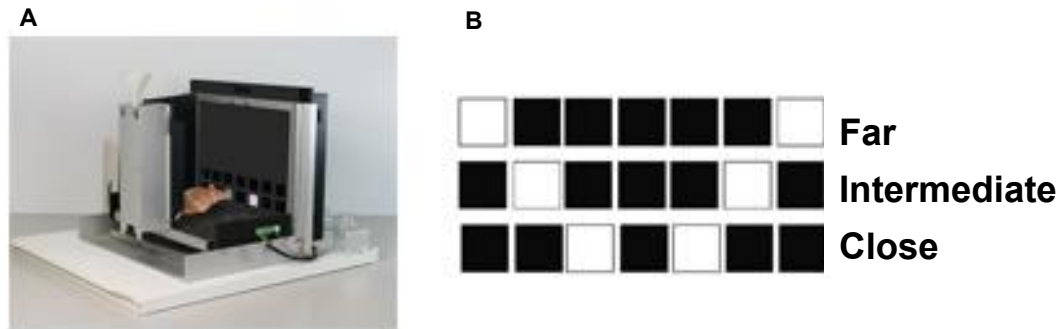
Figure 4.4 Example of the touch screen Location Discrimination (LD) task. A) Mouse performing LD task within touchscreen chamber. The animal must nose poke the correct stimulus, which occupies either the left or right side of the touchscreen. This is varied between trials. The spatial separation of stimuli is also varied between sessions, and is detailed in B. Correct responses are rewarded with condensed milk delivered from a magazine at the rear of the chamber. **B)** Example of stimuli separation conditions. Close discriminations (lower panel) have been shown to preferentially tax pattern separation and thus AHN (Clelland et al., 2009), whereas far discriminations should not tax this computational process to such an extent. Animals are first trained to criterion on an intermediate stimulus separation condition, before being presented with close and far probe trials. Image adapted from McTighe et al. (2009).

compared to WT controls in the LD task, a specific measure of pattern separation that is sensitive to changes in AHN. I also investigated whether these changes impacted upon emotionality, specifically in the form of anxiety-like behaviours measured by the OF and EPM.

Previous reports suggest that absence of the classical complement pathway, and pharmacological antagonism of C3aR, benefits spatial learning and cognitive flexibility (Lian et al. 2015; Perez-Alcazar et al., 2013; Shi et al., 2015; Stephan et al., 2013a). Increased AHN has also been shown to improve performance on the LD task (Creer et al., 2010). I therefore hypothesised that C3$^{-/-}$ and C3aR$^{-/-}$ mice, having greater levels of AHN, would show superior pattern separation abilities in the LD task. Based on prior reports, I also predicted increased cognitive flexibility in C3$^{-/-}$ mice, as measured by the reversal component of the LD task. While the C3aR deficient model has not been subject to behavioural testing before, I hypothesised that if superior reversal learning in C3$^{-/-}$ mice is dependent on C3a/C3aR signalling, then

both C3$^{-/-}$ and C3aR$^{-/-}$ subjects would show improved reversal learning in the LD task.

While the previous literature regarding AHN and anxiety is inconclusive, based on previous reports of an anxiolytic phenotype of aged C3 deficient mice I predicted that these subjects would show lesser anxiety in the OF and EPM. I predicted that this may manifest in greater exploration of the central zone of the OF, and greater exploration of the open arms of the EPM. Again, the C3aR deficient model has not previously been investigated with regard to emotionality. However, if C3/C3aR signalling were responsible for the anti-anxiety phenotype observed in C3$^{-/-}$ mice, one would expect to see a comparable phenotype between C3 and C3aR$^{-/-}$ mice. If not, this may again suggest that alternative signalling pathways are involved.

In light of these hypotheses, It should be noted that at least two of the three reports investigating complement and cognition have suggested that the benefits of C3 deficiency upon memory and anxiety may manifest increasingly with age (Shi et al., 2015). Therefore, I also anticipated that a failure to observe differences to WT in the LD task, OF and EPM might reflect the young age of the experimental subjects used.

4.2 Methods

4.2.1 Subjects

12 C57Bl6 Thy1.1 mice, 12 C3$^{-/-}$ mice and 10 C3aR$^{-/-}$ mice were sourced as detailed in Section 2.2.1. Due to sex differences in AHN in response to hormonal fluctuations (Galea et al., 2013), only male subjects were used. All subjects were aged between two to three months at the beginning of behavioural testing. During the course of the study, five C3$^{-/-}$ mice succumbed to illness. WT littermate controls were not used in these studies due to time constraints.

4.2.2 Housing and maintenance

Animals were group housed where possible, in groups of up to five animals per cage. To prevent fighting, three C3aR$^{-/-}$ subjects had to be singly housed (analyses indicated that this did not affect their behavioural performance). Subjects were housed in conventional caging in a temperature-controlled room with a 12:12 hour light / dark cycle (lights on 7:00am). All behavioural testing was conducted within the light phase. All subjects had *ad libitum* access to food. For the duration of behavioural testing, water was restricted to a two-hour access period per day. Body weight was carefully monitored throughout the period of water deprivation, and animals were maintained at 90% of their free-feeding body weight prior to commencing water restriction. In order to acclimatise animals to the regular handling, each animal was handled daily for a period of two weeks after first arriving in the vivarium. All procedures were carried out in accordance with the UK Animals (Scientific Procedures) Act 1986.

4.2.3 Locomotor activity (LMA)

LMA was assessed over three consecutive days, featuring a 120-minute session per animal, per day. All sessions were conducted in the dark, and were commenced at the same time each day. Subjects were individually placed into Plexiglas chambers (210 x 210 x 365 mm) spanned transversely by two infrared beams, which were located 10 mm from the base, and equally spaced along the length. Due to the large cohort size (total N= 34), LMA was assessed in three separate sessions each day, with a maximum of 12 subjects running per session. After each run, chambers were cleaned with acetic acid to prevent odour cues influencing the activity of the following subject. Genotypes were counterbalanced within each session to control for time of day. A computer running a custom written BBC BASIC V6 programme with additional interfacing by ARACHNID (Campden Instruments, U.K.) recorded the number of beam breaks per box, which served as the dependent variable. For analysis purposes, each 120-minute session on day 1, 2 and 3 was broken down into 30-minute quartiles (Q1-Q4).

4.2.4 Open field (OF)

Apparatus consisted of a white plastic square arena (750 x 750 mm, length x width), evenly illuminated at 15 lux. Using Ethovision XT software (Noldus, NL), the arena floor was virtually subdivided into two concentric squares, featuring an a central 400 x 400 mm area and an outer zone consisting of the peripheral region, within 350 mm of the arena wall (see Figure 4.5). Individual subjects were placed into the centre of the arena, consistently facing the same direction, and allowed to explore the arena for eight minutes. A video camera mounted above the arena linked to a computer operating Ethovision XT software was used to record each animal's position (17 frames/s). The number of entries made into the central and outer zones, as well as the total duration spent per zone, was calculated.
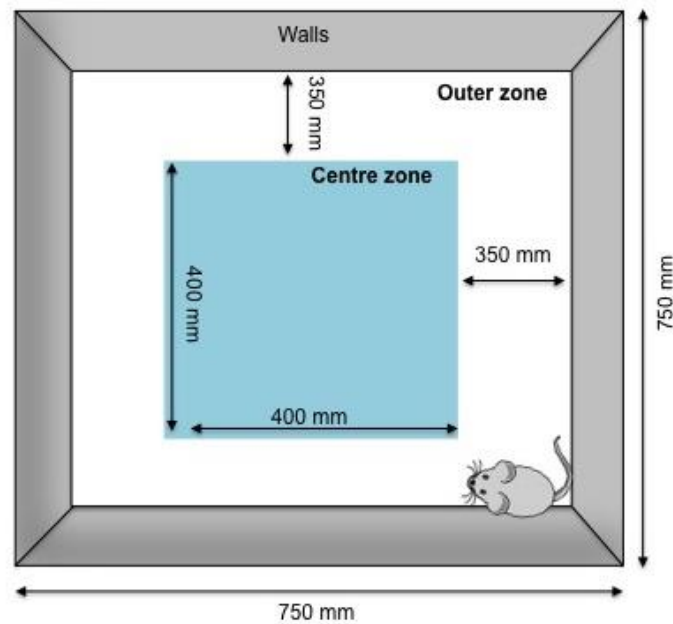
Figure 4.5 Dimensions of open field apparatus and superimposed virtual zones. Drawing not to scale.

4.2.5 Elevated plus maze (EPM)

The apparatus was constructed of white Perspex and consisted of four arms arranged in a cross formation (see Figure 4.6). The two exposed open arms measured 175 x 78 mm (length x width), were positioned opposite each other and converged on a central platform. The closed arms were of equal dimension to the open arms, with the addition of 150 mm high walls. The maze was elevated 300 mm off the floor and evenly illuminated at 15 lux. A video camera linked to a computer running Ethovision XT software was mounted above the maze in order to record each animal's exploratory behaviour. Individual subjects were placed in the central platform between the open and closed arms and allowed to explore the maze for five minutes. Data collected from each pair of arms was combined to calculate the dependent variables of total duration spent in open and closed arms in seconds per animal, and the number of entries into open and closed arms per animal. During the five minute trial, the experimenter manually scored the following behaviours from a monitor situated across the room from the

185

maze; number of head dips from the open arms (defined as downward movement of the rodents head over the edge of an open arm), number of 'stretch attend' postures (defined as an animal stretching forwards into an open arm with their hindquarters remaining in a closed arm) and episodes of grooming.
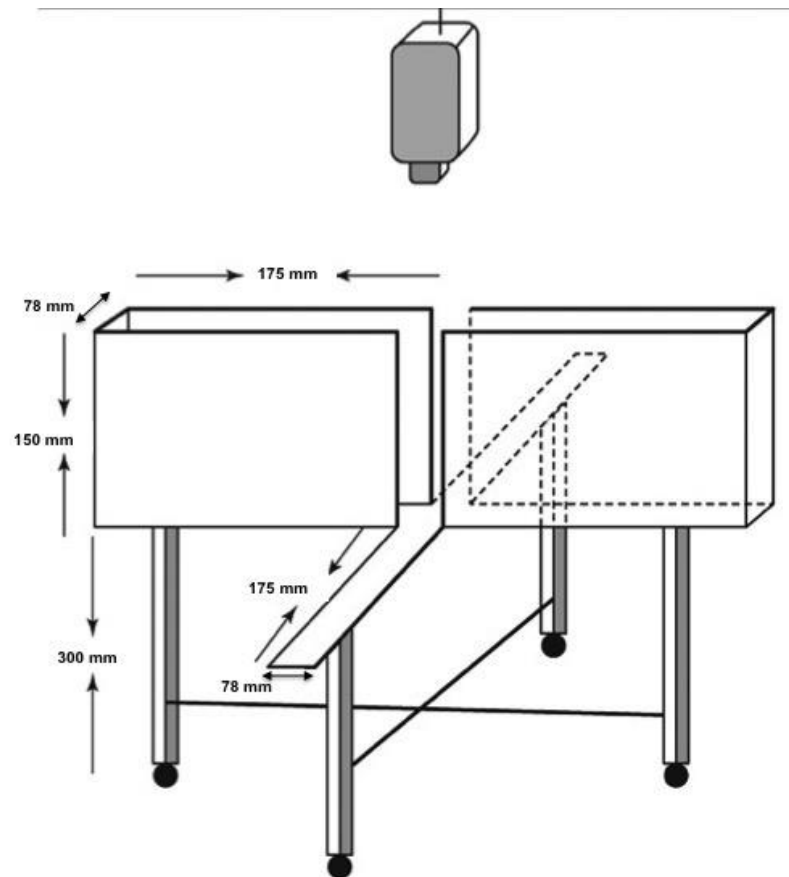
Figure 4.6 Elevated plus maze apparatus with dimensions. Image adapted from Cohen, Matar, & Joseph (2013). Drawing not to scale.

4.2.6 Food neophobia test

As seen in Figure 4.7, two small containers (maximum volume ~3 ml each) were placed towards the rear of a small chamber (285 x 130 x 120 mm, length x width x height). As per Humby, Laird, Davies, & Wilkinson, (1999), each animal completed one ten-minute trial per day for eight consecutive

days. At the onset of testing, all mice were well adjusted to a water deprivation schedule, and testing was carried out before the two-hour water access period in order to increase motivation to drink. During the first two days, both containers were filled with drinking water. In the subsequent five sessions, animals were presented with a choice of either drinking water or a solution of 10% condensed milk (Nestle, UK). Since animals had never encountered condensed milk before, this served as a novel foodstuff. The position of the milk was counterbalanced between the left and right position across sessions. On day eight, both containers were filled with condensed milk. On each day, the containers were weighed before and after the ten-minute trial and the difference calculated. This provided a measure of total consumption, per animal, of water and condensed milk. Animals were weighed throughout the eight-day test duration to obtain an average body weight per animal. Consumption was normalised for body weight differences using Kleiber's 0.75 mass exponent (Kleiber, 1932). The preference for condensed milk was calculated as a percentage of total consumption for each of the five days during which water and milk were available. This task also served to habituate animals to the reward (condensed milk) to be used in the LD task.
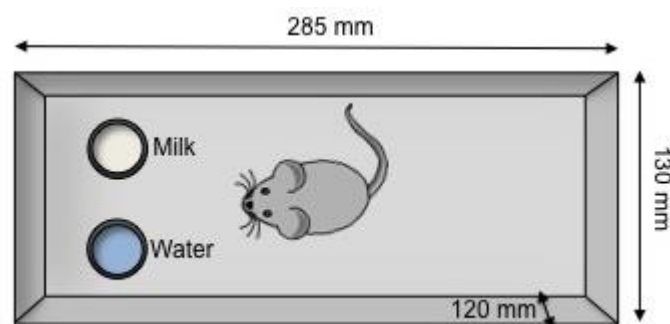
Figure 4.7. Food neophobia test apparatus. The position of water and milk was swapped from left to right each day. Drawing not to scale.

4.2.7 LD task apparatus

Apparatus consisted of a battery of four mouse touchscreen chambers (Campden Instruments Ltd., UK), each housed inside a sound-attenuating fibreboard cubicle. As shown in Figure 4.8, the modular chamber featured a trapezoidal wall shape (250 mm x 180 mm, length x height; touchscreen end), with two black plastic adjoining walls (200 mm x 180 mm). To the rear, the reward delivery area featured a black plastic wall (60 mm x 180 mm, length x height) with a 20 mm x 20 mm aperture at floor level, in which the magazine unit was located. This design is intended to focus the animal's attention towards the touchscreen and the reward delivery area (Hvoslef-Eide et al., 2013). Each chamber was equipped with a fan, tone and click generator, house light (LED), a magazine unit situated in the wall opposite the touchscreen (with a light and infrared beam to detect head entries), a pump connected to a bottle of liquid reward, and a touchscreen at the front of the chamber (screen resolution 600 x 800). The chamber was also supplied with black plastic 'masks' containing either three (70 x 70 mm) or six (25 mm x 25 mm, equally spaced 5 mm apart, 20 mm from chamber floor) horizontally aligned, evenly spaced response windows. The relevant mask (determined by stage of training, see Figure 4.10) was inserted into the chamber and superimposed upon the touchscreen to prevent accidental contact (e.g., with tail) and to allow presentation of stimuli on screen to be spatially localised. The touchscreen featured infrared photocells, meaning that subjects were not required to exert pressure on the screen for a response to be detected. In order to record the subject's movement, two additional photo-beams extended between the sidewalls parallel to the touchscreen (70 mm from screen) and reward delivery area (35 mm from magazine). The chamber floor was a perforated stainless steel raised above a tray filled with sawdust, and had a surface area of 46 mm at the reward delivery area, 238 mm width at touchscreen end and a depth of 170 mm. During testing, each chamber was sealed with a removable clear Perspex roof (working area height 230 mm), through which subjects entered the chamber. The battery of four chambers were controlled by a computer running

Whisker ® Server-based Controller (Campden Instruments Ltd., UK; (Cardinal & Aitken, 2010) and ABET II Touch software (Lafayette Instrument Company, USA).
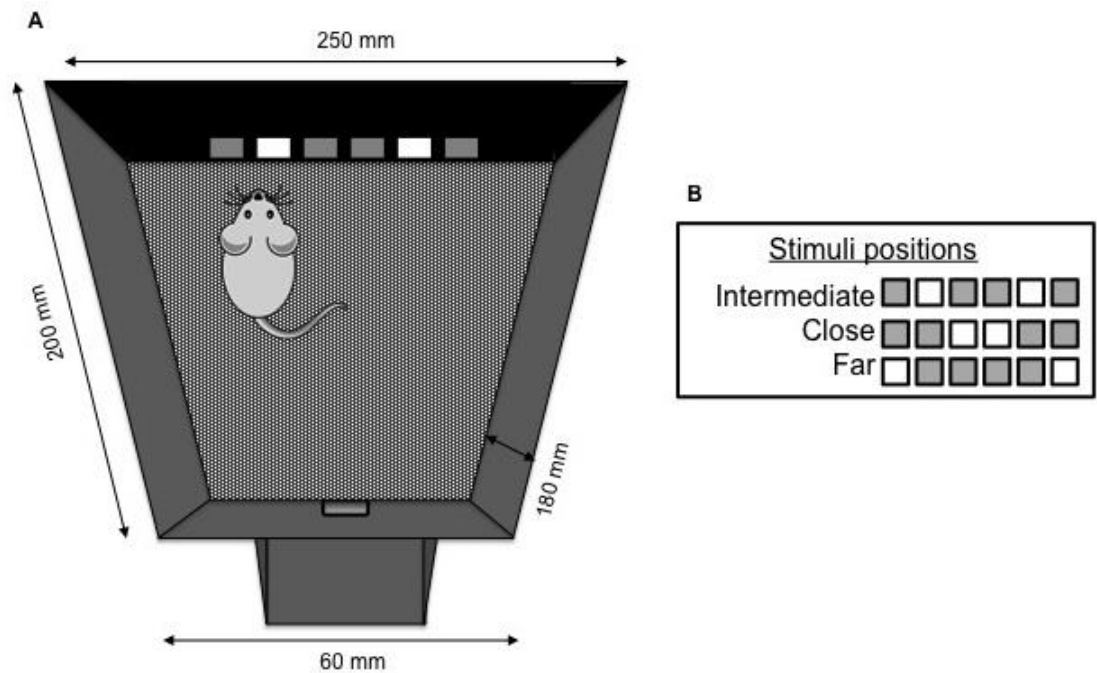
Figure 4.8 Location discrimination task apparatus and stimuli positions. A) Campden Instruments Ltd. mouse touchscreen chamber. Drawing not to scale. **B)** Stimuli positions in intermediate, close and far stimuli separation conditions.

The LD task consisted of a shaping period, followed by an intermediate stimuli separation training stage (Figure 4.9), and finally LD probe trials (see Figure 4.10 for overview of each stage). The following protocol was adapted from that originally developed by McTighe et al. (2009). Throughout the task, animals trained once daily for 13 days, before having the 14th day off to receive 12 hours free water access, in line with Home Office license requirements. Otherwise, subjects were tested at the same time each day, before the two-hour water access period, in order to increase motivation to consume liquid reward. Each subject returned to the same testing chamber each day. Throughout, the reward consisted of 22 μl of 10% v/v condensed

milk solution (Nestle, UK). All sessions terminated after a twenty-minute duration, or after sixty trials had been completed. After completing a session, each subject was removed from the chamber and returned to its home cage. Due to the immunocompromised C3$^{-/-}$ strain used, all inside surfaces of the chamber and the magazine were then cleaned with 70 % (v/v) ethanol before the next subject was placed inside the chamber to minimise spread of infection between animals.

4.2.8 Shaping

In order to prepare animals for the LD task, all subjects went through an initial shaping period in which they were habituated to the testing chamber. This stage also trained subjects to nose poke stimuli locations displayed on the touchscreen for reward. Shaping was comprised of the stages listed below. Individual subjects were advanced to the subsequent stage when they reached specific criteria (detailed in text below) on the prior stage, meaning that individual subjects could advance through shaping and task training in accordance with their speed of learning. This approach was taken to accommodate slow learners whilst preventing overtraining in subjects who acquired the task more rapidly.

Habituation (Hab)

Shaping began with a habituation period during which animals learnt to collect liquid reward from the magazine. At this stage, the touchscreen displayed a black background with no stimuli. An animal was rewarded with condensed milk each time they made a nose poke to the aperture containing the liquid reward dispenser. All subjects spent a minimum of three days at the habituation stage, after which they were advanced to the subsequent stage if they had met the following criterion: twenty trials or more per session, on each of two consecutive days.

Large squares (LS)

The next stage trained subjects to associate stimuli on the screen with a reward. A mask with three response windows (shown in Figure 4.10a) was positioned in front of the touchscreen, on which a single white square stimulus was displayed directly beneath one of the three possible response windows. The stimuli displayed at this stage were larger than those to be used in the following stages, in order to facilitate learning. A subject was required to nose poke the illuminated stimulus. If a subject touched the correct stimulus, reward delivery occurred accompanied with a tone and magazine illumination. The stimulus would remain on screen until touched, and touching the locations not containing stimuli did not generate reward. After each trial, the position of the illuminated stimulus was randomly presented to one of the two other possible positions, and the next trial began automatically. The criterion for advancement at this stage was twenty or more correct trials, completed on each of two consecutive days.

Must touch (MT)

This stage saw introduction of the smaller stimuli to be used for the remainder of the experiment (see Figure 4.10B). A mask with six equally sized squares aligned horizontally towards the bottom of the screen (as described in Section 4.2.7) was placed in front of the touchscreen. Each trial began with one response window out of the six possible locations being illuminated with a white square stimulus, the position of which was selected at random. As before, the subject was required to nose poke the illuminated stimulus in order to collect a reward, which was again accompanied by magazine illumination and a tone. The next trial began automatically after reward collection and saw another response window location illuminated in a different position, again at random. Touches to in the non-illuminated stimuli locations were without consequence. Criterion at this stage required a minimum of twenty trials to be completed on each of two consecutive days.

Must initiate (MI)

This stage taught subjects to self-initiate trials. Stimuli were presented in the same manner as the previous stage. After reward collection on a correct trial, the subject was then required to perform an additional nose poke to the magazine in order to initiate the next trial. Having made the additional nose poke, the magazine light was extinguished and a click sounded to indicate a new trial, and a new stimulus location appeared on the screen. As before, touches in non-illuminated stimuli positions were without consequence. There were three separate sub-stages of the MI stage; MI (1), in which there was a 1000 ms inter-trial-interval (ITI) between the collection of a reward and possible initiation of the next trial, MI (5), in which there was a 5000 ms ITI, and MI (10) which featured a 10,000 ms ITI. These stages were incorporated to gradually increase the ITI, as longer ITIs are thought to facilitate learning (Bussey et al., 2008). The criterion for advancement to the next stage was again a minimum of 20 trials per session, on each of two consecutive days.

Punish incorrect (PI)

This stage was similar to the MI stage preceding it, except for subjects were discouraged from making touches to incorrect response windows during stimulus presentations (referred to as blank touches). In the event of a blank touch, the stimulus was removed from the screen and a time-out period began, during which the house light was illuminated (note that at all other stages, the house light was off during stimulus presentation). This cue served to indicate incorrect responses to subjects. When a subject made correct response, they were able to initiate a new trial after reward collection and a brief ITI. The criterion for advancement to the next stage was completion of twenty trials or more, with minimum 75% correct responses, on each of two consecutive days.

4.2.9 Intermediate task training

Having completed shaping, subjects were moved onto LD task training on a case-by-case basis. This stage saw the introduction of spatial discriminations, owing to the dual presentation of stimuli on the touchscreen, separated by an intermediate distance (response windows 2 and 5, see Figure 4.9). One location was designated as correct, whereas the other illuminated position was incorrect. Prior to commencing intermediate task training, all subjects were assigned to left and right-start groups, which were counterbalanced across each genotype. For those in the left-start group, on their first trial of intermediate task training, the correct response stimuli was situated on the left, where as the right sided stimuli was the correct response option for the right-start group.

As shown in Figure 4.9, a nose poke to the correct location resulted in reward delivery, a tone and magazine illumination. In the case an incorrect response (i.e., to the other stimulus), a 10 s time-out period began which was indicated by house-light illumination. In the case of either response, a 10 s ITI occurred before subjects could initiate a new trial, which was signalled by illumination of the magazine. As shown in Figure 4.9 (right panel), once criterion was attained, the reward-contingency was reversed, meaning that the previously incorrect location was now the rewarded location, and responses to the previously rewarded location were now punished with time-out.

The criterion for achieving a reversal was seven correct responses out of eight consecutive trials. The subject was then required to acquire the reversed contingency by again reaching the same criterion as before, after which another reversal would occur. There was no limit on the number of criteria (or reversals) that could be reached within a single session. Between consecutive sessions, the correct stimulus position remained consistent (e.g., if a session ended with the left stimulus being rewarded, the subsequent session would begin with the left stimulus being rewarded). The intermediate training phase continued until subjects met the following

criterion; completion of twenty trials or more per session, with a minimum of one reversal (i.e., 7 correct out of 8 consecutive trials) per session, on each of three consecutive days.
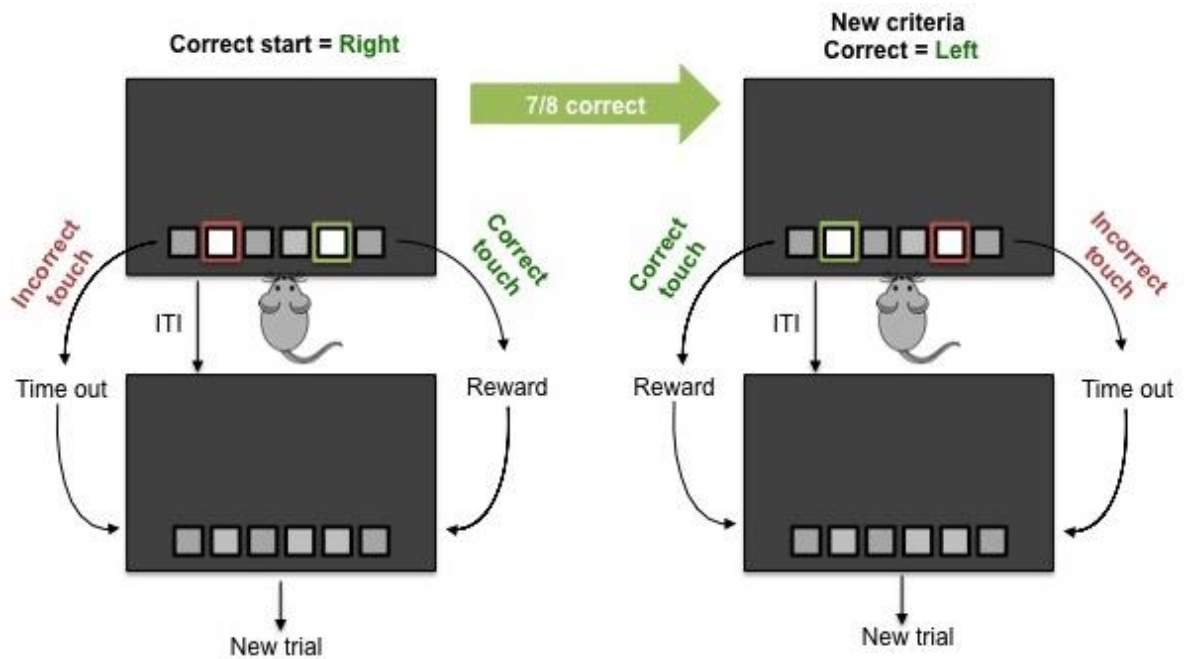
Figure 4.9 Structure of intermediate separation training stage. Left panel shows an example of a subject beginning an intermediate training session with the right-sided location designated correct. If an incorrect response is made, stimuli disappear and time-out occurs followed by a 10 second ITI, after which a new trial can be initiated. If a correct response is made, stimuli disappear, a reward can be collected and a new trial initiated after an 10 second ITI. If the subject makes 7 correct responses in 8 consecutive trials, the reward contingency is reversed and the left sided stimulus is now rewarded (right panel). The same process then ensues until the subject reaches criteria and another reversal occurs.

4.2.10 LD Probe trials

Having met criteria on the intermediate training stage, subjects were moved on to a series of probe sessions. These sessions followed the same structure as those at the intermediate training stage, except for the addition of a spatial discrimination manipulation; conditions featured either far stimulus separations (positions 1 and 6 illuminated) or close stimulus separation

(positions 3 and 4 illuminated; see Figure 4.10 for example). Within one session, all stimulus presentations were either close or far, and each subject received two consecutive sessions of the same probe type (denoted as first and last sessions for analysis purposes, see Figure 4.10D).

As shown in Figure 4.10D, close and far separation conditions were interspersed with two consecutive sessions of intermediate separation probe trials over a period of eight sessions. This process was repeated twice, meaning that each subject completed four sessions of the close separation condition, four sessions of far separation condition trials, and eight sessions of intermediate separation condition trials. For analysis, data was averaged across each first close, last close, first far and last far session for each subject in order to investigate practice effects (see Figure 4.10D).

4.2.11 Data analysis and statistics

Data screening

As detailed in Section 2.2.19, to determine whether assumptions for ANOVA were met, the shape of the distribution was first visually inspected in a histogram of frequency distributions using a bin width of 20 units. D'Agostino-Pearson omnibus K2 test was used to assess normality. To assess departure from horizontal symmetry, skewness was examined, and the peak of the curve was assessed using kurtosis. Equal variance was assessed using the Brown-Forsythe test.

Statistical tests

All statistics were conducted using either GraphPad Prism software (v.6.of, GraphPad Software Inc, USA) or SPSS (v.23.0, IBM Corp, USA). Depending on the task, either one-way or mixed ANOVA was performed to analyse behavioural data. To follow up significant main effects or interactions, pairwise contrasts were made between each possible set of comparisons

using Tukey's HSD test to correct for multiple comparisons. An α – level of 0.05 was used for all statistical tests.
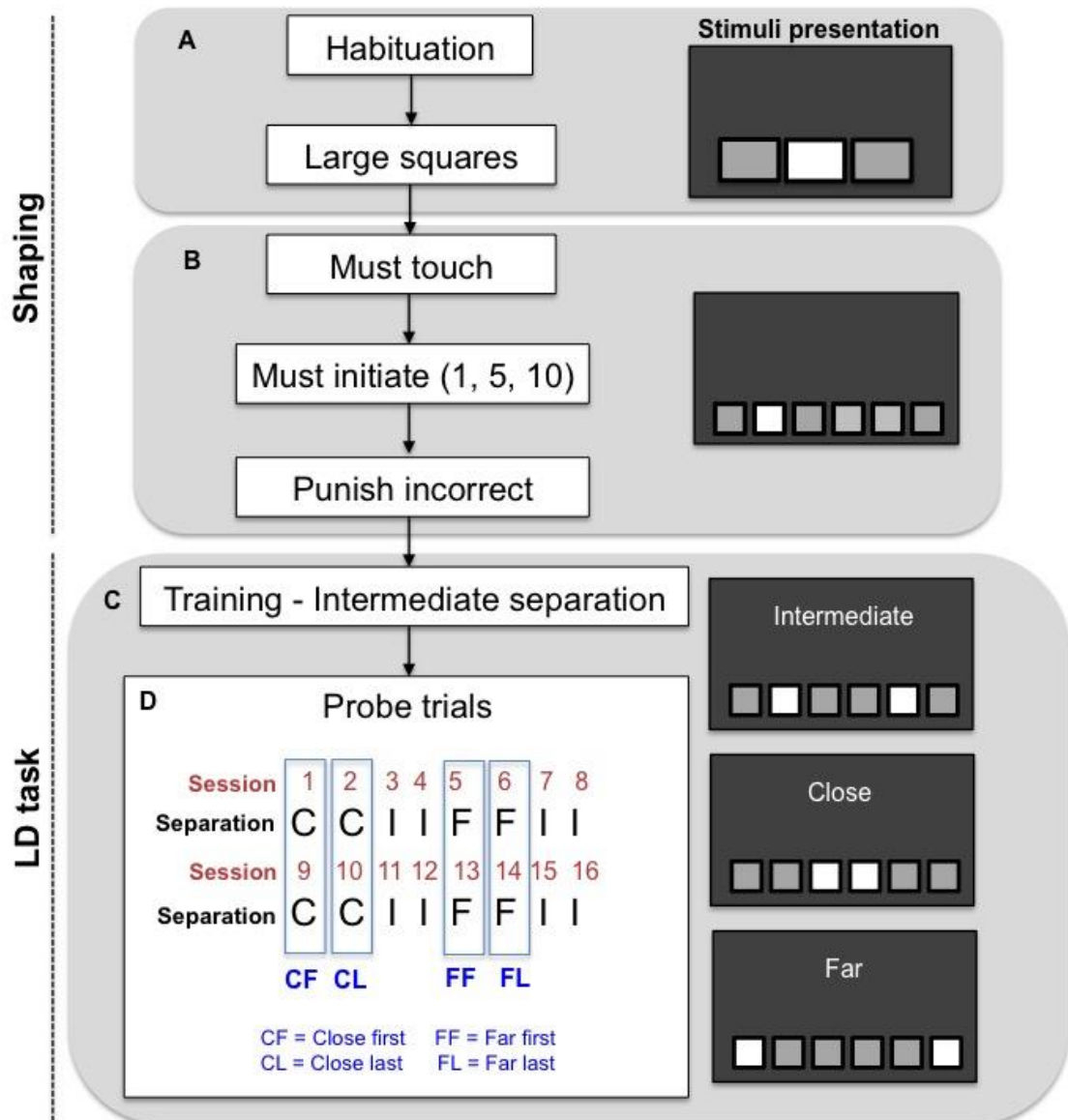
Figure 4.10 Schematic of stages from shaping through to task training and probe trials.
A) The initial stage of shaping consists of habituation and large squares. This stage teaches subjects to touch the screen to obtain reward. **B)** The latter half of the shaping stage trains subjects to responds to smaller stimuli, to self-initiate trials and respond only to the illuminated stimulus. After fulfilling criteria, subjects began training for LD task probe trials with an intermediate separation **(C). D)** Schedule of LD task probe trials. From session 1-8, subjects completed two close sessions (session 1= close first, and session 2 = close last) on two consecutive sessions, succeeded by two intermediate sessions, before two far sessions (session 5 = far first and session 6= far last). This process was replicated between days 9 and 16. For analysis purposes, data from both close first sessions was pooled, as well as from close last, far first and far last.

4.3   Results

4.3.1   Locomotion is normal in C3/C3aR deficient animals

LMA of individual animals during a two-hour testing period was measured over three consecutive days (see Figure 4.11A). The average number of beam breaks per animal, per day and per quartile of the test duration was analysed using a three way ANOVA with a between-subjects factor of genotype (WT, C3$^{-/-}$, C3aR$^{-/-}$) and two repeated measures factors of day (day 1, 2, 3) and time bin (Q1, Q2, Q3, Q4). Results showed no significant main effect of genotype ($F_{(2,31)}$=0.29, p = 0.74), suggesting that genotypes did not vary in their levels of locomotor activity. There was a significant main effect of both day ($F_{(2,31)}$=59.26, p < 0.0001) and time bin ($F_{(3,31)}$=81.86, p < 0.0001).   There was a significant two-way day*genotype interaction ($F_{(4,31)}$=4.96, p < 0.01), and a significant three-way day*genotype*time-bin interaction ($F_{(12,31)}$=2.81, p < 0.001).

To break down this three-way interaction effect, pairwise contrasts were made between genotypes at each level of day (1,2,3) at each time bin of each day (Q1,2,3,4). On day 2, during time bin 4, C3aR$^{-/-}$ mice were significantly more active (433.50 ± 78.89 beam breaks) than C3$^{-/-}$ mice (194.58 ± 72.01 beam breaks, p < 0.05, see Figure 4.11A, middle panel). This was not significantly different to WT however (269.50 ± 72.01 beam breaks, p = 0.13) and the same differences were not present on day 1 or 3 (all p > 0.05). These results suggest that while there were subtle differences in the activity levels of C3aR deficient and C3 deficient mice on day 2, there were no gross differences in activity levels between genotypes, as reflected by the non-significant main effect of genotype.

4.3.2 C3aR deficiency affects habituation to a novel environment

The slight differences observed in the locomotor activity of C3aR$^{-/-}$ animals on day 2 could result from an altered reaction to a novel environment. I therefore examined the rate of long-term behavioural habituation, a basic form of behavioural plasticity. Harris (1943) defined as "response decrement as a result of repeated stimulation" (p. 385), and I therefore analysed the percentage change in the number of beam breaks over the entire testing session, from day 1-2 and 2-3, to examine habituation rates (see Figure 4.11B).

A two-way ANOVA comparing the effect of genotype (WT, C3$^{-/-}$, C3aR$^{-/-}$) and the percentage change in total beam breaks between day 1 and 2, and day 2 and 3, showed a significant main effect of day ($F_{(1,31)}$=5.99, $p < 0.05$) and genotype ($F_{(2,31)}$=4.39, $p < 0.05$). These factors did not interact however ($F_{(2,31)}$=1.29, p=0.28). Pairwise contrasts to follow up the main effect of day showed that across all genotypes, a greater degree of habituation occurred between day 1 and 2 (28.95 $\pm$ 4.28 % change) than between day 2 and 3 (12.00 $\pm$ 4.40 % change, $p < 0.05$). However, follow up tests to investigate the main effect of genotype showed that C3aR$^{-/-}$ animals showed a smaller percentage change in their locomotor activity (13.67 $\pm$ 6.48 %) compared to C3$^{-/-}$ (30.77 $\pm$ 5.54 %) animals ($p < 0.05$), but not to WT (15.86 $\pm$ 4.31%, $p > 0.05$) across days. This result suggests that C3aR deficient animals showed less habituation to the testing environment, which may indicate a learning deficit.
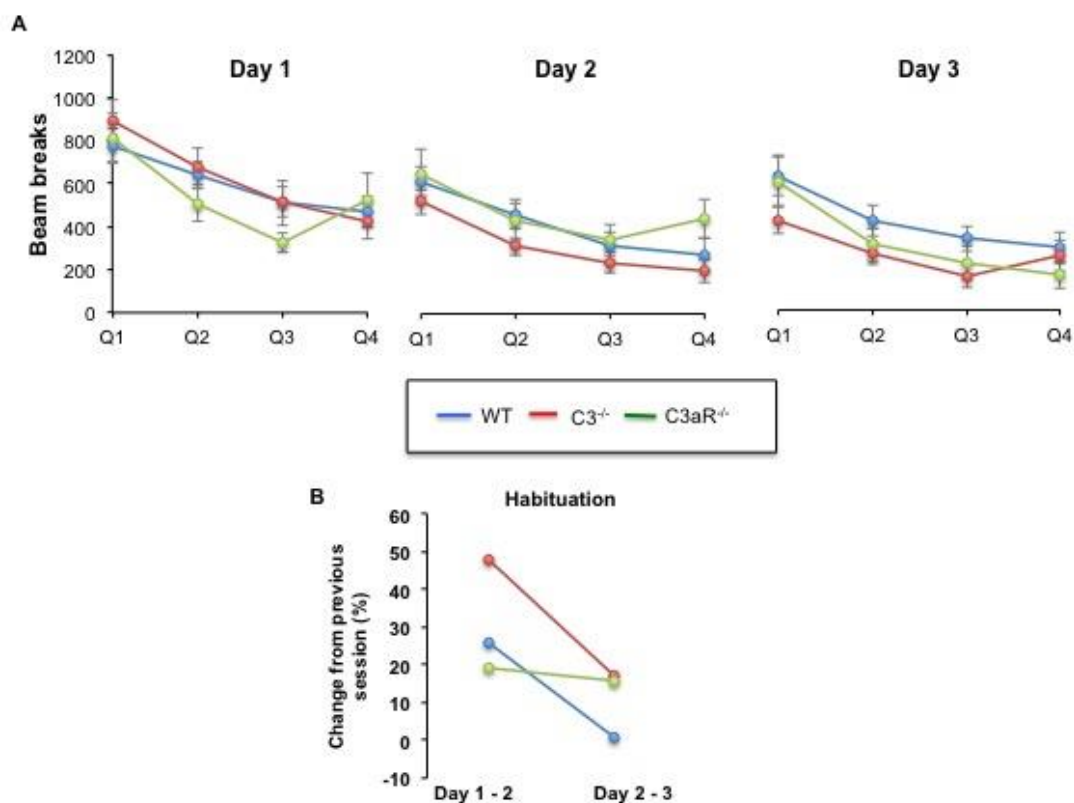
Figure 4.11 Locomotor activity of WT, C3$^{-/-}$ and C3aR$^{-/-}$ animals measured over three consecutive days. Each two-hour long testing session was divided into four time bins consisting of 30 minutes each (Q1-Q4). **A)** Average number of beam breaks made by WT, C3$^{-/-}$ and C3aR$^{-/-}$ animals on days 1-3. **B)** Rate of habituation of WT, C3$^{-/-}$ and C3aR$^{-/-}$ animals calculated as the percentage change in number of total beam breaks from day 1 to 2, and day 2 to 3. WT N=12, C3$^{-/-}$ N= 12, C3aR$^{-/-}$ N=10. Data represents mean + SEM.

4.3.3   C3aR$^{-/-}$ mice show heightened anxiety in the elevated plus maze

The behavioural phenotype of C3$^{-/-}$ and C3aR$^{-/-}$ animals in the EPM and OF was next investigated (Figure 4.12). As can be seen in the heat maps depicted in Figure 4.12A, C3aR$^{-/-}$ showed markedly reduced exploration of the open arms of the EPM compared to both WT and C3$^{-/-}$. Separate two-way ANOVAs with a between-subjects factor of genotype (WT, C3$^{-/-}$, C3aR$^{-/-}$) and repeated-measures factors of zone (open, middle, closed) were used to analyse the number of entries, and duration spent in each maze zone.

Analysis of total number of entries (Figure 4.12B) showed a significant main effect of genotype ($F_{(2,31)}=29.45$, $p < 0.0001$), zone $F_{(2,62)}=383.8$, $p < 0.0001$)

and a significant genotype*zone interaction ($F_{(4,62)}$=25.52, p < 0.0001). Pairwise contrasts were used to break down this interaction and demonstrated that C3aR deficient animals made significantly fewer open arm entries (8.50 ± 1.54) than both WT (22.92 ± 1.63, p < 0.0001) and C3$^{-/-}$ (27.08 ± 1.51, p < 0.0001, Figure 4.12B). A similar pattern of results was present for both the middle zone (C3aR$^{-/-}$ 23.10 ± 3.18 entries, vs. WT 48.92 ± 2.45 entries p < 0.0001, vs. C3$^{-/-}$ 48.42 ± 1.99 entries, p < 0.0001) and closed zone (C3aR$^{-/-}$ 15.50 ± 1.68, vs. WT 27.08 ± 1.26 entries, p < 0.0001, vs. C3$^{-/-}$ 22.67 ± 1.05, p < 0.0001) suggesting that C3aR deficient animals explored all areas of the maze significantly less than other genotypes.

Regarding the duration spent in each zone of the maze, results showed a significant main effect of genotype ($F_{(2,31)}$=8.15, p < 0.01) and zone ($F_{(2,62)}$=107.4, p < 0.0001) and a significant interaction between these factors ($F_{(4,62)}$=17.72, p < 0.0001, Figure 4.12C). Pairwise contrasts showed that C3aR$^{-/-}$ animals spent significantly more time in the closed arms of the maze (221.9 ± 12.06 seconds) compared to WT (146.0 ± 7.01 seconds, p < 0.0001) and C3$^{-/-}$ animals (140.0 ± 8.61 seconds, p < 0.0001) and spent less time in the open arms (16.70 ± 3.73 SEM seconds) than the other genotypes (WT 75.78 ± 8.86 seconds, C3$^{-/-}$ 93.86 ± 9.59 seconds, both p < 0.0001 vs. C3aR$^{-/-}$). There were no significant differences between genotypes in the amount of time spent in the middle region of the maze however (all comparisons p > 0.05). C3aR deficient animals also made fewer head dips compared to WT (see Appendix E) whereas C3 deficient animals performed significantly more of these behaviours compared to both WT and C3aR$^{-/-}$, suggesting anti-anxiety behaviour. Furthermore, C3aR$^{-/-}$ animals were seen to engage in grooming more than WT animals (see Appendix E). Together, the results of reduced exploration and time spent in the open arms indicates that C3aR deficiency induced a highly anxiogenic phenotype.

4.3.4   C3aR$^{-/-}$ explore the open field less, whereas C3$^{-/-}$mice show an anti-anxiety phenotype

C3aR deficient animals also exhibited less exploratory behaviour in the open field (Figure 4.12D). Analysis of the number of entries made per zone (outer vs. centre) demonstrated a main effect of zone ($F_{(1,31)}$=55.97, $p < 0.0001$) and a significant main effect of genotype ($F_{(2,31)}$=4.51, $p < 0.05$). The interaction of these factors was approaching statistical significance ($F_{(2,31)}$=3.00, $p = 0.06$). Post hoc tests demonstrated a tendency for C3aR$^{-/-}$ subjects to make fewer entries into the centre zone (19.10 ± 3.75 entries) than both WT (34.33 ± 3.74 entries, $p < 0.05$) and C3$^{-/-}$ subjects (36.25 ± 5.19 entries, $p < 0.01$). The number of entries made to the outer zone did not significantly differ between genotypes (all $p > 0.05$). In addition to the data obtained from the Elevated plus maze, this data also suggests an anxiogenic phenotype of C3aR deficient mice.

Analysis of the duration spent in either the outer or centre zones of the open field again showed a main effect of zone ($F_{(2,31)}$=0.96, $p = 0.39$), no main effect of genotype ($F_{(2,30)}$=1.33, $p = 0.27$) but a significant zone by genotype interaction ($F_{(2,31)}$=4.02, $p < 0.05$). As seen in Figure 4.12F, C3$^{-/-}$ animals spent a greater duration within the centre region (56.53 ± 7.28 seconds) than WT (37.46 ± 5.84 seconds, $p < 0.05$) and C3aR$^{-/-}$ animals (29.74 ± 2.38 seconds, $p < 0.01$), and less time in the outer region (423.6 ± 7.28 seconds) than did WT (442.5 ± 5.84 seconds, $p < 0.05$) or C3aR$^{-/-}$ (450.3 ± 6.64 seconds, $p < 0.1$). In contrast to C3aR$^{-/-}$, these results suggest an anxiolytic phenotype of C3$^{-/-}$ mice.

201
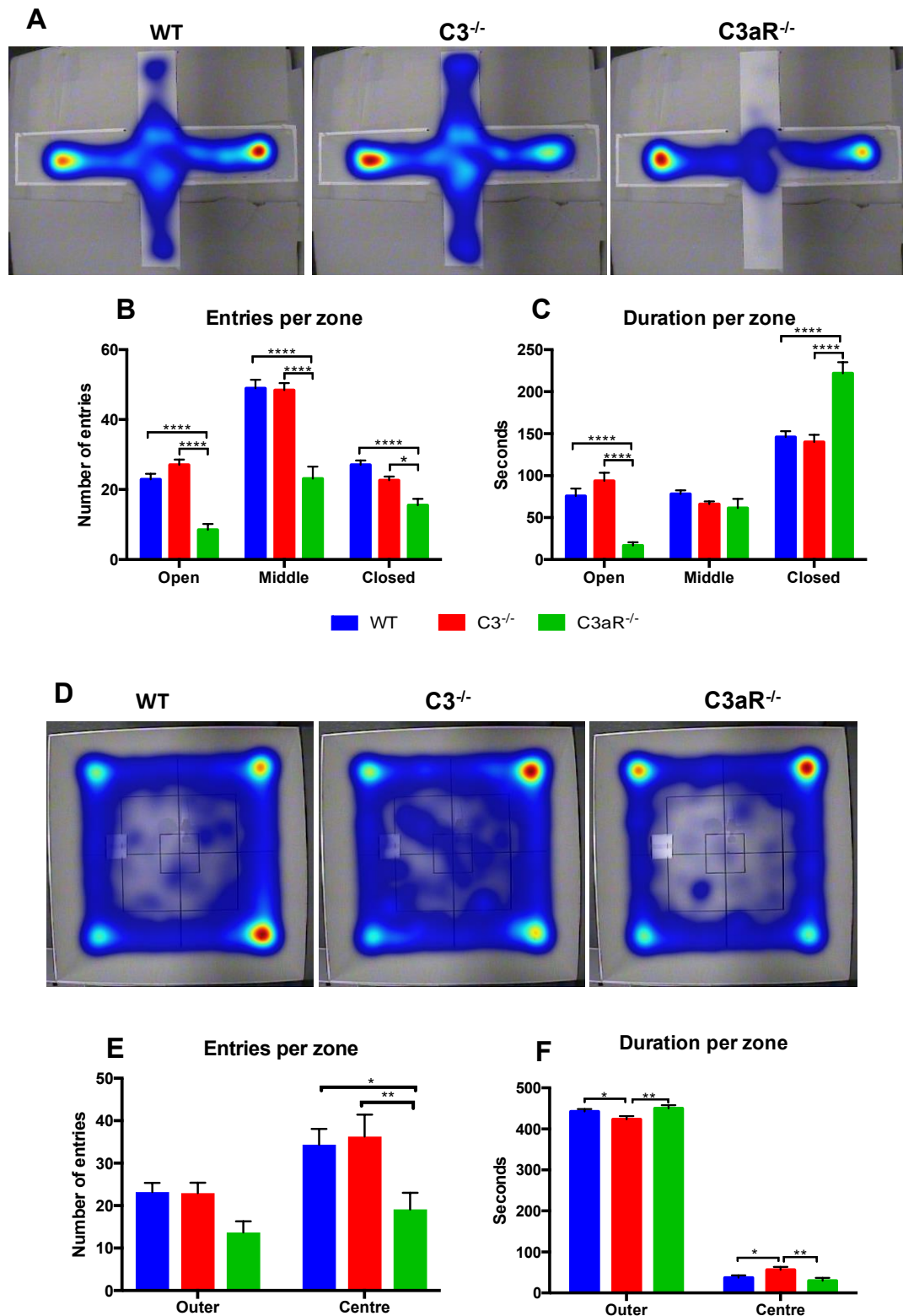
Figure 4.12 Elevated plus maze and Open field-based investigations of anxiety related behaviour in WT, C3$^{-/-}$ and C3aR$^{-/-}$ animals. **A)** Merged heat maps of exploration of EPM by each genotype. **B)** Mean number of entries to open, middle and closed regions of the EPM **C)** Average duration spent in open, middle and closed regions according to genotype **D)** Merged heat map of open field exploration according to genotype **E)** Mean number of entries made to outer and centre regions of the open field according to genotype **F)** Mean duration spent in outer or centre regions in seconds, WT N =12, C3$^{-/-}$ N=12, C3aR$^{-/-}$ N= 10. Data represents mean + SEM. *= p < 0.05, ** = p < 0.01, *** = p < 0.001, ****= p < 0.0001

4.3.5 Food neophobia

We next investigated food neophobia as an extension of the anxiety-related behaviours seen in the EPM and OF. Furthermore, this experiment served to habituate animals to condensed milk, which would later feature as reward in the LD task. It was noted that average body weight assessed during this test differed between genotypes ($F_{(2,31)}$=3.71, $p < 0.05$) due to greater body weight of C3$^{-/-}$ animals (26.23 $\pm$ 0.54 g) compared to WT (24.54 $\pm$ 0.33 g, $p < 0.05$, Figure 4.13A). The weight of C3aR$^{-/-}$ (25.68 $\pm$ 0.47 g) animals was not significantly different to WT or C3$^{-/-}$ animals. Due to these differences, consumption data was adjusted to account for body weight by calculating volume consumed per gram of body weight (denoted vol/g).

As described in Section 4.2.6, all animals were first acclimatised to receiving two pots of water. The amount consumed over two days was measured, before a solution of 10% condensed milk in water was introduced on day 3. As shown in Figure 4.13B & C, all mice showed less consumption of water, and an increasing preference for milk through days 3-8. The preference for milk versus water was calculated for each subject by dividing milk consumption (vol/g) by total consumption (vol/g) for each day water and milk were available (i.e., days 3-7). A two way ANOVA with a between subjects factor of genotype (WT, C3$^{-/-}$, C3aR $^{-/-}$) and a repeated measures factor of day (3,4,5,6,7) showed a significant main effect of genotype ($F_{(2,31)}$=9.79, $p < 0.001$), day ($F_{(4,124)}$=11.37, $p < 0.0001$) and a significant interaction of these factors ($F_{(8,124)}$=3.15, $p < 0.01$). Pairwise contrasts were used to breakdown the significant interaction and showed significant differences between all genotypes on day 3 (see Figure 4.13B). C3aR$^{-/-}$ showed the highest preference for milk (87 ± 5 % of total consumed), whereas C3$^{-/-}$ showed the lowest preference (48 ± 5 %). Both were significantly different to WT (68 ± 10 %, all $p < 0.05$). On day 4, C3$^{-/-}$ again showed a lower preference for condensed milk (55 ± 5 % of total consumption), which was significantly different to both WT (83 ± 4 %, $p <$

0.001) and C3aR$^{-/-}$ (87 ± 4 %, p < 0.001). Preference for condensed milk was comparable between genotypes (all p > 0.05) on days 5, 6 and 7 however. These results suggest that although C3$^{-/-}$ mice were slower than WT and C3aR$^{-/-}$ mice in developing a preference for consumption of condensed milk, all genotypes were equally amenable to milk consumption as a reinforcer by the end of the test. Furthermore, this data suggests that the heightened anxiety seen in C3aR$^{-/-}$ mice in the OF and EPM did not result in food neophobia.
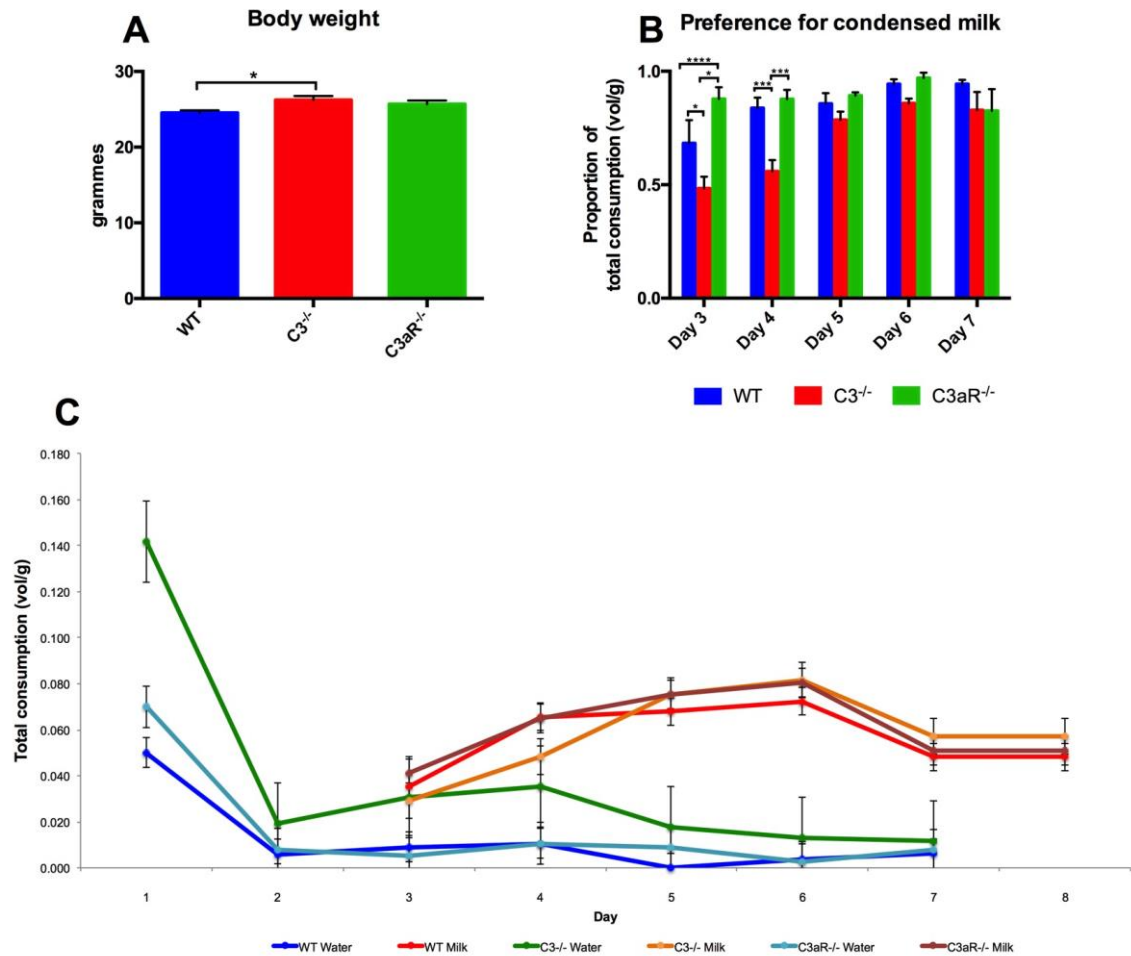
Figure 4.13. Consumption of water versus condensed milk in WT, C3$^{-/-}$ and C3aR$^{-/-}$ animals. **A)** Average body weight over the eight days of testing. **B)** Preference for condensed milk, calculated as proportion of milk consumed (vol/g of body weight) over total consumption (vol/g) for WT, C3$^{-/-}$ and C3aR$^{-/-}$ animals on days three to seven, during which subjects had a choice between water or milk. **C)** Average total consumption (vol/g) per genotype of water (available days 1-7) versus condensed milk (available days 3-8) by WT, C3$^{-/-}$ and C3aR$^{-/-}$ animals. WT N =12, C3$^{-/-}$ N=12, C3aR$^{-/-}$ N= 10. Data represents mean + SEM. *= p < 0.05, ** = p < 0.01, *** = p < 0.001, ****= p < 0.0001.

4.3.6 Location Discrimination task

Shaping and intermediate task training

Having established equivalent locomotor activity and reward preferences across genotypes, animals began a shaping period in preparation for LD task training. In order to examine whether there were any differences in the rate of acquisition across the shaping period (including Hab, LS, MT, MI and PI) and intermediate stimulus separation training, the mean number of sessions required to reach criterion in each stage of training was analysed with separate one-way ANOVAs. There was a significant difference between genotypes in the average number of sessions to complete shaping ($F_{(2,23)}$=9.52, p < 0.001, Figure 4.14). Tukey post-hoc comparisons showed that C3$^{-/-}$ (36.78 ± 3.07) reached criterion in fewer sessions that WT (58.45 ± 3.86 sessions, p < 0.001). C3aR$^{-/-}$ (48.17 ± 4.04 sessions) did not significantly differ to WT (p=0.18) or C3$^{-/-}$ (p=0.14) in the number of sessions required to meet criterion during the shaping stage. Therefore, these results suggest that the absence of C3 enhanced task acquisition during the shaping stage relative to WT.

I next examined whether there were any genotype differences in the baseline training for the LD task, in which animals were trained to make discriminations between stimuli separated by an intermediate distance (as described in Section 4.2.9, Figure 4.9). Importantly, this was the first stage during which spatial discriminations were introduced. C3$^{-/-}$ (4.66 ± 0.72 sessions) and C3aR$^{-/-}$ (11.83 ± 2.34) did not significantly differ to WT (8.54 ± 1.60 sessions) in the number of sessions required to reach criterion, suggesting an equal baseline level of performance between knockout and WT strains (all p > 0.05). However, C3aR$^{-/-}$ animals required significantly more sessions to reach criterion compared to C3$^{-/-}$ (p < 0.05; Figure 4.14).

Number of sessions to criteria
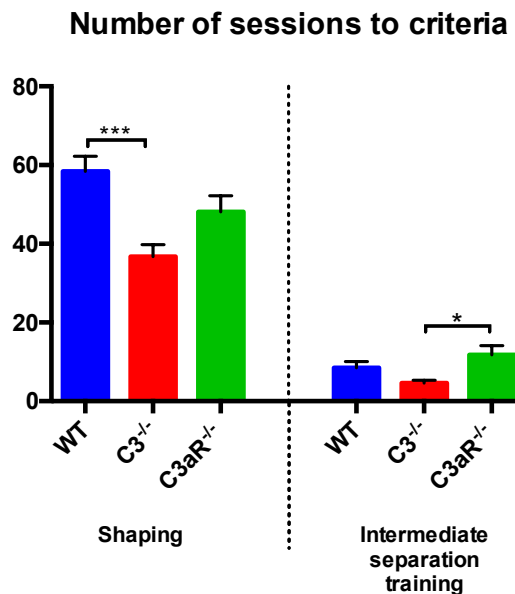
Figure 4.14 C3^{-/-} animals progressed through the shaping stage faster than WT animals, whereas C3aR^{-/-} animals were slower to acquire the LD task than C3^{-/-} animals. The average number of sessions to criteria was calculated for the following shaping (including habituation, large squares, must touch, must initiate and punish incorrect stages) and intermediate separation training. WT N =12, C3^{-/-} N=12, C3aR^{-/-} N= 10. Data represents mean + SEM. *= $p < 0.05$, ** = $p < 0.01$, *** = $p < 0.001$, ****= $p < 0.0001$.

4.3.7 LD task probe sessions

After completion of the training period, mice were presented with probe sessions during which the stimuli were presented either close together, or far apart, as detailed in Section 4.2.10.

Sample attrition

Three C3^{-/-} animals succumbed to illness before beginning probe sessions and a C3aR^{-/-} subject showed skin lesions due to excessive grooming. Therefore, their data were not included in the analyses. One WT and three C3aR^{-/-} animals were also excluded as they did not meet criteria at the intermediate stimulus separation training stage (i.e., completion of twenty trials or more per session, with a minimum of one reversal, per session, on three consecutive days). Therefore, the final N equalled 11 WT, 9 C3^{-/-} and 6 C3aR^{-/-} mice.

LD task probe session parameters

A series of mixed ANOVAs with the between subject factor of genotype (WT, C3$^{-/-}$ and C3aR$^{-/-}$) and repeated-measures factors of separation (close, far) and session (first, last) were used to analyse the following; the average number of criteria achieved per session (Figure 4.15B), the average number of trials taken to reach first criterion per session (Figure 4.15C), the average percentage of correct responses until first criterion per session (Figure 4.15D), the average correct response time (s) until first criterion per session (Figure 4.15E), the average incorrect response time (s) until first criterion per session (Figure 4.15F), the average number of inter-trial interval touches made per session (Figure 4.15G), and the average number of trials completed per session (Figure 4.15H). I also calculated the number of trials between criteria in a session, to give an indication of perseverative response tendency (Figure 4.16).

Percentage of mice reaching criteria

Firstly, I calculated the percentage of all mice reaching criteria during close and far stimuli separation conditions regardless of session (Data not shown). Across all genotypes, a significantly larger percentage of animals met criteria in the far stimuli separation condition (70 ± 8.31 %) compared to the close stimuli separation (41 ± 6.58 %, paired *t*-test, p < 0.01). Individually, subjects made more correct responses in the trials preceding their first criterion in the far condition (63.46 ± 1.65 % correct) than in the close condition (50.23 ± 2.61 % correct, paired *t*-test, p < 0.0001). Trial number was also significantly higher in the far condition (41.73 ± 1.95) compared to close (26.17 ± 1.34, paired *t*-test, p < 0.0001). This data suggests that, as intended, the close discrimination was more challenging than the far discrimination.

Next, I determined the percentage of mice per genotype that were able to reach criteria in close and far stimuli separation conditions, as a descriptive measure (Figure 4.15A). In the first session of the close stimuli separation condition, 27% of WT animals reached criterion, compared to 38% of C3$^{-/-}$ and 58% of C3aR$^{-/-}$, suggesting that both mutant genotypes

showed enhanced pattern separation. There was an interesting pattern of data pertaining to the second session of the close discrimination however. WT were unable to better their performance, again with 27% of animals reaching criterion. Performance in the C3$^{-/-}$ group improved to 64% in the second session, suggesting a benefit of practice. On the other hand, the performance of the C3aR$^{-/-}$ group fell to near WT levels in the second session (33% reaching criteria). Overall, this pattern of data suggests a greater ability to correctly discriminate close stimuli separations by C3$^{-/-}$ and C3aR$^{-/-}$ animals compared to WT, but indicates differential effects of practice between the two mutant strains.

 C3 and C3aR$^{-/-}$ were also superior to WT in the less taxing far stimuli separation condition. As shown in Figure 4.15A, in the first session of the far separation condition, 33% of WT mice met criteria, compared to 77% and 75% of C3$^{-/-}$ and C3aR$^{-/-}$, respectively. In the last session of the far separation condition, WT animals showed improvement, with 76% of animals reaching criterion. C3$^{-/-}$ mice also improved, with 94% of animals reaching criterion. However, again the performance of C3aR$^{-/-}$ animals declined slightly, with 66% of the group reaching criterion.

Mean number of criteria reached per session

I next examined the mean number of criteria reached per animal, per session in close and far stimuli separation conditions. Again, there was a trend indicative of improved performance of C3 and C3aR$^{-/-}$ subjects compared to WT, on both close and far conditions, that was again influenced by practice (Figure 4.15B). Statistical analyses showed a significant main effect of genotype ($F_{(2,23)}=136.92$, p < 0.01), and separation ($F_{(1,23?)}=42.06$, p < 0.0001) but not session ($F_{(1,23)}=1.81$, p= 0.19). There was no significant interaction between these three factors combined ($F_{(2,23)}=1.22$, p=0.31), however there was a significant genotype by separation interaction ($F_{(1,23)}=3.83$, p < 0.05). All other potential interactions (session*genotype, session*separation) were non-significant (p > 0.05). To break down the significant interaction of genotype and

separation, contrasts were performed to compare the performance of each genotype at each level of separation (close versus far) collapsed across both sessions (first versus last). Results demonstrated that in the close stimuli separation condition, C3aR$^{-/-}$ animals achieved a significantly greater mean number of criteria (0.79 ± 0.13) than WT animals (0.29 ±0.08, p < 0.05). Although C3$^{-/-}$ animals attained on average 0.55 ± 0.10 criteria per session, this was not significantly different to WT, or C3aR$^{-/-}$ (p= 0.21 and p=0.39, respectively). In the far stimuli separation conditions, C3$^{-/-}$ attained a significantly greater average number of criteria per session (1.27 ± 0.13) than WT (0.59 ± 0.08, p < 0.0001). C3aR$^{-/-}$ animals achieved on average 0.87 ± 0.16 criteria per session, however this was not significantly different to WT (p =0.23) or C3$^{-/-}$ (p=0.07; Figure 4.15B).

Mean number of trials taken to reach first criterion

The average number of trials completed to reach first criterion in close and far stimuli separation conditions were analysed per genotype, across the first and last sessions of each condition. On this measure, there was a trend indicative of poorer performance by C3$^{-/-}$ mice in the close condition, compared to both WT and C3aR$^{-/-}$ (Figure 4.15C). Analyses showed no significant main effects of the factors genotype and session, but a significant main effect of separation was found ($F_{(1,23)}$=7.87, p < 0.01). There was also a significant interaction effect of genotype and separation ($F_{(2,23)}$=5.01, p < 0.05). All other potential interaction effects (session*genotype, session*genotype*separation) were non-significant. Pairwise contrasts were performed to breakdown the significant interaction between genotype and separation, collapsed across session. Results showed that C3$^{-/-}$ mice required a greater number of trials to reach their first criterion in the close stimuli separation condition (21.53 ± 2.21) than did WT (15.95 ± 1.45, p <0.05) or C3aR$^{-/-}$ animals (14.92 ± 1.44 p < 0.05), suggesting that C3$^{-/-}$ were impaired on discriminating closely separated stimuli. Pairwise contrasts showed no differences between
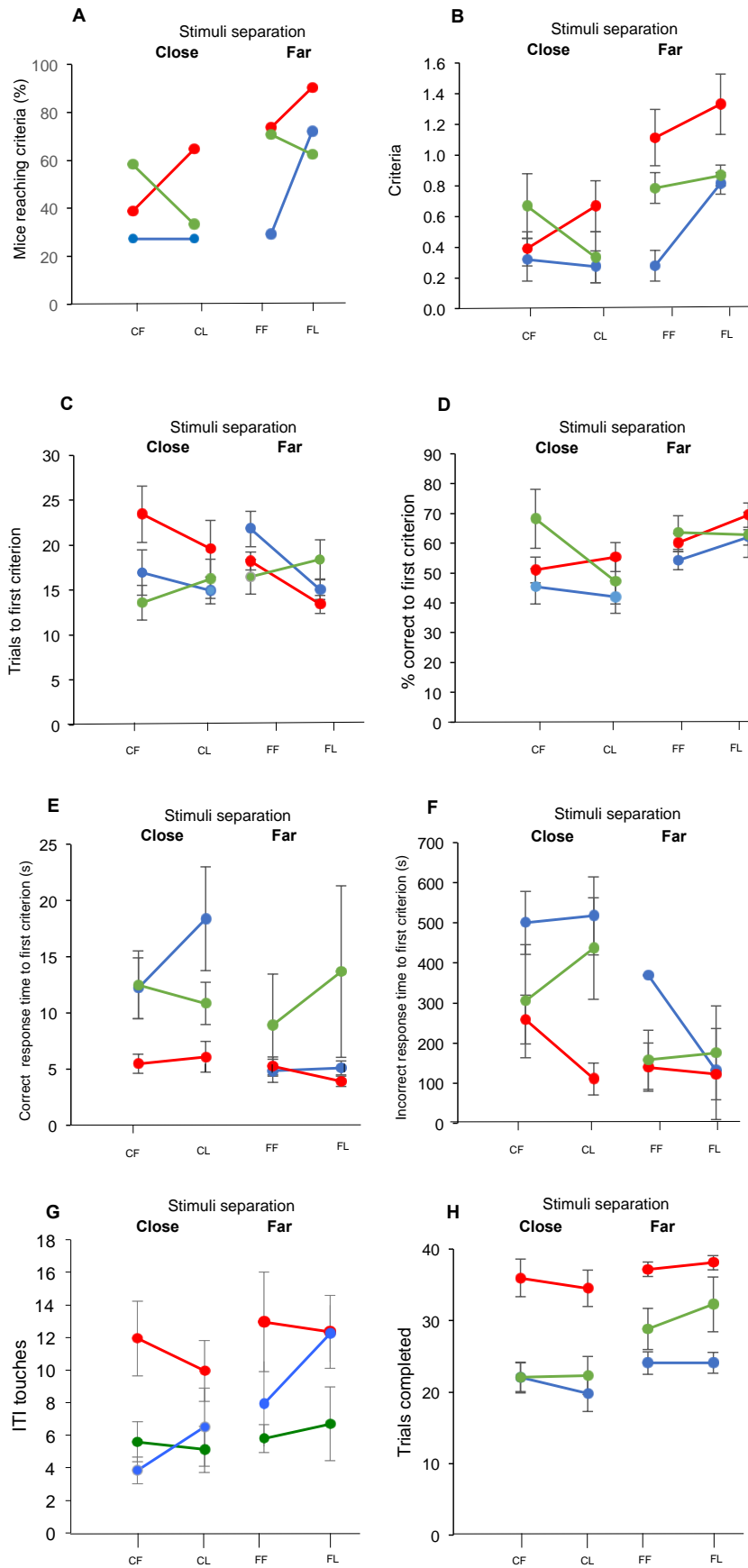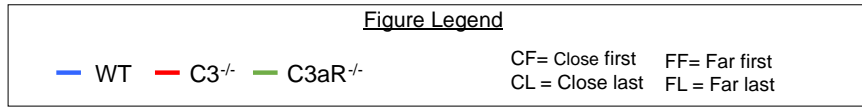
Figure 4.15 Performance of WT, C3^-/- and C3aR^-/- mice in the location discrimination (LD) task, in first and last sessions of close and far stimulus separation conditions. **A)** Mean percentage of mice per genotype reaching criterion **B)** Mean number of criteria reached. **C)** Mean number of trials taken to reach first criteria **D)** Mean percentage of correct responses in trials preceding first criterion **E)** Mean correct response latency in seconds. **F)** Mean incorrect response latency in seconds **G)** Mean number of inter-trial-interval (ITI) touches. **H)** Mean number of trials completed. Data represents the mean + SEM. WT N= 11, C3^-/- N= 9, C3aR^-/- N=6. *= p < 0.05, ** = p < 0.01, *** = p < 0.001, ****= p < 0.0001. CF= Close first, CL=Close last, FF=Far first, FL=Far last.

genotypes in the number of trials to first criterion in the far stimuli separation condition.

Percentage of correct responses to first criterion

Of the total number of trials to first criterion, the percentage of correct responses was calculated per animal, per session. The average correct percentage of responses was then analysed. Again, there was a trend towards better performance by C3 and C3aR^-/- in the close condition, but this was dependent on session (Figure 4.15D). Analyses showed a significant main effect of separation ($F_{(1,23)}$=15.94 , p < 0.001), reflecting fewer correct responses in the close stimuli separation condition across all genotypes. The main effect of genotype was approaching significance ($F_{(2,23)}$=3.04 , p= 0.06) and there was no main effect of session ($F_{(1,23)}$=0.08 , p= 0.77). There was a significant interaction effect between the factors of genotype and session however ($F_{(2,23)}$=3.92 , p < 0.05), and the interaction of session and separation was borderline significant ($F_{(1,23)}$=3.95 , p= 0.059). There was no significant three-way interaction effect between the factors examined (p > 0.05). Pairwise contrasts were used to break down the significant genotype*session interaction. Regardless of stimuli separation, in the first session, C3aR^-/- animals made a significantly higher proportion of correct responses (66.80 ± 5.42 %) compared to WT animals (50.87 95 ± 3.43 %, p < 0.05). On average, 56.54 ± 2.87 % of responses made by C3^-/- animals in the run up to their first criterion, in the first session of either close or far, were correct. This was not statistically significant in comparison to either WT (p=

0.53) or C3aR$^{-/-}$ (p=0.22). Pairwise contrasts showed no significant differences between genotypes on the last session. While this statistical result does not take account of the critical task manipulation of stimuli separation, it suggests that C3aR$^{-/-}$ animals were differentially affected by session, as their performance was improved relative to other genotypes only on the first session of each condition.

Correct response time to first criterion

I then probed the nature of responses made in the run up to each subject's first criterion (Figure 4.15E). The average time in seconds (s) required for animals to make a correct response after stimulus presentation was analysed according to genotype, session and separation. Significant main effects of genotype ($F_{(2,23)}$=4.16 , p < 0.05) and separation ($F_{(1,23)}$=5.80 , p < 0.05) were found, in absence of a main effect of session ($F_{(1,23)}$=0.74 , p= 0.39). The interaction between factors of genotype and separation was statistically significant ($F_{(2,23)}$=3.65 , p < 0.05). There was no significant interaction effect of factors of session and genotype jointly, nor session, genotype and separation combined. To break down the interaction between genotype and separation, pairwise contrasts were made between genotypes at each level of separation (close vs. far) collapsed across the two levels of session. Comparisons showed that C3$^{-/-}$ mice were significantly faster in making correct responses (5.77 ± 0.78 s) than WT (15.28 ± 2.69 s, p < 0.001) in the close stimuli separation condition. On average, C3aR$^{-/-}$ animals made correct responses within 11.65 ± 1.71 s, and were not significantly different to either WT (p=0.44) or C3$^{-/-}$ (p=0.14). There were no significant differences between genotypes in the speed of correct responses made in the far stimuli separation condition.

Incorrect response time to first criterion

I was also interested in the latency of incorrect responses in the trials preceding the first criterion. The average latency of incorrect responses made per animal was analysed by genotype, in close vs. far stimuli separations across two sessions was analysed (Figure 4.15F). There was a significant

main effect of genotype ($F_{(2,23)}$=38.11 , p < 0.0001), separation ($F_{(1,23)}$=10.27 , p < 0.01) and session ($F_{(1,23)}$=33.48 , p < 0.0001). There was a significant two way interaction between genotype and session ($F_{(2,23)}$=3.51 , p < 0.01), and a significant three way interaction between genotype, separation and session ($F_{(2,23)}$=3.46 , p < 0.05). Session and genotype did not interact significantly (p > 0.05).

In order to break down the significant three-way interaction between genotype, separation and session, contrasts between genotypes were made at each level of separation (close vs. far) in each session (first vs. last). In the first session of the close stimuli separation condition, C3$^{-/-}$ mice made incorrect responses with shorter latencies (5.45 ± 2.34 s) than WT (12.19 ± 2.11 s, p < 0.05). The speed of incorrect responding in C3aR $^{-/-}$ mice was comparable to that of WT (12.48 ± 2.86 s, p = 0.93). On session two of the close stimuli separation condition, there were no significant differences between genotypes in their latency to make an incorrect response. In the first session of the far stimuli separation condition, C3 deficient mice were again faster to select an incorrect response (110.65 ± 88.96 s) compared to WT (517.21 ± 80.47 s, p < 0.05) and C3aR deficient mice (436.27 ± 108.96 s, p < 0.05). Again, no differences in incorrect response time were found in the second session of the far stimuli separation condition. Together with the correct response time data, this pattern suggests that C3 deficient mice were faster at making responses in general, regardless of whether they were correct or incorrect.

Inter-trial-interval (ITI) touches

The number of nose pokes made to the touchscreen during ITIs was recorded per session, and gives an indication of indiscriminate responding. Analyses showed a significant main effect of genotype ($F_{(2,23)}$=5.08 , p < 0.0001). As shown in Figure 4.15G, C3$^{-/-}$ animals made a significantly higher number of ITI touches (11.85 ± 9.47), across both first and last sessions of far and close stimuli separations. This was significantly higher than both WT (5.84 ± 0.74, p < 0.0001) and C3aR$^{-/-}$ animals (7.66 ± 1.14, p < 0.05). There was also a

significant main effect of session ($F_{(1,23)}$=7.32 , p < 0.05), however contrasts did not find any significant differences in ITI touches between the first and last session across genotypes or separation conditions. There was no significant main effect of separation ($F_{(1,23)}$=0.64 , p = 0.43) and there were no significant interactions (all p > 0.05). This result suggests that C3$^{-/-}$ subjects engaged in more indiscriminate responding than did WT and C3aR$^{-/-}$ subjects.

Total number of trials completed

I also compared the average number of trials subjects completed per session (Figure 4.15H). There was a significant main effect of genotype ($F_{(2,23)}$=11.79 , p < 0.0001) and separation ($F_{(1,23)}$=14.23 , p < 0.001). There was no significant main effect of session however ($F_{(2,23)}$=0.03 , p = 0.86). These factors did not interact significantly, and therefore significant main effects were followed up with pairwise contrasts. C3 $^{-/-}$ animals performed a significantly greater number of trials (36.32 ± 1.47) regardless of stimulus separation condition or session, compared to both WT (22.43 ± 0.98, p < 0.0001) and C3aR$^{-/-}$ (26.29 ± 1.62, p < 0.0001). Follow up analyses of the main effect of separation showed that regardless of genotype and session, animals performed a significantly greater number of trials (30.09 ± 1.33) in the far stimuli separation than in the close stimuli separation condition (26.17 ± 1.34, p < 0.001).

Perseverative response tendencies

The LD tasks incorporates reversal learning, which requires subjects to constantly adapt their responses to changing stimulus-reward contingencies. Therefore, I was interested in whether subjects displayed perseverative response tendencies. This is characterised by persistent selection of the previously relevant response, and impaired learning of the new stimulus-reward contingency (Clark et al., 2004). I therefore examined the average number of intervening trials between subjects achieving separate criteria (see Figure 4.16). If an animal did not reach criterion again during a session, the number of trials until the end of the session was used. There was no significant main effect of separation ($F_{(1,23)}$=0.07 , p = 0.79) but there was a

significant main effect of genotype ($F_{(2,23)}$=4.91 , $p < 0.05$). These factors did not significantly interact ($p > 0.05$). C3$^{-/-}$ animals completed on average 22.99 ± 1.73 trials before reaching another criterion or terminating the session. This was significantly higher than both WT (14.92 ± 1.31 trials, $p < 0.001$) and C3aR$^{-/-}$ (16.48 ± 1.34 trials, $p < 0.05$). Therefore, C3$^{-/-}$ mice displayed perseverative response tendencies, and were not able to adapt their responses to changing contingencies as rapidly as WT or C3aR$^{-/-}$ animals.
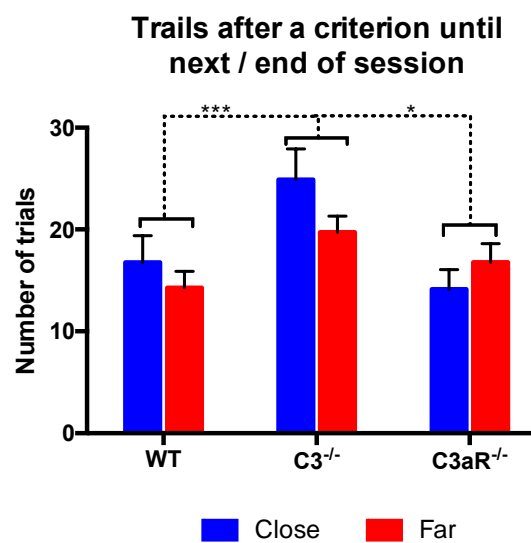
Figure 4.16. C3$^{-/-}$ subjects showed a tendency to perseverate after achieving criterion. Data represents the mean number of trials between criteria within a session per animal, or if another criterion was not reached, the number of trials until session termination. Error bars represent SEM. WT N= 11, C3$^{-/-}$ N= 9, C3aR$^{-/-}$ N=6. *= $p < 0.05$, ** = $p < 0.01$, *** = $p < 0.001$, ****= $p < 0.0001$.

4.4 Discussion

Summary of results

In this chapter, I investigated whether the previously observed C3/C3aR-mediated increases in AHN had functional consequences in terms of the cognitive and affective processes often attributed to newly born neurons. I therefore tested C3 and C3aR deficient mice on a battery of behavioural tasks to assess their ability to perform fine pattern separation, and to probe anxiety.

The LD task proved a successful measure of fine pattern separation, as all genotypes performed significantly worse on close than far discriminations. In terms of their ability to perform fine pattern separation, both C3 and C3aR deficient mice were superior to WT. Such improvements in performance have previously been linked to increases in AHN (Creer et al., 2010), tentatively suggesting that the superior performance observed is a correlate of, or may even be causally linked to, the increases in AHN seen in these strains.

Furthermore, AHN and the process of pattern separation have also been linked to affective processes including anxiety (Kheirbek & Hen, 2014). Using the OF and EPM, two classical tests of anxiety, the here data provides converging evidence for abnormal anxiety phenotypes in both C3 and C3aR deficient models. Interestingly, absence of C3 was anxiolytic in the OF, whereas the absence of C3aR was anxiogenic in the EPM and OF. These results suggest a novel role for C3 and C3aR signalling in mediating anxiety.

4.4.1   C3/C3aR did not affect locomotor activity but C3aR deficiency altered habituation to a novel environment

Prior to beginning cognitive and affective behavioural testing, it was important to ensure comparable activity levels between genotypes, as such

differences can confound results of exploration based paradigms such as the OF and EPM. Previously, Perez-Alcazar et al. (2013) reported lower levels of activity in young adult C3$^{-/-}$ mice compared to WT controls. I did not observe differences in the overall locomotor activity of C3 or C3aR$^{-/-}$ mice over three successive days of testing however. Methodological differences are likely to explain these differing results, since Perez-Alcazar et al. (2013) recorded activity levels of animals within in their home cage environment. In contrast, these experiments took place in purpose-built chambers designed to measure locomotor activity. Inherent in this design is the use of a novel environment, which also allowed insight into habituation. Interestingly, compared to their WT and C3 deficient counterparts, C3aR$^{-/-}$ mice showed a smaller decrement in their activity levels between consecutive days. This suggests a deficit in habituation or learning about a novel context in the absence of C3aR. However, in light of the results obtained through the OF and EPM, which will be discussed in turn, this result may be explained by their anxiogenic phenotype.

4.4.2   C3aR deficiency is profoundly anxiogenic in the elevated plus maze

I was also interested in the affective phenotype of C3/C3aR deficient mice, since AHN and pattern separation have been proposed to play a role in pathological anxiety (Kheirbek & Hen, 2014). In the EPM, C3aR deficiency proved anxiogenic. In terms of the duration spent in the zones of the maze, C3aR$^{-/-}$ mice spent dramatically less time in the open arms, and greater time in the closed arms than WT or C3$^{-/-}$ subjects. The genotypes did not differ in their duration spent in the middle zone however. With regard to the number of entries made per zone, C3aR$^{-/-}$ entered the open, closed and middle regions less than WT or C3$^{-/-}$ mice. In absence of any genotype differences in the aforementioned locomotor activity test, I am confident that these results reflect a valid readout of the affective state of anxiety.

I also measured ethological parameters within the EPM; head dips, stretch-attend postures, and grooming (see Appendix E). Head dips, which involve the rodent peering over the edge of an open arm, were performed considerably less, and for a shorter duration, by C3aR$^{-/-}$ mice compared to WT and C3$^{-/-}$ mice, again confirming their anxious phenotype. Interestingly, C3$^{-/-}$ mice performed the most head dips, which may represent a reduced level of anxiety due to greater willingness to approach the open arms. Otherwise, C3 deficient animals were comparable to WT on all variables measured in this paradigm. This is in line with the report of Shi et al. (2015), who did not find any changes in the behaviour of young adult C3 deficient mice in the EPM.

4.4.3   C3 deficiency is anxiolytic in the open field

It has been demonstrated that the EPM has predictive validity in terms of performance in other behavioural tests; for example, greater exploration of the open arms of the EPM is predictive of greater exploration of the central zone in the OF (Frye, Petralia, & Rhodes, 2000; Walf & Frye, 2007). In agreement, C3aR$^{-/-}$ mice made fewer entries into the central and outer zones of the OF, and heat maps illustrated a greater degree of thigmotaxis than the other genotypes, consistent with their elevated anxiety in the EMP.

In contrast to the results of the EPM however, an anxiolytic phenotype of C3 deficient mice manifested in the OF; C3 deficient mice spent a greater duration in the centre of the OF, and a less of their time was spent in the peripheral region compared to other genotypes. This is in line with my hypotheses, although I had expected to observe less anxiety in both the OF and EPM. While the EPM and OF do measure overlapping anxiety-related behavioural constructs, and despite their mutual predictive validity in terms of task performance, each task has different sensitivities to varying facets of behaviour (Carola, D'Olimpio, Brunamonti, Mangia, & Renzi, 2002). In

support of this argument, the anxious phenotype of C3aR deficient mice did not manifest in the test of food neophobia, and the anti-anxiety phenotype of C3 deficient mice was not associated with greater consumption of a novel foodstuff. Therefore, the data obtained in the OF implies that the absence of C3 is anxiolytic in young adult mice, but suggests that the phenotype is perhaps more task-specific than in aged C3$^{-/-}$ mice.

4.4.4 Relevance of affective phenotype to AHN and dependence on C3/C3aR signalling

The current literature regarding alterations in AHN and their impact on anxiety lacks clarity, with many conflicting results (Hill, Sahay, & Hen, 2015a; Marques et al., 2016; Revest et al., 2009). In the case of the data described here, since both knockout genotypes had comparable increases in adult neurogenesis, it is unlikely that the affective phenotypes observed are a consequence of increased AHN. It is likely that the mutations affect other undiscovered circuits within the brain, which may contribute to the phenotypes observed.

Whether this phenotype can be attributed to C3a signalling via C3aR is also unlikely, due to the differences in behaviour observed. Interestingly, the VGF neuropeptide has been shown to be downregulated in the hippocampus on exposure to stress, and is involved in affective behaviour (Thakker-Varia et al., 2007). It is the peptide derivative of VGF, TLQP-21, which has been shown to bind C3aR (Hannedouche et al., 2013). Therefore, I tentatively suggest that the anxiety phenotype observed in C3aR deficient animals may be mediated by TLQP-21/C3aR signalling as opposed to C3a/C3aR signalling. C3a can also interact with other pathways as outlined in Section 1.6.3, which may explain the anti-anxiety behaviours displayed by C3$^{-/-}$ mice. These possibilities will be considered further in the general discussion.

4.4.5   C3/C3aR deficient genotypes showed comparable preference for food reward

Due to the LD task being appetitive in nature, it was important to check for strain differences in reactivity to reward. The food neophobia test therefore served to habituate animals to the reinforcer to be used in the LD task, condensed milk. Interestingly, $C3^{-/-}$ showed a slower acquisition of preference for consumption of condensed milk compared to WT and $C3aR^{-/-}$. However, their preference for milk was comparable to that of the other strains by day three, suggesting that condensed milk served as an equally motivating reward for all genotypes in the LD task. Nonetheless, their delayed uptake of reward preference is of interest as it may indicate either sensory differences in taste perception, or alternatively altered hedonic responses in the absence of C3.

4.4.6 $C3^{-/-}$ and $C3aR^{-/-}$ were comparable to WT on their baseline spatial discrimination performance

Before moving onto the testing of pattern separation, it was imperative to establish equivalent baseline performance in the location discrimination task between genotypes. Throughout shaping, $C3^{-/-}$ animals required fewer sessions to reach criteria than did WT or $C3aR^{-/-}$ animals. Therefore, it seems that $C3^{-/-}$ mice have improved associative learning; they were quicker to learn to touch the screen, or stimuli, in order to obtain a reward, than were WT and C3aR deficient mice. However, they also competed more trials per session throughout the entire shaping period suggesting that they allowed themselves greater opportunity for learning than did the other groups, which may be related to their decreased anxiety. Since there was not increased locomotion in this genotype, their greater trial number is likely a related to their superior ability to perform the task at hand. Critically, when spatial discriminations were first introduced in the intermediate separation training

stage, both mutant strains did not differ to WTs in the number of sessions required to reach criterion. This suggests a common baseline between the mutant and WT strains in their ability to discriminate stimuli separated by an intermediate distance.

4.4.7 Close discriminations were more difficult than far discriminations

In LD probe sessions, subjects had to discriminate stimulus locations that were either close together or far apart. This manipulation was originally designed by McTighe et al. (2009) with the intention of influencing task difficulty, and thereby the computational process of pattern separation, which is preferentially required for close discriminations (Clelland et al., 2009). In agreement with previous reports (Clelland et al. 2009; Creer et al. 2010), my experimental subjects found the close discrimination considerably more difficult. This was evidenced by the percentage of animals (regardless of genotype) able to reach criterion on the close discrimination ($\sim$40 %) compared to the far discrimination ($\sim$70 %). Furthermore, trial number and accuracy of responding was reduced in the close condition indicating elevated task difficulty. Therefore, the stimuli separation condition successfully manipulated task difficulty.

4.4.8 $C3^{-/-}$ and $C3aR^{-/-}$ mice showed enhanced fine pattern separation in the LD task

In close stimuli separation sessions, a higher percentage of animals in $C3^{-/-}$ and $C3aR^{-/-}$ groups were able to reach criterion, and there was a trend towards both C3 and $C3aR^{-/-}$ achieving a greater number of criteria per session than did WT subjects. Results also indicated that C3 and $C3aR^{-/-}$ animals made more correct responses in the trials preceding their first

criterion than did WT animals. This pattern of data suggests that these subjects were better at discriminating closely separated stimuli. In support of my hypothesis, this suggests improved pattern separation in C3 and C3aR deficient mice, consistent with their elevated levels of AHN.

In these analyses, only C3aR$^{-/-}$ reached statistical significance in comparison to WT however, with C3$^{-/-}$ subjects showing intermediate levels of performance in between that of WT and C3aR$^{-/-}$. Statistically, the LD task is complex to analyse due to the inclusion of three groups, two time points and two stimulus separation conditions. Furthermore, analyses may not have been sensitive enough to detect differences in the face of consistent cross-over interactions, which were seen in both C3 and C3aR$^{-/-}$ subjects between the first and last sessions of each separation condition (as seen in Figure 4.15, A,B,C and D). Due to this pattern of data, significant interactions and main effects of the session variable may have been lost due to the values cancelling out. Furthermore, the relatively small final N may have compromised the results. However, given the presence of significant effects in the C3aR$^{-/-}$ group, which had the smallest N, this suggests a large effect size and reasonable power in the analyses. Nonetheless, follow up experiments will try to replicate these data with a larger cohort of animals.

It is interesting to note that C3aR deficient animals required a greater number of trials to reach criteria during the intermediate stimuli separation training than did C3 deficient mice. This is a surprising result given their superior performance on close stimuli separation probe trials, which is a more difficult discrimination. This may be explained by the idea that the benefit of increased AHN may vary according to task demands, and may actually compromise performance on easy tasks due to over-generalisation of responses (Clemenson et al., 2015).

4.4.9 C3$^{-/-}$ mice showed an altered approach to the LD task, and a perseverative response tendency

Despite the aforementioned trend towards better performance by C3$^{-/-}$ subjects in the close stimuli separation relative to WT, they required significantly more trials to reach their first criterion than did WT or C3aR$^{-/-}$. One possible interpretation of this result is that the benefit of elevated AHN on pattern separation, and thus task performance, was partly jeopardised by the strategy used by C3$^{-/-}$ animals to perform the task. Results indicated a perseverative response tendency in C3 deficient subjects, who required a greater number of trials after reaching criterion to attain another than did WT or C3aR$^{-/-}$ subjects. This may explain their increased number of trials to first criterion, as they may have needed more trials to correct an incorrect response, even in the run up to their first criterion. Furthermore, analyses pertaining to the manner in which responses were made suggested that C3$^{-/-}$ subjects approached the task in a differing manner to other genotypes. Response latency data showed that C3$^{-/-}$ subjects were less hesitant in making responses, regardless of whether they were correct or incorrect. They also made significantly more ITI touches than did C3aR$^{-/-}$ or WT subjects. This may suggest that C3$^{-/-}$ subjects were somewhat 'impatient' or impulsive in their responding, but were still able to perform the task better than WT animals on most measures, but not as well as C3aR$^{-/-}$ subjects.

Contrary to previous reports and my hypotheses, the observation of perseverative responding in C3$^{-/-}$ subjects suggests the possibility of impaired reversal learning or cognitive flexibility in the absence of C3. Methodological differences between past and present studies may explain this difference. Using young adult C3$^{-/-}$ mice, Perez-Alcazar et al. (2013) tested spatial reversal learning within the home-cage environment, within which it is difficult to disentangle purely cognitive effects from the surrounding social milieu. Furthermore, Shi et al. (2015) used the MWM, which is aversive in nature. It is possible that cognitive flexibility is

differentially affected or modulated by the nature of the cognitive task and whether it is appetitive or aversive.

Furthermore, the fact that I did not observe any significant perseveration in the responses of C3aR deficient animals suggests that this behaviour is not due to C3a/C3aR signalling. C3 deficiency has broader effects upon neuronal networks than merely impacting upon the number of new neurons present in the adult DG. As discussed in Section 3.1.2, the classical complement cascade plays an important role in synaptic pruning and refinement, and consequently adult C3 and C1q deficient animals show an excess of synapses (Chu et al., 2010; Stevens et al., 2007) and altered functionality of neuronal networks (Perez-Alcazar et al., 2013). Therefore it is possible that this mechanism, dependent on C3b/CR3 signalling, may be responsible for the impaired reversal learning observed in C3 deficient mice.

4.4.10   The effect of practice varied between genotypes

The LD task also revealed other altered facets of cognition; there were distinctive effects of practice that were dependent on task difficulty, and varied between genotypes. Previous testing usually has a beneficial impact upon subsequent performance. However, in the close stimuli separation condition, performance related measures (Figure 4.15 A-D) suggest that WT animals found the discrimination so difficult that practice did not confer them any benefit. Their performance on the last session of the close condition was therefore comparable to their performance on the first session. In the far separation condition however, WT subjects improved considerably between first and last sessions. Again, this pattern of results suggests that our task was sensitive to changes in AHN, since the control group were at floor level in the condition requiring pattern separation.

Interestingly, practice effects deviated between the C3 and C3aR$^{-/-}$ models. C3$^{-/-}$ subjects improved their performance considerably between the first and last session of the close stimulus condition, and they consistently outperformed the other two genotypes on the last session of the close separation condition. Paradoxically, despite superior performance on the first session of the close discrimination, C3aR$^{-/-}$ mice showed a large decrement in their performance on the second session of the close discrimination. The sessions occurred on two consecutive days, and the possibility of physical exhaustion is negated by the fact that their trial number remained consistent on both days (see Figure 4.15H). It is difficult to name a psychology that may underlie this result, although it may be related to altered habituation to recently acquired patterns of stimuli (Sanderson and Bannerman, 2012), but this is a possibility that requires further investigation.

4.4.11 Methodological considerations

The use of touch screen testing in rodents is known to be technically challenging. In the LD task in particular, mice are known to display variable performance as well as complete fewer trials than rats (Hvoslef-Eide et al., 2013). This is evidenced by the need to exclude some subjects from the task due to their inability to reach criterion within the parameters used (as detailed in Section 4.3.7). Moreover, this meant group sizes fell below optimum, in addition to the added complication of fatalities in the C3$^{-/-}$ group.

Furthermore, a methodological difficulty with this task is that if a subject does not reach criterion within a session, data regarding the number of trials to criterion is not generated. Therefore, the number of trials until the end of session must be used in substitute of this information. In future, allowing a longer testing session of up to 60 minutes, as recommended in the published LD task protocol, could avert this problem (Hvoslef-Eide et al., 2013).

However, considering that from beginning to end, the LD task featuring 20-minute daily sessions for each subject took four months to complete, it would not have been possible to use the longer session duration due to time constraints. However, this has been tested with other knockout strains in our laboratory, and no significant increases in the number of criteria achieved were noted, despite increased session duration. Therefore, the current data is likely to be reflective of the true ability WT and C3/C3aR deficient mice. Furthermore, this data shows that the LD task was effective in manipulating task difficulty, and the finding of improved pattern separation in C3 and C3aR deficient animals suggest that the task was sensitive to changes in AHN.

4.4.12 Future work

The next step in this line of work will involve histological analyses of the present experimental cohort, and will correlate DCX cell counts in the DG with pattern separation performance on a case-by-case basis. Pharmacological interventions could also be used to back up the results of the genetically modified strains used. Testing pattern separation and anxiety both before and after administration of C3aRA SB290157 (Ames et al., 2001) to WT animals may prove a more feasible option, which would hopefully mimic the effects seen in the constitutive C3aR$^{-/-}$ model.

Future work will aim to provide further evidence for improved pattern separation in the absence of C3/C3aR using complementary behavioural paradigms. For example, an open field pattern separation task has been developed by Bekinschtein et al., (2013) based on the spontaneous location recognition task originally reported by Ennaceur, Neave, & Aggleton (1997). The task has been modified to place varying demands on pattern separation. Within an open field surrounded by wall mounted spatial cues, a rodent is exposed to three identical objects during the sample phase, two of which are close together and one is placed further away (Figure 4.17). In order to vary

the load placed on pattern separation at the encoding phase, two of the objects are either in close proximity to each other (e.g., 50° angle, close separation), or are situated further apart (e.g., 120° angle, far separation). After a 24-hour delay, animals are reintroduced to the arena, containing two of the previously encountered objects. However, one object is repositioned to occupy a space in a novel location between and equidistant to the location of the previously close-together items. The animals' exploration time is then measured during the test phase. If an animal has successfully encoded and 'separated' the memory of the proximal items locations, then it should show a preference for exploring the novel location. Bekinschtein et al. (2013) have demonstrated that this is a valid test of pattern separation, as blocking adult neurogenesis via lentiviral inhibition of Wnt signalling impaired performance on the highly similar, close separation condition, but not when items were in dissimilar, distal locations. Amongst the advantages of this paradigm are exploitation of the natural exploratory response to novelty and thus minimal requirement for training. Furthermore, the task manipulates pattern separation demands during the encoding phase of the task, which is when the computational process of pattern separation is thought to occur (Bekinschtein et al., 2013).

Future work will also investigate other aspects of cognition these results have suggested may be altered by C3/C3aR signalling. An advantage of the touchscreen operant platform I have used to conduct the LD task is that a variety of other cognitive tests (including tests of attention, impulsivity and reversal learning) are available for this system, and can be implemented within the same testing environment in an automated manner (Hvoslef-Eide et al., 2013; Talpos, McTighe, Dias, Saksida, & Bussey, 2010). Furthermore, another attractive line of investigation is to repeat this battery of behavioural tests with aged cohorts to assess age-dependent cognitive decline. It has previously been documented that $C3^{-/-}$ mice do not show the normal rate of cognitive decline (Shi et al., 2015). It would be interesting to determine whether $C3aR^{-/-}$ mice show a similar phenotype, and if so, whether these changes are attributable altered AHN.
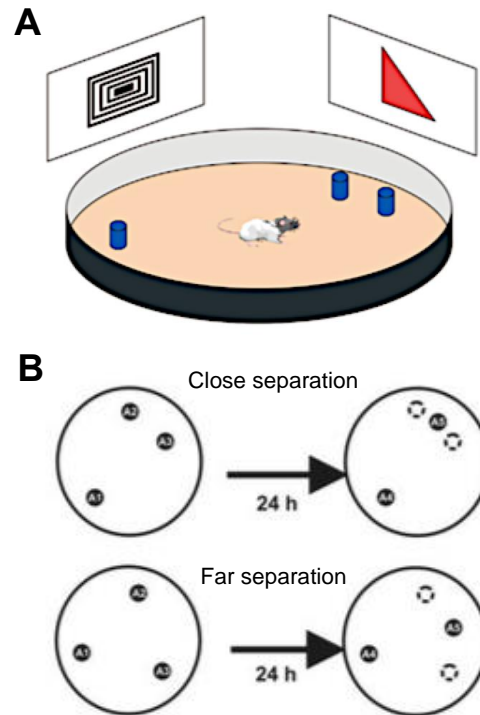
Figure 4.17. Spontaneous location recognition (SLR) task. The rodent is placed in an open field with distal spatial cues, containing three identical objects. A pair of objects are placed close together, and one object is placed in isolation to the others. In order to manipulate pattern separation, the distance of the pair of objects is changed between acquisition and probe trials. The animals exploration of the displaced versus static objects is recorded. Images adapted from Bekinschtein et al., (2013).

4.4.13 Concluding remarks

In this chapter, I have shown that C3 and C3aR deficient subjects have enhanced fine pattern separation, consistent with their elevated levels of AHN. This supports the emerging literature suggesting that the immune system can exert a broad range of effects upon cognition (Pugh et al., 2001; Kipnis et al., 2012). Furthermore, the LD task revealed other potentially altered facets of cognition in the absence of C3, including cognitive flexibility and impulsivity, which will be addressed in future work. Intriguingly, C3aR$^{-/-}$ was highly anxiogenic in the elevated plus maze and open field, where as C3$^{-/-}$ was anxiolytic in the open field paradigm. This demonstrates a novel role for C3a and C3aR in the mediation of anxiety, although it is unlikely that this is a correlate of enhanced AHN.

5.   General Discussion

5.1 Overview

New neurons are constantly added to the DG throughout adult life, a process which supports episodic memory formation and successful retrieval (Kempermann, 2004). AHN is thought to have evolved to allow organisms to flexibly learn and therefore adapt to novel environments (Kempermann, 2012). As such, the process of AHN is exquisitely regulated by a myriad of factors that convey macroscopic behavioural-level conditions to NPCs via network level changes, which then impact upon the process of neurogenesis at molecular and cellular levels (Aimone et al., 2014). Much regulation impinges upon the survival of newborn neuronal progenitors and immature neurons, as opposed to early stem cell proliferation (Dayer et al., 2003; Kuhn, 2015). This is of significance to the net level of neurogenesis, increases in which have been associated with performance improvements in cognitive tasks that challenge pattern separation (Clelland et al., 2009). Of the select population of immature neurons that survive, a period of drastic morphological change occurs during which GC morphology and synaptic profile is developed. Dendritic branches are functional units that may be needed for memory storage (Govindarajan et al., 2011), and the extent of dendritic arborisation affects the integration, connectivity and ultimate functionality of newly born neurons within the hippocampal network (Llorens-Martín et al., 2016). The factors controlling this stage of development are less well understood than those overseeing the earlier milestones of neurogenesis however. Nonetheless, the continual regulation of the many facets of AHN allows constant structural plasticity and network remodelling throughout life, in line with environmental demands.

The immune system has emerged as a critical regulator of AHN, through both cell-cell interactions and secreted molecules, including complement. This system lies at the heart of innate and adaptive immunity, and our

understanding of its function has been revolutionised within the last decade. It is now regarded as a vital participant in several non-immune, homeostatic and regenerative processes within the CNS (Mastellos, 2014). While the activation of complement was traditionally regarded as restricted to pathogenic or pathological contexts, it is now recognised that there is a consistent, albeit low level of complement activation within the CNS due to spontaneous C3 and C1 tickover (Manderson et al., 2001; Nataf et al., 1999). These processes may allow complement to exert regulatory effects within the CNS (Orsini et al., 2014).

Complement has been implicated in regulating AHN under physiological conditions via the central component, C3 (Moriyama et al., 2011; Rahpeymai et al., 2006). However, the mechanisms through which complement acts on AHN required greater clarification, and I therefore investigated the role of C3/C3aR signalling with regard to the developmental milestones of AHN. C3 is also involved in maintaining normal neuronal morphology (Lian et al., 2015) and conducting developmental synapse elimination (Stevens et al., 2007), although to date these processes have been documented in embryonic and early postnatal hippocampal neurons only (Lian et al., 2015). The DG is not morphologically formed until postnatal day 7, and until then neurons are unlikely to be representative of adult born GC neurons (Namba et al., 2005). Therefore, I speculated that such mechanisms would be well suited to mediate to the constant structural remodelling required in the DG, and therefore investigated their relevance to AHN.

5.1.1   C3aR regulates AHN and newborn neuronal morphology via distinct pathways

Previous studies of C3 breakdown products C3a and C3d suggested opposing roles for these molecules in regulating AHN. C3a was shown to exert a pro-neurogenic effect on newly born neurons within the adult DG through C3aR, (Rahpeymai et al., 2006), whereas C3d signalling via CR2 had an anti-

proliferative effect on newly born DCX expressing neurons *in vivo* (Moriyama et al., 2011)*.* Using both C3^{-/-} and C3aR^{-/-} mice, my results demonstrate a clear regulatory role for C3/C3aR signalling in regulating AHN. In contrast to a previous report by Rahpeymai et al. (2006), I observed a significant increase in the number of DCX^{+} immature neurons in the DG of C3^{-/-} mice, and a strong trend of similar magnitude in C3aR^{-/-} mice. Both strains had significantly increased GCL volume compared to WT, suggesting that the increase in immature neurons is not transient, and instead leads to elevated neurogenesis. Furthermore, due to the observation of equivalent phenotypes between the two strains, these data suggest that C3d/CR2 does not regulate AHN since C3d signalling is intact in the C3aR^{-/-} mouse. Therefore, this project suggests that C3/C3aR signalling is anti-neurogenic under physiological conditions, and may discourage either neuronal-lineage adoption, or the survival of immature neurons. As discussed in Section 2.4.8, further experiments will attempt to distinguish these possibilities.

I also examined the morphological characteristics of immature DCX^{+} neurons in the adult brain using Sholl analysis (Sholl, 1953). In the absence of C3aR, these cells had less complex morphology, reflected in decreased ramification and neurite length, than those in the brains of WT or C3 deficient mice. In agreement with previous report by Lian et al. (2016), this suggests that C3aR is important for normal neurite outgrowth and dendritic arborisation and extends this mechanism to adult born neurons.

These data also suggest that the role of C3aR upon morphology is not mediated by C3. The only known alternative ligand for C3aR is the recently discovered VGF-derived peptide TLQP-21 (Cero et al., 2014; Hannedouche et al., 2013). VGF has been implicated in neuronal development (Synder et al., 1998) and is expressed in adult hippocampal GCs from soon after their formation in the postnatal brain (Synder et al., 1998). VGF expression is itself activity-dependent (Salton et al., 1991) and is also induced by neurotrophic factors including NGF and BDNF (Ferri et al. 2011), the latter of which is integral to activity-dependent regulation of AHN (Waterhouse et al., 2011; Ge

et al., 2007). These characteristics of VGF make it ideally suited to participate in the regulation of AHN. Indeed, VGF has been implicated in regulating AHN as a downstream signal of BDNF (Thakker-Varia et al., 2007). The functions of TLQP-21 are less well understood due to its recent discovery, although initial research suggests pleiotropic roles in the stress response, metabolism and nociception, amongst others (Cero et al., 2014; Hannedouche et al., 2013). Though I have not yet investigated the involvement of this pathway experimentally, I suggest that TLQP-21 is a probable candidate in modulating C3aR dependent effects on newborn neuron morphology.

Due to the relatively late discovery of diverging C3/C3aR effects within the timescale of this project, I was unable to experimentally test the possibility of VGF/C3aR mediated effects. Follow up experiments will first test for VGF mRNA expression in WT primary hippocampal cultures, followed by ELISA for TLQP-21 protein. I then aim to characterise AHN and the behavioural phenotype of VGF knockout mice. Despite this missing link, and the possibility that yet more undiscovered C3aR ligands may exist, VGF and TLQP-21 seem highly likely candidates in the mediation of the effects observed.

Therefore, this body of work suggests a novel mechanism through which C3aR regulates AHN; anti-neurogenic effects are mediated via the canonical C3a/C3aR pathway, and I tentatively propose that the TLQP-21/C3aR pathway modulates the dendritic maturation of newborn neurons (see Figure 5.1). Interestingly, there is potential for interaction to occur between these pathways via microglia and astrocytes. C3a can stimulate NGF expression in both cell types via C3aR (Heese, Hock, & Otten, 1998; Jauneau et al., 2006; Sayah et al., 2003). It is this neurotrophic factor that has been shown to potently induce VGF expression, which is the peptide precursor for TLQP-21 (Ferri et al., 2011). In principal, these pathways could work together to simultaneously inhibit differentiation or survival of immature neurons and promote the maturation of already established immature GCs. Such selective elimination and survival of newborn neurons has been

demonstrated to be necessary for hippocampus-dependent cognition (Dupret et al., 2007).

In order to begin testing this hypothesis, I will first examine neuronal morphology in WT hippocampal cultures in each of three treatment conditions; cobra venom factor, which depletes C3a (CVF; Wu et al., 2016); VGF-neutralising antibody, or C3aRA SB290157. Should my hypothesis be true, one would expect to see similarly altered morphology in the presence of SB290157 and the VGF-neutralising antibody, but normal morphology in cultures treated with CVF. Furthermore, the potential role for microglia could be tested *in vitro* through microglial depletion. This can be achieved using a saporin-conjugated anti-CD11b monoclonal antibody known as MAC-1-SAP. This approach has proven successful for microglial depletion from primary rat hippocampal cultures in our laboratory (Nunan et al., 2014). This experimental design would show whether VGF/TLQP-21/C3aR binding was mediated by C3a induction of microglial NGF.

Furthermore, there is scope for crosstalk with several other factors that are important for regulation of AHN. For example, VGF expression is also induced by BDNF (Ferri et al., 2011). Many studies have demonstrated that BDNF promotes dendritic maturation of adult born neurons in the DG (Horch & Katz, 2002; Tolwani, Buckmaster, Varma, & Cosgaya, 2002; Waterhouse et al., 2012). It has been suggested that VGF mediates the downstream effects of BDNF (Thakker-Varia et al., 2007), a hypothesis that would fit with my observation of impaired dendritic development in the absence of C3aR, should this effect be VGF dependent.
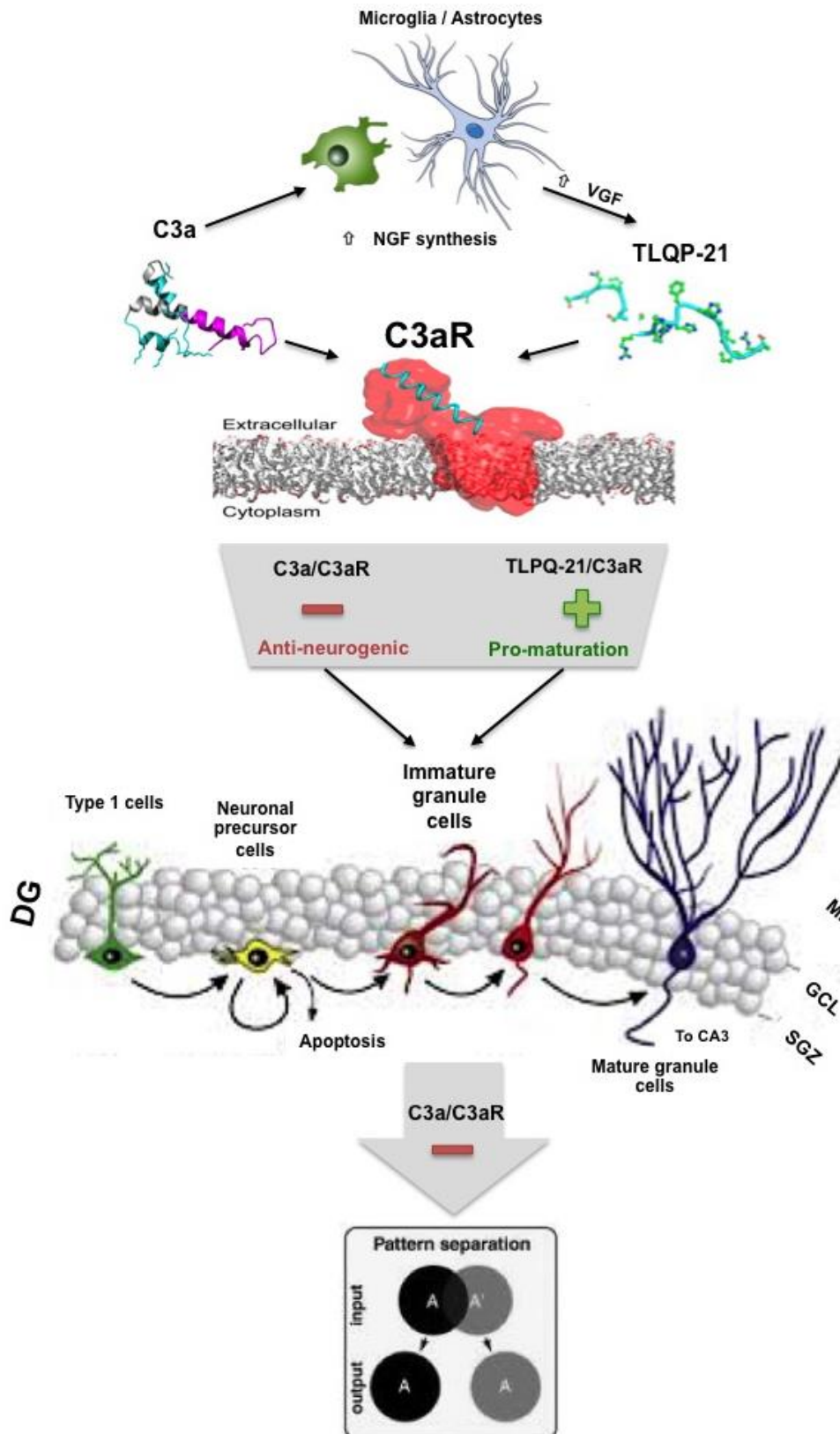
Figure 5.1 Proposed mechanism for C3aR dependent regulation of AHN and newborn neuronal morphology via C3a and VGF-derivative TLQP-21. C3a/C3aR signalling exerts an anti-neurogenic effect on immature neurons in the adult DG, which may have detrimental functional consequences for the ability of these cells to perform pattern separation. I also propose that TLQP-21/C3aR provide pro-maturation signals to the same population of immature neurons, the functional consequences of which are unknown. These pathways may interact. C3a induces NGF expression in microglia and astrocytes via C3aR, which in turn stimulates production of VGF.

5.1.2   Dissociations between C3/C3aR knockout models

In addition to the difference between C3aR$^{-/-}$ cells and C3$^{-/-}$ cells in terms of morphology, I observed several other interesting dissociations between C3 and C3aR deficient models. Behaviourally, there was a dramatic difference in the anxiety phenotype of C3 and C3aR deficient animals. Furthermore, I documented a unique perseverative and potentially impulsive phenotype of C3$^{-/-}$ mice, which was absent from C3aR$^{-/-}$ subjects. Moreover, C3aR deficiency seemed to alter habituation and the effect of practice within the spatial working memory paradigm used. These results suggest considerable divergence of C3 and its canonical receptor, C3aR.

In agreement, a previously unforeseen complexity in the functionality of C3a is now being acknowledged in the literature (Coulthard & Woodruff, 2015). C3a is often regarded as purely pro-inflammatory, due to being grouped conceptually with C5a. However, it is rapidly emerging that the actions of C3a are nuanced and highly dependent on cell type and context. However, much remains to be understood. Similarly, the ligand binding, and therefore the signalling of C3aR remain poorly characterised. This is in part due to its unusually large second extracellular loop (Gao et al., 2003; Hannedouche et al., 2013), the observation of which originally led speculation that other ligands may exist for C3aR (Gao et al., 2003). This received experimental confirmation in 2013, with the report of Hannedouche et al. (2013) confirming TLQP-21/C3aR binding in the CHO-K1 cell line.

While this interaction may explain phenotypes that were observed in C3aR, but not C3 deficient animals, there are other possible pathways that may explain phenotypes seen in C3 but not C3aR deficient animals that are independent of C3aR. These include C3a-desArg/C5aR and C5L2 mediated effects. The time window in which C3a is an intact molecule is limited, supposedly to limit its capacity for self-damage (Coulthard & Woodruff, 2015). Therefore, C3a is rapidly inactivated to the C3a des Arg form. It is however still able to modulate pro-inflammatory cytokines including TNF-α

(Takabayashi et al., 1996), although much of its functionality remains unknown. C3a des Arg binding to C5aR and C5L2 has been documented (Kalant et al., 2005). Potentially, this could underlie effects seen in C3$^{-/-}$ animals that are not seen in C3aR$^{-/-}$ animals, as C3a des Arg and C5aR/C5L2 are preserved in the latter. Furthermore, another potential factor that may interact with C3a through an unknown receptor, is the chemokine SDF-1. Interestingly, this molecule can either promote or inhibit NPC migration depending on C3a concentration (Shinjyo et al., 2009). Moreover, SFD-1 is co-released with GABA from niche interneurons (Masiulis et al., 2011) and can sensitise type 2 NPCs to GABAergic signals (Bhattacharyya et al., 2008). This mechanism may therefore contribute to activity-dependent regulation of AHN, and the effects of it may depend on local complement C3a expression. However, this remains speculatory but may nonetheless be an interesting future direction. Therefore, my results are in line with the evolving body of literature that is broadening our knowledge of C3a and C3aR.

5.1.2   C3/C3aR regulation of AHN is of functional relevance to cognition

The function of the DG in performing pattern separation is affected by net levels of AHN (Clelland et al., 2009; Creer, Romberg, Saksida, van Praag, & Bussey, 2010). The effect of newborn neuronal morphology is difficult to quantify in this regard, although is likely to have important consequences upon the connectivity of the region, and may therefore be expected to impact upon function. Therefore, I tested the ability of C3 and C3aR deficient animals to make discriminations that required pattern separation. C3 and C3aR deficient animals were superior at discriminating closely separated spatial locations, suggesting enhanced pattern separation. The LD task has been shown to be sensitive to changes in both increased (Creer et al., 2010) and decreased AHN (Clelland et al., 2009), which specifically improve or impair

discrimination of the close stimuli separation condition, respectively. Therefore, it is likely that the improved pattern separation shown by C3 and C3aR deficient animals is attributable to their elevated levels of immature DCX$^+$ cells. Thus, the C3 mediated cellular-level changes observed were of functional relevance in augmenting the ability of newborn neurons to perform fine pattern separation. This demonstrates that the negative regulatory role played by C3/C3aR in the healthy brain is also detrimental to the functioning of newborn neurons in performing fine pattern separation (see Figure 5.1).

However, the deficit in newborn neuron morphology did not compromise the pattern separation abilities of C3aR$^{-/-}$ mice, suggesting that in terms of functionality, the overall number of immature neurons takes precedence over their morphology. This is perhaps surprising given that differences were observed in the suprapyramidal blade, where immature neurons are preferentially recruited by spatial learning (Chawla, Guzowski, & Amaya, 2005; Snyder et al., 2009). However, there is age-dependent involvement of immature neurons in hippocampal learning (Nakashiba et al., 2012). I used DCX immunohistochemistry as a surrogate marker of newborn neurons, and this protein is expressed for two to three weeks after neuronal-lineage commitment (Zhao et al., 2006). Therefore, I likely sampled a broad age-range of immature neurons, and it may be that those displaying impaired morphology were not yet of the age where their participation in spatial tasks is crucial.

5.1.3 AHN and C3/C3aR signalling as neurobiological substrates of altered anxiety

Due to the potential involvement of AHN in affective processes (Kheirbek & Hen, 2014; Strange et al., 2014), I also investigated anxiety in C3 and C3aR

deficient animals. An interesting phenotype emerged in the elevated plus maze and open field paradigms, whereby C3aR was profoundly anxiogenic in both paradigms, and C3 was mildly anxiolytic in the open field. These results suggest a novel role for C3/C3aR in the mediation of anxiety.

Currently, our knowledge regarding the impact of altered AHN on anxiety lacks clarity, and there have been many conflicting reports (Hill, Sahay, & Hen, 2015; Marques et al., 2016; Revest et al., 2009). As both C3 and C3aR deficient animals showed increases of a comparable magnitude in AHN, it is improbable that the anxiety phenotypes observed are solely related to AHN. However, in the C3aR$^{-/-}$ strain, it is possible that any potential anxiolytic benefit of C3a/C3aR mediated-increases in AHN were negated by the morphological deficits seen in these newly born neurons. This is difficult to test experimentally however. Moreover, it is likely that the mutation affects many other brain circuits, which are beyond the scope of this current project, but nevertheless may contribute to the behaviours examined.

These data suggest that complement mediates anxiety, but this may not be through direct interaction between C3 and C3aR, since the two knockout strains displayed opposing phenotypes. These effects may instead be mediated by other ligands for C3aR, or receptors for C3a. Interestingly, VGF has also been implicated in affective processes, and shows downregulation in the hippocampus when animals are exposed to stress (Thakker-Varia et al., 2007). Therefore the prevention of TLQP-21 binding via C3aR could play a roll in the profoundly anxiogenic phenotype of C3aR$^{-/-}$ mice. VGF has also been reported to have anti-depressant properties (Thakker-Varia et al., 2007). In future experiments, the anxiety phenotype of VGF deficient mice could therefore be examined, as well as the consequences of intra-hippocampal infusion of VGF on anxiety measures in WT animals.

An important point to consider is to what extent the observed behavioural outcomes can be linked to changes in AHN. For reasons already discussed, it

is likely that improved pattern separation in C3 and C3aR deficient mice is attributable to their increased levels of AHN. On the other hand, it is unlikely that the anxiety phenotype observed is a product of increased AHN. However, it is acknowledged that these results are correlative, not causative. Follow up histological analyses of the experimental cohort will attempt to correlate DCX$^+$ cell counts with pattern separation ability, which will provide greater insight into how closely linked pattern separation and C3/C3aR mediated increased in AHN are. I also intend to repeat these behavioural experiments using WT animals treated with C3aRA antagonist, which will provide a degree of causal evidence regarding the involvement of the C3aR. However, in order to establish causative evidence linking AHN to our behavioural results, the ideal design would utilise an inducible, conditional knockout of C3/C3aR specifically in the newborn neurons of the adult DG. While an attractive option, such a model does not currently exist and would be costly to produce.

5.1.4 The regulatory effects of C3/C3aR on AHN depend on the environment

I also investigated the capacity for C3/C3aR signalling to regulate neurogenesis in culture. Previous *in vitro* studies investigating either C3a/C3aR or C3d/CR2 signalling have used cell types which were not relevant to AHN, either through use of whole mouse brain progenitor cells, which disregard the unique aspects of the hippocampal niche, or through use of neurosphere cultures subjected to many passages and high selection. While the latter creates a relatively pure NSC population, it discounts the important influence of other cell types on NPCs, such as microglia and astrocytes (Reynolds & Rietze, 2005). Furthermore, it is unclear from previous *in vivo* studies whether the purported effects of complement are mediated via direct interactions with the cells that constitute the neurogenic niche, as opposed to the many peripheral factors that intervene in whole

organisms. I therefore used an *in vitro* model of AHN to investigate whether C3/C3aR signalling exerts direct effects upon the survival, proliferation, fate choice and maturation of NPCs within a defined environment. Primary cultures were generated from the postnatal hippocampus, and maintained for up to 14 days. These cultures consisted largely of NPCs and their progeny, however other cell types have also been shown to be present in this paradigm, including microglia, astrocytes, endothelial cells and oligodendrocytes (Babu et al., 2007; 2011; Howell et al., 2003; Zaben et al., 2009).

The result I obtained again suggest that C3/C3aR signalling can regulate the process of AHN, and the use of a controlled culture environment permits the conclusion that this regulation takes place between NPCs and other cell types found in the hippocampal niche. However, I observed different effects to those seen in my *in vivo* experiments. *In vitro,* the absence of C3/C3aR signalling caused a phenotypic shift in the culture population towards type 1 radial glia, and increased their proliferation. This may be via complement-mediated effects on division symmetry. The consequence of this was temporarily declined levels of subsequent cell types, although this was restored after 14DIV, suggesting it may be an artefact of a culture system heavily dependent on growth factors. I also observed that despite a decrease in the number of TUJ1$^+$ neurons at 5DIV, their morphology was significantly more complex in the absence of C3aR. This again suggests a direct role for C3aR in modulating the morphology of adult born neurons.

The differences between these results and those observed *in vivo* suggest that the regulation of AHN and neuronal morphology by complement is heavily dependent on the environment. While cells in culture still make cell-cell contact, and receive autocrine and paracrine signals, the principal difference between the *in vitro* and *in vivo* contexts is the lack of surrounding cytoarchitechture. Within the neurogenic niche, type 1 radial glia have been shown to guide neuronal progenitors in the GCL as they differentiate

(Shapiro, Korn, Shan, & Ribak, 2005), and astrocytes sitting immediately outside the GCL support synaptogenesis and dendritic maturation (Toni & Sultan, 2011). These principles clearly do not apply within monolayer cultures. An alternative approach that may circumvent this issue in future would be to examine AHN and neuronal morphology in hippocampal slice cultures, which preserve the cycoarchitechture that is so important for maintaining normal AHN.

Furthermore, the finding that the regulatory effects of complement vary based on the environment is perhaps not surprising given the diverse array of immune and non-immune cell types that complement interacts with, many of which also regulate AHN. For example, complement interacts with both T cells and mast cells (Ricklin et al., 2010; Strainic et al., 2008), which are known to modulate AHN (Nautiyal et al., 2012; Ziv et al., 2006). C3a can also regulate IL-1β and TFN-α (Takabayashi et al., 1996) which again impact upon AHN (Koo & Duman, 2008; Widera et al., 2006). C3 also interacts with astrocytes (Sayah et al., 2003), endothelial cells (Wu et al., 2016), and can activate microglia (Ramaglia et al., 2012). Although microglia were present in our cultures at low levels, I assume that many of these other cell types and molecules are absent from the culture system. Low levels of microglia may also explain why I did not observe changes in synapse density in the absence of C3, as the synaptic pruning mechanism has been proposed to be microglia-dependent (Schafer et al., 2012). Therefore, both the lack of cytoarchitechture and complement-responsive cell types may explain the differences in the *in vitro* and *in vivo* paradigms used. However, the fact that I observed effects in culture in absence of the aforementioned factors does suggest that C3/C3aR may be able to affect NPCs directly, perhaps via direct C3a binding to NPC C3aR, which has been demonstrated previously by Shinjyo et al. (2009).

5.2 Methodological considerations regarding C3$^{-/-}$ and C3aR$^{-/-}$ animals

The use of constitutive germ line knockout models mean that the mutations likely impact upon many aspects of physiology, both within the CNS and periphery. For example, due to the role of C3 in developmental synaptic pruning, it is difficult to attribute the phenotype of the C3$^{-/-}$ model entirely to changes in AHN, in confidence that this is not related to their altered synaptic phenotype, which appears to affect the CNS from the early postnatal period (Stevens et al., 2007). Furthermore, the mutations are present from birth, and therefore it cannot be concluded that the effects observed are due to immediate involvement of the gene in the measured behaviour or cellular phenotype. It is equally possible that the mutation may impact upon distant factors such as early postnatal rearing or stress reactivity, which may carry over to later cognitive and affective phenotypes measured in adulthood. This is especially the case since the strains used were bred in homozygous colonies, and pups were therefore were reared by mutant mothers. Maternal behaviours have been shown to impact upon adult anxiety and stress reactivity (Priebe, Brake, & Romeo, 2005). With regard to the profound anxiety phenotype seen in the C3aR$^{-/-}$ model, this may alter mother-litter interactions and social interactions throughout development. One way to address this issue would be through the generation of heterozygous breeding colonies, to eventually attain homozygous and WT littermates. This was not possible during this project due to time-constraints and experimental practicalities. The additional manipulation of cross-fostering experiments would also allow us to temporally distinguish adult phenotypes from rearing-induced changes.

With these limitations in mind, I am confident that the use of genetically manipulated models is of value in investigating complement-mediated regulation of AHN. There are several advantages of this approach over pharmacological alternatives. Firstly, murine C3a is not available commercially and is difficult to isolate in the laboratory. Therefore,

commercially available C3a tends to be human in origin, and despite considerably homology to murine C3a, it is unknown whether binding to murine C3aR is of identical consequence. Furthermore, C3a is rapidly degraded upon thawing, making it impractical and cost-ineffective with frequent experimental use. Furthermore, some doubt surrounds the validity of the C3aR antagonist SB290157 originally described by (Ames et al., 2001), as it has been reported to have agonist activity in certain cell types (Mathieu et al., 2005; Therien, Baelder, & Köhl, 2005; Woodruff & Tenner, 2015). Therefore, the use of genetic manipulations has proved a valid and efficient method of investigating complement regulation of AHN.

5.3 Future directions

Complement is also involved in the genesis and sequela of various neuropathologies (Orsini et al., 2014). In the case of injury, molecules released from apoptotic and/or necrotic cells within injured tissue are potent activators of complement (Bellander, Singhrao, Ohlsson, Mattsson, & Svensson, 2001; Cowell, Plane, & Silverstein, 2003). Therefore, a recurrent theme in the literature is the rapid, uncontrolled activation of complement in response to disease or injury, the ensuing inflammation thereby propagating pathology (Orsini et al., 2014). This is juxtaposed against the body of literature this project has focused on, which instead portrays complement as essential for homeostatic and developmental processes within the brain (Veerhuis et al., 2011). Thus, the notion of complement as a 'double-edged sword' is highly appropriate (Orsini et al., 2014; Ricklin et al., 2010; Veerhuis et al., 2011).

The role of complement in the pathogenesis of mTLE
In particular, complement has been shown to be upregulated in the epileptic brain and may contribute to epileptogenesis. Pasinetti, Johnson, & Rozovsky,
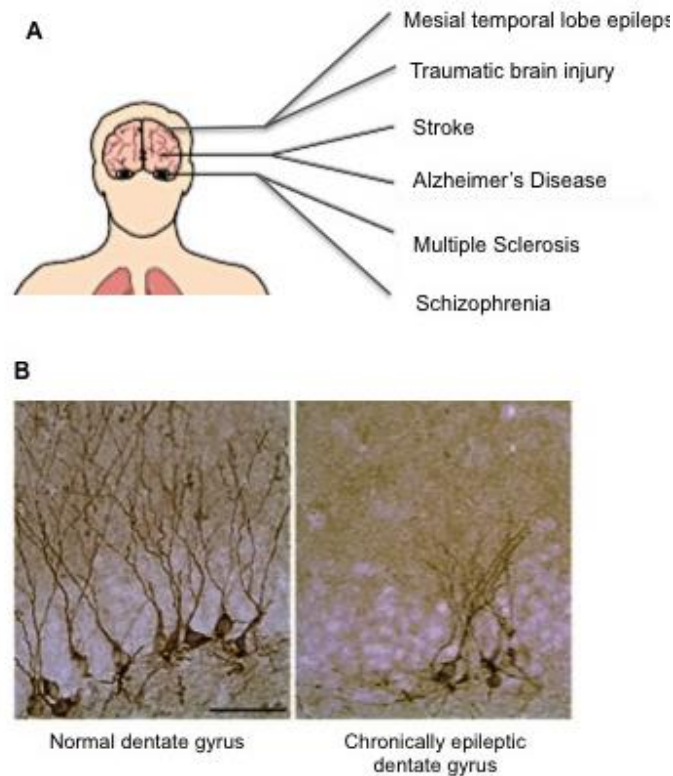
Figure 5.2 Involvement of complement in neuropathology. **A)** Complement related neuropathologies. Image adapted from Ricklin & Lambris, (2007). **B)** Severely declined adult hippocampal neurogenesis in an experimental model of chronic seizures. Image sourced from Shetty & Hattiangady (2007).

(1992) first documented an increase in C1q mRNA within CA3 pyramidal cells after systemic administration of convulsant kainic acid (KA) in rats, an observation that was replicated by Morita, Suzuki, Mori, & Yasuhara in 2006. Immunoreactivity was witnessed within CA1 and CA3 pyramidal neurons and also in microglia. Furthermore, C3 expression in hippocampal pyramidal neurons coincided with DNA fragmentation, suggesting a direct link between complement C3 deposition and neuronal death in the epileptic hippocampus. A recent report by Benson et al. (2015) also showed upregulation of complement proteins a rodent model of chronic epilepsy, which persisted 12 months after status epilepticus. This suggests that C3 remains upregulated during the chronic stages of the disease, indicating a sustained inflammatory response.

These observations have been mirrored in human mTLE tissue specimens, which showed occurrence of C3 activation products near areas of cell death (Aronica et al., 2007). This may indicate a benign role of complement, in which opsonisation and phagocytosis are recruited to remove debris from the site of injury. However, the terminal complement component, the membrane attack complex, has been observed within the epileptic hippocampus also (Morita et al., 2006) suggesting a causative role in cell death. This is in line with the observation that the presence of complement regulators is limited within context of brain injury, leading to the possibility that complement activation is poorly controlled within the epileptic brain (Vezzani & Friedman, 2011).

It has been suggested that uncontrolled, sustained neuroinflammation may destabilise neuronal networks and therefore contribute to recurrent seizures (Aronica et al., 2007). Xiong et al. (2003) reported that activation of the terminal pathway, from C5 through to C9 leading to the formation of MAC, consistently evoked seizures in rodents. In several cell types, MAC has been shown to cause influx of Ca^{2+} and Na^{2+} and efflux of K^+, consequently causing depolarization before cell lysis occurs (Xiong et al. 2003). Therefore MAC deposition on hippocampal neurons may stimulate similar depolarization events, which may induce spontaneous firing in synaptically coupled neighbouring neurons, thus leading to seizures. In support of this, C3 activation is correlated with the severity of epileptic seizures in a mouse model of mTLE (Kharatishvili et al., 2013).

Furthermore, this potentially causative role of complement in epilepsy opens up the possibility of pharmacological interventions. Using a variety of models of rodent epilepsy, including pilocarpine and chronic intra-hippocampal kainate, Benson et al. (2015) reported that C5aR antagonist PMX53 provides anticonvulsant effects, with treated animals showing reduced seizure frequency and neuropathology compared to vehicle treated controls.

Complement and AHN in mTLE

As described in Section 1.5.4, seizures are a potent regulator of AHN, and induce a transient surge in proliferation (Bengzon et al., 1997; Parent et al., 1997; Gray & Sundstrom, 1998), followed by a subsequent severe decline in AHN with the onset of chronic seizures (Hattiangady, Reo, & Shetty, 2004). Not surprisingly, mTLE is associated with significant cognitive and affective impairments (Helmstaedter, Kurthen, Lux, Reuber, & Elger, 2003; Illman, Moulin, & Kemp, 2015). In patients, the *ex vivo* proliferative capacity of hippocampal stem cells has been correlated with declarative memory performance (Coras et al., 2010). AHN has therefore received considerable interest as a therapeutic target for restoring learning and memory deficits in mTLE, which remains an unmet therapeutic need (Kuruba & Shetty, 2007; Shetty & Hattiangady, 2007). Treatment of chronically epileptic rats with the anti-depressant fluoxetine has been shown to restore neurogenesis and learning and memory deficits (Barkas et al., 2012), suggesting that AHN is a feasible therapeutic focus. Interestingly, fluoxetine also has anti-inflammatory effects. Since neuroinflammation can be detrimental to AHN (Monje et al., 2003; Ekdahl et al.; 2003), it is likely that the effect was partly mediated by the anti-inflammatory effects of treatment. Therefore, neuroinflammation is likely to contribute to declined AHN and cognitive deficits in mTLE.

This project has demonstrated anti-neurogenic regulation of C3/C3aR signalling under physiological conditions. Several previous studies have shown that whether complement is protective or damaging is concentration dependent (Lian et al., 2015; Petersen et al, 2015). Therefore, It can be speculated that sustained upregulation of C3 in the epileptic brain may exert anti-neurogenic effects of greater magnitude, potentially contributing to the severe decline in AHN seen with chronic seizures. Uncontrolled complement activation may also further propagate seizures (Xiong et al., 2003).

Furthermore, abnormal AHN may be both a cause and a consequence of chronic, recurring seizures. It has recently been shown that the aberrant AHN induced by recurrent seizures may exacerbate and perpetuate epileptogenesis, as ablating neurogenesis prior to seizures prevented development of chronic recurrent seizures (Cho et al., 2015). Therefore it is of great importance that we continue to expand our knowledge of how complement activation may negatively regulate AHN both within the healthy brain and the epileptic brain. A starting point in this line of work will be to assess the impact of chronic seizures on AHN in C3 and C3aR deficient animals, and to assess whether absence of these factors ameliorates abnormal neurogenesis, epileptogenesis and learning and memory deficits.

5.4 Concluding remarks

This work demonstrates that the complement system is a key regulator of AHN and neuronal morphology. I have identified a novel mechanism whereby C3/C3aR signalling exerts an anti-neurogenic effect upon immature neurons born in the adult dentate gyrus. Furthermore, I reported changes in the morphology of newly born neurons, which appeared to be mediated via a separate pathway. The most likely candidate for this is TLQP-21/C3aR signalling, which has only recently been discovered, and therefore requires validation in further experimental studies. Together, these pathways may interact to selectively control the neuronal differentiation or survival of neuronal precursor cells and the dendritic maturation and integration of surviving granule cells. This constitutes a novel-mechanism for the neuroimmune regulation of AHN.

References

Aggleton, J. P., & Brown, M. W. (2006a). Interleaving brain systems for episodic and recognition memory. Trends in Cognitive Sciences, 10(10), 455–463.

Ahmed, A. I., Shtaya, A. B., Zaben, M. J., Owens, E. V., Kiecker, C., & Gray, W. P. (2012). Endogenous GFAP-positive neural stem/progenitor cells in the postnatal mouse cortex are activated following traumatic brain injury. Journal of Neurotrauma, 29(5), 828–842.

Aimone, J. B., Deng, W., & Gage, F. H. (2011). Resolving New Memories: A Critical Look at the Dentate Gyrus, Adult Neurogenesis, and Pattern Separation. Neuron, 70(4), 589–596.

Aimone, J. B., Li, Y., Lee, S. W., Clemenson, G. D., Deng, W., & Gage, F. H. (2014). Regulation and function of adult neurogenesis: from genes to cognition. Physiological Reviews, 94(4), 991–1026.

Alexander, J. J., Anderson, A. J., Barnum, S. R., Stevens, B., & Tenner, A. J. (2008). The complement cascade: Yin-Yang in neuroinflammation - Neuro-protection and - degeneration. Journal of Neurochemistry, 107(5), 1169–1187.

Altman, J. (1963). Autoradiographic investigation of cell proliferation in the brains of rats and cats. The Anatomical Record, 145(4), 573–591.

Altman, J., & Bayer, S. A. (1990). Migration and distribution of two populations of hippocampal granule cell precursors during the perinatal and postnatal periods. The Journal of Comparative Neurology, 301(3), 365–381.

Amaral, D. G., & Pierre, L. (2009). The Hippocampus Book. In Hippocampal Neuroanatomy (pp. 37–114). Oxford University Press.

Amaral, D. G., Scharfman, H. E., & Lavenex, P. (2007). The dentate gyrus: fundamental neuroanatomical organization (dentate gyrus for dummies). Progress in Brain Research, 163, 3–22.

Ames, R. S., Lee, D., Foley, J. J., Jurewicz, A. J., Tornetta, M. A., Bautsch, W., et al. (2001). Identification of a selective non-peptide antagonist of the anaphylatoxin C3a receptor that demonstrates anti-inflammatory activity in animal models. Journal of Immunology , 166(10), 6341–6348.

Ames, R. S., Li, Y., Sarau, H. M., Nuthulaganti, P., Foley, J. J., Ellis, C., et al. (1996). Molecular Cloning and Characterization of the Human Anaphylatoxin C3a Receptor. Journal of Biological Chemistry, 271(34), 20231–20234.

Andersen, P., BLISS, T. V. P., & Skrede, K. K. (1971). Lamellar organization of hippocampal excitatory pathways. Experimental Brain Research, 13(2), 222–238.

Annett, L. E., McGregor, A., & Robbins, T. W. (1989). The effects of ibotenic acid lesions of the nucleus accumbens on spatial learning and extinction in the rat. Behavioural Brain Research, 31(3), 231–242.

Arellano, J. I., & Rakic, P. (2011). Neuroscience: Gone with the wean. Nature, 478(7369), 333–334.

Aronica, E., Boer, K., van Vliet, E. A., Redeker, S., Baayen, J. C., Spliet, W. G. M., et al. (2007). Complement activation in experimental and human temporal lobe epilepsy. Neurobiology of Disease, 26(3), 497–511.

Babu, H., Cheung, G., Kettenmann, H., Palmer, T. D., & Kempermann, G. (2007). Enriched monolayer precursor cell cultures from micro-dissected adult mouse dentate gyrus yield functional granule cell-like neurons. PloS One, 2(4), e388.

Babu, H., Claasen, J.-H., Kannan, S., Rünker, A. E., Palmer, T., & Kempermann, G. (2011). A protocol for isolation and enriched monolayer cultivation of neural precursor cells from mouse dentate gyrus. Frontiers in Neuroscience, 5, 89.

Bachstetter, A. D., Morganti, J. M., Jernberg, J., Schlunk, A., Mitchell, S. H., Brewster, K. W., et al. (2011). Fractalkine and CX3CR1 regulate hippocampal neurogenesis in adult and aged rats. Neurobiology of Aging, 32(11), 2030–2044.

Bakker, A., Kirwan, C. B., Miller, M., & Stark, C. E. L. (2008). Pattern Separation in the Human Hippocampal CA3 and Dentate Gyrus. Science, 319(5870), 1640–1642.

Bannerman, D. M., Sprengel, R., & Sanderson, D. J. (2014). Hippocampal synaptic plasticity, spatial memory and anxiety. Nature Reviews Neuroscience, 15(3), 181-192.

Barkas, L., Redhead, E., Taylor, M., Shtaya, A., Hamilton, D. A., & Gray, W. P. (2012). Fluoxetine restores spatial learning but not accelerated forgetting in mesial temporal lobe epilepsy. Brain, 135(8), 2358–2374.

Barkho, B. Z., Song, H., Aimone, J. B., Smrt, R. D., Kuwabara, T., Nakashima, K., et al. (2006). Identification of Astrocyte-expressed Factors That Modulate Neural Stem/Progenitor Cell Differentiation. Stem Cells and Development, 15(3), 407–421.

Barnum, S. R. (1995). Complement Biosynthesis in the Central-Nervous-System. Critical Reviews in Oral Biology and Medicine, 6(2), 132–146.

Battista, D., Ferrari, C. C., Gage, F. H., & Pitossi, F. J. (2006). Neurogenic niche modulation by activated microglia: transforming growth factor beta increases neurogenesis in the adult dentate gyrus. *The European Journal of Neuroscience*, *23*(1), 83–93.

Beek, J., Elward, K., & Gasque, P. (2003). Activation of Complement in the Central Nervous System. Annals of the New York Academy of Sciences, 992(1), 56–71.

Bekinschtein, P., Kent, B. A., Oomen, C. A., Clemenson, G. D., Gage, F. H., Saksida, L. M., & Bussey, T. J. (2013). BDNF in the Dentate Gyrus Is Required for Consolidation of ``Pattern-Separated" Memories. Cell Reports, 5(3), 759–768.

Bekinschtein, P., Kent, B. A., Oomen, C. A., Clemenson, G. D., Gage, F. H., Saksida, L. M., & Bussey, T. J. (2014). Brain-derived neurotrophic factor interacts with adult-born immature cells in the dentate gyrus during consolidation of overlapping memories. Hippocampus, 24(8), 905–911.

Bellander, B. M., Singhrao, S. K., Ohlsson, M., Mattsson, P., & Svensson, M. (2001). Complement activation in the human brain after traumatic head injury. Journal of Neurotrauma, 18(12), 1295–1311.

Benard, M., Raoult, E., Vaudry, D., Leprince, J., Falluel-Morel, A., Gonzalez, B. J., et al. (2008). Role of complement anaphylatoxin receptors (C3aR, C5aR) in the development of the rat cerebellum. Molecular Immunology, 45(14), 3767–3774.

Bengzon, J., Kokaia, Z., Elmér, E., Nanobashvili, A., Kokaia, M., & Lindvall, O. (1997). Apoptosis and proliferation of dentate gyrus neurons after single and intermittent limbic seizures. Proceedings of the National Academy of Sciences of the United States of America, 94(19), 10432–10437.

Benson, M. J., Thomas, N. K., Talwar, S., Hodson, M. P., Lynch, J. W., Woodruff, T. M., & Borges, K. (2015). A novel anticonvulsant mechanism via inhibition of complement receptor C5ar1 in murine epilepsy models. Neurobiology of Disease, 76, 87–97.

Bhattacharyya, B. J., Banisadr, G., Jung, H., Ren, D., Cronshaw, D. G., Zou, Y., & Miller, R. J. (2008). The Chemokine Stromal Cell-Derived Factor-1 Regulates GABAergic Inputs to Neural Progenitors in the Postnatal Dentate Gyrus. Journal of Neuroscience, 28(26), 6720–6730.

Bilimoria, P. M., & Stevens, B. (2015). Microglia function during brain development_ New insights from animal models. Brain Research, 1617(C), 7–17.

Binley, K. E., Ng, W. S., Tribble, J. R., Song, B., & Morgan, J. E. (2014). Sholl analysis: A quantitative comparison of semi-automated methods. Journal of Neuroscience Methods, 225, 65–70.

Bliss, T. V. P. (1988). Long-term potentiation of synaptic transmission in the hippocampus: properties and mechanisms. Long Term-Potentiation: From Biophysics to Behavior, 3–72.

Bohanakashtan, O. (2004). Cell signals transduced by complement. Molecular Immunology, 41(6-7), 583–597.

Bonfanti, L. (2013). Neural Stem Cells: New Perspectives. Rijeka, Croatia: InTech

Bonaguidi, M. A., Song, J., Ming, G. L., & Song, H. (2012). A unifying hypothesis on mammalian neural stem cell properties in the adult hippocampus. Current Opinion in Neurobiology, 22(5) 754-761.

Bonaguidi, M. A., Wheeler, M. A., Shapiro, J. S., Stadel, R. P., Sun, G. J., Ming, G.-L., & Song, H. (2011). In Vivo Clonal Analysis Reveals Self-Renewing and Multipotent Adult Neural Stem Cell Characteristics. Cell, 145(7), 1142–1155.

Bosma, M. J., & Carroll, A. M. (1991). The SCID mouse mutant: definition, characterization, and potential uses. Annual Review of Immunology, 9, 323-350

Boulanger, L. M. (2009). Immune Proteins in Brain Development and Synaptic Plasticity. Neuron, 64(1), 93–109.

Brandt, M. D., Jessberger, S., Steiner, B., Kronenberg, Reuter, K., Bick-Sander, A., von der Behrens, W. & Kempermann, G. (2003) Transient calretinin expression defines early postmitotic step of neuronal differentiation in adult hippocampal neurogenesis of mice. Molecular and Cellular Neuroscience, 24(3), 603-613

Brennan, F. H., Anderson, A. J., Taylor, S. M., Woodruff, T. M., & Ruitenberg, M. J. (2012). Complement activation in the injured central nervous system: another dual-edged sword?. Journal of Neuroinflammation, 9, 137

Brown, M. B., & Forsythe, A. B. (1974). Robust tests for the equality of variances. Journal of the American Statistical Association, 69 (346) 364-367.

Brown, M. W., & Aggleton, J. P. (2001). Recognition memory: What are the roles of the perirhinal cortex and hippocampus? Nature Reviews Neuroscience, 2(1), 51–61.

Burgess, N., Maguire, E. A., & O'Keefe, J. (2002). The Human Hippocampus and Spatial and Episodic Memory. Neuron, 35(4), 625–641.

Bussey, T. J., Padain, T. L., Skillings, E. A., Winters, B. D., Morton, A. J., & Saksida, L. M. (2008). The touchscreen cognitive testing method for rodents: How to get the best out of your rat. Learning & Memory, 15(7), 516–523.

Butovsky, O., Ziv, Y., Schwartz, A., Landa, G., Talpalar, A. E., Pluchino, S., et al. (2006). Microglia activated by IL-4 or IFN-γ differentially induce neurogenesis and oligodendrogenesis from adult stem/progenitor cells. Molecular and Cellular Neuroscience, 31(1), 149–160.

Cacci, E., Ajmone Cat, M. A., Anelli, T., Biagioni, S., & Minghetti, L. (2008). In vitro neuronal and glial differentiation from embryonic or adult neural precursor cells are differently affected by chronic or acute activation of microglia. Glia, 56(4), 412–425.

Cameron, H. A., & Gould, E. (1994). Adult neurogenesis is regulated by adrenal steroids in the dentate gyrus. Neuroscience, 61(2), 203–209.

Cao, L., Jiao, X., Zuzga, D. S., Liu, Y., Fong, D. M., Young, D., & During, M. J. (2004). VEGF links hippocampal activity with neurogenesis, learning and memory. Nature Genetics, 36(8), 827–835.

Cardinal, R. N., & Aitken, M. R. F. (2010). Whisker: A client—server high-performance multimedia research control system. Behavior Research Methods, 42(4), 1059–1071.

Cardona, A. E., Pioro, E. P., Sasse, M. E., Kostenko, V., Cardona, S. M., Dijkstra, I. M., et al. (2006). Control of microglial neurotoxicity by the fractalkine receptor. Nature Neuroscience, 9(7), 917–924.

Carola, V., D'Olimpio, F., Brunamonti, E., Mangia, F., & Renzi, P. (2002). Evaluation of the elevated plus-maze and open-field tests for the assessment of anxiety-related behaviour in inbred mice. Behavioural Brain Research, 134(1-2), 49–57.

Carroll, M. C. (2004). The complement system in regulation of adaptive immunity. Nature Immunology, 5(10), 981–986.

Cero, C., Vostrikov, V. V., Verardi, R., Severini, C., Gopinath, T., Braun, P. D., et al. (2014). The TLQP-21 peptide activates the G-protein-coupled receptor C3aR1 via a folding-upon-binding mechanism. Structure, 22(12), 1744–1753.

Chan, J. P., Cordeira, J., Calderon, G. A., Iyer, L. K., & Rios, M. (2008). Depletion of central BDNF in mice impedes terminal differentiation of new granule neurons in the adult hippocampus. Molecular and Cellular Neuroscience, 39(3), 372–383.

Chancey, J. H., Adlaf, E. W., & Sapp, M. C. (2013). Chancey: GABA depolarization is required for experience-dependent synapse unsilencing in adult born neurons. Journal of Neuroscience, 33(15), 6614-6622.

Chawla, M. K., Guzowski, J. F., Ramirez Amaya, V., Lipa, P., Hoffman, K. L., Marriott, L. K., et al. (2005). Sparse, environmentally selective expression of Arc RNA in the upper blade of the rodent fascia dentata by brief spatial experience. Hippocampus, 15(5), 579–586.

Chen, N.-J., Mirtsos, C., Suh, D., Lu, Y.-C., Lin, W.-J., McKerlie, C., et al. (2007). C5L2 is critical for the biological activities of the anaphylatoxins C5a and C3a. Nature, 446, 203–207.

Chen, Y., Al, Y., Slevin, J., Maley, B., & Gash, D. (2005). Progenitor proliferation in the adult hippocampus and substantia nigra induced by glial cell line-derived neurotrophic factor. Experimental Neurology, 196(1), 87–95.

Cho, K. O., Lybrand, Z. R., Ito, N., Brulet, R., Tafacory, F., Zhang, L., et al. (2015). Aberrant hippocampal neurogenesis contributes to epilepsy and associated cognitive decline. Nature Communications, 6, 6606.

Chow, W.-N., Lee, Y.-L., Wong, P.-C., Chung, M.-K., Lee, K.-F., & Yeung, W. S.-B. (2009). Complement 3 deficiency impairs early pregnancy in mice. Molecular Reproduction and Development, 76(7), 647–655.

Chu, Y., Jin, X., Parada, I., Pesic, A., Stevens, B., Barres, B., & Prince, D. A. (2010). Enhanced synaptic connectivity and epilepsy in C1q knockout mice. Proceedings of the National Academy of Sciences of the United States of America, 107(17), 7975–7980.

Cieślar Pobuda, A., & Los, M. J. (2013). Prospects and limitations of "Click-Chemistry-"based DNA labeling technique employing 5-ethynyl-2'deoxyuridine (EdU). Cytometry Part A, 83(11), 977–978.

Claiborne, B. J., Amaral, D. G., & Cowan, W. M. (1990). Quantitative, three-dimensional analysis of granule cell dendrites in the rat dentate gyrus. Journal of Comparative Neurology, 302(2), 206–219.

Clark, L., Cools, R., & Robbins, T. W. (2004). The neuropsychology of ventral prefrontal cortex: decision-making and reversal learning. Brain and Cognition, 55(1), 41–53.

Clelland, C. D., Choi, M., Romberg, C., Clemenson, G. D., Fragniere, A., Tyers, P., et al. (2009). A functional role for adult hippocampal neurogenesis in spatial pattern separation. Science, 325(5937), 210–213.

Clemenson, G. D., Lee, S. W., Deng, W., Barrera, V. R., Iwamoto, K. S., Fanselow, M. S., & Gage, F. H. (2014). Enrichment rescues contextual discrimination deficit associated with immediate shock. Hippocampus, 25(3), 385–392.

Cohen, H., Matar, M. A., & Joseph, Z. (2013). Animal Models of Post-Traumatic Stress Disorder. Current Protocols in Neuroscience, 64:9.45.1-9.45.18.

Cole, D. S., & Morgan, B. P. (2003). Beyond lysis: how complement influences cell fate. Clinical Science, 104(5), 455–466.

Colgin, L. L., Moser, E. I., & Moser, M.-B. (2008). Understanding memory through hippocampal remapping. Trends in Neurosciences, 31(9), 469–477. .

Coras, R., Siebzehnrubl, F. A., Pauli, E., Huttner, H. B., Njunting, M., Kobow, K., et al. (2010). Low proliferation and differentiation capacities of adult hippocampal

stem cells correlate with memory dysfunction in humans. Brain, 133, 3359–3372.

Coulthard, L. G., & Woodruff, T. M. (2015). Is the Complement Activation Product C3a a Proinflammatory Molecule? Re-evaluating the Evidence and the Myth. Journal of Immunology, 194(8), 3542–3548.

Cowell, R. M., Plane, J. M., & Silverstein, F. S. (2003). Complement activation contributes to hypoxic-ischemic brain injury in neonatal rats. The Journal of Neuroscience, 23(28), 9459–9468.

Crawley, J. N. (1985). Exploratory behavior models of anxiety in mice. Neuroscience & Biobehavioral Reviews, 9(1), 37–44.

Creer, D. J., Romberg, C., Saksida, L. M., van Praag, H., & Bussey, T. J. (2010). Running enhances spatial pattern separation in mice. Proceedings of the National Academy of Sciences of the United States of America, 107(5), 2367–2372.

Cryan, J. F., & Holmes, A. (2005). The ascent of mouse: advances in modelling human depression and anxiety. Nature Reviews Drug Discovery, 4(9), 775–790.

Cummings, B. S., & Schnellmann, R. G. (2001). Measurement of Cell Death in Mammalian Cells. Curr Protoc Pharmacol, 1, 1–30.

Cunningham, M., Cho, J.-H., Leung, A., Savvidis, G., Ahn, S., Moon, M., et al. (2014). hPSC-Derived Maturing GABAergic Interneurons Ameliorate Seizures and Abnormal Behavior in Epileptic Mice. Stem Cell, 15(5), 559–573.

Daha, M. R., van Kooten, C., & Roos, A. (2006). Compliments from complement: a fourth pathway of complement activation? Nephrology Dialysis Transplantation, 21(12), 3374–3376.

Damoiseaux, J. G., Döpp, E. A., Calame, W., Chao, D., MacPherson, G. G., & Dijkstra, C. D. (1994). Rat macrophage lysosomal membrane antigen recognized by monoclonal antibody ED1. Immunology, 83(1), 140–147.

Dantzer, R., O'Connor, J. C., Freund, G. G., Johnson, R. W., & Kelley, K. W. (2008). From inflammation to sickness and depression: when the immune system subjugates the brain. Nature Reviews Neuroscience, 9(1), 46–56.

Davoust, N., Jones, J., Stahel, P. F., Ames, R. S., & Barnum, S. R. (1999). Receptor for the C3a anaphylatoxin is expressed by neurons and glial cells. Glia, 26(3), 201–211.

Dayer, A. G., Ford, A. A., Cleaver, K. M., Yassaee, M., & Cameron, H. A. (2003). Short-term and long-term survival of new neurons in the rat dentate gyrus. The Journal of Comparative Neurology, 460(4), 563–572.

DeCarolis, N. A., & Eisch, A. J. (2010). Hippocampal neurogenesis as a target for the treatment of mental illness: A critical evaluation. Neuropharmacology, 58(6), 884–893.

Deisseroth, K., Singla, S., Toda, H., Monje, M., Palmer, T. D., & Malenka, R. C. (2004). Excitation-neurogenesis coupling in adult neural stem/progenitor cells. Neuron, 42(4), 535–552.

Deng, W., Aimone, J. B., & Gage, F. H. (2010). New neurons and new memories: how does adult hippocampal neurogenesis affect learning and memory? Nature, 11(5), 339–350.

Desmond, N. L., & Levy, W. B. (1985). Granule cell dendritic spine density in the rat hippocampus varies with spine shape and location. Neuroscience Letters, 54(2-3), 219–224.

D'Hooge, R., & De Deyn, P. P. (2001). Applications of the Morris water maze in the study of learning and memory. Brain Research. Brain Research Reviews, 36(1), 60–90.

Doetsch, F. (2003). A niche for adult neural stem cells. Current Opinion in Genetics & Development, 13(5), 543–550.

Dolorfo, C. L., & Amaral, D. G. (1998). Entorhinal cortex of the rat: Topographic organization of the cells of origin of the perforant path projection to the dentate gyrus. Journal of Comparative Neurology, 398(1), 25–48.

Dupret, D., Fabre, A., Döbrössy, M. D., Panatier, A., Rodríguez, J. J., Lamarque, S., et al. (2007). Spatial Learning Depends on Both the Addition and Removal of New Hippocampal Neurons. PLoS Biology, 5(8), e214–12.

Edmondson, J. M., Armstrong, L. S., & Martinez, A. O. (1988). A rapid and simple MTT-based spectrophotometric assay for determining drug sensitivity in monolayer cultures. Journal of Tissue Culture Methods, 11(1), 15–17.

Ehninger, D., & Kempermann, G. (2006). Paradoxical effects of learning the Morris water maze on adult hippocampal neurogenesis in mice may be explained by a combination of stress and physical activity. Genes, Brain and Behavior, 5(1), 29–39.

Eichenbaum, H. (2004). Hippocampus: Cognitive Processes and Neural Representations that Underlie Declarative Memory. Neuron, 44(1), 109–120.

Ekdahl, C. T. (2012). Microglial activation - tuning and pruning adult neurogenesis. Frontiers in Pharmacology, 3, 41.

Ekdahl, C. T., Claasen, J. H., Bonde, S., Kokaia, Z., & Lindvall, O. (2003). Inflammation is detrimental for neurogenesis in adult brain. Proceedings of the National Academy of Sciences of the United States of America, 100(23), 13632–13637.

Encinas, J. M., Michurina, T. V., Peunova, N., Park, J.-H., Tordo, J., Peterson, D. A., et al. (2011). Division-coupled astrocytic differentiation and age-related depletion of neural stem cells in the adult hippocampus. Cell Stem Cell, 8(5), 566–579.

Encinas, J. M., Vaahtokari, A., & Enikolopov, G. (2006). Fluoxetine targets early progenitor cells in the adult brain. Proceedings of the National Academy of Sciences of the United States of America, 103(21), 8233–8238.

Ennaceur, A., Neave, N., & Aggleton, J. P. (1997). Spontaneous object recognition and object location memory in rats: the effects of lesions in the cingulate cortices, the medial prefrontal cortex, the cingulum bundle and the fornix. Experimental Brain Research, 113(3), 509–519.

Eriksson, P. S., Perfilieva, E., Björk-Eriksson, T., Alborn, A.-M., Nordborg, C., Peterson, D. A., & Gage, F. H. (1998). Neurogenesis in the adult human hippocampus. Nature Medicine, 4(11), 1313–1317.

Esposito, M. S. (2005). Neuronal Differentiation in the Adult Hippocampus Recapitulates Embryonic Development. Journal of Neuroscience, 25(44), 10074–10086.

Fabel, K, Wolf, S. A., Ehninger, D., Babu, H., Leal-Galicia, P. & Kempermann, G. (2009). Additive effects of physical exercise and environmental enrichment on adult hippocampal neurogenesis in mice. Frontiers in Neuroscience.

Fabel, K., Fabel, K., Tam, B., Kaufer, D., Baiker, A.,Simmons, N., Kuo, C. J. & Palmer, T. D. (2003). VEGF is necessary for exercise-induced adult hippocampal neurogenesis. European Journal of Neuroscience, 18(10), 2803–2812.

Farioli-Vecchioli, S., Micheli, L., Saraulli, D., Ceccarelli, M., Cannas, S., Scardigli, R., Leonardi, L., Cina, I., Costanzi, M., Ciotti, M. T., Moreira, P., Roualt, J. P., Cestari, V.& Tirone, F. (2012). Btg1 is Required to Maintain the Pool of Stem and Progenitor Cells of the Dentate Gyrus and Subventricular Zone. Frontiers in Neuroscience, 6(124), e00124.

Farioli-Vecchioli, S., Saraulli, D., Costanzi, M., Leonardi, L., Cinà, I., Micheli, L., et al. (2009). Impaired terminal differentiation of hippocampal granule neurons and defective contextual memory in PC3/Tis21 knockout mice. PloS One, 4(12), e8339.

Feng, L., Hatten, M. E., & Heintz, N. (1994). Brain lipid-binding protein (BLBP): A novel signalling system in the developing mammalian CNS. Neuron, 12(4), 895–908.

Ferland, R. J., Gross, R. A., & Applegate, C. D. (2002). Differences in hippocampal mitotic activity within the dorsal and ventral hippocampus following flurothyl seizures in mice. Neuroscience Letters, 332(2), 131–135.

Ferragud, A., Haro, A., Sylvain, A., Velázquez-Sánchez, C., Hernández-Rabaza, V., & Canales, J. J. (2010). Enhanced habit-based learning and decreased neurogenesis in the adult hippocampus in a murine model of chronic social stress. Behavioural Brain Research, 210(1), 134–139.

Ferri, G.-L., Noli, B., Brancia, C., D'Amato, F., & Cocco, C. (2011). VGF: An inducible gene product, precursor of a diverse array of neuro-endocrine peptides and tissue-specific disease biomarkers. Journal of Chemical Neuroanatomy, 42(4), 249–261.

Ferrini, F., & De Koninck, Y. (2013). Microglia control neuronal network excitability via BDNF signalling. Neural Plasticity, 2013, 429815.

Filippov, V., Kronenberg, G., Pivneva, T., Reuter, K., Steiner, B., Wang, L.P., et al. (2003). Subpopulation of nestin-expressing progenitor cells in the adult murine hippocampus shows electrophysiological and morphological characteristics of astrocytes. Molecular and Cellular Neuroscience, 23(3), 373–382.

Fitzsimons, C. P., van Hooijdonk, L. W. A., Schouten, M., Zalachoras, I., Brinks, V., Zheng, T., et al. (2013). Knockdown of the glucocorticoid receptor alters

functional integration of newborn neurons in the adult hippocampus and impairs fear-motivated behavior. Molecular Psychiatry, 18(9), 993–1005.

Franklin, K. B. J. & Paxinos, G. (2008) The Mouse Brain in Stereotactic Coordinates, Third Edition. New York, USA: Academic Press.

Frielingsdorf, H., Simpson, D. R., Thal, L. J., & Pizzo, D. P. (2007). Nerve growth factor promotes survival of new neurons in the adult hippocampus. Neurobiology of Disease, 26(1), 47–55.

Frye, C. A., Petralia, S. M., & Rhodes, M. E. (2000). Estrous cycle and sex differences in performance on anxiety tasks coincide with increases in hippocampal progesterone and 3α,5α-THP. Pharmacology Biochemistry and Behavior, 67(3), 587–596.

Fukuda, S., Kato, F., Tozuka, Y., Yamaguchi, M., Miyamoto, Y., & Hisatsune, T. (2003). Two distinct subpopulations of nestin-positive cells in adult mouse dentate gyrus. The Journal of Neuroscience, 23(28), 9357–9366.

Furutachi, S., Matsumoto, A., Nakayama, K. I., & Gotoh, Y. (2013). p57 controls adult neural stem cell quiescence and modulates the pace of lifelong neurogenesis. The EMBO Journal, 32(7), 970–981.

Fuss, J., Ben Abdallah, N. M. B., Hensley, F. W., Weber, K.-J., Hellweg, R., & Gass, P. (2010a). Deletion of Running-Induced Hippocampal Neurogenesis by Irradiation Prevents Development of an Anxious Phenotype in Mice. PLoS ONE, 5(9), e12769.

Fuss, J., Ben Abdallah, N. M. B., Vogt, M. A., Touma, C., Pacifici, P. G., Palme, R., et al. (2010b). Voluntary exercise induces anxiety-like behavior in adult C57BL/6J mice correlating with hippocampal neurogenesis. Hippocampus, 20(3), 364–376.

Gage, F. H. (2000). Mammalian Neural Stem Cells. Science, 287(5457), 1433–1438.

Galea, L. A. M., Wainwright, S. R., Roes, M. M., Duarte Guterman, P., Chow, C., & Hamson, D. K. (2013). Sex, Hormones and Neurogenesis in the Hippocampus: Hormonal Modulation of Neurogenesis and Potential Functional Implications. Journal of Neuroendocrinology, 25(11), 1039–1061.

Gan, W. B., Grutzendler, J., Wong, W. T., & Wong, R. (2000). Multicolor "DiOlistic" labeling of the nervous system using lipophilic dye combinations. Neuron, 27(2), 219–225.

Gao, J., Choe, H., Bota, D., Wright, P. L., Gerard, C., & Gerard, N. P. (2003). Sulfation of Tyrosine 174 in the Human C3a Receptor Is Essential for Binding of C3a Anaphylatoxin. Journal of Biological Chemistry, 278(39), 37902–37908.

Garcia-Segura, L. M., & Perez-Marquez, J. (2014). A new mathematical function to evaluate neuronal morphology using the Sholl analysis. Journal of Neuroscience Methods, 226, 103–109.

Garthe, A., Roeder, I., & Kempermann, G. (2015). Mice in an enriched environment learn more flexibly because of adult hippocampal neurogenesis. Hippocampus, 26(2) 261-271.

Gasque, P. (2004). Complement: a unique innate immune sensor for danger signals. Molecular Immunology, 41(11), 1089–1098.

Gasque, P., Chan, P., Fontaine, M., Ischenko, A., Lamacz, M., Götze, O., & Morgan, B. P. (1995a). Identification and characterization of the complement C5a anaphylatoxin receptor on human astrocytes. The Journal of Immunology, 155(10), 4882-4889.

Gasque, P., Chan, P., Mauger, C., Schouft, M. T., Singhrao, S., Dierich, M. P., et al. (1996). Identification and characterization of complement C3 receptors on human astrocytes. Journal of Immunology, 156(6), 2247–2255.

Gasque, P., Fontaine, M., & Morgan, B. P. (1995b). Complement expression in human brain. Biosynthesis of terminal pathway components and regulators in human glial cells and cell lines. The Journal of Immunology, 154(9), 4726-4733.

Gavrilyuk, V., Kalinin, S., & Hilbush, B. S. (2005). Identification of complement 5a-like receptor (C5L2) from astrocytes: characterization of anti-inflammatory properties Journal of Neurochemistry, 92(5), 1140-1149. -

Ge, S., Goh, E. L. K., Sailor, K. A., Kitabatake, Y., Ming, G.-L., & Song, H. (2006). GABA regulates synaptic integration of newly generated neurons in the adult brain. Nature, 439(7076), 589–593.

Ge, S., Pradhan, D. A., Ming, G.-L., & Song, H. (2007a). GABA sets the tempo for activity-dependent adult neurogenesis. Trends in Neurosciences, 30(1), 1–8.

Ge, S., Yang, C.-H., Hsu, K.-S., Ming, G.-L., & Song, H. (2007c). A Critical Period for Enhanced Synaptic Plasticity in Newly Generated Neurons of the Adult Brain. Neuron, 54(4), 559–566.

Gebara, E., Bonaguidi, M. A., Beckervordersandforth, R., Sultan, S., Udry, F., Gijs, P. J., et al. (2016). Heterogeneity of Radial Glia-Like Cells in the Adult Hippocampus. Stem Cells, 34(4), 997–1010.

Ginhoux, F., Lim, S., Hoeffel, G., Low, D., & Huber, T. (2013). Origin and differentiation of microglia. Front Cell Neurosci. 2013; 7: 45.

Gomez-Lira, G. (2005). Programmed and Induced Phenotype of the Hippocampal Granule Cells. Journal of Neuroscience, 25(30), 6939–6946.

Gonzalez-Perez, O., Gutierrez-Fernandez, F., Lopez-Virgen, V., Collas-Aguilar, J. Quinones-Hinojosa, A., & Garcia-Verdugo, J. M. (2012). Neuroimmunological regulation of neurogenic niches in the adult brain. Neuroscience, 226,270–281.

Gould, E., & Tanapat, P. (1999). Stress and hippocampal neurogenesis. Biological Psychiatry, 46(11), 1472–1479.

Gould, E., Beylin, A., Tanapat, P., Reeves, A., & (, T. J. (1999). Learning enhances adult neurogenesis in the hippocampal formation. Nature Neuroscience, 2(3), 260–265.

Gould, E., Cameron, H. A., Daniels, D. C., Woolley, C. S., & McEwen, B. S. (1992). Adrenal hormones suppress cell division in the adult rat dentate gyrus. Journal of Neuroscience, 12(9), 3642–3650.

Govindarajan, A., Israely, I., Huang, S.-Y., & Tonegawa, S. (2011). The dendritic branch is the preferred integrative unit for protein synthesis-dependent LTP. Neuron, 69(1), 132–146.

Gray, W. P., & Sundstrom, L. E. (1998). Kainic acid increases the proliferation of granule cell progenitors in the dentate gyrus of the adult rat. Brain Research, 790(1-2), 52–59.

Groeticke, I., Hoffmann, K., & Loescher, W. (2008). Behavioral alterations in a mouse model of temporal lobe epilepsy induced by intrahippocampal injection of kainate. Experimental Neurology, 213(1), 71–83.

Gutierrez, H., & Davies, A. M. (2007). A fast and accurate procedure for deriving the Sholl profile in quantitative studies of neuronal morphology. Journal of Neuroscience Methods, 163(1), 24–30.

Gutiérrez, R. (2003). The GABAergic phenotype of the "glutamatergic" granule cells of the dentate gyrus. Progress in Neurobiology, 71(5), 337–358.

Hanisch, U.-K. (2002). Microglia as a source and target of cytokines. Glia, 40(2), 140–155.

Hannedouche, S., Beck, V., Leighton-Davies, J., Beibel, M., Roma, G., Oakeley, E. J., et al. (2013). Identification of the C3a Receptor (C3AR1) as the Target of the VGF-derived Peptide TLQP-21 in Rodent Cells. Journal of Biological Chemistry, 288(38), 27434–27443.

Harris, J. D. (1943). Habituatory response decrement in the intact organism. Psychological Bulletin, 40(6), 385-422.

Hattiangady, B., RAO, M., & SHETTY, A. (2004). Chronic temporal lobe epilepsy is associated with severely declined dentate neurogenesis in the adult hippocampus. Neurobiology of Disease, 17(3), 473–490.

Hawksworth, O. A., Coulthard, L. G., Taylor, S. M., Wolvetang, E. J., & Woodruff, T. M. (2014). Brief Report: Complement C5a Promotes Human Embryonic Stem Cell Pluripotency in the Absence of FGF2. Stem Cells, 32: 3278-3284.

Heese, K., Hock, C., & Otten, U. (1998). Inflammatory signals induce neurotrophin expression in human microglial cells. Journal of Neurochemistry, 70(2), 699–707.

Helmstaedter, C., Kurthen, M., Lux, S., Reuber, M., & Elger, C. E. (2003). Chronic epilepsy and cognition: a longitudinal study in temporal lobe epilepsy. Annals of Neurology, 54(4), 425–432.

Hernández-Rabaza, V., Llorens-Martín, M., Velázquez-Sánchez, C., Ferragud, A., Arcusa, A., Gumus, H. G., et al. (2009). Inhibition of adult hippocampal neurogenesis disrupts contextual learning but spares spatial working memory, long-term conditional rule retention and spatial reversal. Neuroscienec, 159(1), 59–68.

Hill, A. S., Sahay, A., & Hen, R. (2015). Increasing Adult Hippocampal Neurogenesis is Sufficient to Reduce Anxiety and Depression-Like Behaviors. Neuropsychopharmacology, 40(10), 2368–2378.

Horch, H. W., & Katz, L. C. (2002). BDNF release from single cells elicits local dendritic growth in nearby neurons. Nature Neuroscience, 5(11), 1177–1184.

Horner, A. E., Heath, C. J., Hvoslef-Eide, M., Kent, B. A., Kim, C. H., Nilsson, S. R. O., et al. (2013). The touchscreen operant platform for testing learning and memory in rats and mice. Nature Protocols, 8(10), 1961–1984.

Hosokawa, M., Klegeris, A., Maguire, J., & McGeer, P. L. (2003). Expression of complement messenger RNAs and proteins by human oligodendroglial cells. Glia, 42(4), 417–423.

Howell, O. W., Doyle, K., Goodman, J. H., Scharfman, H. E., Herzog, H., Pringle, A., et al. (2005). Neuropeptide Y stimulates neuronal precursor proliferation in the post-natal and adult dentate gyrus. Journal of Neurochemistry, 93(3), 560–570.

Howell, O. W., Scharfman, H. E., Herzog, H., Sundstrom, L. E., Beck-Sickinger, A., & Gray, W. P. (2003). Neuropeptide Y is neuroproliferative for post-natal hippocampal precursor cells. Journal of Neurochemistry, 86(3), 646–659.

Hsieh, J. (2004). Histone deacetylase inhibition-mediated neuronal differentiation of multipotent adult neural progenitor cells. Proceedings of the National Academy of Sciences, 101(47), 16659–16664.

Huber-Lang, M., Sarma, J. V., Zetoune, F. S., Rittirsch, D., Neff, T. A., McGuire, S. R., et al. (2006). Generation of C5a in the absence of C3: a new complement activation pathway. Nature Medicine, 12(6), 682–687.

Hughes, V. (2012). The Constant Gardeners. Nature, 485(7400), 570–572.

Humby, T., Laird, F. M., Davies, W., & Wilkinson, L. S. (1999). Visuospatial attentional functioning in mice: interactions between cholinergic manipulations and genotype. European Journal of Neuroscience, 11(8), 2813–2823.

Huttmann, K., Sadgrove, M., Wallraff, A., Hinterkeuser, S., Kirchhoff, F., Steinhauser, C., & Gray, W. P. (2003). Seizures preferentially stimulate proliferation of radial glia-like astrocytes in the adult dentate gyrus: functional and immunocytochemical analysis. European Journal of Neuroscience, 18(10), 2769–2778.

Hvoslef-Eide, M., Heath, C. J., Mar, A. C., Horner, A. E., Bussey, T. J., Saksida, L. M., & Oomen, C. A. (2013). The touchscreen operant platform for testing working memory and pattern separation in rats and mice. Nature Protocols, 8(10), 2006–2021.

Illman, N. A., Moulin, C. J. A., & Kemp, S. (2015). Assessment of everyday memory functioning in temporal lobe epilepsy and healthy adults using the multifactorial memory questionnaire (MMQ). Epilepsy Research, 113, 86–89.

Jacob, A., Bao, L., Brorson, J., Quigg, R., & Alexander, J. (2010). C3aR inhibition reduces neurodegeneration in experimental lupus. Lupus, 19(1), 73–82.

Jakubs, K., Bonde, S., Iosif, R. E., Ekdahl, C. T., Kokaia, Z., Kokaia, M., & Lindvall, O. (2008). Inflammation Regulates Functional Integration of Neurons Born in Adult Brain. Journal of Neuroscience, 28(47), 12477–12488.

Janeway, C. A., Travers, P., Walport, M. & Schlomchik (2001). Immunobiology: The Immune System in Health and Disease. 6th Edition. New York: Garland Science

Jauneau, A.-C., Ischenko, A., Chatagner, A., Benard, M., Chan, P., Schouft, M.-T., et al. (2006). Interleukin-1β and anaphylatoxins exert a synergistic effect on NGF expression by astrocytes. Journal of Neuroinflammation, 3(1), 8.

Jerome Engel, J. (2001). Mesial Temporal Lobe Epilepsy: What Have We Learned? The Neuroscientist, 7(4), 340–352.

Jessberger, S., Aigner, S., Clemenson, G. D., Toni, N., Lie, D. C., Karalay, O., et al. (2008). Cdk5 regulates accurate maturation of newborn granule cells in the adult hippocampus. PLoS Biology, 6(11), e272.

Jessberger, S., Nakashima, K., Clemenson, G. D., Mejia, E., Mathews, E., Ure, K., et al. (2007). Epigenetic Modulation of Seizure-Induced Neurogenesis and Cognitive Decline. The Journal of Neuroscience : the Official Journal of the Society for Neuroscience, 27(22), 5967–5975.

Jessberger, S., Römer, B., Babu, H., & Kempermann, G. (2005). Seizures induce proliferation and dispersion of doublecortin-positive hippocampal progenitor cells. Experimental Neurology, 196(2), 342–351.

Jin, K., Zhu, Y., Sun, Y., Mao, X. O., Xie, L., & Greenberg, D. A. (2002). Vascular endothelial growth factor (VEGF) stimulates neurogenesis in vitro and in vivo. Proceedings of the National Academy of Sciences of the United States of America, 99(18), 11946–11950.

Jinno, S. (2011). Topographic differences in adult neurogenesis in the mouse hippocampus: A stereology-based study using endogenous markers. Hippocampus, 21(5), 467–480.

Johnson, S. A., Pasinetti, G. M., & Finch, C. E. (1994). Expression of complement C1qB and C4 mRNAs during rat brain development. Brain Research. Developmental Brain Research, 80(1-2), 163–174.

Johnston, D., & Narayanan, R. (2008). Active dendrites: colorful wings of the mysterious butterflies. Trends in Neurosciences, 31(6), 309–316.

Johnston, S. T., Shtrahman, M., Parylak, S., Gonçalves, J. T., & Gage, F. H. (2015). Paradox of pattern separation and adult neurogenesis: A dual role for new neurons balancing memory resolution and robustness. Neurobiology of Learning and Memory, 129:60-68.

Jones, B., & Mishkin, M. (1972). Limbic lesions and the problem of stimulus--reinforcement associations. Experimental Neurology, 36(2), 362–377.

Kalant, D., MacLaren, R., Cui, W., Samanta, R., Monk, P. N., Laporte, S. A., & Cianflone, K. (2005). C5L2 is a functional receptor for acylation-stimulating protein. Journal of Biological Chemistry, 280(25), 23936–23944.

Kaneko, N., Kudo, K., Mabuchi, T., Takemoto, K., Fujimaki, K., Wati, H., et al. (2006). Suppression of Cell Proliferation by Interferon-Alpha through Interleukin-1 Production in Adult Rat Dentate Gyrus. Neuropsychopharmacology, 31(12), 2619–2626.

Kaneko, T., Fujiyama, F., & Hioki, H. (2002). Immunohistochemical localization of candidates for vesicular glutamate transporters in the rat brain. The Journal of Comparative Neurology, 444(1), 39–62.

Kee, N., Sivalingam, S., Boonstra, R., & Wojtowicz, J. M. (2002). The utility of Ki-67 and BrdU as proliferative markers of adult neurogenesis. Journal of Neuroscience Methods, 115(1), 97–105.

Kee, N., Teixeira, C. M., Wang, A. H., & Frankland, P. W. (2007). Preferential incorporation of adult-generated granule cells into spatial memory networks in the dentate gyrus. Nature Neuroscience, 10(3), 355–362.

Kempermann, G. (2004). Functional significance of adult neurogenesis. Current Opinion in Neurobiology, 14(2), 186–191.

Kempermann, G. (2006). Natural variation and genetic covariance in adult hippocampal neurogenesis. Proceedings of the National Academy of Sciences, 103(3), 780–785.

Kempermann, G. (2012). New neurons for "survival of the fittest,". Nature Reviews Neuroscience, 13(727) 1–10.

Kempermann, G. (2013). An old test for new neurons: refining the Morris water maze to study the functional relevance of adult hippocampal neurogenesis. Frontiers in Neuroscience, 7(63), 1–11.

Kempermann, G. (2015). Activity Dependency and Aging in the Regulation of Adult Neurogenesis. Cold Spring Harbor Perspectives in Biology, 7(11), a018929–19.

Kempermann, G., Gast, D., Kronenberg, G., Yamaguchi, M., & Gage, F. H. (2003). Early determination and long-term persistence of adult-generated new neurons in the hippocampus of mice. Development and Disease, 130, 391-399.

Kempermann, G., Jessberger, S., Steiner, B., & Kronenberg, G. (2004). Milestones of neuronal development in the adult hippocampus. Trends in Neurosciences, 27(8), 447–452.

Kempermann, G., Krebs, J., & Fabel, K. (2008). The contribution of failing adult hippocampal neurogenesis to psychiatric disorders. Current Opinion in Psychiatry, 21(3), 290–295.

Kempermann, G., Kuhn, H. G., & Gage, F. H. (1997). More hippocampal neurons in adult mice living in an enriched environment. Nature.

Kempermann, G., Song, H., & Gage, F. H. (2015). Neurogenesis in the Adult Hippocampus. Cold Spring Harbor Perspectives in Biology, 7(9), a018812–15.

Kheirbek, M. A., & Hen, R. (2014). Add neurons, subtract anxiety. Scientific American, 311(1), 62–67.

Kheirbek, M. A., Drew, L. J., Burghardt, N. S., Costantini, D. O., Tannenholz, L., Ahmari, S. E., et al. (2013). Differential Control of Learning and Anxiety along the Dorsoventral Axis of the Dentate Gyrus. Neuron, 77(5), 955–968.

Kheirbek, M. A., Klemenhagen, K. C., Sahay, A., & Hen, R. (2012). Neurogenesis and generalization: a new approach to stratify and treat anxiety disorders. Nature Neuroscience, 15(12), 1613–1620.

Kirby, E. D., Muroy, S. E., Sun, W. G., Covarrubias, D., Leong, M. J., Barchas, L. A., et al. (2013). Acute stress enhances adult rat hippocampal neurogenesis and activation of newborn neurons via secreted astrocytic FGF2. eLife, 2, e00362.

Kleiber, M. (1932). Body size and metabolism. Journal of Agricultural Science, 6(11) 315-353.

Klos, A., Tenner, A. J., Johswich, K.-O., Ager, R. R., Reis, E. S., & Köhl, J. (2009). The role of the anaphylatoxins in health and disease. Molecular Immunology, 46(14), 2753–2766.

Koo, J. W., & Duman, R. S. (2008). IL-1beta is an essential mediator of the antineurogenic and anhedonic effects of stress. Proceedings of the National Academy of Sciences, 105(2), 751–756.

Kronenberg, G., Reuter, K., Steiner, B., Brandt, M. D., Jessberger, S., Yamaguchi, M., & Kempermann, G. (2003). Subpopulations of proliferating cells of the adult hippocampus respond differently to physiologic neurogenic stimuli. The Journal of Comparative Neurology, 467(4), 455–463.

Kuhn, H. G. (2015). Control of Cell Survival in Adult Mammalian Neurogenesis. Cold Spring Harbor Perspectives in Biology. 7(12) a018895.

Kuhn, H. G., Biebl, M., Wilhelm, D., Li, M., Friedlander, R. M., & Winkler, J. (2005). Increased generation of granule cells in adult Bcl-2-overexpressing mice: a role for cell death during continued hippocampal neurogenesis. European Journal of Neuroscience, 22(8), 1907–1915.

Kuruba, R., & Shetty, A. K. (2007). Could hippocampal neurogenesis be a future drug target for treating temporal lobe epilepsy? CNS & Neurological Disorders Drug Targets, 6(5), 342–357.

Kuwabara, T., Hsieh, J., Muotri, A., Yeo, G., Warashina, M., Lie, D.-C., et al. (2009). Wnt-mediated activation of NeuroD1 and retro-elements during adult neurogenesis. Nature Neuroscience, 12(9), 1097–1105.

Lassalle, J.-M., Bataille, T., & Halley, H. (2000). Reversible Inactivation of the Hippocampal Mossy Fiber Synapses in Mice Impairs Spatial Learning, but neither Consolidation nor Memory Retrieval, in the Morris Navigation Task. Neurobiology of Learning and Memory, 73(3), 243–257.

Lee, I., & Kesner, R. P. (2004). Encoding versus retrieval of spatial memory: Double dissociation between the dentate gyrus and the perforant path inputs into CA3 in the dorsal hippocampus. Hippocampus, 14(1), 66–76.

Leiter, O., Kempermann, G., & Walker, T. L. (2016). A Common Language: How Neuroimmunological Cross Talk Regulates Adult Hippocampal Neurogenesis. Stem Cells International, 2016(9), 1–13.

Leventhal, C., Rafii, S., Rafii, D., Shahar, A., & Goldman, S. A. (1999). Endothelial Trophic Support of Neuronal Production and Recruitment from the Adult Mammalian Subependyma. Molecular and Cellular Neuroscience, 13(6), 450–464.

Lever, C., & Burgess, N. (2012). The virtues of youth and maturity (in dentate granule cells). Cell, 149(1), 18–20.

Lévi-Strauss, M., & Mallat, M. (1987). Primary cultures of murine astrocytes produce C3 and factor B, two components of the alternative pathway of complement activation. Journal of Immunology , 139(7), 2361–2366.

Li, G., Kataoka, H., Coughlin, S. R., & Pleasure, S. J. (2008). Identification of a transient subpial neurogenic zone in the developing dentate gyrus and its regulation by Cxcl12 and reelin signalling. Development, 136(2), 327–335.

Lian, H., Yang, L., Cole, A., Sun, L., Chiang, A., Fowler, S. W., Shim, D. J., Rodriguez-Rivera, J., Taglialatela., J. L., Jankowsky, J. L., Lu., H. and Zheng., H. (2015). NFkappaB-Activated Astroglial Release of Complement C3 Compromises Neuronal Morphology and Function Associated with Alzheimer's Disease. Neuron, 85, 101-115.

Liaury, K., Miyaoka, T., Tsumori, T., Furuya, M., Wake, R., Ieda, M., et al. (2012). Morphological features of microglial cells in the hippocampal dentate gyrus of Gunn rat: a possible schizophrenia animal model. Journal of Neuroinflammation, 9(1), 56.

Lie, D. C., Colamarino, S. A., Song, H.-J., Désiré, L., Mira, H., Consiglio, A., et al. (2005). Wnt signalling regulates adult hippocampal neurogenesis. Nature, 437(7063), 1370–1375.

Lindsey, B. W., & Tropepe, V. (2006). A comparative framework for understanding the biological principles of adult neurogenesis. Progress in Neurobiology, 80(6), 281–307.

Liu, M., Pleasure, S. J., Collins, A. E., Noebels, J. L., Naya, F. J., Tsai, M. J., & Lowenstein, D. H. (2000). Loss of BETA2/NeuroD leads to malformation of the dentate gyrus and epilepsy. Proceedings of the National Academy of Sciences, 97(2), 865–870.

Lledo, P.-M., Alonso, M., & Grubb, M. S. (2006). Adult neurogenesis and functional plasticity in neuronal circuits. Nature Reviews Neuroscience, 7(3), 179–193.

Llorens-Martín, M., Jurado-Arjona, J., Fuster-Matanzo, A., Hernández, F., Rábano, A., & Avila, J. (2014). Peripherally triggered and GSK-3|[beta]|-driven brain inflammation differentially skew adult hippocampal neurogenesis, behavioral pattern separation and microglial activation in response to ibuprofen. Translational Psychiatry, 4(10), e463.

Llorens-Martín, M., Rábano, A., & Ávila, J. (2016). The Ever-Changing Morphology of Hippocampal Granule Neurons in Physiology and Pathology. Frontiers in Neuroscience, 9(145), 4217–20.

Logue, S. F., Paylor, R., & Wehner, J. M. (1997). Hippocampal lesions cause learning deficits in inbred mice in the Morris water maze and conditioned-fear task. Behavioral Neuroscience, 111(1), 104–113.

Lopez-Rojas, J., & Kreutz, M. R. (2016). Mature granule cells of the dentate gyrus—Passive bystanders or principal performers in hippocampal function? Neuroscience & Biobehavioral Reviews, 64, 167–174.

Lugert, S., Basak, O., Knuckles, P., Haussler, U., Fabel, K., Götz, M., et al. (2010). Quiescent and Active Hippocampal Neural Stem Cells with Distinct Morphologies Respond Selectively to Physiological and Pathological Stimuli and Aging. Stem Cell, 6(5), 445–456.

Ma, D. K., Kim, W. R., Ming, G.-L., & Song, H. (2009). Activity-dependent Extrinsic Regulation of Adult Olfactory Bulb and Hippocampal Neurogenesis. Annals of the New York Academy of Sciences, 1170(1), 664–673.

Manderson, A. P., Pickering, M. C., Botto, M., Walport, M. J., & Parish, C. R. (2001). Continual low-level activation of the classical complement pathway. The Journal of Experimental Medicine, 194(6), 747–756.

Marques, A. A., Bevilaqua, M. C. D. N., da Fonseca, A. M. P., Nardi, A. E., Thuret, S., & Dias, G. P. (2016). Gender Differences in the Neurobiology of Anxiety: Focus on Adult Hippocampal Neurogenesis. Neural Plasticity, 2016, 5026713.

Marr, D. (1971). Simple memory: a theory for archicortex. Philosophical Transactions of the Royal Society B: Biological Sciences, 262(841), 23–81.

Masiulis, I., Yun, S., & Eisch, A. J. (2011). The Interesting Interplay Between Interneurons and Adult Hippocampal Neurogenesis. Molecular Neurobiology, 44(3), 287–302.

Mastellos, D. C. (2014). Complement emerges as a masterful regulator of CNS homeostasis, neural synaptic plasticity and cognitive function. Experimental Neurology, 261, 469–474.

Mathieu, M.-C., Sawyer, N., Greig, G. M., Hamel, M., Kargman, S., Ducharme, Y., et al. (2005). The C3a receptor antagonist SB 290157 has agonist activity. Immunology Letters, 100(2), 139–145.

McHugh, T. J., Jones, M. W., Quinn, J. J., Balthasar, N., Coppari, R., Elmquist, J. K., et al. (2007). Dentate gyrus NMDA receptors mediate rapid pattern separation in the hippocampal network. Science, 317(5834), 94–99.

McIlwain, D. R., Berger, T., & Mak, T. W. (2013). Caspase functions in cell death and disease. Cold Spring Harbor Perspectives in Biology, 5(4), a008656–a008656.

McTighe, S. M., Mar, A. C., Romberg, C., Bussey, T. J., & Saksida, L. M. (2009). A new touchscreen test of pattern separation: effect of hippocampal lesions. Neuroreport, 20(9), 881–885.

Mineur, Y. S., Belzung, C., & Crusio, W. E. (2007). Functional implications of decreases in neurogenesis following chronic mild stress in mice. Neuroscience, 150(2), 251–259.

Mirescu, C., & Gould, E. (2006). Stress and adult neurogenesis. Hippocampus, 16(3), 233–238.

Molina, H., Perkins, S. J., Guthridge, J., Gorka, J., Kinoshita, T., & Holers, V. M. (1995). Characterization of a complement receptor 2 (CR2, CD21) ligand binding site for C3. An initial model of ligand interaction with two linked short consensus repeat modules. Journal of Immunology, 154(10), 5426–5435.

Monje, M. L., Toda, H., & Palmer, T. D. (2003). Inflammatory blockade restores adult hippocampal neurogenesis. Science, 302(5651), 1760–1765.

Morgan, B. P., & Gasque, P. (1996). Expression of complement in the brain: role in health and disease. Immunology Today, 17(10), 461–466.

Morita, H., Suzuki, K., Mori, N., & Yasuhara, O. (2006). Occurrence of complement protein C3 in dying pyramidal neurons in rat hippocampus after systemic administration of kainic acid. Neuroscience Letters, 409(1), 35–40.

Moriyama, M., Fukuhara, T., Britschgi, M., He, Y., Narasimhan, R., Villeda, S., et al. (2011). Complement Receptor 2 Is Expressed in Neural Progenitor Cells and Regulates Adult Hippocampal Neurogenesis. Journal of Neuroscience, 31(11), 3981–3989.

Morris, R. (1984). Developments of a water-maze procedure for studying spatial learning in the rat. Journal of Neuroscience Methods, 11(1), 47–60.

Morris, R. G., Garrud, P., Rawlins, J. N., & O'Keefe, J. (1982). Place navigation impaired in rats with hippocampal lesions. Nature, 297(5868), 681–683.

Moser, E. I. (2011). The multi-laned hippocampus. Nature Publishing Group, 14(4), 407–408.

Motulsky, H. J., & Brown, R. E. (2006). Detecting outliers when fitting data with nonlinear regression-a new method based on robust nonlinear regression and the false discovery rate. BMC Bioinformatics, 7(1), 123–20.

Nakashiba, T., Cushman, J. D., Pelkey, K. A., Renaudineau, S., Buhl, D. L., McHugh, T. J., et al. (2012). Young Dentate Granule Cells Mediate Pattern Separation, whereas Old Granule Cells Facilitate Pattern Completion. Cell, 149(1), 188–201.

Namba, T., Mochizuki, H., Onodera, M., Namiki, H., & Seki, T. (2007). Postnatal neurogenesis in hippocampal slice cultures: early in vitro labeling of neural precursor cells leads to efficient neuronal production. *Journal of Neuroscience Research*, *85*(8), 1704–1712.

Namba, T., Mochizuki, H., Onodera, M., Mizuno, Y., Namiki, H., & Seki, T. (2005). The fate of neural progenitor cells expressing astrocytic and radial glial markers in the postnatal rat dentate gyrus. European Journal of Neuroscience, 22(8), 1928–1941.

Nataf, S., Stahel, P. F., Davoust, N., & Barnum, S. R. (1999). Complement anaphylatoxin receptors on neurons: new tricks for old receptors? Trends in Neurosciences, 22(9), 397–402.

Nautiyal, K. M., Dailey, C. A., Jahn, J. L., Rodriquez, E., Son, N. H., Sweedler, J. V., & Silver, R. (2012). Serotonin of mast cell origin contributes to hippocampal function. European Journal of Neuroscience, 36(3), 2347–2359.

Nimmerjahn, A., Kirchhoff, F., & Helmchen, F. (2005). Resting microglial cells are highly dynamic surveillants of brain parenchyma in vivo. Science, 308(5726), 1314–1318.

Nunan, R., Sivasathiaseelan, H., Khan, D., Zaben, M., & Gray, W. (2014). Microglial VPAC1R mediates a novel mechanism of neuroimmune-modulation of hippocampal precursor cells via IL-4 release. Glia.

Olson, A. K., Eadie, B. D., Ernst, C., & Christie, B. R. (2006). Environmental enrichment and voluntary exercise massively increase neurogenesis in the adult hippocampus via dissociable pathways. Hippocampus, 16(3), 250–260.

O'Reilly, R. C., & Norman, K. A. (2002). Hippocampal and neocortical contributions to memory: advances in the complementary learning systems framework. Trends in Cognitive Sciences, 6(12), 505–510.

Orsini, F., De Blasio, D., Zangari, R., Zanier, E. R., & De Simoni, M.-G. (2014). Versatility of the complement system in neuroinflammation, neurodegeneration and brain homeostasis. Frontiers in Cellular Neuroscience, 8, 389.

Overstreet-Wadiche, L. S., Bromberg, D. A., Bensen, A. L., & Westbrook, G. L. (2006). Seizures accelerate functional integration of adult-generated granule cells. Journal of Neuroscience, 26(15), 4095–4103.

Palmer, T. (1997). The Adult Rat Hippocampus Contains Primordial Neural Stem Cells. Molecular and Cellular Neuroscience, 8(6), 389–404.

Palmer, T. D., Willhoite, A. R., & Gage, F. H. (2000). Vascular niche for adult hippocampal neurogenesis. Journal of Comparative Neurology, 425(4), 479–494.

Pan, Y.-W., Chan, G. C. K., Kuo, C. T., Storm, D. R., & Xia, Z. (2012). Inhibition of adult neurogenesis by inducible and targeted deletion of ERK5 mitogen-activated protein kinase specifically in adult neurogenic regions impairs contextual fear extinction and remote fear memory. The Journal of Neuroscience : the Official Journal of the Society for Neuroscience, 32(19), 6444–6455.

Parent, J. M., Yu, T. W., Leibowitz, R. T., Geschwind, D. H., Sloviter, R. S., & Lowenstein, D. H. (1997). Dentate Granule Cell Neurogenesis Is Increased by Seizures and Contributes to Aberrant Network Reorganization in the Adult Rat Hippocampus. The Journal of Neuroscience, 17(10) 3727-3738.

Pasinetti, G. M., Johnson, S. A., & Rozovsky, I. (1992). Complement C1qB and C4 mRNAs responses to lesioning in rat brain. Experimental Neurology, 118, 117-125.

Pauli, E., Hildebrandt, M., Romstöck, J., Stefan, H., & Blumcke, I. (2006). Deficient memory acquisition in temporal lobe epilepsy is predicted by hippocampal granule cell loss. Neurology, 67(8), 1383-1389.

Pekna, M., Hietala, M. A., Rosklint, T., Betsholtz, C., & Pekny, M. (1998). Targeted disruption of the murine gene coding for the third complement component (C3). Scandinavian Journal of Immunology, 47(1), 25–29.

Pellow, S., Chopin, P., File, S. E., & Briley, M. (1985). Validation of open : closed arm entries in an elevated plus-maze as a measure of anxiety in the rat. Journal of Neuroscience Methods, 14(3), 149–167.

Perez-Alcazar, M., Daborg, J., Stokowska, A., Wasling, P., Björefeldt, A., Kalm, M. Zetterberg H., Carlstrom, K. E., Blomgren, K., Ekdahl C. T., Hanse, E. & Pekna, M. (2013). Altered cognitive performance and synaptic function in the hippocampus of mice lacking C3. Experimental Neurology, 253, 154–164.

Peterson, S. L., Nguyen, H. X., Mendez, O. A., & Anderson, A. J. (2015). Complement protein C1q modulates neurite outgrowth in vitro and spinal cord axon regeneration in vivo. The Journal of Neuroscience : the Official Journal of the Society for Neuroscience, 35(10), 4332–4349.

Phillips, R. G., & Ledoux J. E. (1992). Differential Contribution of Amygdala and Hippocampus to Cued and Contextual Fear Conditioning. Behavioral Neuroscience, 106(2), 274–285.

Piazzini, A., Canevini, M. P., Maggiori, G., & Canger, R. (2001). Depression and Anxiety in Patients with Epilepsy. Epilepsy & Behavior, 2(5), 481–489.

Plümpe, T., Ehninger, D., Steiner, B., Klempin, F., Jessberger, S., Brandt, M., et al. (2006). Variability of doublecortin-associated dendrite maturation in adult hippocampal neurogenesis is independent of the regulation of precursor cell proliferation. BMC Neuroscience, 7(1), 77–14.

Poot, M., Zhang, Y. Z., Krämer, J. A., Wells, K. S., Jones, L. J., Hanzel, D. K., et al. (1996). Analysis of mitochondrial morphology and function with novel fixable fluorescent stains. The Journal of Histochemistry and Cytochemistry : Official Journal of the Histochemistry Society, 44(12), 1363–1372.

Priebe, K., Brake, W. G., & Romeo, R. D. (2005). Maternal influences on adult stress and anxiety-like behavior in C57BL/6J and BALB/cJ mice: A cross-fostering study. Developmental Psychobiology, 47(4), 1098-2303.

Qu, Q., Sun, G., Murai, K., Ye, P., Li, W., Asuelime, G., et al. (2013). Wnt7a regulates multiple steps of neurogenesis. Molecular and Cellular Biology, 33(13), 2551–2559.

Rahimi, O., & Claiborne, B. J. (2007). Morphological development and maturation of granule neuron dendrites in the rat dentate gyrus. In The Dentate Gyrus: A Comprehensive Guide to Structure, Function, and Clinical Implications. Vol. 163, pp. 167–181.

Rahpeymai, Y., Hietala, M. A., Wilhelmsson, U., Fotheringham, A., Davies, I., Nilsson, A.K., et al. (2006). Complement: a novel factor in basal and ischemia-induced neurogenesis. The EMBO Journal, 25(6), 1364–1374.

Rakic, P. (1981). Neuronal-glial interaction during brain development. Trends in Neurosciences, 4, 184–187.

Ramaglia, V., Hughes, T. R., Donev, R. M., Ruseva, M. M., Wu, X., Huitinga, I., et al. (2012). C3-dependent mechanism of microglial priming relevant to multiple sclerosis. Proceedings of the National Academy of Sciences, 109(3), 965–970.

Rani Das, K. (2016). A Brief Review of Tests for Normality. American Journal of Theoretical and Applied Statistics, 5(1), 5–8.

Ransohoff, R. M. (2016). A polarizing question: do M1 and M2 microglia exist? Nature Neuroscience, 19(8), 987–991.

Ransohoff, R. M., & Perry, V. H. (2009). Microglial physiology: unique stimuli, specialized responses. Annual Review of Immunology, 27, 119–145.

Rao, M. S., & Shetty, A. K. (2004). Efficacy of doublecortin as a marker to analyse the absolute number and dendritic growth of newly generated neurons in the adult dentate gyrus. European Journal of Neuroscience, 19(2), 234–246.

Ray, J., & Gage, F. H. (2006). Differential properties of adult rat and mouse brain-derived neural stem/progenitor cells. Molecular and Cellular Neurosciences, 31(3), 560–573.

Reca, R., Wysoczynski, M., Yan, J., Lambris, J. D., & Ratajczak, M. Z. (2006). The role of third complement component (C3) in homing of hematopoietic stem/progenitor cells into bone marrow. Current Topics in Complement, 586(Chapter 3), 35–51.

Redila, V. A., & Christie, B. R. (2006). Exercise-induced changes in dendritic structure and complexity in the adult hippocampal dentate gyrus. Neuroscience, 137(4), 1299–1307.

Redondo, R. L., & Morris, R. G. M. (2011). Making memories last: the synaptic tagging and capture hypothesis. Nature Reviews Neuroscience, 12(1), 17–30.

Reiman, R., Torres, A. C., Martin, B. K., Ting, J. P., Campbell, I. L., & Barnum, S. R. (2005). Expression of C5a in the brain does not exacerbate experimental autoimmune encephalomyelitis. Neuroscience Letters, 390(3), 134–138.

Revest, J.-M., Dupret, D., Koehl, M., Funk-Reiter, C., Grosjean, N., Piazza, P. V. & Abrous, D. N. (2009). Adult hippocampal neurogenesis is involved in anxiety-related behaviors. Molecular Psychiatry, 14(10), 959–967.

Reynolds, B. A., & Rietze, R. L. (2005). Neural stem cells and neurospheres—re-evaluating the relationship. Nature Methods, 2(5), 333–336.

Ricklin, D., & Lambris, J. D. (2007). Complement-targeted therapeutics. Nature Biotechnology, 25(11), 1265–1275.

Ricklin, D., Hajishengallis, G., Yang, K., & Lambris, J. D. (2010). Complement: a key system for immune surveillance and homeostasis. Nature Immunology, 11(9), 785–797.

Riquelme, P. A., Drapeau, E., & Doetsch, F. (2008). Brain micro-ecologies: neural stem cell niches in the adult mammalian brain. Philosophical Transactions of the Royal Society B: Biological Sciences, 363(1489), 123–137.

Rodrigo, C., Zaben, M., Lawrence, T., Laskowski, A., Howell, O. W., & Gray, W. P. (2010). NPY augments the proliferative effect of FGF2 and increases the expression of FGFR1 on nestin positive postnatal hippocampal precursor cells, via the Y1 receptor. Journal of Neurochemistry, 113(3), 615–627.

Rolls, E. T., & Kesner, R. P. (2006). A computational theory of hippocampal function, and empirical tests of the theory. Progress in Neurobiology, 79(1), 1–48.

Rossi, C., Angelucci, A., Costantin, L., Braschi, C., Mazzantini, M., Babbini, F., et al. (2006). Brain-derived neurotrophic factor (BDNF) is required for the enhancement of hippocampal neurogenesis following environmental enrichment. European Journal of Neuroscience, 24(7), 1850–1856.

Ruan, B. H., Li, X., Winkler, A. R., Cunningham, K. M., Kuai, J., Greco, R. M., et al. (2010). Complement C3a, CpG oligos, and DNA/C3a complex stimulate IFN-α production in a receptor for advanced glycation end product-dependent manner. Journal of Immunology, 185(7), 4213–4222.

Rudy, J. W., Huff, N. C., & Matus-Amat, P. (2004). Understanding contextual fear conditioning: insights from a two-process model. Neuroscience & Biobehavioral Reviews, 28(7), 675–685.

Rutkowski, M. J., Sughrue, M. E., Kane, A. J., Mills, S. A., Fang, S., & Parsa, A. T. (2010). Complement and the central nervous system: emerging roles in development, protection and regeneration. Immunology and Cell Biology, 88(8), 781–786.

Sahay, A., & Hen, R. (2007). Adult hippocampal neurogenesis in depression. Nature Neuroscience, 10(9), 1110–1115.

Sahay, A., Scobie, K. N., Hill, A. S., O'Carroll, C. M., Kheirbek, M. A., Burghardt, N. S., et al. (2011). Increasing adult hippocampal neurogenesis is sufficient to improve pattern separation. Nature, 472(7344), 466–470.

Salton, S. R., Fischberg, D. J., & Dong, K. W. (1991). Structure of the gene encoding VGF, a nervous system-specific mRNA that is rapidly and selectively induced by nerve growth factor in PC12 cells. Molecular and Cellular Biology, 11(5), 2335–

Sanderson, D. J. & Bannerman., D., M. (2012). The Role of Habituation in Hippocampus-Dependent Spatial Working Memory Tasks: Evidence from GluA1 AMPA Receptor Subunit Knockout Mice. Hippocampus, 22(5), 981-994.

Santarelli, L. (2003). Requirement of Hippocampal Neurogenesis for the Behavioral Effects of Antidepressants. Science, 301(5634), 805–809.

Saxe, M. D., Battaglia, F., Wang, J.-W., Malleret, G., David, D. J., Monckton, J. E., et al. (2006). Ablation of hippocampal neurogenesis impairs contextual fear conditioning and synaptic plasticity in the dentate gyrus. Proceedings of the National Academy of Sciences of the United States of America, 103(46), 17501–

Saxe, M. D., Malleret, G., Vronskaya, S., Mendez, I., Garcia, A. D., Sofroniew, M. V., et al. (2007). Paradoxical influence of hippocampal neurogenesis on working memory. Proceedings of the National Academy of Sciences of the United States of America, 104(11), 4642–4646.

Sayah, S., Jauneau, A. C., Patte, C., Tonon, M. C., Vaudry, H., & Fontaine, M. (2003). Two different transduction pathways are activated by C3a and C5a anaphylatoxins on astrocytes. Molecular Brain Research, 112(1-2), 53–60.

Schafer, D. P., Lehrman, E. K., Kautzman, A. G., Koyama, R., Mardinly, A. R., Yamasaki, R., et al. (2012). Microglia Sculpt Postnatal Neural Circuits in an Activity and Complement-Dependent Manner. Neuron, 74(4), 691–705.

Scharfman, H. E. (2007). The CA3 "backprojection" to the dentate gyrus. In The Dentate Gyrus: A Comprehensive Guide to Structure, Function, and Clinical Implications. Vol. 163, 627–637.

Schmidt-Hieber, C., Jonas, P., & Bischofberger, J. (2004). Enhanced synaptic plasticity in newly generated granule cells of the adult hippocampus. Nature, 429, 184-187.

Scholzen, T., & Gerdes, J. (2000). The Ki-67 protein: From the known and the unknown. Journal of Cellular Physiology, 182(3), 311–322.

Schwab, M. H., Bartholomae, A., Heimrich, B., Feldmeyer, D., Druffel-Augustin, S., Goebbels, S., et al. (2000). Neuronal Basic Helix-Loop-Helix Proteins (NEX and BETA2/Neuro D) Regulate Terminal Granule Cell Differentiation in the Hippocampus. The Journal of Neuroscience, 20(10), 3714-3724.

Scola, A.-M., Johswich, K.-O., Morgan, B. P., Klos, A., & Monk, P. N. (2009). The human complement fragment receptor, C5L2, is a recycling decoy receptor. Molecular Immunology, 46(6), 1149–1162.

Scoville., W. B., & Milner, B. (1957). Loss of recent memory after bilateral hippocampal lesions. Journal of Neurology, Neurosurgery & Psychiatry, 20(1), 11–21.

Seaberg, R. M., & van der Kooy, D. (2002). Adult rodent neurogenic regions: the ventricular subependyma contains neural stem cells, but the dentate gyrus contains restricted progenitors. The Journal of Neuroscience, 22(5), 1784–1793.

Seaberg, R. M., & van der Kooy, D. (2003). Stem and progenitor cells: the premature desertion of rigorous definitions. Trends in Neurosciences. 26(3), 125-131.

Sekar, A., Bialas, A. R., de Rivera, H., Davis, A., Hammond, T. R., Kamitaki, N., et al. (2016). Schizophrenia risk from complex variation of complement component 4. Nature, 530, 177-183.

Seki, T. (2002). Expression patterns of immature neuronal markers PSA-NCAM, CRMP-4 and NeuroD in the hippocampus of young adult and aged rodents. Journal of Neuroscience Research, 70(3), 327–334.

Seri, B., Garcia-Verdugo, J. M., McEwen, B. S., & Alvarez-Buylla, A. (2001). Astrocytes give rise to new neurons in the adult mammalian hippocampus. Journal of Neuroscience, 21(18), 7153–7160.

Shapiro, L. A., Korn, M. J., Shan, Z., & Ribak, C. E. (2005). GFAP-expressing radial glia-like cell bodies are involved in a one-to-one relationship with doublecortin-immunolabeled newborn neurons in the adult dentate gyrus. Brain Research, 1040(1-2), 81–91.

Shen, Y., Li, R., McGeer, E. G., & McGeer, P. L. (1997). Neuronal expression of mRNAs for complement proteins of the classical pathway in Alzheimer brain. Brain Research, 769(2), 391–395.

Shetty, A. K., & Hattiangady, B. (2007). Concise Review: Prospects of Stem Cell Therapy for Temporal Lobe Epilepsy. Stem Cells, 25(10), 2396–2407.

Shetty, A. K., Hattiangady, B., & Shetty, G. A. (2005). Stem/progenitor cell proliferation factors FGF-2, IGF-1, and VEGF exhibit early decline during the course of aging in the hippocampus: Role of astrocytes. Glia, 51(3), 173–186.

Shi, Q., Colodner, K. J., Matousek, S. B., Merry, K., Hong, S., Kenison, J. E., et al. (2015). Complement C3-Deficient Mice Fail to Display Age-Related Hippocampal Decline. Journal of Neuroscience, 35(38), 13029–13042.

Shinjyo, N., de Pablo, Y., Pekny, M., & Pekna, M. (2015). Complement Peptide C3a Promotes Astrocyte Survival in Response to Ischemic Stress. Molecular Neurobiology, 53, 3076-3087.

Shinjyo, N., Ståhlberg, A., Dragunow, M., Pekny, M., & Pekna, M. (2009). Complement-derived anaphylatoxin C3a regulates in vitro differentiation and migration of neural progenitor cells. Stem Cells, 27(11), 2824–2832.

Sholl, D. A. (1953). Dendritic organization in the neurons of the visual and motor cortices of the cat. Journal of Anatomy, 87(4), 387–406.

Shors, T. J., Miesegaes, G., Beylin, A., Zhao, M., Rydel, T., & Gould, E. (2001). Neurogenesis in the adult is involved in the formation of trace memories. Nature, 410(6826), 372–376.

Shors, T. J., Townsend, D. A., Zhao, M., Kozorovitskiy, Y., & Gould, E. (2002). Neurogenesis may relate to some but not all types of hippocampal-dependent learning. Hippocampus, 12(5), 578–584.

Sierra, A., Encinas, J. M., Deudero, J. J. P., Chancey, J. H., Enikolopov, G., Overstreet-Wadiche, L. S., et al. (2010). Microglia Shape Adult Hippocampal Neurogenesis through Apoptosis-Coupled Phagocytosis. Cell Stem Cell, 7(4), 483–495.

Sierra, A., Martín-Suárez, S., Valcárcel-Martín, R., Pascual-Brazo, J., Aelvoet, S.-A., Abiega, O., et al. (2015). Neuronal Hyperactivity Accelerates Depletion of Neural Stem Cells and Impairs Hippocampal Neurogenesis. Stem Cell, 16(5), 488–503.

Sisti, H. M., Glass, A. L., & Shors, T. J. (2007). Neurogenesis and the spacing effect: learning over time enhances memory and the survival of new neurons. Learning & Memory, 14(5), 368–375.

Snyder, J. S., Ferrante, S. C., & Cameron, H. A. (2012). Late Maturation of Adult-Born Neurons in the Temporal Dentate Gyrus. PLoS ONE, 7(11), e48757–8.

Snyder, J. S., Hong, N. S., McDonald, R. J., & Wojtowicz, J. M. (2005). A role for adult neurogenesis in spatial long-term memory. Neuroscience, 130(4), 843–852.

Snyder, J. S., Radik, R., Wojtowicz, J. M., & Cameron, H. A. (2009). Anatomical gradients of adult neurogenesis and activity: Young neurons in the ventral dentate gyrus are activated by water maze training. Hippocampus, 19(4), 360–370.

Snyder, J. S., Soumier, A., Brewer, M., Pickel, J., & Cameron, H. A. (2011). Adult hippocampal neurogenesis buffers stress responses and depressive behaviour. Nature, 476(7361), 458–461

Snyder, S. E., Cheng, H. W., Murray, K. D., Isackson, P. J., McNeill, T. H., & Salton, S. R. (1998a). The messenger RNA encoding VGF, a neuronal peptide precursor, is rapidly regulated in the rat central nervous system by neuronal activity, seizure and lesion. Neuroscience, 82(1), 7–19.

Snyder, S. E., Pintar, J. E., & Salton, S. R. (1998b). Developmental expression of VGF mRNA in the prenatal and postnatal rat. The Journal of Comparative Neurology, 394(1), 64–90.

Song, H., Stevens, C. F., & Gage, F. H. (2002). Astroglia induce neurogenesis from adult neural stem cells. Nature, 417(6884), 39–44.

Song, J., Olsen, R. H. J., Sun, J., Ming, G.-L., & Song, H. (2016). Neuronal Circuitry Mechanisms Regulating Adult Mammalian Neurogenesis. Cold Spring Harbor Perspectives in Biology, 8(8).

Song, J., Zhong, C., Bonaguidi, M. A., Sun, G. J., Hsu, D., Gu, Y., et al. (2012). Neuronal circuitry mechanism regulating adult quiescent neural stem-cell fate decision. Nature, 489(7414), 150–154.

Spalding, K. L., Bergmann, O., Alkass, K., Bernard, S., Salehpour, M., Huttner, H. B., et al. (2013). Dynamics of hippocampal neurogenesis in adult humans. Cell, 153(6), 1219–1227.

Squire, L. R., & Zola, S. M. (1996). Structure and function of declarative and nondeclarative memory systems. Proceedings of the National Academy of Sciences of the United States of America, 93(24), 13515–13522.

Squire, L. R., Stark, C. E. L., & Clark, R. E. (2004). The Medial Temporal Lobe. Annual Review of Neuroscience, 27(1), 279–306.

Steffenach, H.-A., Witter, M., Moser, M.-B., & Moser, E. I. (2005). Spatial Memory in the Rat Requires the Dorsolateral Band of the Entorhinal Cortex. Neuron, 45(2), 301–313.

Steiner, B., Klempin, F., Wang, L., Kott, M., Kettenmann, H., & Kempermann, G. (2006). Type-2 cells as link between glial and neuronal lineage in adult hippocampal neurogenesis. Glia, 54(8), 805–814.

Stephan, A. H., Barres, B. A., & Stevens, B. (2012). The complement system: an unexpected role in synaptic pruning during development and disease. Annual Review of Neuroscience, 35, 369–389.

Stephan, A. H., Madison, D. V., Mateos, J. M., Fraser, D. A., Lovelett, E. A., Coutellier, L., et al. (2013). A dramatic increase of C1q protein in the CNS during normal aging. The Journal of Neuroscience, 33(33), 13460–13474.

Stevens, B. (2008). The classical complement cascade mediates CNS synapse elimination. Journal of Neurochemistry, 104, 143–143.

Stevens, B., Allen, N. J., Vazquez, L. E., Howell, G. R., Christopherson, K. S., Nouri, N., et al. (2007). The classical complement cascade mediates CNS synapse elimination. Cell, 131(6), 1164–1178.

Strainic, M. G., Liu, J., Huang, D., An, F., Lalli, P. N., Muqim, N., et al. (2008). Locally Produced Complement Fragments C5a and C3a Provide Both Costimulatory and Survival Signals to Naive CD4+ T Cells. Immunity, 28(3), 425–435.

Strange, B. A., Witter, M. P., Lein, E. S., & Moser, E. I. (2014). Functional organization of the hippocampal longitudinal axis. Nature, 15(10), 655–669.

Sultan, S., Li, L., Moss, J., Petrelli, F., Cassé, F., Gebara, E., et al. (2015). Synaptic Integration of Adult-Born Hippocampal Neurons Is Locally Controlled by Astrocytes. Neuron, 88(5), 957–972.

Sunyer, J. O., Zarkadis, I. K., & Lambris, J. D. (1998). Complement diversity: a mechanism for generating immune diversity? Immunology Today, 19(11), 519–523.

Swanson, L. W., & Cowan, W. M. (1979). The connections of the septal region in the rat. Journal of Comparative Neurology, 186(4), 621–655.

Takabayashi, T., Vannier, E., Clark, B. D., Margolis, N. H., Dinarello, C. A., Burke, J. F., & Gelfand, J. A. (1996). A new biologic role for C3a and C3a desArg: regulation of TNF-alpha and IL-1 beta synthesis. The Journal of Immunology, 156(9), 3455-3460.

Talpos, J. C., McTighe, S. M., Dias, R., Saksida, L. M., & Bussey, T. J. (2010). Trial-unique, delayed nonmatching-to-location (TUNL): A novel, highly hippocampus-dependent automated touchscreen test of location memory and pattern separation. Neurobiology of Learning and Memory, 94(3), 341–352.

Tamashiro, T. T., Dalgard, C. L., & Byrnes, K. R. (2012). Primary microglia isolation from mixed glial cell cultures of neonatal rat brain tissue. Journal of Visualized Experiments : JoVE, (66), e3814–e3814.

Taupin, P. (2007). BrdU immunohistochemistry for studying adult neurogenesis: Paradigms, pitfalls, limitations, and validation. Brain Research Reviews, 53(1), 198–214.

Terai, K., Walker, D. G., McGeer, E. G., & McGeer, P. L. (1997). Neurons express proteins of the classical complement pathway in Alzheimer disease. Brain Research, 769(2), 385–390.

Thakker-Varia, S., Krol, J. J., Nettleton, J., Bilimoria, P. M., Bangasser, D. A., Shors, T. J., et al. (2007). The neuropeptide VGF produces antidepressant-like behavioral effects and enhances proliferation in the hippocampus. The Journal of Neuroscience : the Official Journal of the Society for Neuroscience, 27(45), 12156–12167.

Therien, A. G., Baelder, R., & Köhl, J. (2005). Agonist Activity of the Small Molecule C3aR Ligand SB 290157. Journal of Immunology, 174(12), 7479–7480.

Thoma, E. C., Wischmeyer, E., Offen, N., Maurus, K., Sirén, A.-L., Schartl, M., & Wagner, T. U. (2012). Ectopic expression of neurogenin 2 alone is sufficient to induce differentiation of embryonic stem cells into mature neurons. PloS One, 7(6), e38651.

Thomas, A., Gasque, P., Vaudry, D., Gonzalez, B., & Fontaine, M. (2000). Expression of a complete and functional complement system by human neuronal cells in vitro. International Immunology, 12(7), 1015–1023.

Tirone, F., Farioli-Vecchioli, S., Micheli, L., Ceccarelli, M., & Leonardi, L. (2013). Genetic control of adult neurogenesis: interplay of differentiation, proliferation and survival modulates new neurons function, and memory circuits. Frontiers in Cellular Neuroscience, 14(7), 59.

Tolwani, R. J., Buckmaster, P. S., Varma, S., & Cosgaya, J. M. (2002). BDNF overexpression increases dendrite complexity in hippocampal dentate gyrus. Neuroscience, 114(3): 795-805.

Toni, N., & Sultan, S. (2011). Synapse formation on adult-born hippocampal neurons. European Journal of Neuroscience, 33(6), 1062–1068.

Tozuka, Y., Fukuda, S., Namba, T., Seki, T., & Hisatsune, T. (2005). GABAergic Excitation Promotes Neuronal Differentiation in Adult Hippocampal Progenitor Cells. Neuron, 47(6), 803–815.

Tran, P. B., Banisadr, G., Ren, D., Chenn, A., & Miller, R. J. (2007). Chemokine receptor expression by neural progenitor cells in neurogenic regions of mouse brain. Journal of Comparative Neurology, 500(6), 1007–1034.

Tronel, S., Charrier, V., Sage, C., Maitre, M., Leste-Lasserre, T., & Abrous, D. N. (2015). Adult-born dentate neurons are recruited in both spatial memory encoding and retrieval. Hippocampus, 22, 292-298.

Tronel, S., Fabre, A., Charrier, V., Oliet, S. H. R., Gage, F. H., & Abrous, D. N. (2010). Spatial learning sculpts the dendritic arbor of adult-born hippocampal neurons. Proceedings of the National Academy of Sciences of the United States of America, 107(17), 7963–7968.

van Beek, J., Nicole, O., Ali, C., Ischenko, A., MacKenzie, E. T., Buisson, A., & Fontaine, M. (2001). Complement anaphylatoxin C3a is selectively protective against NMDA-induced neuronal cell death. Neuroreport, 12(2), 289–293.

van Praag, H., Kempermann, G., & Gage, F. H. (1999). Running increases cell proliferation and neurogenesis in the adult mouse dentate gyrus. Nature Neuroscience, 2(3), 266–270.

van Praag, H., Schinder, A. F., Christie, B. R., Toni, N., Palmer, T. D., & Gage, F. H. (2002). Functional neurogenesis in the adult hippocampus. Nature, 415(6875), 1030–1034.

Veerhuis, R., Janssen, I., De Groot, C. J. A., Van Muiswinkel, F. L., Hack, C. E., & Eikelenboom, P. (1999). Cytokines Associated with Amyloid Plaques in Alzheimer's Disease Brain Stimulate Human Glial and Neuronal Cell Cultures to Secrete Early Complement Proteins, But Not C1-Inhibitor. Experimental Neurology, 160(1), 289–299.

Veerhuis, R., Nielsen, H. M., & Tenner, A. J. (2011). Complement in the brain. Molecular Immunology, 48(14), 1592–1603.

Vezzani, A. (2008). Innate Immunity and Inflammation in Temporal Lobe Epilepsy: New Emphasis on the Role of Complement Activation. Epilepsy Currents, 8(3), 75–77

Vezzani, A., & Friedman, A. (2011). Brain inflammation as a biomarker in epilepsy. Biomarkers in Medicine, 5(5), 607–614.

Vezzani, A., Aronica, E., Mazarati, A., & Pittman, Q. J. (2013). Experimental Neurology. Experimental Neurology, 244(C), 11–21.

Vorhees, C. V., & Williams, M. T. (2006). Morris water maze: procedures for assessing spatial and related forms of learning and memory. Nature Protocols, 1(2), 848–858.

Wadiche, L. O., Bromberg, D. A., Bensen, A. L., & Westbrook, G. L. (2005). GABAergic Signalling to Newborn Neurons in Dentate Gyrus. Journal of Neurophysiology, 94(6), 4528–4532.

Walf, A. A., & Frye, C. A. (2007). The use of the elevated plus maze as an assay of anxiety-related behavior in rodents. Nature Protocols, 2(2), 322–328.

Walker, T. L., White, A., Black, D. M., Wallace, R. H., Sah, P., & Bartlett, P. F. (2008). Latent Stem and Progenitor Cells in the Hippocampus Are Activated by Neural Excitation. The Journal of Neuroscience, 28(20), 5240–5247.

Wall, P. M., & Messier, C. (2001). Methodological and conceptual issues in the use of the elevated plus-maze as a psychological measurement instrument of animal anxiety-like behavior. Neuroscience & Biobehavioral Reviews, 25(3), 275–286.

Waterhouse, E. G., An, J. J., Orefice, L. L., Baydyuk, M., Liao, G.-Y., Zheng, K., et al. (2012). BDNF promotes differentiation and maturation of adult-born neurons through GABAergic transmission. The Journal of Neuroscience, 32(41), 14318–14330.

Wei, L. C., Shi, M., Chen, L. W., Cao, R., Zhang, P., & Chan, Y. S. (2002). Nestin-containing cells express glial fibrillary acidic protein in the proliferative regions of central nervous system of postnatal developing and adult mice. Developmental Brain Research, 139(1), 9–17.

Wessels, M. R., Butko, P., Ma, M., Warren, H. B., Lage, A. L., & Carroll, M. C. (1995). Studies of group B streptococcal infection in mice deficient in complement component C3 or C4 demonstrate an essential role for complement in both innate and acquired immunity. Proceedings of the National Academy of Sciences of the United States of America, 92(25), 11490–11494.

Widera, D., Mikenberg, I., Elvers, M., Kaltschmidt, C., & Kaltschmidt, B. (2006). Tumor necrosis factor receptor 1 is a negative regulator of progenitor proliferation in adult hippocampal neurogenesis. BMC Neuroscience, 7(1), 64.

Wiedenmann, B., & Franke, W. W. (1985). Identification and localization of synaptophysin, an integral membrane glycoprotein of Mr 38,000 characteristic of presynaptic vesicles. Cell, 41(3), 1017–1028.

Winocur, G., Wojtowicz, J. M., Sekeres, M., Snyder, J. S., & Wang, S. (2006). Inhibition of neurogenesis interferes with hippocampus-dependent memory function. Hippocampus, 16(3), 296–304.

Winters, B. D. (2004). Double Dissociation between the Effects of Peri-Postrhinal Cortex and Hippocampal Lesions on Tests of Object Recognition and Spatial Memory: Heterogeneity of Function within the Temporal Lobe. Journal of Neuroscience, 24(26), 5901–5908.

Wirenfeldt, M., Dalmau, I., & Finsen, B. (2003). Estimation of absolute microglial cell numbers in mouse fascia dentata using unbiased and efficient stereological cell counting principles. Glia, 44(2), 129–139.

Witter, M. P. (1993). Organization of the entorhinal—hippocampal system: A review of current anatomical data. Hippocampus, 3(S1), 33–44.

Wojtowicz, J. M., & Kee, N. (2006). BrdU assay for neurogenesis in rodents. Nature Protocols, 1(3), 1399–1405.

Woodruff, T. M., & Tenner, A. J. (2015). A Commentary On: "NFκB-Activated Astroglial Release of Complement C3 Compromises Neuronal Morphology and Function Associated with Alzheimer's Disease." A cautionary note regarding C3aR. Frontiers in Immunology, 6, 1–2.

Woodruff, T. M., & Tenner, A. J. (2015). A Commentary On: "NFκB-Activated Astroglial Release of Complement C3 Compromises Neuronal Morphology and

Function Associated with Alzheimer's Disease." A cautionary note regarding C3aR. Frontiers in Immunology, 6, 1–2.

Woodruff, T. M., Ager, R. R., Tenner, A. J., Noakes, P. G., & Taylor, S. M. (2010). The Role of the Complement System and the Activation Fragment C5a in the Central Nervous System. Neuromolecular Medicine, 12(2), 179–192.

Wright, S. P. (1992). Adjusted p-values for simultaneous inference. Biometrics, 48(4), 1005–1013.

Wu, F., Zou, Q., Ding, X., Shi, D., Zhu, X., Hu, W., et al. (2016). Complement component C3a plays a critical role in endothelial activation and leukocyte recruitment into the brain. Journal of Neuroinflammation, 13(23), 1-14.

Xiong, Z. Q., et al. (2003). Formation of complement membrane attack complex in mammalian cerebral cortex evokes seizures and neurodegeneration. Journal of Neuroscience, 23(3), 955-960

Yassa, M. A., & Stark, C. E. L. (2011). Pattern separation in the hippocampus. Trends in Neurosciences, 34(10), 515–525.

Yeckel, M. F., & Berger, T. W. (1990). Feedforward excitation of the hippocampus by afferents from the entorhinal cortex: redefinition of the role of the trisynaptic pathway. Proceedings of the National Academy of Sciences of the United States of America, 87(15), 5832–5836.

Yonelinas, A. P., Aly, M., Wang, W.-C., & Koen, J. D. (2010). Recollection and familiarity: Examining controversial assumptions and new directions. Hippocampus, 20(11), 1178–1194.

Young, D., Lawlor, P. A., Leone, P., Dragunow, M., & During, M. J. (1999). Environmental enrichment inhibits spontaneous apoptosis, prevents seizures and is neuroprotective. Nature Medicine, 5(4), 448–453.

Zabel, M. K., & Kirsch, W. M. (2013). From development to dysfunction: Microglia and the complement cascade in CNS homeostasis. Ageing Research Reviews, 12(3), 749–756.

Zaben, M., John Sheward, W., Shtaya, A., Abbosh, C., Harmar, A. J., Pringle, A. K., & Gray, W. P. (2009). The Neurotransmitter VIP Expands the Pool of Symmetrically Dividing Postnatal Dentate Gyrus Precursors via VPAC 2Receptors or Directs Them Toward a Neuronal Fate via VPAC 1receptors. Stem Cells, 27(10), 2539–2551.

Zander, J.-F., Münster-Wandowski, A., Brunk, I., Pahner, I., Gómez-Lira, G., Heinemann, U., et al. (2010). Synaptic and vesicular coexistence of VGLUT and VGAT in selected excitatory and inhibitory synapses. The Journal of Neuroscience, 30(22), 7634–7645.

Zhang, J., Malik, A., Choi, H. B., Ko, R. W. Y., Dissing-Olesen, L., & MacVicar, B. A. (2014a). Microglial CR3 Activation Triggers Long-Term Synaptic Depression in the Hippocampus via NADPH Oxidase. Neuron, 82(1), 195–207.

Zhang, Y., Chen, K., Sloan, S. A., Bennett, M. L., Scholze, A. R., O'Keeffe, S., et al. (2014b). An RNA-sequencing transcriptome and splicing database of glia,

neurons, and vascular cells of the cerebral cortex. The Journal of Neuroscience, 34(36), 11929–11947.

Zhao, C. E., Teng, M., Sumners, R. G., Ming, G. & Gage, F. H. (2006). Distinct Morphological Stages of Dentate Granule Neuron Maturation in the Adult Mouse Hippocampus. Journal of Neuroscience, 26(1), 3–11.

Clemenson, G. D., Deng, W., & Gage, F. H. (2014). Regulation and function of adult neurogenesis: from genes to cognition. Physiological Reviews, 94(4), 991–1026.

Zhao, C., Deng, W., & Gage, F. H. (2008). Mechanisms and Functional Implications of Adult Neurogenesis. Cell, 132(4), 645–660.

Zhao, M., Li, D., Shimazu, K., Zhou, Y.-X., Lu, B., & Deng, C.-X. (2007). Fibroblast Growth Factor Receptor-1 is Required for Long-Term Potentiation, Memory Consolidation, and Neurogenesis. Biological Psychiatry, 62(5), 381–390.

Zipfel, P. F., & Skerka, C. (2009). Complement regulators and inhibitory proteins. Nature Reviews Immunology, 9(10), 729–740.

Ziv, Y., Ron, N., Butovsky, O., Landa, G., Sudai, E., Greenberg, N., et al. (2006). Immune cells contribute to the maintenance of neurogenesis and spatial learning abilities in adulthood. Nature Neuroscience, 9(2), 268–275.

Appendices

Appendix A. Table of primary and secondary antibodies

Antibody	Working concentration		Supplier & Cat. No
	ICC	ICH	
Mouse α-nestin	1:500	1:500	Millipore MAB353
Rat α-GFAP	1:1000	1:1000	Invitrogen 13-0300
Rabbit α-GFAP	1:1000	1:1000	Dako Z033429-2
Goat α-DCX	1:500	1:200	Santa Cruz Biotech. sc-8066
Rabbit α-TUJ1	1:500	Not used	BioLegend MRB-435P-100
Mouse α-TUJ1	1:500	Not used	BioLegend MMS-435P-100
Rabbit α-Ki67	Not Used	1:1000	Abcam Ab15580
Rabbit α-Iba1	1:1000	Not used	Wako Chemicals (via Alpha Laboratires UK) 019-19741
Rat α- C3/C3b/iC3b/ C3d/C3dg (Clone 11H9)	1:200	Not Used	Hycult Biotechnology HM1045
Mouse α-Synaptophysin 1	1:1000	Not Used	Abcam Ab8049
Rabbit α-VGluT 1	1:1000	Not Used	Synaptic Systems 135 302
Mouse α-VGAT 1	1:1000	Not used	Synaptic Systems 131 011
Alexa Fluor® 488 Donkey α-rat	1:1000	1:2000	Life Technologies A21208
Alexa Fluor® 488 Donkey α-mouse	1:1000	Not used	Life Technologies A21202
Alexa Fluor® 488 Donkey α-rabbit	1:1000	Not used	Life Technologies A21206
Alexa Fluor® 555 Donkey α-mouse	1:1000	Not used	Life Technologies A31570
Alexa Fluor® 555 Donkey α-Rabbit	1:1000	1:2000	Life Technologies A-31572

Alexa Fluor® 647 Donkey α-Rabbit	1:1000	Not used	Life Technologies A31571
Alexa Fluor® 647 Donkey α-mouse	1:1000	Not used	Life Technologies A31573
Alexa Fluor® 647 Donkey α-goat	1:1000	1:2000	Life Technologies A-21447

Appendix B. Table of primer sequences and complement gene names.

Target gene	Forward Primer		Reverse Primer		Product size
	Sequence (5'-> 3')	Tm	Sequence (5'-> 3')	Tm	
C1r	TGTATGCCTACTCCCTCCTT	57.13	CAAAGAGCCACATGTCTCAAG	57.13	98
C1s	CAGCTCCTGAAGGTGACA	56.14	TTGGAGGTAAAGGGCAGTC	56.64	109
C2	ACTGACGGAAAGTCCAACAT	57.07	TCTTTCCAGTCCACATCCAG	56.84	143
Complement Factor I	CGGGCAAGAAAGAATGTGAA	56.63	TGGTTATCTTTCCCTCGACC	56.64	121
C1-INH	ACACACTGATTCTCTGCGAC	57.93	ATGTCAGCTGCGTCCAAA	57.2	90
C5	TCAGAAGAGGCAGAAATCCC	56.91	TAACCTGTGCCTTGATGGAA	56.74	118
CD59	GGTTTGCATTGCTGTGTACT	56.91	GGGCTACCAAATCTGCAATC	56.84	113
Cd59a	CTAAGATTGCAGGGTTGAAGG	56.59	AGCACTATCTTGAGCCACAT	56.61	95
CD55 (DAF)	GAGCCTAACACAGGTGGTG	57.77	TTCGTAACTCTTCGTTGGCT	57.19	120
Cfh	ATGCAAAGATAATTCCTGTGTGG	57.41	CACTTGCCCAAATAGTTCCAA	56.71	136
Clusterin	CGCTATAAATAGGGCGCTTC	56.56	TGGAATCTGGAGTCCGGT	57.11	92
CD46	GTTATTACGTCAATTGTTGGAGTTT	56.61	GAACAGTAATGACTTCCACACA	56.31	126
Cr2	CTTCCTCTCCTTGCTACAGG	57.02	GAGGGTCACAAGAAATCTCAAG	56.71	160
Itgam	CAGGAGTCGTATGTGAGGTC	57.15	CTTGAAAAAGCCAAGCTTGTATAG	56.82	150
Itgb2	CAGGAATGCACCAAGTACAAA	56.72	TCCAGTGAAGTTCAGCTTCTG	57.88	93
Itgax	CCAACTGTTCACTTCACACC	56.86	ACTTCGGAGGTCACCTAGT	56.92	147
CD93	GGAGAATCAGTACAGCCCAA	56.92	CCCCCTCATCTAAGAAGGT	56.73	103
C5aR2	GCAGCCGGTGTCTGG	56.91	CGGAAGGTCACTGTAGTGTT	57.19	92
C6	ACTAGGTCGATTTGAAGGGTC	57.11	GTCACAGAAACAGGCTTCAC	56.95	112
C7	AATAATCCCCCTCCCAGAGA	56.78	ATGTGGCTCAAGTAATCGCA	57.6	108

C8g	GAACCTGCGAAGTGGGG	57.54	CCTGCAAACTGCCTCCC	57.85	92
C9	CAGATGCCAATACCCGTTTC	56.68	CTTCTTGAGCGAAACCTTTGT	57.08	131
Cfb	GGAGAACAGCAGAAGAGGAA	56.86	TAACTCGCCACCTTCTCAAT	56.56	149
Cfd	GATGGAGTGACGGATGACGA	59.26	TACACTCTGCACATCATACCA	56.46	99
Cfp	CAAGTACCCGCCTACAGTTT	57.53	ATGACCGTTTCTCTTCCACC	57.53	128
CR1	GTTTGATCTGGTGGGTGAGA	57.14	TTCAATTTCTGGCATTGGGC	57.23	121
C3	TTCACTATGGGACCAGCTTC	56.92	AGTAATGATGGAATACATGGGGA	56.81	102
C3AR1	GCTTCCTGGTGCCGTTTTTC	58.4	GTTTTGTTCCGAGACTTGGTGAA	58.5	94
C5AR1	ATCTCCCAAGTGTCGGACT	56.3	TCCATTAAATACCATTCCTGAAAACA	56.3	95
C1qa	CCGCAAAGGGTCGCATTTAC	58.2	CGCAGGAGATGGCAGGATG	58.3	114
C4A	GCCAGTATTCTTCTCCAGATGC	57.4	TGCTCACAGGTACGCTTCAT	57.4	79

| Approved Symbol	Approved Name
C1QA	complement component 1, q subcomponent, A chain
C1QB	complement component 1, q subcomponent, B chain
C1QC	complement component 1, q subcomponent, C chain
C1R	complement component 1, r subcomponent
C1S	complement component 1, s subcomponent
C2	complement component 2
C3	complement component 3
C3AR1	complement component 3a receptor 1
C4A	complement component 4A (Rodgers blood group)
C4B	complement component 4B (Chido blood group)
C5	complement component 5
C5AR1	complement component 5a receptor 1

C6	complement component 6
C7	complement component 7
C8A	complement component 8, alpha polypeptide
C8B	complement component 8, beta polypeptide
C8G	complement component 8, gamma polypeptide
C9	complement component 9
CD46	CD46 molecule, complement regulatory protein
CD59	CD59 molecule, complement regulatory protein
CFB	complement factor B
CFD	complement factor D (adipsin)
CFH	complement factor H
CFHR1	complement factor H-related 1
CFHR2	complement factor H-related 2
CFHR3	complement factor H-related 3
CFHR4	complement factor H-related 4
CFHR5	complement factor H-related 5
CFI	complement factor I
CFP	complement factor properdin
CR1	complement component (3b/4b) receptor 1 (Knops blood group)
CR1L	complement component (3b/4b) receptor 1-like
CR2	complement component (3d/Epstein Barr virus) receptor 2
ITGAM	integrin, alpha M (complement component 3 receptor 3 subunit)
ITGAX	integrin, alpha X (complement component 3 receptor 4 subunit)
ITGB2	integrin, beta 2 (complement component 3 receptor 3 and 4 subunit)

**Appendix C.** Microglia in primary hippocampal cultures at 5DIV.
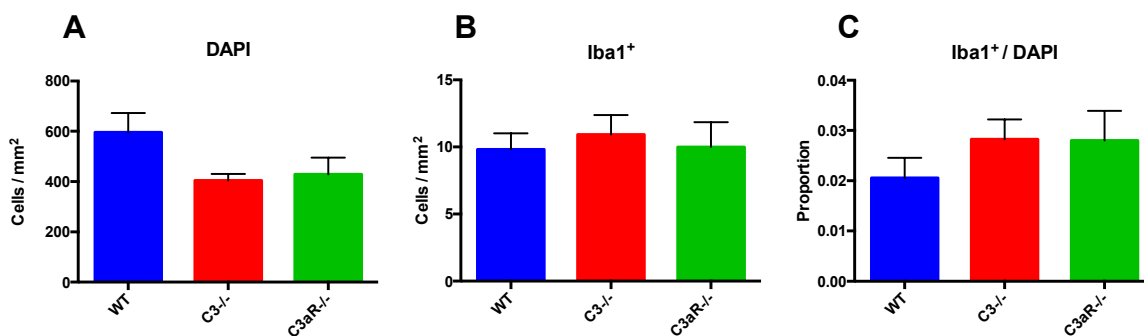
The number of microglia was unchanged between genotypes. A) DAPI cells per mm^2 in WT, $C3^{-/-}$ and $C3aR^{-/-}$ cultures. B) $Iba1^+$ cells per per mm^2. WT 9.81 ± 1.20 per mm^2, $C3^{-/-}$ 10.92 ± 1.45 per mm^2, $C3aR^{-/-}$ 9.99 ± 1.84 per mm^2. Overall ANOVA $F_{(2,33)}=0.15$, p = 0.75. **C)** $Iba1^+$ cells as a proportion of the total cell count. WT 2.0 ± 0.4 %, $C3^{-/-}$ 2.8 ± 0.3% , $C3aR^{-/-}$ 0.28 ± 0.5 %. Overall ANOVA $F_{(2,33)}=0.85$, p = 0.64. N= minimum 12 wells per experiment, from 3 independent cultures per genotype. Data represents mean $\pm$ SEM.

Appendix D. Type 3 cells (DCX$^+$ Nestin$^-$) and DCX/TUJ1 expression in primary hippocampal cultures at 5DIV.
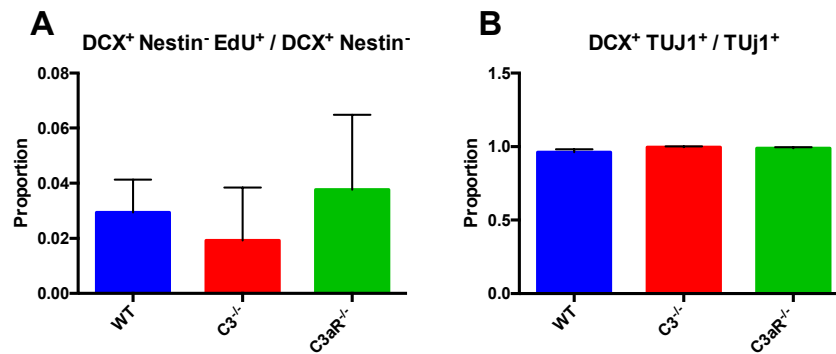
Type 3 cells (DCX$^+$ Nestin$^-$) and DCX/TUJ1 expression in primary hippocampal cultures at 5DIV. A) Proliferating type 3 cells (DCX$^+$ Nestin$^-$) account for a small proportion of the type 3 cell population. WT 2.9 ± 1.1%, C3$^{-/-}$ 1.9 ± 1.9 %, C3aR$^{-/-}$ 3.7 ± 2.7 %. One way ANOVA $F_{(2,25)}$=0.21, p = 0.81. **B)** The majority of the TUJ1$^+$ population co-express DCX. WT 96 ± 1.9 %, C3$^{-/-}$ 99 ± 0.5 %, C3aR$^{-/-}$ 98 ± 0.8 %. One way ANOVA $F_{(2,25)}$=1.85, p = 0.18. N= minimum 4 wells per experiment, from 3 independent cultures per genotype. Data represents mean ± SEM. Data represents mean + SEM. *= p < 0.05, ** = p < 0.01, *** = p < 0.001, ***= p < 0.0001

Appendix E. Ethological parameters measured in the Elevated plus maze
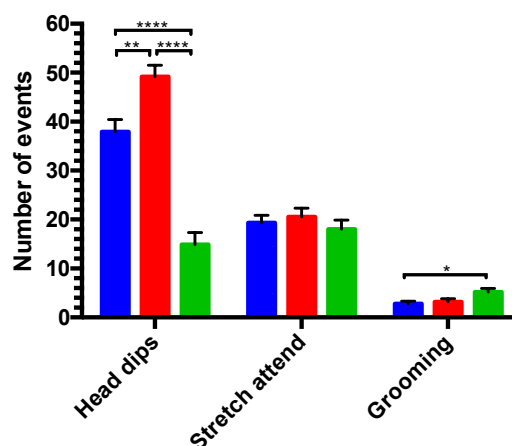
Ethological parameters measured in the Elevated plus maze included head dips, stretch attend postures and grooming events. C3aR$^{-/-}$ mice made fewer head dips (14.90 ± 2.22) compared to WT (37.92 ± 2.53, p < 0.0001). C3$^{-/-}$ mice made significantly more head dips (49.17 ± 2.37) compared to both WT and C3aR$^{-/-}$ (p < 0.01 and p <0.0001, respectively). There were no differences between genotypes in the number of stretch attend postures observed. C3aR$^{-/-}$ animals engaged in significantly more grooming than WT animals (p < 0.05; C3aR $^{-/-}$5.20 ± 0.66, WT 2.75 ± 3.51, C3$^{-/-}$ 3.17 ± 0.65). Data represents mean ± SEM. WT N =12, C3$^{-/-}$ N=12, C3aR$^{-/-}$ N= 10. Data represents mean + SEM. *= p < 0.05, ** = p < 0.01, *** = p < 0.001, ***= p < 0.0001